KU LEUVEN
VRIJE UNIVERSITEIT AMSTERDAM

SENSITIVITY OF FLOODPLAIN GEOECOLOGY TO HUMAN IMPACT IN THE DIJLE CATCHMENT

ACADEMISCH PROEFSCHRIFT

ter verkrijging van de graad Doctor aan
de Vrije Universiteit Amsterdam
en de graad Doctor in de Wetenschappen aan de KU Leuven
op gezag van de rector magnifici
prof.dr. F.A. van der Duyn Schouten en prof.dr. R. Torfs,
in het openbaar te verdedigingen
ten overstaan van de gezamenlijke promotiecommissie
van de faculteit der Aard- en Levenswetenschappen van de Vrije Universiteit Amsterdam en
de Faculteit Wetenschappen van de KU Leuven,
op dinsdag 21 oktober 2014 om 17.00 uur
te Leuven, en
op donderdag 29 januari 2015 om 11.45 uur
in de aula van de universiteit,
De Boelelaan 1105
te Amsterdam

door

Nils Broothaerts

geboren te Mechelen, België

promotoren:	prof.dr. G. Verstraeten (KU Leuven)
	prof.dr. J.F. Vandenberghe (Vrije Universiteit Amsterdam)
copromotoren:	dr. C. Kasse (Vrije Universiteit Amsterdam)
	dr. S.J.P. Bohncke (Vrije Universiteit Amsterdam)

Dit proefschrift is tot stand gekomen op basis van een daartoe tussen de Vrije Universiteit en de KU Leuven, België, overeengekomen samenwerkingsverband ter regeling van een gezamenlijke promotie als bedoeld in het Promotiereglement Vrije Universiteit, hetgeen mede tot uiting wordt gebracht door de weergave van de beeldmerken van beide universiteiten op deze pagina.

KU LEUVEN

VU VRIJE UNIVERSITEIT AMSTERDAM

Leescommissie – Leden van de Examencommissie: prof.dr. J. Poesen (voorzitter)
prof.dr. G. Govers
dr. E. Marinova
prof.dr. H. Middelkoop
prof.dr. R.T. van Balen

This research was carried out at:

KU Leuven
Faculty of Science
Department of Earth and Environmental Sciences
Geography Division
Celestijnenlaan 200E, box 2409
B-3001 Leuven
Belgium
tel. +32 16 32 78 00
www.ees.kuleuven.be

VU University Amsterdam
Faculty of Earth and Life Sciences
Department of Earth Sciences
De Boelelaan 1085
1081 HV Amsterdam
The Netherlands

ISBN 978-90-8649-760-7
D/2014/10705/68

Sensitivity of floodplain geoecology to human impact in the Dijle catchment

In Dutch: Gevoeligheid van de geo-ecologie van overstromingsvlaktes voor menselijke impact in het Dijlebekken

Author: Nils Broothaerts

Uitgegeven in eigen beheer, NILS BROOTHAERTS, MECHELEN

Dankwoord

Deze thesis is het resultaat van vier jaar hard werken. Het werken aan een doctoraatsthesis is een interessante ontdekkingsreis geworden doorheen de wetenschappelijke wereld. Gedurende deze vier jaar heb ik van heel wat mensen steun en hulp gekregen. Ik wil deze mensen dan ook graag bedanken.

Ten eerste dank ik mijn promotoren, prof. Gert Verstraeten en prof. Jef Vandenberghe. Bedankt om me de kans te bieden om een 'dubbel-doctoraat' te starten. Bedankt ook voor de zeer leerrijke discussies en de vele nuttige commentaren op mijn werk. Jullie advies en begeleiding waren zeer inspirerend en apprecieer ik ten zeerste. Gert, bedankt ook voor de leuke informele momenten, zoals de fietstochten door het Dijlebekken, de leuke avonden op congressen en de teambuilding-activiteiten. Zeer veel dank ook aan mijn copromotoren, dr. Kees Kasse en dr. Sjoerd Bohncke, voor de vlotte samenwerking, de interessante discussies op het veld en de uitstekende begeleiding die ik van jullie heb gekregen. Ik heb onze samenwerking over de universiteits- en landsgrenzen heen steeds als zeer leerrijk ervaren, en dank jullie allen dan ook hiervoor. Sjoerd, bedankt ook voor de hulp bij de pollentellingen en voor de gastvrijheid in Lelystad. Bedankt ook aan alle mensen aan de VU Amsterdam die me hielpen tijdens mijn studieverblijven, en die mijn verblijf steeds weer tot een aangename en leerrijke periode maakten.

I would like to thank all other members of the examination committee – prof. Jean Poesen, prof. Gerard Govers, prof. Hans Middelkoop, prof. Ronald van Balen, and dr. Elena Marinova – for their valuable comments on my PhD thesis.

Daarnaast wil ik ook Bastiaan Notebaert bedanken. Van hem kreeg ik dagdagelijkse tips en nuttige commentaren die mijn werk naar een hoger niveau brachten. Zijn enthousiasme voor alles wat te maken heeft met wetenschappelijk onderzoek werkte aanstekelijk en inspirerend. Hij hielp me ook meermaals op het veld, bedankt daarvoor. Bedankt ook Koen D'Haen, voor de hulp bij de boringen en om me te introduceren in de wondere wereld van R, en Hanne De Brue en Bert Dusar voor de hulp bij het veldwerk en de vele nuttige discussies. Gedurende 4 jaar heb ik het bureau mogen delen met heel wat boeiende mensen: Matthias, Bastiaan, Hanne, Steven en Wouter. Bedankt allen voor de hulp bij kleine en grote problemen, maar vooral voor de mooie tijd in ons bureau.

Bedankt ook alle huidige en voormalige collega's in het geo-instituut, in toren 3 en daarbuiten, voor jullie hulp in allerlei vormen en voor de leuke tijd die we samen hebben doorgebracht. Speciale dank aan Bart Vanmontfort voor de vele nuttige discussies over het Neolithicum in het Dijlebekken, Prof. Martin Hermy en zijn team voor de nuttige tips in verband met de statistische analyses van mijn pollen data, en Elena Marinova voor de hulp bij het selecteren van dateerbaar materiaal.

Tijdens mijn doctoraat heb ik ook verschillende studenten begeleid bij hun bachelor- en masterthesis, en hun werk vormt een belangrijke bijdrage aan dit doctoraat. Bedankt Rick Assendelft, Maartje Buijs, Jesper Van Schilt en Bart Coenen voor jullie grondig werk, en de hulp bij het veldwerk en de pollentellingen. Thanks also to Jing Qian, for your work and interest in the Dijle River, although thousands of miles away from your hometown.

Bedankt ook familie en vrienden voor de steun gedurende mijn studies en mijn doctoraat, en vooral voor de vele ontspannende en leuke momenten.

Een speciaal woordje van dank gaat uit naar mijn ouders, voor hun onvoorwaardelijke steun tijdens mijn studies, mijn doctoraat en bij alles daarbuiten. Weten dat jullie altijd – waar we ook zijn – klaar staan voor ons, geeft me steeds de nodige rust en kracht om elke uitdaging aan te gaan. Bedankt!

En bovenal, bedankt Veerle, om er altijd voor mij te zijn, voor je liefde en voor de leuke tijd. Ook bedankt voor je steun en je goede zorgen tijdens mijn wetenschappelijke ontdekkingsreis. Ik hoop dat we de komende jaren samen nog heel wat leuke ontdekkingstochten mogen maken!

Nils Broothaerts

Leuven, oktober 2014

Abstract

Many fluvial systems in West and Central European have undergone important changes in their sediment dynamics and sediment storage during the Holocene, and it is important to understand the driving forces of these changes in order to understand the sensitivity of fluvial systems to environmental changes. The overall objective of this PhD thesis is to provide a better understanding of the sensitivity of floodplain geomorphology and ecology ('geoecology') to human impact in the landscape and to attain a detailed insight in the timing, nature and extent of human impact on floodplain geoecology. The Dijle catchment (758 km²), located within the Belgian loess belt, can serve as a model for most lowland rivers in the European loess area and is selected as the main study area in this thesis.

Previously gathered data on sediment dynamics and floodplain geomorphology were combined with new detailed field-based sediment data, palynological data and radiocarbon ages to provide a more comprehensive overview of the changing floodplain geoecology in the Dijle catchment for the Holocene period. These data showed that during the Middle Holocene, the floodplain was mainly a relatively stable environment and consisted of a strongly vegetated marsh (dominated by an alder carr forest), which resulted in peat accumulation. Throughout the Late Holocene, floodplain geoecology changed with clearing of the Alder carr forest, the development of a single channel river and the dominance of minerogenic overbank sedimentation.

A detailed chronology of the floodplain changes indicated that the end of the peat growth and the transition towards clastic overbank deposition was diachronous at the scale of the entire catchment, ranging between 6500 and 500 cal a BP. Moreover, a well-dated cross-section at the downstream end of the study area suggested that were the floodplain is wide, floodplain changes were asynchronous at cross-section scale, caused by a gradual increasing sediment input in the floodplain that first affected the near-channel parts. These results indicate that conclusions with respect to past changes in sedimentation rate and floodplain morphology should be based on a multi-transect and multi-core dating approach.

In order to understand the role human impact has played in changing the floodplain geoecology, a reconstruction of vegetation changes and a semi-quantification of anthropogenic land cover changes were made, based on palynological and statistical analysis (cluster analysis and non-metric multidimensional scaling (NMDS)). The results show that the pollen records and the NMDS analysis could not detect Mesolithic or Neolithic human activities in the Dijle catchment. In these periods, human impact in the catchment was limited to local disturbances and small-scale forest clearances. The Dijle catchment was covered by deciduous forest, dominated by *Quercus*, *Corylus* and *Tilia*, the natural vegetation for the catchment. Only from the Bronze Age onwards (ca. 3900 cal a BP) human impact clearly increased and vegetation gradually changed. Human impact further increased from the Iron Age onwards, except for a temporary halt between ca. 1900 and 1600 cal a BP, possibly coupled with the Migration Period in Europe. The intensity and onset of the increasing human impact differs between the different study sites.

The relationship between pollen deposited in the floodplain and the vegetation abundance in the landscape was provided based on simulations in the HUMPOL software suite. Such model simulations are needed to translate the modern pollen signal from alluvial sites into vegetation abundance in the

surroundings of the sampling site. Our results indicate that HUMPOL simulations provide a better similarity to the observed pollen signal in the modern alluvial deposits, compared to the observed pollen and the vegetation in the catchment of the sampling site. However, more information on the importance of fluvial pollen transport is needed to correctly interpret the outcome of the multiple scenario approach (MSA), applied to fossil pollen assemblages from alluvial sites and to select the most likely reconstruction of past vegetation.

Finally, the observed floodplain changes were evaluated against the available data on human impact, for the headwaters and for the entire Dijle catchment. This integrated approach demonstrated that during the Neolithic Period, human impact in the catchment was nearly absent and floodplains consisted of a strongly vegetated marshy environment where organic material accumulated, which is considered as the natural state of the floodplain. The increase in human impact from Bronze Age onwards caused an increase in soil erosion and in hillslope-floodplain connectivity. Consequently, sediment input in the floodplain system increased and floodplain geoecology changed towards a more open floodplain dominated by clastic overbank deposits, mainly as the indirect result of an intensification of agricultural activities. At the scale of the entire Dijle catchment, the gradual changes in floodplain morphology coincided with the gradually increasing human impact in the catchment, which suggests a linearity between the external forcing (human impact)and geomorphic response (floodplain change). However, at the narrow floodplains in the headwaters, the gradual increase in human impact contrasts with the abrupt change in floodplain geoecology, only triggered when human impact reached a threshold. Observed differences in the process-response model at catchment scale are attributed to differences in hillslope-floodplain connectivity, the location within the catchment and mainly to differences in the timing and intensity of human activities between different subcatchments.

Samenvatting

Vele riviersystemen in West en Centraal Europa hebben belangrijke veranderingen gekend op vlak van sedimentdynamiek tijdens het Holoceen. Het is belangrijk om de drijvende krachten van deze veranderingen te begrijpen, om op die manier meer inzicht te verkrijgen in de gevoeligheid van riviersystemen en overstromingsvlaktes voor toekomstige omgevingsveranderingen. Het globale doel van dit doctoraatsonderzoek is om meer inzicht te verkrijgen in de gevoeligheid van de geomorfologie en ecologie ('geo-ecologie') van overstromingsvlaktes voor menselijke impact in het landschap, en in de timing, de aard en de omvang van menselijke impact op overstromingsvlaktes. Het Dijlebekken (758 km²) werd geselecteerd als het studiegebied. Het kan gezien worden als een model voor de meeste laaglandrivieren in de Europese loessgordel.

Eerder verzamelde data over sedimentdynamiek en de geomorfologie van overstromingsvlaktes in het Dijlebekken werd gecombineerd met nieuwe gedetailleerde gegevens van sedimenten en pollen, en aangevuld met een reeks nieuwe radiokoolstof (C^{14}) dateringen om een meer volledig inzicht te verkrijgen in de veranderende geo-ecologie van de overstromingsvlakte gedurende het Holoceen. Deze gegevensset toont dat gedurende het Midden Holoceen de overstromingsvlakte een relatief stabiele omgeving was die bestond uit een sterk begroeid moeras (gedomineerd door een elzenbroekbos) waarin geen duidelijke waterloop aanwezig was. In deze stabiele en moerassige overstromingsvlakte kon zich eeuwenlang een dik pakket veen opbouwen. Doorheen het Laat Holoceen veranderde de geo-ecologie van de overstromingsvlakte: het elzenbroekbos verdween, er werd een rivier gevormd met één enkele bedding en oeverwal, en de rivier zette metersdikke pakketten fijnkorrelige sediment af.

Een gedetailleerde chronologie van de veranderingen in de overstromingsvlakte toont dat, op de schaal van het gehele bekken, het einde van de veengroei en de omslag naar klastische overstromingssedimenten asynchroon verliep, variërend tussen 6500 en 500 cal jaren BP. Bovendien toont een in detail gedateerde dwarssectie door een brede overstromingsvlakte, dat de veranderingen ook asynchroon waren op schaal van een individuele sectie. Deze resultaten illustreren dat studies in overstromingsvlaktes steeds gebaseerd moeten worden op resultaten van verschillende dwarsssecties en dat meerdere boringen in een sectie gedateerd moeten worden.

Om de rol van de mens in de veranderingen in de overstromingsvlaktes beter te begrijpen, werd een reconstructie gemaakt van de vegetatieveranderingen. Tevens werd op basis van palynologische en statistische analyses (clusteranalyse en non-metric multidimensional scaling (NMDS)) een semi-kwantificatie van de menselijke impact gemaakt. Deze statistische analyse van de pollengegevens kon geen menselijke activiteiten detecteren tijdens het Mesolithicum en het Neolithicum in het Dijlebekken. In deze periodes was menselijke impact afwezig of beperkt tot lokale verstoringen en kleinschalige ontginningen. Het Dijlebekken werd bedekt door een loofwoud, gedomineerd door eik, hazelaar en linde, wat geïnterpreteerd wordt als de natuurlijke vegetatie van het bekken. Enkel vanaf de Bronstijd (ca. 3900 cal jaren BP) steeg de menselijke impact duidelijk. Menselijke impact nam verder toe met enkel een tijdelijke stagnatie tussen 1900 en 1600 cal jaren BP, wat gekoppeld kan worden met de Grote Volksverhuizingen in Europa. De intensiteit en de start van de toename van menselijke impact verschilt tussen de verschillende bestudeerde valleigebieden in het Dijlebekken.

Verder werd gebruik gemaakt van bestaande simulatiemodellen (HUMPOL) om het pollen signaal van alluviale sites te vertalen naar vegetatie in de omgeving van de site. Deze resultaten tonen dat de HUMPOL simulaties een betere gelijkenis vertonen met het geobserveerde pollensignaal, dan wanneer de vegetatie in het stroomgebied van de site vergeleken wordt met het geobserveerde pollensignaal. Zulke modellen zijn dus nodig om pollengegevens te vertalen naar het relatief voorkomen van de overeenkomstige vegetatietypes in het landschap. De bestaande pollen simulatiemodellen gaan er echter vanuit dat het pollen overwegend via de wind worden getransporteerd. Meer informatie is echter nodig omtrent het belang van fluviatiel pollentransport om de modeluitkomsten correct te interpreteren en om realistische vegetatiereconstructies te maken op basis van pollen die uit alluviale sedimenten worden gehaald.

Tenslotte werden de geobserveerde veranderingen in de overstromingsvlakte gecombineerd met de beschikbare data van menselijke impact, zowel voor de bovenloop als voor het gehele Dijlebekken. Deze geïntegreerde aanpak toont aan dat gedurende het Neolithicum menselijke impact in het bekken afwezig was en de overstromingsvlaktes bestonden uit een sterk begroeide moerasomgeving waar veen accumuleerde. Dit wordt dan ook beschouwd als de natuurlijke toestand van de overstromingsvlakte in het Dijlebekken. De toename in menselijke impact vanaf de Bronstijd veroorzaakte een toename in bodemerosie en in connectiviteit tussen helling en overstromingsvlakte. Als gevolg hiervan steeg de sedimentaanvoer in het riviersysteem en veranderde de geo-ecologie van de overstromingsvlakte naar een meer open vegetatie gedomineerd door klastische overstromingssedimenten. Deze veranderingen worden dus voornamelijk toegeschreven aan een toename van menselijke activiteiten in het bekken. Op de schaal van het gehele Dijlebekken valt de graduele verandering in de overstromingsvlakte samen met de graduale toename in menselijke impact in het bekken. Dit suggereert een lineair verband tussen de externe factoren (menselijke impact) en de geomorfologische respons (veranderingen in de overstromingsvlakte). Daarentegen, op de schaal van de kleine overstromingsvlaktes in de bovenloop van het bekken, verschilt de graduele toename in menselijke impact van de abrupte veranderingen in de overstromingsvlakte. De veranderingen in de overstromingsvlakte worden daar enkel veroorzaakt wanneer menselijke impact een drempelwaarde overschrijdt. De verschillen op bekkenschaal kunnen toegeschreven worden aan verschillen in connectiviteit tussen helling en overstromingsvlakte, de locatie in het bekken en voornamelijk aan verschillen in timing en intensiteit van menselijke activiteit tussen verschillende deelbekkens.

List of abbreviations

a	year (annum)
AF	alder forest
AMS	accelerator mass spectrometry
AP	arboreal pollen taxa
BP	before present
cal a BP	calibrated years before present
CA	correspondence analysis
CAI	centrale archeologische inventaris
CCA	canonical correspondence analysis
CHAR	charcoal accumulation rate
CI	cultural indicator
CPF	cumulative probability function
FSP	fall speed of pollen
HUMPOL	Hull method of pollen simulation
HSDR	Hillslope sediment delivery ratio
LiDAR	light detection and ranging
LOI	loss of ignition
LRA	landscape reconstruction algorithm
M	Median grain size
MSA	multiple scenario approach
NAP	non-arboreal pollen taxa
NMDS	non-metric multidimensional scaling
OSL	optical stimulated luminescence
PAR	pollen accumulation rate
PCA	Principal component analysis
PPE	pollen productivity estimate

R	open source statistical software package (http://www.r-project.org)
SPI	surface peat index

List of symbols

C	compaction of the peat layer (%)
CP_bottom	cumulative probability of the available radiocarbon ages of the bottom of the peat layer
CP_top	cumulative probability of the available radiocarbon ages of the top of the peat layer
D	burial depth (m)
DBD_{MS}	dry bulk density of the mineral sediment mass (Mg m^{-3})
DBD_{OM}	dry bulk density of organic matter (Mg m^{-3})
F_0	initial porosity
OM	organic matter (%)
S_i	initial solidity
t_0	oldest radiocarbon age of peat in the catchment
t_{end}	youngest radiocarbon age of peat in the catchment

Table of Contents

Chapter 1 Introduction

1.1 Problem statement

1.1.1 Floodplain changes during the Holocene

Fluvial systems are an important part of the sedimentary cascade, and herein floodplains play an important role in the redistribution of eroded soils and sediments. Sedimentary records in floodplains form important archives, which can indirectly be related to environmental changes, such as climatic forcing, anthropogenic land use changes (e.g. Kalis et al., 2003; Zolitschka, 2003), and directly be related to engineering works in the floodplain such as terrace or dam building (e.g. Walter and Merritts, 2008). As a consequence, fluvial archives contain valuable information on past sediment dynamics caused by natural or anthropogenic forcings. In addition, fluvial archives contain other valuable proxies to study environmental changes, such as pollen records which can provide more information on vegetation changes in the floodplain and in the catchment. Consequently, fluvial archives are a valuable data source of past environmental changes. The response of the fluvial system to environmental change is, however, complex and often non-linear (e.g. Vandenberghe, 1995; Erkens et al., 2011). Due to different sensitivities to changing environmental factors, similar changes may cause different responses in the fluvial system. Vice versa, contrasting directions in the evolution of environmental factors may finally result in a similar response of the fluvial system (e.g. Van De Wiel and Coulthard, 2010). This complicates the correct interpretation of fluvial archives in terms of its driving forces (e.g. Kalis et al., 2003). Catchment size, for instance, is an important factor in the interpretation of these archives. Large river systems (>10^4 km²) integrate the effects of different sub-catchments and can buffer sediment fluxes to a large extent, through sediment storage in floodplains (Wilkinson and McElroy, 2007). Sediment archives in small to medium-sized river systems, however, reflect the conditions of the individual catchment, and are more sensitive to local variations. Integrated investigation of entire river catchments is therefore necessary.

Many fluvial systems have undergone important changes in their sediment dynamics and sediment storage during the Holocene (Notebaert and Verstraeten, 2010), and it is important to understand the driving forces of these changes in order to understand the sensitivity of fluvial systems to environmental changes. The sensitivity of the fluvial system is defined here as the “susceptibility of a system to disturbance” (Thomas and Allison, 1993), a definition used in many other studies. During the Middle Holocene, most floodplains in the West and Central European lowlands were rather stable environments, typically for interglacial periods (Vandenberghe, 1995). These environments mainly consisted of large marshes where river channels were absent or small and with limited floodplain aggradation. This resulted in the formation of peat in the floodplain of many river systems, e.g. in central Belgium (e.g. De Smedt, 1973; Rommens et al., 2006; Notebaert et al., 2011b) and in the Paris basin (e.g. Pastre et al., 2002). In Germany, often so called ‘black floodplain soils’ were formed during this period, i.e. a layer rich in clay and humic material (e.g. Rittweger, 2000; Kalis et al., 2003; Houben, 2007). However, in some larger catchments (>10^4 km²) in West and Central Europe, like the Rhine catchment, floodplain sedimentation dominated during the same period due to a reworking of clastic sediments from the previous cold stadial (Hoffmann et al., 2007; Erkens, 2009).

The transformation of the floodplains in West and Central Europe has often been attributed to an increasing human impact. From the Neolithic Period onwards, human impact indeed increased through human induced land use changes (e.g. deforestation) and the development of agriculture (e.g. Kalis et al., 2003; Dotterweich, 2008). One of the consequences of the Neolithic Revolution is the increased rate of soil erosion, hillslope sediment delivery and also floodplain sedimentation compared to the pre-agricultural situation (for an overview see e.g. Dotterweich, 2008; Notebaert and Verstraeten, 2010). In West and Central Europe, the first increase in floodplain sedimentation related to the development of agriculture started between ca. 5500 and 2500 cal a BP, although in some catchments early farming activities did not influence floodplain sedimentation to the extent that it would be visible in the sediment record (e.g. Kalis et al., 2003; Rommens et al., 2006). As a result of the increased sediment supply, the floodplains became dominated by clastic sedimentation and their morphology changed towards an aggrading floodplain with a single-channel meandering river. Examples of this changing floodplain geomorphology can be found in Germany (e.g. Rittweger, 2000; Kalis et al., 2003; Houben, 2007), France (e.g. Pastre et al., 2002; Lespez et al., 2008) and Belgium (e.g. De Smedt, 1973; Rommens et al., 2006; Verstraeten et al., 2009b; Notebaert et al., 2011b).

Floodplain sedimentation in many West and Central European catchments increased dramatically during the High Middle Ages (e.g. Pastre et al., 2002; Rommens et al., 2006; Houben, 2007), which can be related to the increased human pressure on the landscape and the associated increase in soil erosion (e.g. Notebaert and Verstraeten, 2010). Modelling results demonstrated that little evidence exists for the influence of climatic variations on the changing sediment delivery to the fluvial system, and showed the importance of land cover changes, e.g. in the Geul (De Moor and Verstraeten, 2008), Dijle (Notebaert et al., 2011c) and Meuse catchment (Ward et al., 2009). In some catchments in Germany, the peak in sedimentation during the Medieval Period is attributed to the introduction of hydraulic water milling infrastructure on valley floors (Houben et al., 2013). Local variations in floodplain aggradation rates in these catchments are related to the local breakdowns of the hydraulic milling infrastructure. Similar changes in floodplain morphology can be found in the eastern USA, where the floodplain changes are attributed to mill dam construction following European colonization (Walter and Merritts, 2008).

Although the increase in sedimentation in floodplains can be related to the development of agriculture in the catchment (see above), several studies point out that the timing of the increased sedimentation in the floodplain does not correspond with the timing of the development of agriculture. Such a temporal offset between the beginning of the agricultural hillslope colluviation and the massive alluvial aggradation is observed in different West and Central European catchments (Lang and Nolte, 1999; Trimble, 1999; Rommens et al., 2006; De Moor and Verstraeten, 2008; Macklin et al., 2010; Notebaert et al., 2011b); an overview is provided by Notebaert and Verstraeten (2010) and Houben et al. (2013). This temporal offset between the increase in colluvial and floodplain sedimentation can be attributed to a time lag between catchment disturbance and its influence on the floodplain system. Such time lags are often related to a threshold value or tipping point that needs to be reached or crossed before an external pressure on the system (e.g. land use change) will result in a change in system behavior (e.g. changing floodplain geoecology) (e.g. Schumm, 1973). Many authors have pointed out that this temporal offset can be explained by changes in hillslope-floodplain connectivity (Lang et al., 2003; Verstraeten et al., 2009b; Houben et al., 2013). First Neolithic agricultural activities were poorly connected to the fluvial system, and sediments did not reach the floodplains. Only when the introduction of new techniques for working the land and the change in spatial pattern of land occupation, with intense cultivation on hillslopes, caused a better connectivity between hillslopes and floodplains, floodplain sedimentation increased. Moreover, the removal of valley-side vegetation as well as the increase in roads and animal paths contributed to the increased hillslope-floodplain connectivity (Verstraeten et al., 2009b; Houben et al., 2013).

Identifying such temporal offsets relies on a sufficient dating resolution. Dating the alluvial sediments can, however, be problematic. Alluvial deposits are frequently characterized by low concentrations of radiocarbon datable material. Due to this lack of datable material, but also due to financial restrictions, past studies have often been based on limited dating evidence for individual catchments (see e.g. Notebaert and Verstraeten, 2010). Moreover, radiocarbon dating does not necessarily provide data on the sedimentation process itself, due to erosion and reworking of organic material (e.g. Hoffmann et al., 2008; Lang, 2008; Chiverrell et al., 2011). These restrictions often lead to studies with a low temporal resolution. As a result, averaging effects might be introduced and only long-term trends can be discerned but short- to medium-range variations or events are not discernable. The lack of a detailed chronology makes it hard to retrieve unambiguous information on the driving forces for the observed sediment dynamics and floodplain changes. Thus, more detailed and precise chronologies are clearly needed (Verstraeten et al., 2009a).

Next to the changing floodplain morphology, also the floodplain vegetation and floodplain ecology underwent an important evolution during the Holocene. Pollen records from alluvial study sites showed that during the Middle Holocene floodplains in West and Central Europe were dominated by wet woodland, mainly dominated by *Alnus* (e.g. Brown et al., 1997; Klimo and Hager, 2001). Floodplain ecology changed during the Holocene under direct influence of human impact in the floodplain, e.g. with the clearance of the floodplain forests (Brown, 1988; Brown, 2002), or due to the increasing sediment input in the river system, which altered the geomorphology and hydrology of the floodplain. Currently, most floodplain forests disappeared and almost no lowland floodplain in West and Central Europe is in a natural, pre-human impact state (Tockner and Stanford, 2002).

An important interplay exists between floodplain geomorphology and floodplain ecology. For instance, floodplain vegetation plays a significant role in trapping sediments, and the vegetation itself is influenced by the sediment input in the floodplain (e.g. Hughes, 1997). Also beavers (*Castor fiber*) can influence floodplain sedimentation by constructing beaver dams (e.g. Hughes, 1997; Brown, 2002). This combination of floodplain geomorphology and floodplain ecology is often called ‘floodplain geoecology’. Geoecology is used in literature in different ways and several different definition are given (e.g. Trofimov, 2009), including this definition. This term will be used in this study, although the focus will mainly be on the interplay between floodplain geomorphology and floodplain vegetation.

Understanding the changing floodplain geoecology is not only scientifically relevant but is also very useful for river restoration and management (e.g. Wohl et al., 2005; Newson and Large, 2006). Since at present no lowland rivers are in a natural state (e.g. Tockner and Stanford, 2002), the study of past river systems during times that human impact was limited is very useful (e.g. Montgomery, 2008). By understanding how past river systems reacted on catchment disturbance, more insights can be gathered about the potential vulnerability of the fluvial system to future disturbances (e.g. Brown, 2002). In this thesis we consider a natural river as a river for which all components are still in a pristine situation, including the non-direct impact e.g. through changes in water or sediment fluxes. Consequently, the natural reference situation is considered as the situation before significant catchment deforestation and anthropogenic management of floodplain systems (e.g. Brown, 2002). Moreover, (quantitative) data on vegetation changes throughout the Holocene are very useful for archaeological research, landscape management, climate change research (e.g. Anderson et al., 2006; Gaillard et al., 2008), understanding past soil erosion (e.g. Enters et al., 2008) and natural ecology conservation management (e.g. Petit et al., 2008).

Furthermore, floodplains play an important role in global biochemical cycles, such as the global carbon cycle (e.g. Aufdenkampe et al., 2011). Increasing human impact throughout the Holocene has played an important role in the long-term erosion and storage of carbon in floodplains (e.g. Van Oost et al., 2012). However, data on human impact on carbon storage in floodplains on a Holocene timescale are scarce. In many West and Central European floodplain systems, organic rich peaty layers are buried by clastic sedimentation (e.g. Notebaert and Verstraeten, 2010), which is a largely underestimated process of carbon storage (Chaopricha and Marin-Spiotta, 2014; Marin-Spiotta et al., 2014). More information on changing floodplain geoecology throughout the Holocene due to human impact can help to unravel the role that floodplain marshes in West and Central Europe played as a carbon sink. It can help to get a better understanding of the global carbon cycle and a better understanding of the early human impact on it.

1.1.2 Reconstructing human impact

To be able to unravel the role human impact has played in altering the floodplain geoecology, good reconstructions of anthropogenic land cover changes and high-quality data on human pressure are needed (e.g. Verstraeten et al., 2009a). Detailed reconstructions of land cover history during the Holocene Period have previously been made based on archeological and palynological records. Archaeological data has previously been used to obtain reliable estimates of population densities (e.g. Zimmermann et al., 2009; Shennan et al., 2013). Detailed quantitative and spatially distributed data on archaeological findings is, however, not available for every region.

Palynological records can also be used to reconstruct human impact at the regional landscape scale, and have widely been applied in several studies (e.g. Behre, 1981; Kalis et al., 2003; Gaillard et al., 2008). Nevertheless, translating pollen percentages in estimations of vegetation abundances is far from straightforward (e.g. Sugita, 1994). Several factors complicate pollen-vegetation relationships, such as defining the pollen source area. The pollen source area depends on different factors, including basin size and pollen transport mechanisms. Larger sedimentary basins have a larger pollen source area than smaller basins. The pollen transport mechanism (e.g. water versus wind transport) depends in turn on the type of study site (e.g. peat bog, lake or alluvial site) (Tauber, 1967; Sugita, 1994). Also inter-taxonomic differences in pollen productivity and dispersal make pollen-vegetation relationships problematic.

Different approaches have been proposed to deal with these problems and to translate pollen data into measures of land cover. One widely used technique is the indicator species approach, broadly discussed in Behre (1981). In this approach, pollen types – such as anthropogenic indicators – are grouped and summed to describe different land cover types. Anthropogenic indicators are pollen of cultivated plants, plants supported by human activities such as treading, browsing or ploughing, or plants tolerating human impact (Behre, 1981). The indicator species approach is nowadays still used by environmental archaeologists (Gaillard, 2007; Fyfe et al., 2010). An even more simple approach is the use of ratio of arboreal to non-arboreal pollen taxa (AP/NAP ratio) (e.g. Faegri and Iversen, 1989), which have been applied in several studies (see e.g. Favre et al., 2008). However, the AP/NAP ratio has proven to be not a suitable proxy for the representation of openness of the landscape (e.g. Brostrom et al., 1998; Sugita et al., 1999), since it depends on many other factors, such as variations in pollen productivity and pollen transport, and it tense to over-represent local input. Overall, these traditional interpretations of pollen diagrams are mainly qualitative approaches, and detailed determination of causal factors or detailed comparisons of different study sites are difficult. Moreover, traditional pollen studies are mostly based on a limited number of study sites (Figure 1.1). However, in order to fully understand all involved factors, a catchment-wide approach is needed. Investigating several study sites within a catchment will help to minimize the effect of local variations and will provided more representative data. Moreover a catchment-wide approach will help to identify catchment wide patterns and to assess the spatial and temporal variation within a catchment.

Recently, advances in pollen studies have been made and new approaches have been proposed to (semi-) quantify vegetation cover based on pollen data. An easy to apply approach is the pseudobiomisation method (Fyfe et al., 2010), which builds further on the indicator species approach and assigns pollen taxa to land cover classes to summarise the dominant land-cover type from individual pollen records (Fyfe et al., 2010; Woodbridge et al., 2012). Other recently developed techniques are the model-based correction approaches, which are based on the empirical understanding of the relationship between pollen values and vegetation cover for individual pollen taxa (e.g. Gaillard et al., 2008), such as the Landscape Reconstruction Algorithm (LRA; Sugita, 2007a and b) and the Multiple Scenario Approach (MSA; Bunting and Middleton, 2009). The LRA of Sugita (Sugita, 2007a and b) aims to quantify vegetation cover using pollen proportions retrieved from large lakes. Although the LRA has been validated in southern Sweden (Hellman et al., 2008) and successfully applied in e.g. Switzerland (Soepboer et al., 2010), several restrictions are associated with it, limiting its use. For instance, the LRA is only validated for pollen data from large lakes. Not every pollen study can, however, rely on pollen data from such large lakes, and often only pollen data from wetland or alluvial sites are available. The MSA (Bunting and Middleton, 2005) starts with generating possible vegetation maps, based on rules of plant requirements combined with environmental parameters. The HUMPOL software suite (i.e. a pollen dispersal and deposition model; Bunting and Middleton, 2005) is then used to simulate the pollen assemblage at a known sampling point in the landscape for each possible map. These simulated pollen assemblages are in a next step compared with known pollen data from the same location to select which of those maps can be considered as the most likely reconstruction of past vegetation (Bunting and Middleton, 2009). Both MSA and LRA have their limitations. For instance, both models rely on good approximations of pollen productivity which are not available for many regions (e.g. Brostrom et al., 1998). Moreover, different studies have indicated that the pollen source area of the aerial component, used in both models, is a poor starting point, since pollen influx in lakes is often dominated by waterborne pollen (e.g. Bonny, 1978; Xu et al., 2012). In alluvial sites one can expect that waterborne pollen are an important contributor to the pollen influx (Brown et al., 2007). Due to the importance of waterborne pollen and the presence of wetland surface vegetation, the pollen signal of wetlands and alluvial sites is not always easy to interpret (e.g. Bunting, 2007)

Alternatively, statistical analysis of pollen diagrams has recently been used to characterize vegetation changes and to extract (semi-)quantitative data on human impact based on the entire pollen signal. Principal component analysis (PCA; Kaniewski et al., 2008; Bakker et al., 2012; Lopez-Merino et al., 2012; Etienne et al., 2013), canonical correspondence analysis (CCA; Lechterbeck et al., 2009) and non-metric multidimensional scaling (NMDS; Oswald et al., 2007; Ghilardi and O'Connell, 2013) have successfully been applied to pollen data in previous studies. These statistical techniques allow a comparison of pollen records from different study sites (Lechterbeck et al., 2009) and are easily applied. They do not rely on a good understanding of pollen productivity and are less complex than the numerical models mentioned above. However, additional insights can be extracted from the pollen data compared with the more traditional approaches, since these statistical techniques include the entire pollen signal. Although these statistical methods can provide more insights in vegetation changes throughout the Holocene, they do not translate pollen percentages in estimations of vegetation abundance, in contrast to the numerical models. To do so, more insight is needed in pollen transport and deposition mechanisms.

1.2 Objectives and research questions

As discussed above, many studies have discussed anthropogenic-driven land cover changes during the Holocene. Also floodplain changes in West and Central European catchments have widely been discussed, and from these studies it is clear that the present-day small meandering river channels in many West and Central European catchments are thought to be the indirect result of anthropogenic land use changes. Although this general framework of changes in floodplain geoecology throughout the Holocene is well established, many uncertainties on the exact nature and timing, and the relation to increasing human impact still exist. First, reconstructing human impact during the Holocene is still challenging, and translating pollen data into land cover changes remains complex. Second, it remains unclear whether the floodplain geomorphology and ecology gradually changed, coinciding with the gradually increasing human impact in the catchment (Kalis et al., 2003; Dotterweich, 2008), or that floodplain changes were abrupt and only occurred when a certain threshold in human impact has been reached (e.g. Kalicki, 2008; Lespez et al., 2008; Notebaert et al., 2011b). Such abrupt changes are associated with systems with a short relaxation time (less than a few hundred years) and such systems are typically more sensitive to disturbances. On the other hand, gradual changes are associated with systems with a longer relaxation time (more than a few thousand years) and such systems are less sensitive (e.g. Huggett, 2007). Moreover, a threshold or tipping point that human impact must cross, has not yet been defined. It can thus be questioned how intense human pressure on the land has to be before any observable change in the fluvial system behaviour occurs. Estimating the level of human activities needed to trigger environmental changes, is recently indicated as one of the priority research question in palaeoecology (Seddon et al., 2014). Related to this, the question remains when exactly the observed floodplain changes occurred and if they occurred at the same time throughout a river catchment. If not, and if floodplain changes appear to be non-uniform and asynchronous at catchment scale, the question remains whether this can be attributed to heterogeneity in the timing and nature of the external forcings, or to differences in intrinsic sensitivity towards the same environmental disturbances – which can indicate an additional non-linearity in the process-response relationship. Due to these uncertainties, it is still unknown what exactly the natural state of the floodplains of lowland rivers was in West and Central Europe.

Overall, we lack a detailed reconstruction or model of the impact-response relationships that is needed to fully grasp how, when and to what extent humans have reshaped fluvial systems. It remains unclear which role human impact and land use changes have exactly played in transforming the floodplain. To answer these uncertainties and to fully understand the process-response relationship, geomorphic fieldwork needs to be complemented by an accurate reconstruction of vegetation changes and quantitative measures of human impact in the landscape (e.g. Verstraeten et al., 2009a). These data need to be collected with a high spatial and temporal resolution. Therefore, more robust chronologies of floodplain changes and land cover changes are necessary at several locations within a single catchment (Verstraeten et al., 2009a). A better understanding of human-environment interactions requires a holistic, multi-disciplinary and spatially integrated approach, which combines results from e.g. geomorphological, archaeological and palynological studies and which integrates data from several study sites (e.g. Foulds and Macklin, 2006; Brown, 2008; Verstraeten et al., 2009a). Traditional palaeo-environmental studies, focussing on one or a few study sites, are not sufficient (Figure 1.1). Therefore, in this study, data will be gathered at a catchment scale (Figure 1.1). Catchments in the West and Central European loess belt have a long history of intense anthropogenic land use, and are therefore very useful to study the effect of anthropogenic land use changes on river systems. The Dijle catchment (758 km²), located within the European loess belt can serve as a model for most intermediate scaled lowland rivers in this loess belt (Notebaert and Verstraeten, 2010). Catchments with such as intermediate scale (a few hundred to 2000 km²) are important as they provide a link between small scaled catchments (< 10^2 km²), where local variations are dominant, and large scaled catchments (> 10^4 km²) integrating signals from different regions.

The aim of this thesis is to address the above research gaps, which can be summarized in the following **research questions**:

- When exactly did the transformation of the floodplain geoecology occur? Are the floodplain changes uniform and synchronous at catchment scale (10^2 – 10^3 km²), or can we observe non-linearities in space and/or time ?
- Did floodplain geoecology change gradually or abrupt? Are these changes coinciding with the increase in human impact or can a temporal offset (time lag) be observed?
- Can statistical methods be used to extract quantitative data of human impact based on alluvial pollen records?
- How are human impact and land use changes related to changes in floodplain geoecology?

Overall, the objective of this thesis is to provide a better understanding of the sensitivity of floodplain geoecology to human impact in the landscape, and **to attain a detailed understanding of the timing, nature and extent of human impact on the floodplain geoecology**. Therefore, in this research

- a detailed reconstruction of the changing floodplain geoecology and a precise chronology of these changes is collected;
- a detailed reconstruction of the vegetation changes in the catchment and a (semi–)quantitative measure of human impact based on palynological and statistical analysis is provided;
- a first attempt is presented to link pollen assemblages deposited in floodplains to vegetation abundances; and
- data on floodplain changes and human impact are combined to attain a detailed model of the impact-response relationship.

These data are gathered at the scale of the Dijle catchment (758 km²). Intensive research on sediment dynamics and vegetation changes has been carried out in this catchment (e.g. Mullenders and Gullentops, 1957; Mullenders et al., 1966; Rommens et al., 2006; Notebaert et al., 2009b; Verstraeten et al., 2009b), which provide useful data and a framework to position our own research. The study will mainly focus on the period starting from the beginning of Neolithic agriculture (ca. 7200 cal a BP) until the onset of widespread agriculture in the entire landscape (ca. 1000 cal a BP). It is expected that before this period, human impact in the landscape was almost non-existing whereas afterwards human impact was overwhelming.

1.3 Outline of the thesis

The structure of this thesis is schematically shown in Figure 1.2. The thesis is divided in six chapters. Following this introduction chapter, chapter 2 discusses the changes in floodplain geomorphology and ecology during the Holocene in the Dijle catchment. Several studies have previously provided data on changes in floodplain geomorphology in the Dijle catchment (e.g. De Smedt, 1973; Rommens et al., 2006; Notebaert et al., 2009b; Verstraeten et al., 2009b). However, these studies were performed with different objectives and lack an integrated approach investigating both geomorphological and ecological changes, nor do they provide a good spatial coverage of the entire catchment. In chapter 2, these previously gathered data will be combined with new detailed field-based sediment data, palynological data and radiocarbon ages to provide a more comprehensive overview of the changing floodplain geoecology in the Dijle catchment for the Holocene period.

Chapter 3 discusses the changes in floodplain morphology and sedimentation patterns by means of a detailed chronology. Chronological information on changes in floodplain geomorphology is retrieved from previous studies in the Dijle catchment (Rommens et al., 2006; Notebaert et al., 2011b) and from newly obtained radiocarbon dating results, providing a detailed chronological database. Such a robust chronology of floodplain changes is necessary to identify their relationship to land use changes, and separate the potential driving forces and processes involved (e.g. Verstraeten et al., 2009a).

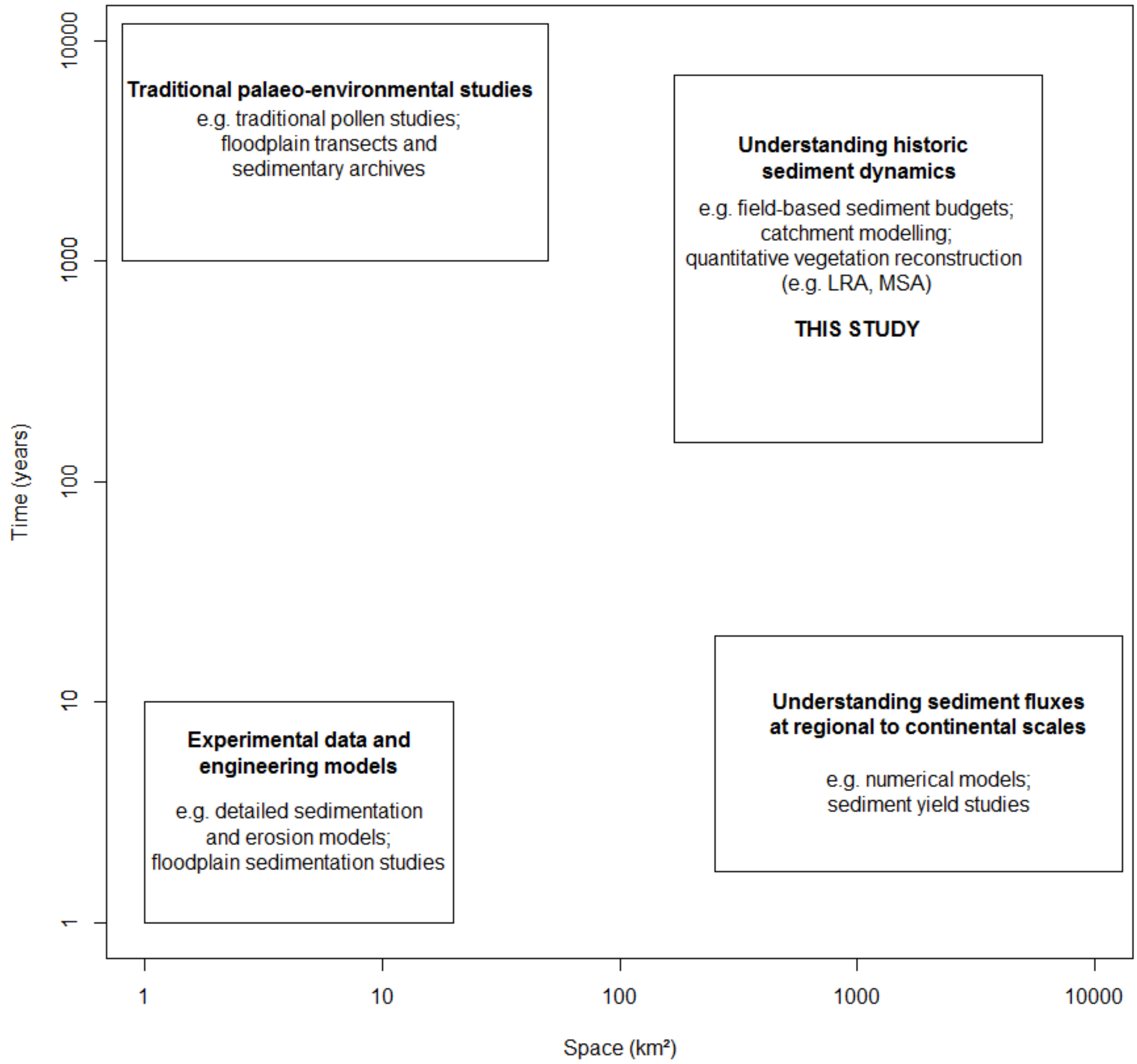

Figure 1.1. Position of this study and the different research fields within geomorphology (with focus on floodplain changes and sediment dynamics) (based on Verstraeten, 2012).

In chapter 4, a reconstruction of vegetation changes in the Dijle catchment throughout the Holocene is presented, based on palynological data. A detailed reconstruction and semi-quantification of human impact in the catchment is extracted from the palynological study based on statistical analysis (non-metric multidimensional scaling (NMDS)) of the pollen records. NMDS is used to compare vegetation changes through time in different subcatchments of the Dijle catchment. In chapter 4, a pilot study is presented as well to link pollen assemblages deposited in floodplains to vegetation abundances in the landscape.

In chapter 5 and 6, the data gathered in the previous chapters are integrated to provide a model of the impact-response relationship that is needed to fully grasp how, when and to what extent humans have changed the floodplain geoecology. The observed floodplain changes in chapter 2 and 3 are evaluated against the available data on human impact – presented in chapter 4. In chapter 5, this is done for the headwaters of the Dijle catchment. In chapter 6, a catchment-wide approach is used to provide more insight in the differences between different subcatchments and therefore it provides a better understanding of the process-response relationships and the sensitivity of floodplain geoecology to human impact. Consequently, chapter 6 integrates the different chapters to come to a general synthesis and general conclusions.

Parts of this thesis have already been published or are under review. Chapter 3 is based on Broothaerts et al. (2014a), chapter 4 on Broothaerts et al. (2014b), chapter 5 on Broothaerts et al. (2013), and chapter 6 on Broothaerts et al. (under review). In citing this research, reference should be made to these publications. Since most of the chapters are based on publications, the chapters are written to stand on their own. Therefore, some overlap between the different chapters is possible and unavoidable, e.g. in the introduction and material and method sections.

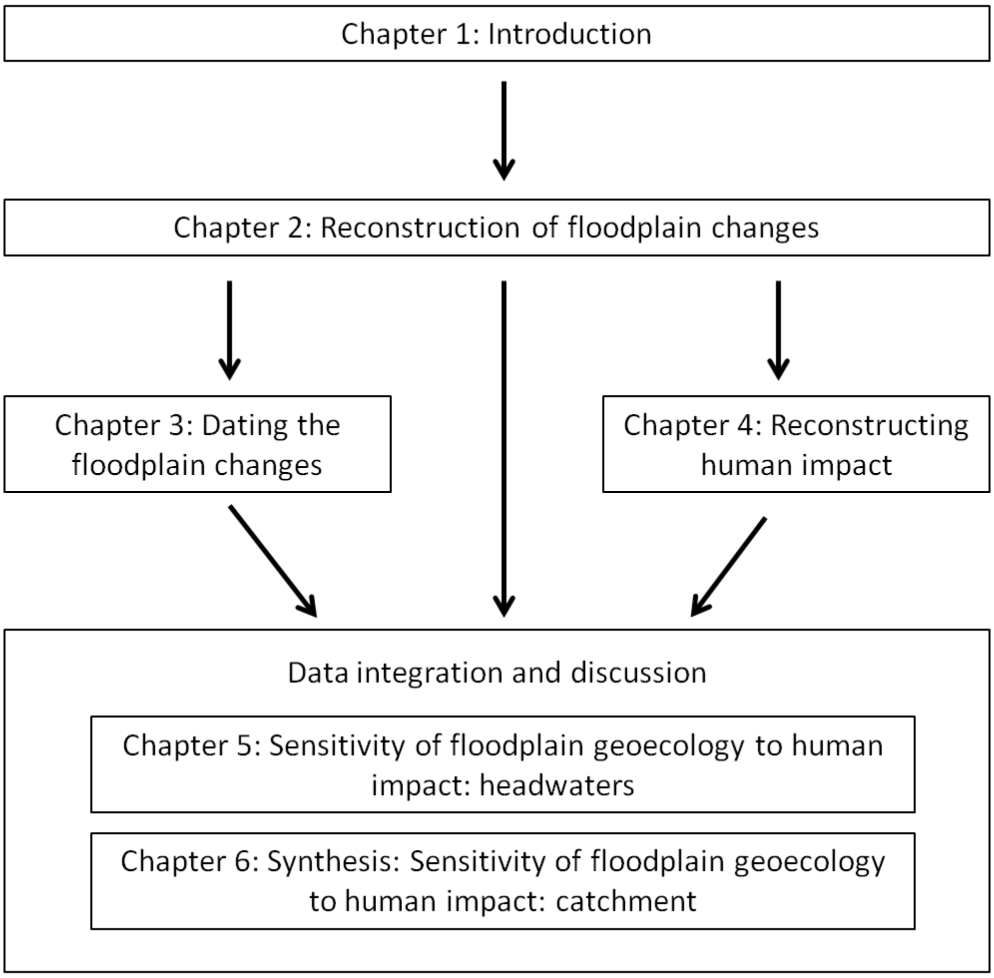

Figure 1.2. General outline of the PhD Thesis.

Chapter 2 Reconstruction of Holocene floodplain changes in the Dijle catchment

2.1 Introduction

Changes in floodplain geomorphology have previously been reconstructed for many catchments in West and Central Europe. These studies have shown that many fluvial systems have undergone important changes in their sediment dynamics and sediment storage during the Holocene (see overview in chapter 1 and Notebaert and Verstraeten 2010). Floodplain vegetation has shown to change during the Holocene period. Floodplain vegetation changed under direct influence of human impact in the floodplain, e.g. with the clearance of the floodplain forest, or due to the increasing sediment input in the river system, which altered the geomorphology and hydrology of the floodplain (Brown, 1988; Brown, 2002).

Also in the Dijle catchment, several studies have provided data on changes in floodplain geomorphology (e.g. De Smedt, 1973; Rommens et al., 2006; Notebaert et al., 2009b; Verstraeten et al., 2009b). However, these studies were done with different objectives and lack e.g. a combined approach investigating both geomorphological and ecological changes, a reliable chronostratigraphical framework, a detailed core-based lithogenic classification, or a good spatial coverage of the entire catchment. Consequently, several questions remained unanswered. It remains a question how the floodplain geomorphology and ecology exactly changed and whether these changes were similar and simultaneous within one catchment. Moreover, it remains unclear whether the floodplain geoecology gradually changed or that these changes were abrupt and only occurring when a certain threshold in external forcing has been reached. To answer these uncertainties, a detailed reconstruction of the floodplain geoecology is necessary, both on a spatial and temporal scale.

In this chapter, we aim to provide such a detailed reconstruction of the changing floodplain geoecology during the Holocene for the Dijle catchment, with a high temporal and spatial resolution. For this purpose, the data gathered in previous studies were combined with new detailed data to provide a more comprehensive understanding of the changing floodplain geoecology in the catchment. Based on detailed field-based sediment coring, different lithostratigraphical units were identified, the fluvial architecture of the Dijle River was described and the floodplain geomorphology reconstructed. For reconstructing the floodplain vegetation, palynological data were used. Information on the timing of the floodplain changes is facilitated by radiocarbon dates of crucial lithological and palynological transitions. First, we present a general overview of the Dijle catchment, the main study area of this thesis, and a general description of the different study sites.

2.2 Study area

2.2.1 Introduction

In this study we will mainly focus on the Dijle catchment upstream of Leuven (758 km²), which is part of the Scheldt catchment (ca. 20 000 km²). The Dijle catchment is located in the Central Belgian loess belt, and has a long history of intense anthropogenic land use. Intensive research on land use changes, vegetation changes and sediment dynamics has been carried out in this catchment (e.g. Mullenders and Gullentops, 1957; Mullenders et al., 1966; De Smedt, 1973; Geurts, 1976; Vanwalleghem et al., 2003; Rommens et al., 2006; Rommens et al., 2007; Notebaert et al., 2009b; Verstraeten et al., 2009b; Notebaert et al., 2011b; Van Oost et al., 2012; De Brue and Verstraeten, 2014). These previous studies provide useful data and a framework for positioning our own results. But, as stated above in section 2.1, they do also raise a lot of questions, and indicate gaps in our knowledge regarding human impact on the landscape. Therefore, the Dijle catchment upstream of Leuven is selected as the main study area within this research.

The geology of the Dijle catchment upstream of Leuven mainly consists of Paleogene sands and clays covered by Pleistocene loess. Locally, where loess has been eroded, sandy outcrops occur. In the incised river valleys in the southern part of the catchment, Palaeozoic basement rocks crop out. Soils in the catchment are mainly Luvisols and Albeluvisols (European Soil database; European Union, http://eusoils.jrc.ec.europa.eu) developed in the loess deposits. Locally, Podzols, Cambisols and Regosols can be found, developed in outcrops of sandy and clayey Paleogene deposits. In the valleys Fluvisols can be found. The topography of the Dijle catchment consists of an undulating plateau in which several rivers are incised. Height in the Dijle catchment varies between 180 m a.s.l. in the south of the catchment and 25 m a.s.l. near the outlet of the studied catchment. Slope gradients are usually less than 5%, although along the valley axis maximum slope angles of 50% can be found (Figure 2.3). The Dijle River has a length of 43 km in the catchment upstream of Leuven. Important tributaries are the Thyle and the Orne, joining the Dijle River near Court-St-Etienne. More downstream other tributaries join the Dijle River: Train, Laan, Nethen and IJse (Figure 2.1). Floodplain width in the headwaters of the Dijle catchment does not exceed 150 m, whereas floodplains in the downstream part of the catchment, near Leuven, are 1000 to 1500 m wide. Floodplain slope gradients in the main valley range between 0.1 and 0.2%. In the headwaters, the maximum floodplain slope gradient is 1.5%, and even 2.5% for the Orne River. Base discharge near Leuven is around 4 $m^3 s^{-1}$, peak discharge reaches 25 $m^3 s^{-1}$.

In addition to the Dijle catchment upstream of Leuven, an explorative study was done downstream of Leuven. Our study site is located near Rotselaar (Figure 2.2), situated at the transition of the loess deposits (Middle Belgium) and the sandy deposits (Lower Belgium) (Figure 2.3). In this part of the Dijle catchment, i.e. the Dijle-Demer confluence area, previous research was done by De Smedt (1973) and Vandenberghe and De Smedt (1979), investigating the Late Glacial and Holocene changes in river activity and vegetation. Here, the fluvial landscape is dominated by palaeo-meanders (Figure 2.6). De Smedt (1973) and Vandenberghe and De Smedt (1979) hypothesised that these meanders were active during the Younger Dryas and became abandoned from the Preboreal Period onward and were built up by peat (Boreal and Atlantic Period) and clayey to sandy loams (Atlantic to Subatlantic Period). However, these studies lack a good chronostratigraphical framework and raise new questions on the role human impact played in changing the floodplain geoecology (chapter 1).

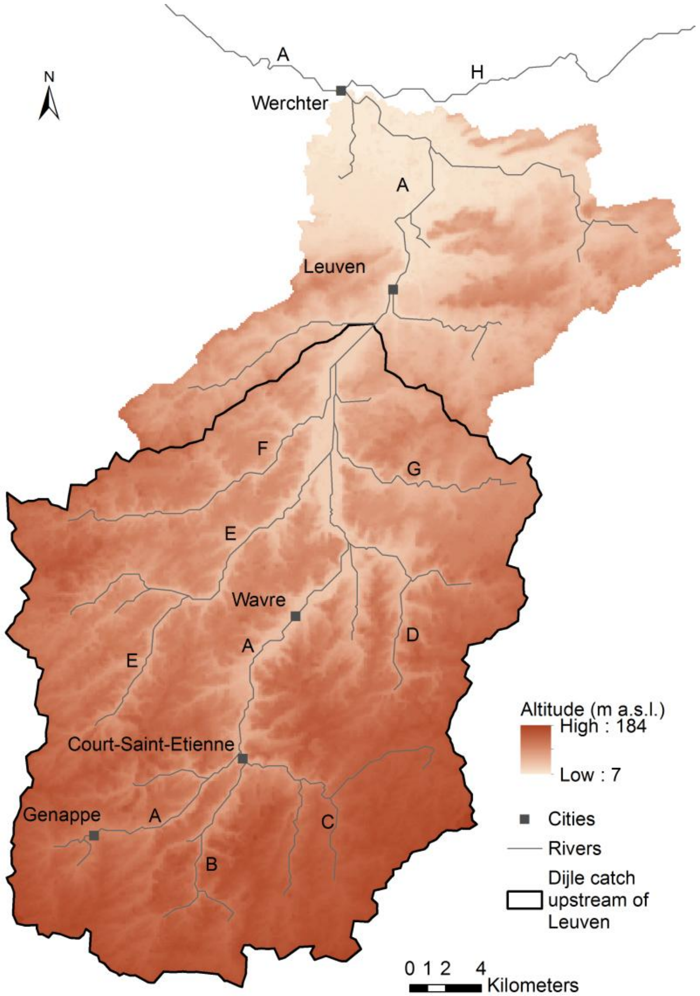

Figure 2.1. Overview of the Dijle catchment upstream of the Dijle-Demer confluence (1040 km²), with indication of the Dijle catchment upstream of Leuven (758 km²). A) Dijle River; B) Thyle River; C) Orne River; D) Train River; E) Laan River; F) Ijse River; G) Nethen River; H) Demer River.

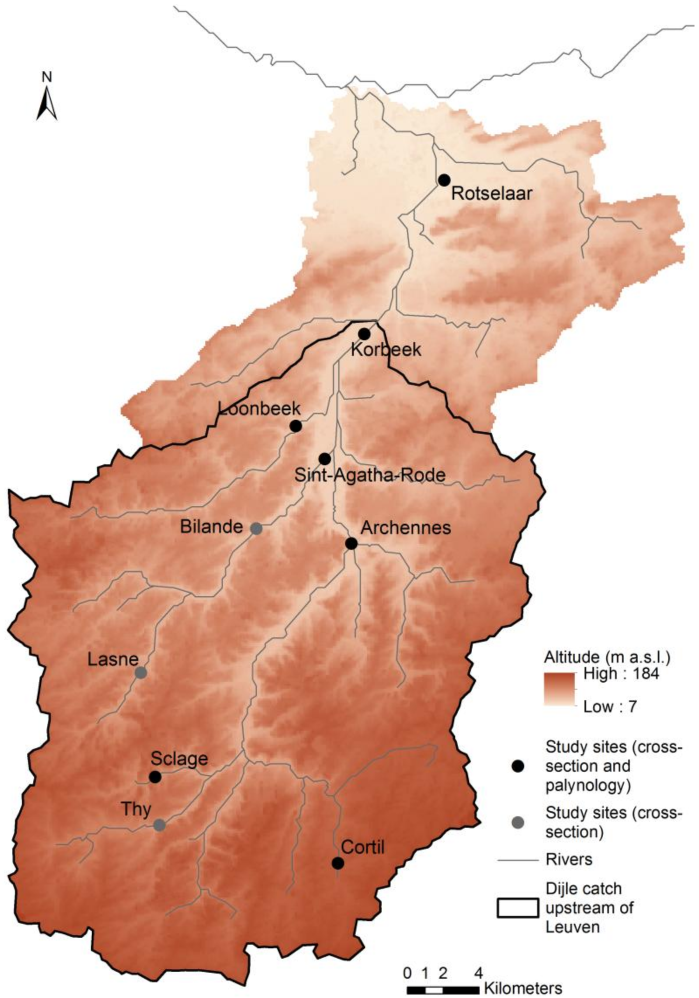

Figure 2.2. Location of the study sites in the Dijle catchment upstream of the Dijle-Demer confluence (1040 km²), with indication of the Dijle catchment upstream of Leuven (758 km²).

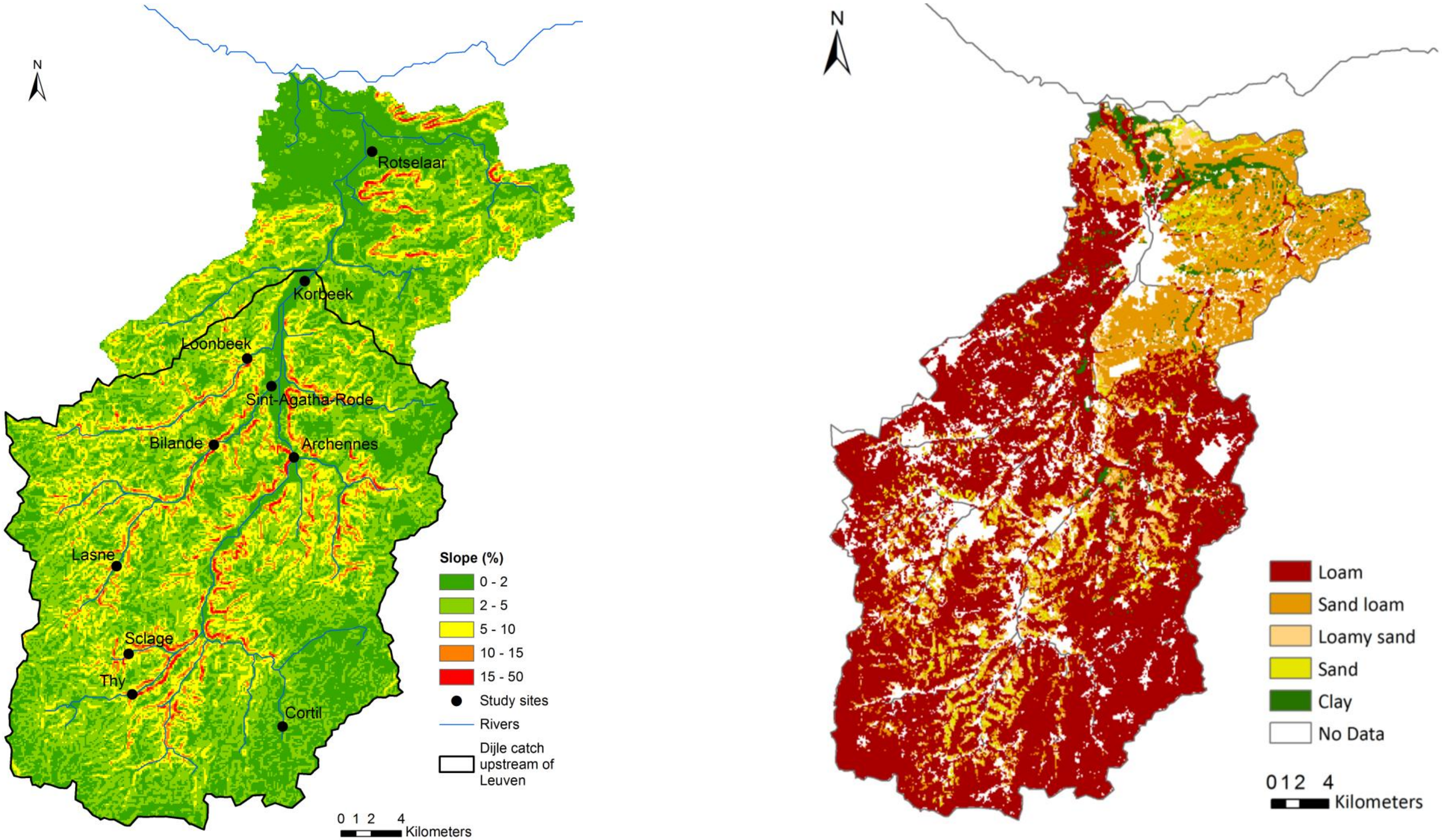

Figure 2.3. (Left) Slope map of the Dijle catchment upstream of the Dijle-Demer confluence (1040 km²), with indication of the Dijle catchment upstream of Leuven (758 km²) and the location of the study sites. (Right) Soil texture map of the Dijle catchment upstream of the Dijle-Demer confluence, according to the Belgian soil classification system.

2.2.2 Previous research on land cover history in the Dijle catchment

Previous palynological studies in the Dijle catchment show that the catchment was mainly forested during the first half of the Holocene (Mullenders and Gullentops, 1957; Mullenders et al., 1966; De Smedt, 1973). The Neolithic Linearbandkeramik culture arrived in the Belgian loess belt around 7200 cal a BP, however, no indications of the presence of this culture in the Dijle catchment are present (Vanmontfort, 2007). The Neolithic Period in the Belgian loess belt lasted from ca. 7200 to 3900 cal a BP (Table 2.1) (CAI, 2014). The oldest known Neolithic settlement in the Dijle catchment ('Ottenburg site') dates from ca. 6200 cal a BP (Crombé and Vanmontfort, 2007; Vanmontfort, 2007). The Bronze Age in the Belgian loess belt lasted from ca. 3900 to 2700 cal a BP, the Iron Age from ca. 2700 to 2050 cal a BP (Table 2.1) (CAI, 2014). Mullenders and Gullentops (1957) and Mullenders et al. (1966) proposed that anthropogenic disturbances in the landscape became evident in the pollen assemblages from 2500 cal a BP, but these palynological data had a poor chronological control. Archaeological data for the Dijle catchment is fragmentary. For the Flemish part of the catchment, an extensive database is available (Centrale Archeologische Inventaris (CAI, 2014)). For the Walloon part, such a detailed database is still missing. Consequently, the archaeological data for the Walloon part is limited to overviews provided by Rommens (2006) and Notebaert (2009), which are not as detailed as the extensive database available for Flanders. Moreover, the overview of Rommens (2006) is restricted to the Nethen subcatchment.

Current land use in the Dijle catchment is dominated by cropland, except for some large deciduous forests in the northeast (Meerdaal Forest) and northwest (Zonien Forest) of the catchment. Historical documents indicate that these areas have remained forested for several centuries, the Meerdaal Forest since the 14^{th} century (Vanwalleghem et al., 2005), and Zonien Forest even since the 12^{th} century (Langohr, 2001). No agricultural activities took place in these forests since the 14^{th} century, as it was protected by the Dukes of Brabant (Langohr, 2001). In the Meerdaal Forest, man-made closed depressions and gullies dated to the Bronze Age and Roman Period have been preserved, indicating that this forest was not prone to severe erosion for the last centuries (e.g. Vanwalleghem et al., 2006).

Table 2.1. Archaeological periods in the Belgian loess belt. Based on CAI (2014) and Buntgen et al. (2011).

Archeological period	**start date (cal a BP)**	**end date (cal a BP)**
Paleolithic Period		11500
Mesolitic Period	11500	7200
Neolithic Period	7200	3900
Bronze Age	3900	2700
Iron Age	2700	2050
Roman Period	2050	1750
Migration Period	1750	1600
Medieval to Modern Period	1600	0

2.2.3 Location of the study sites

Core-based floodplain transects in the Dijle catchment are available from Mullenders and Gullentops (1957), Mullenders et al. (1966), De Smedt (1973), Rommens et al. (2006) and Notebaert (2009). Additional sites were selected for our study, since some of the floodplain transects from previous research lack a good chronological control or an adequate detail. Nevertheless, they provide useful data on floodplain changes in the Dijle catchment.

In this research, ten study sites were selected in the Dijle catchment: nine in the Dijle catchment upstream of Leuven and one in the Dijle catchment downstream of Leuven (Figure 2.2 and Table 2.2). These study sites were selected based on the availability of previous research and their accessibility, but mainly on their location in the catchment. We tried to achieve a good spatial coverage across the whole Dijle catchment. Six out of the nine study sites upstream of Leuven were selected for palynological analysis (Figure 2.2). Two of them (Sclage and Cortil) are located in the headwaters of the catchment. Two study sites (Archennes and Korbeek) are located in the main valley of the Dijle River, and two study sites (Sint-Agatha-Rode and Loonbeek) are located along important tributaries of the Dijle River in the northern part of the catchment (Table 2.2). By selecting these study sites, we were able to study differences between different subcatchments, differences between the tributaries and the main valley, and the importance of scale effects since they all have different catchment areas (Table 2.2). Such a selection of study areas is necessary to answer our research questions posed in chapter 1.

The locations of the different study sites are indicated in detail on the topographic map (Figures 2.4, 2.5 and 2.6). Hillshade maps of the valley were calculated based on hydrological corrected LiDAR data (light detection and ranging), with a resolution of 5m. Previous research has demonstrated the added value of LiDAR data for interpretative geomorphological mapping of floodplains (e.g. Jones et al., 2007; Notebaert et al., 2009a). LiDAR data are available for the whole of Flanders, but in the Walloon region LiDAR data are only available for the floodplains of the larger rivers. So a hillshade map is only shown for study sites with a wide floodplain (Figures 2.5 and 2.6).

Palynological and geomorphological data of Cortil and Sint-Agatha-Rode are partly based on Assendelft (2012), data of Loonbeek are partly based on Buijs (2013), data of Lasne and Archennes are partly based on Van Schilt (2013), and data of Rotselaar are partly based on Qian (2013).

Table 2.2. Properties of the different study sites

Study site	River	catchment area (km²)	floodplain width (m)	floodplain transect	palynological analysis	Location (Lat Lon)
Sclage	Cala	13	90	x	x	50°35'00" N 4°38'15" E
Cortil	Orne	13	70	x	x	50°34'55" N 4°38'20" E
Lasne	Laan	25	140	x		50°41'15"N 4°29'15"E
Thy	Dijle	40	180	x		50°36'30" N 4°29'30" E
Loonbeek	Ijse	65	130	x	x	50°48'45" N 4°36'50" E
Bilande	Laan	130	250	x		50°45'40" N 4°35'40" E
St-Agatha-Rode	Laan	190	350	x	x	50°47'20" N 4°37'40" E
Archennes	Dijle	360	400	x	x	50°45'10" N 4°39'30" E
Korbeek	Dijle	750	1050	x	x	50°51'00" N 4°39'30" E
Rotselaar	Dijle	1040	-	x	x	50°56'17" N 4°43'20" E

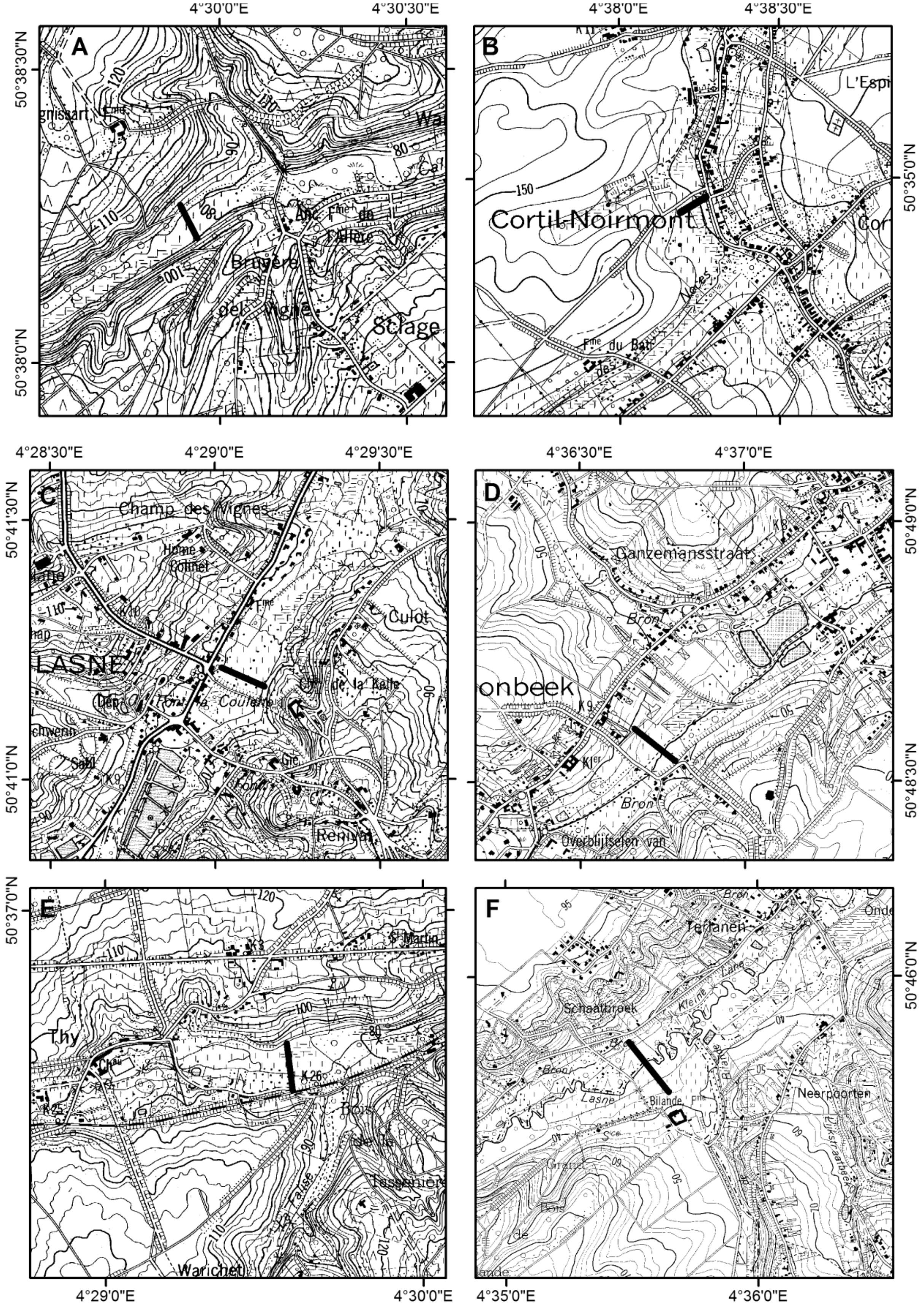

Figure 2.4. Location of the coring transects, indicated by the black lines. (A) Sclage, (B) Cortil, (C) Lasne, (D) Loonbeek, (E) Thy, (F) Bilande.

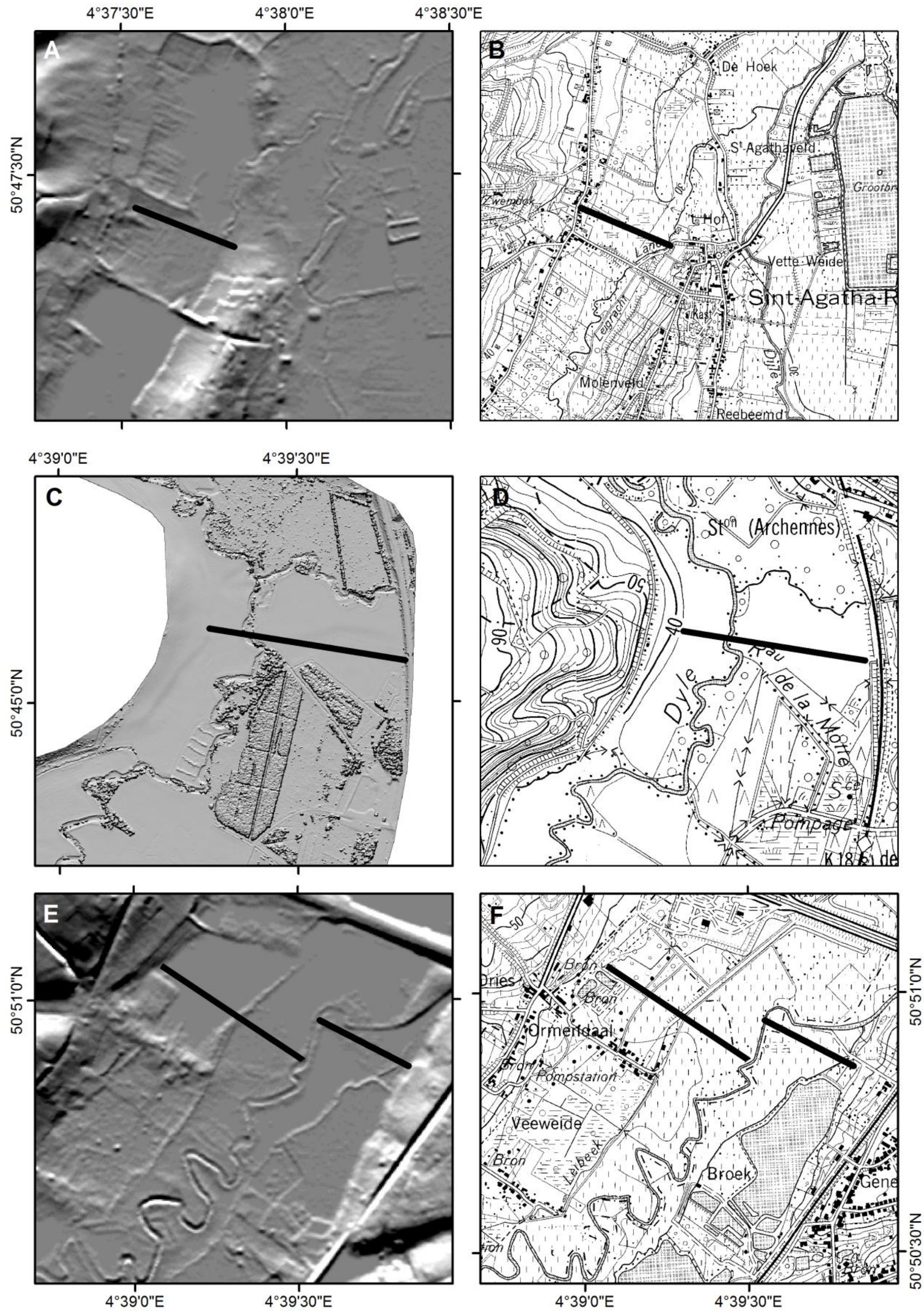

Figure 2.5. Location of the coring transects (black lines). Indicated on hillshade maps with hillshade azimuth at 0° based on hydrological corrected LiDAR data (left) and indicated on the topographic map (right). (A and B) Sint-Agatha-Rode, (C and D) Archennes, and (E and F) Korbeek.

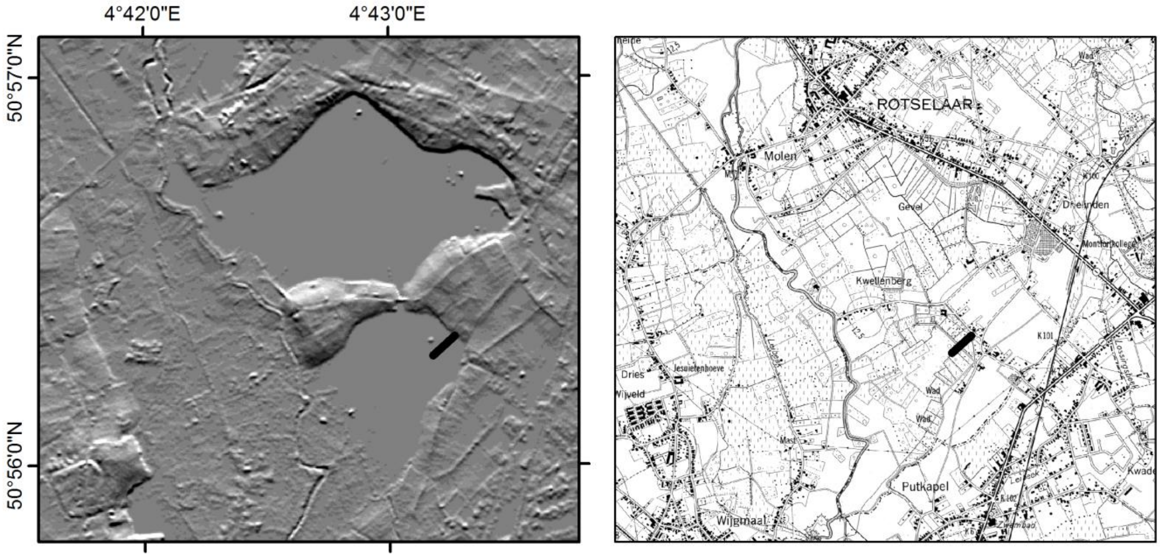

Figure 2.6. Location of the coring transect (black line) at Rotselaar. Indicated on hillshade maps with hillshade azimuth at 0° based on hydrological corrected LiDAR data (left) and indicated on the topographic map (right).

2.3 Material and Methods

2.3.1 Coring and sediment analysis

Alluvial architecture and floodplain evolution of the Dijle catchment was reconstructed based on coring data, along transects across the floodplain, one at each study site (Figure 2.2). For each coring a lithological field description was made with a vertical resolution of 5 cm. The field descriptions contained texture and sorting determined by palpation, colour description, description of soil horizons, and determining of inclusions (such as plant material, gravel and artefacts). A gouge auger was used for the corings. In order to understand the complete architecture of the floodplain, corings should be spaced at a distance smaller than the width of the smallest architectural element, which is often the river channel in European river systems (e.g. Houben, 2007). This can however be very time-demanding. In this study, the coring density is around one coring each 20 m, which is larger than the width of the smallest architectural element. Consequently, at some places small fluvial architectural elements could be missed, however such a detailed reconstruction of the fluvial architecture is beyond the scope of this research. For some study sites, thermogravimetric analysis (loss of ignition, LOI) was performed to determine organic matter (OM) and carbonate content, to describe and characterize the different lithostratigraphical units. Grain-size analyses were performed on selected depth ranges using laser diffraction particle size analyzers (Coulter LS 13 320 and Helos KR Laser Particle Sizer), to further describe the different units. Based on the detailed field descriptions, grain-size analysis and thermogravimetric analysis, the sediments were grouped in different lithostratigraphical units representing different depositional environments, similar to the study of Notebaert et al. (2011a).

To compare the sediment texture of the palaeo-floodplain deposits with the sediment texture of modern floodplain deposits at different depositional environments, a CM diagram was used at one study site (Korbeek). A CM diagram (Passega, 1957) is constructed by plotting the 99% or 95%

percentile (C, coarsest fraction) on the Y-axis and the median grain size on the X-axis (M, median fraction), using log-log scales. It has previously been used in several studies (e.g. Passega, 1957; Bravard and Peiry, 1999; Notebaert et al., 2011a; Houbrechts et al., 2013). Sediment texture of modern floodplain deposits are based on data from Broothaerts (2008) and Notebaert et al. (2011a). T-tests were used to test the statistical differences between the different lithostratigraphical units.

2.3.2 Palynological analysis

For seven study sites, one sediment core was collected for pollen analysis (Appendix 2). Since the focus of this research is on the lithological transition in floodplain deposition from organic to clastic deposits, the location of these pollen profiles was chosen based on a good preservation of this transition (e.g. no indications of erosion of the peat). For the same reason a specific depth range was selected around this transition on which pollen analyses and additional lab analysis were performed: for Sclage between 285 and 415 cm, for Cortil between 215 and 370 cm, for Korbeek between 170 and 275 cm, for Archennes between 260 and 540 cm, Loonbeek between 70 and 410 cm, for Sint-Agatha-Rode between 220 and 440 cm, and for Rotselaar between 150 and 325 cm (Appendix 2). Pollen samples were extracted from the sediment using a sampler of defined volume (100 mm^3 for organic rich sediments, 200 mm^3 for minerogenic sediments), and were prepared following the standard techniques of Faegri and Iversen (1989). A know quantity of *Lycopodium* spores was added, to allow the calculation of charcoal accumulation rates (CHAR) and pollen accumulation rates (PAR). Samples were studied under a 630x and 1000x magnification using oil immersion. Moore et al. (1991), Beug (2004) and a modern reference collection were used for the identification of the pollen types. Non-pollen palynomorphs were identified by using Van Geel (1978). A total of at least 500 pollen grains were counted for each pollen slide. Pollen data are expressed as relative frequencies (percentages) of the pollen sum. Since the focus in this chapter is on the local vegetation, the pollen sum only contains the local pollen, i.e. wetland vegetation (e.g. *Alnus*, *Salix*, Cyperaceae and Typhaceae). Percentage diagrams were constructed using *C2* computer program (Juggins, 2007). Regional vegetation changes will be discussed in chapter 4. Raw pollen data are added in Appendix 3.

2.3.3 Cluster analysis

To provide more objective insight in the local pollen signal of the study sites and to divide the local pollen signal in different zones, a hierarchical cluster analysis was applied on the local pollen signal of each study site separately. Cluster analysis is a method for combining similar objects into groups of clusters; pollen samples that contain a similar pollen signal will be grouped together (e.g. Hammer and Harper, 2006; Birks et al., 2012). The used clustering method is ‘average linkage clustering’, where the distance between two clusters is defined as the average of all possible distances between members of the two clusters (e.g. McCune and Grace, 2002; Hammer and Harper, 2006). The distance between two clusters was defined as the Euclidean distance.

2.3.4 Radiocarbon dating and floodplain accumulation rates

AMS radiocarbon dating results (appendix 1) were used to provide a chronostratigraphical framework for the pollen assemblages and the floodplain changes. Each sample was sieved at 250 µm and datable material was handpicked. Terrestrial plant and wood remains were selected to avoid hard-water effects, reservoir effect or incorporation of older organic material (e.g. Törnqvist et al., 1992). Ages were calibrated using the IntCal13 calibration curve (Reimer et al., 2013) and *Oxcal 4.2* software (Ramsey, 2009). An age-depth model was established for each study site using the *clam.R* package version 2.2 (Blaauw, 2010), based on the obtained ages from the sediment core of each study site (Appendix 1). The age-depth models were established using linear interpolation between the dated levels. This age-depth model was then used to derive a timescale for the whole pollen sequence for each study site. Dating results were used to calculate floodplain accumulation rates (mm a^{-1}).

Such simple age-depth curves can be used to provide more insights in the temporal changes in floodplain deposition rates. However, these age-depth curves have some disadvantages. First, age-depth curves represent floodplain accumulation rates, including clastic sedimentation as well as organic accumulation (e.g. peaty deposits). So in order to study the evolution of accumulated floodplain sediment mass resulting from soil erosion and incision processes, the autochthonous organic matter fraction needs to be excluded. Therefore, to calculate the accumulated sediment mass, the thickness of each sediment layer was multiplied with the average mineral sediment bulk density of that layer ($DBD_{MS,layer}$). This value was calculated for each sediment layer following Verstraeten and Poesen (2001):

$$DBD_{MS,layer} = (1 - OM\%)\,\frac{DBD_{MS}\left(\frac{100}{100-OM\%}\right)}{\left(1+\frac{DBD_{MS}\;OM\%}{DBD_{OM}\;(100-OM\%)}\right)} \qquad \text{equation (2.1)}$$

with OM% the percentage organic matter, DBD_{MS} the dry bulk density of mineral sediment and DBD_{OM} the dry bulk density of organic matter. The percentage organic matter (OM%) of the peat units in the Dijle floodplain were calculated in Van Oost et al. (2012) and in this study. Values range between 40 and 60 %. For DBD_{MS} a value of 1.35 g cm^{-3} for silt loam was taken (van Asselen et al., 2010), which is the mean sediment texture in the Dijle floodplain. Values for DBD_{OM} highly depend on the degree of compaction. Most of the peat units in the Dijle floodplain are overlain by 2-3 meter thick mineral sediment. Based on the pressure that is applied to the peat by a 2-3 m thick sediment unit, the mean peat compaction was estimated at 50%, whereby values ranged between 40 and 60% (following Van Asselen, 2011). As a result, the values for DBD_{OM} are estimated to range between 0.37 and 0.56 g cm^{-3}, with a mean value of 0.45 g cm^{-3}. Secondly, to be able to compare accumulated sediment mass for different study sites, relative accumulated sediment mass needs to be calculated. This can be defined as the fraction of sediment mass per unit floodplain area deposited after the moment of sample deposition divided by the total Holocene sediment accumulation for the considered coring (cf. Notebaert et al., 2011b). The relative accumulated sediment mass was calculated according to the formulas of Notebaert et al. (2011b) and was plotted versus age for the different dated corings, allowing a comparison over different study sites. Such curves can be calculated based on the data of De Smedt (one study site) and Notebaert (five study sites). In this study, data of six additional study sites are available.

2.4 Results

2.4.1 Floodplain architecture

In this section, a synthesis of all available cross-section is presented. For the detailed results of each individual cross-section, we refer to Appendix 2. Figure 2.7 shows the typical grain-size distribution for several units. Based on all the available floodplain transects, the data on texture (Figures 2.7 and 2.12), organic matter (OM) and carbonate content (Figure 2.12) and other sedimentological properties, different lithostratigrahical units were identified (Table 2.3) following Notebaert et al. (2011a).

Unit 1A can be found at each floodplain transect (Appendix 2) at the base of the floodplain deposits. The unit mainly consists of compact silty to loamy sediments (Figure 2.7), with low OM content (< 10%). In the floodplain transect at Lasne (Appendix 2i), a layer with higher organic content can be observed within this unit. At most floodplain transects (Appendix 2) the top of this layer is not horizontal, and shows the presence of shallow channel remains. On the higher parts (at the edges of the floodplain) a weakly developed A-horizon can be found at the top of unit 1A, indicated by accumulation of organic material and the decalcification of the sediments. On the lower parts (mainly in the centre of the floodplain) this A-horizon is less developed and sediments are not decalcified. Unit 1A is interpreted as Weichselian Late Glacial river deposits or as in situ loess deposits, following Notebaert et al. (2011a). At some places in the Dijle catchment, loamy sands to coarse sand deposits can be found (Notebaert, 2009). This is indicated as unit 1B. The top of this layer is not horizontal with indications of shallow channels. A single OSL (optical stimulated luminescence) age is available from this unit: 26000 ± 4000 BP (2σ uncertainty; Notebaert et al. 2011b). Unit 1B is interpreted as Weichselian Late Glacial river deposits.

Unit 2 can be found in floodplain transects Cortil (Appendix 2A), Sclage (Appendix 2B) and Thy (Appendix 2H). It consists of gyttja and contains high amount of organic matter (LOI values above 40%). Small freshwater shells are often observed in this unit. Gyttja deposits are interpreted to be deposited in open stagnant water such as small floodplain ponds or shallow floodplain lakes (see e.g. Van Geel et al., 1983; Hoek et al., 1999). Unit 2 is not present across the whole valley, but interfingers laterally with unit 3.

Unit 3 is a peat layer and can be found in all floodplain transects except for transect Thy (Appendix 2). OM is high (LOI values above 40%). The mineral component of the peat layer has a texture of silty clay loam (Figure 2.7). The unit is between 0.5 and 3 m thick. The type of the peat differs in the Dijle catchment. At Sclage (Appendix 2B) and Sint-Agatha-Rode (Appendix 2C), mainly wood peat has been found, characterized by large amount of unidentified wood remains. In the wide floodplains in the downstream part of the catchment, at Korbeek (Appendix 2D) and Archennes (Appendix 2E), the peat layer mainly consists of reed peat. At Cortil, Loonbeek, Bilande and Lasne (Appendix 2A, F, G and I respectively), the peat type is variable, both reed peat and wood peat were found. The formation of this unit 3 is related to a marshy environment with limited sediment discharge and deposition, resulting in peat accumulation.

Unit 4 can be found in floodplain transect Loonbeek (Appendix 2F) and Thy (Appendix 2H) and was previously identified in the Nethen valley (Rommens et al., 2006). Unit 4 are calcium carbonate rich deposits. This layer varies between calcareous gyttja deposits and deposits of calcium carbonate nodules. At some places, this layer contains high amount of organic material. In the Train River (tributary of the Dijle River; Figure 2.1) this layer was previously identified as travertine by Geurts (1976).

Unit 5 is found in all floodplain transects (Appendix 2). This unit has a texture of silty clay loam or silt loam (Figure 2.7), is very homogenous and there are no sedimentary structures visible in the sediments. OM content is low (LOI values < 10%), only in a few places identifiable organic material, except for roots, were found within this unit. Based on these characteristics, unit 5 is mainly interpreted as formed by vertical accretion of overbank deposits. The thickness varies between 0.5 m in Bilande (Appendix 2G) and 6 m in Archennes (Appendix 2E). Unit 5 overlays unit 2, 3 and 4, and is present across almost the whole floodplain (Appendix 2). The transition from unit 2, 3 and 4 towards unit 5 is abrupt but not erosive in most corings, indicated by the absence of a sandy layer on top of the peat layer and the absence of abrupt variations in grain-size. At some places the overbank deposits have higher OM content (LOI values of ca 15%). This organic silty layer is indicated as unit 5A. Grain-size distributions of unit 5 and unit 5A are similar (Figure 2.7).

Unit 6A consists of alternations of strong organic silty to clayey deposits and fine sandy layers. It is only found in transect Cortil (Appendix 2A), within the peaty deposits (unit 3). This unit is interpreted as low-energetic multichannel deposits. On the other hand unit 6B is distinguished, containing sandy loam and fine sand deposits without intermediate finer layers. In some cross-sections, a textural fining up can be observed (Notebaert et al., 2011a). This unit often contains small wood fragments. At some places in floodplain transect Sint-Agatha-Rode (Appendix 2C) and Korbeek (Appendix 2D), unit 6B forms a depression in unit 3. In that case, the transition to the underlying unit is sharp, indicating erosion of the peat unit. This is probably also the case in Loonbeek (Appendix 2F) and Bilande (Appendix 2G). According to its position and texture, unit 6B is interpreted as river channel and point bar deposits. Unit 6B is mostly confined to a part of the floodplain, except for Korbeek (Appendix 2D), where the river channel crosses the floodplain transect several times.

Unit 7 consists of heterogeneous and alternating silty clay loam to sandy deposits, and often containing brick fragments and charcoal. Unit 7 is positioned at the edges of the floodplain, and connects to colluvial fans. The thickness increases towards the valley sides. It can be found at Cortil (Appendix 2A), Sint-Agatha-Rode (Appendix 2C), Loonbeek (Appendix 2F), Archennes (Appendix 2E), Thy (Appendix 2H) and Lasne (Appendix 2I). Because of its position and its characteristics, it is interpreted as colluvial deposits. Locally, these colluvial deposits are intercalated with the overbank deposits (unit 5).

Overall the Holocene lithostratigraphical units can be summarised in 2 large groups of units which can be found in all floodplain cross-sections in the Dijle catchment south of Leuven. A first group includes unit 2, 3 and 4 and forms a large complex of organic and/or calcium carbonate rich deposits. The thickness of this first group varies but most often it is 1 to 3 m thick. This first group of units is overlain by the second group of mainly clastic deposits (unit 5, 5A, 6 and 7). Beside some local variations, these two groups of lithostratigraphical units are present in all study sites in the Dijle catchment (see also Rommens et al., 2006; Notebaert, 2009).

Similar patterns in Holocene floodplain deposition can be found in the Dijle catchment downstream of Leuven (e.g. De Smedt, 1973). In our study, one transect was made in this part of the Dijle catchment, i.e. near Rotselaar (Figure 2.2 and Appendix 2J). At the base of this floodplain transect sandy deposits can be found (unit 1B). The texture varies between loamy sand and coarse sand, without organic material. The top of this layer is not horizontal, but with the shape of a river channel. These deposits are interpreted as channel bed deposits. Pollen present in the top 5 cm of this sandy layer were dated at 11588 ± 123 cal a BP, indicating that these river bed deposits were deposited during the Younger Dryas. The sandy deposits are overlain by loamy sediments (unit 1A), which can be interpreted as the infilling of the abandoned river channel. The top of this loamy layer has been dated at 10504 ± 82 cal a BP. Consequently, abandoned channel accumulation rate was ca. 1 mm a^{-1} on average during this infilling phase. On top of the loamy sediments, a peat layer was found (unit 3). Peat composition is variable, both reed peat and wood peat were found. The middle of this peat layer has been dated at 9988 ± 27 cal a BP. De Smedt (1973) interpreted this peaty unit to be deposited in a marshy environment, with diffuse water transport. In the western part of the transect, the peaty layer grades into organic overbank deposits (unit 5A). Unit 3 and unit 5A are overlain by a mixture of fluvial overbank deposits and colluvial deposits (unit 7). Radiocarbon dating results and pollen data (see below: Figure 2.9 and 2.12) indicate that the main floodplain changes occurred in the Late Glacial and Early Holocene Period. At this stage, human influence on the floodplain changes is not really expected, and the Late Glacial – Early Holocene period is out of the scope of this research. Therefore, the study site Rotselaar will not be included in the analysis in the next chapters, but will only briefly be discussed in this chapter.

Table 2.3. Lithostratigrahical units identified in the Dijle catchment. Similar units were found by Notebaert et al. (2011a).

Unit	Texture	Position	Interpreted depositional environment	Age
1A	Compact silty to loamy sediments	Base of the floodplain deposits	River channel and overbank, and loess deposits	Pre-Holocene
1B	Loamy sands to coarse sands	Base of the floodplain deposits	River channel	Pre-Holocene
2	Gyttja deposits	Above unit 1, covered by unit 3 or 5	Shallow lake	From early Holocene to ca. 2500 cal a BP, depending on location
3	Peat	Above unit 1 and 2, covered by unit 5	Marshy floodplain	From early Holocene to ca. 500 cal a BP, depending on location
4	Calcium carbonate rich deposits, often organic	Above unit 2 or included in unit 5	Calcium carbonate rich shallow lake	Holocene, depending on location
5	Silty clay loam to loam	Upper part of floodplain	Overbank	From ca. 2500 cal a BP, depending on location
5A	organic silty clay loam to silt loam	Above unit 2 and 3, covered by or included in unit 5	Organic overbank	From ca. 2500 to 600 cal a BP, depending on location
6A	Alterations of organic silty clay loam and fine sand deposits	Included in unit 2 and 3	Low energetic channels	From early Holocene to ca. 500 cal a BP, depending on location
6B	Sandy loam and sands	Above or included in unit 2, 3 and 5	River channel and point bar	After ca. 2500 cal a BP, depending on location
7	Alternating silty clay loam to sand deposits, arranged in layers	Valley margins at location of colluvial fans	Alternation of colluvium and overbank	After ca. 2500 cal a BP

2.4.2 Grain-size analysis

Results of the grain size analysis for sediment cores in 6 study sites are shown in Figures 2.7 and 2.12. The median grain-size varies between 10-50 µm (Figure 2.12), which is comparable with the median grain-size of modern overbank deposits in the Dijle catchment (Broothaerts, 2008; Notebaert et al., 2011a). At some study sites (e.g. in Sint-Agatha-Rode (Figure 2.12c) and Archennes (Figure 2.12e)), an increase in median grain-size and in the percentage of sand can be observed at the transition from peat (unit 3) towards clastic overbank deposits (unit 5). Moreover, median grain-size and percentage of sand decrease again during the deposition of organic overbank deposits (unit 5A) (e.g. in Sint-Agatha-Rode (Figure 2.c)). However, these variations in grain-size are not abrupt, which can be expected when erosion of the peat would have had occurred, but show a smooth trend.

When plotting the results of the grain size analysis for the sediment core in Korbeek together with the modern deposits from the same study site (Broothaerts, 2008; Notebaert et al., 2011a) in a CM diagram (Figure 2.8), it is clear that unit 5 (clastic overbank deposits) plots together with the modern overbank deposits (not statistically different on a 0.05 interval; Table 2.4). Furthermore, also unit 5A (organic overbank deposits), and unit 3 (mineral component of peat layer) plot together with the modern overbank deposits (Figure 2.8; Table 2.4). Unit 1A (pre-Holocene deposits) is statistically different from units 3, 5 and 5A, and also from the modern deposits, including the modern channel deposits (Table 2.4). This indicates that these sediments were deposited in a different depositional environment. Unit 1A represents the final low energy river stages of the Late Glacial river system before the river system became inactive, whereas the modern channel deposits represent an active meandering river. This is also illustrated by the fact that the pre-Holocene deposits (unit 1A) can be found over the entire floodplain width, whereas the channel deposits (corresponding with unit 6B) are confined to a part of the floodplain (Appendix 2).

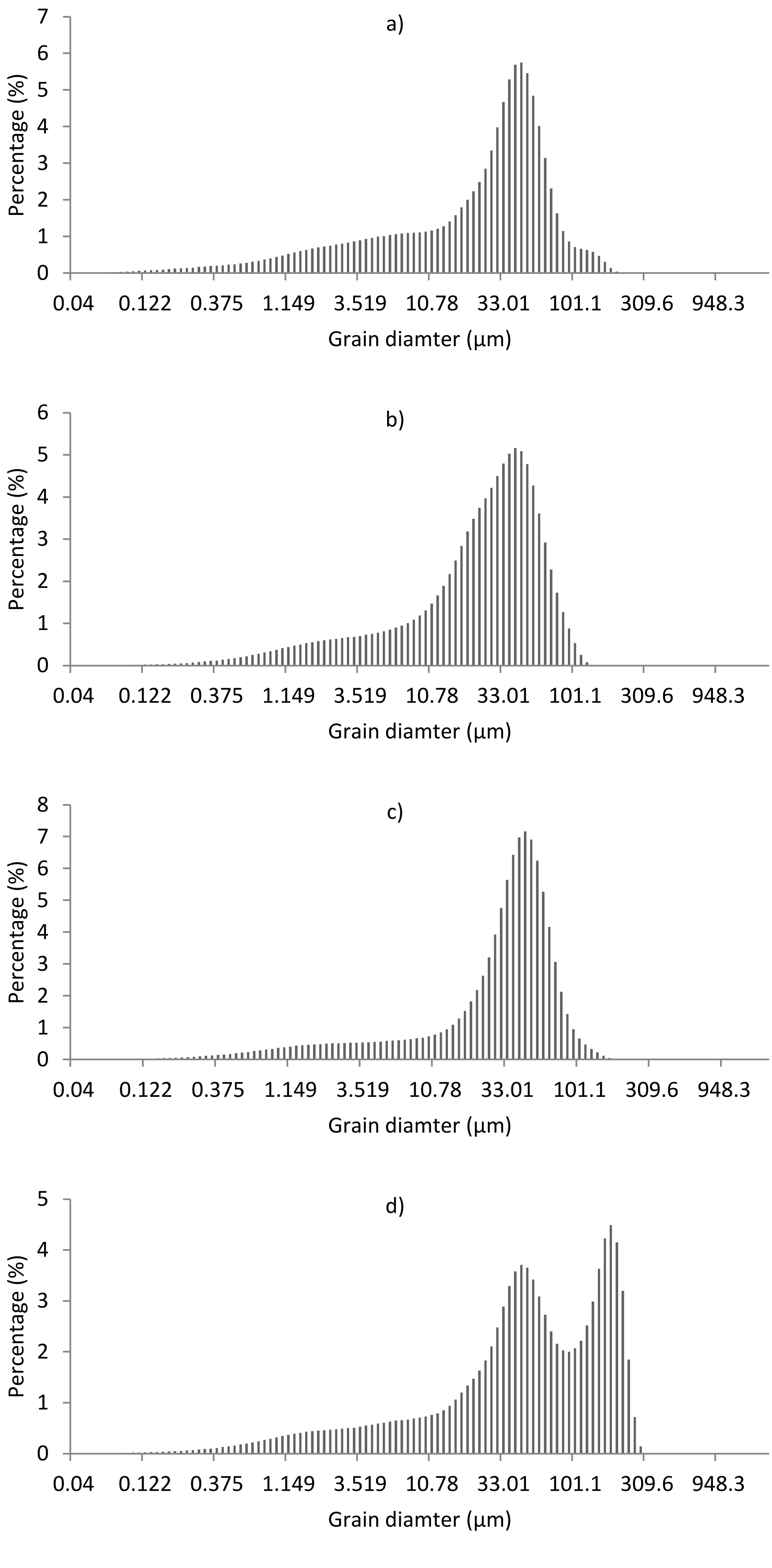

Figure 2.7. Typical grain-size distributions, calculated using laser diffraction particle size analyzer, for (a) unit 5, (b) unit 5A, (c) unit 3 and (d) unit 1A (see Table 2.3). Partly based on Coenen (2013).

Table 2.4. T-tests for the textural percentiles of the modern and palaeo-deposition environments. M: Median grain size; 90: 90 % percentile. *: significant different on a 0.1 interval; **: significant different on a 0.05 interval; ***: significant different on a 0.01 interval; –: not significant different on a 0.1 interval.

	Modern levee deposits	Modern overbank deposits	Modern channel and point bar deposits	Unit 5	Unit 5A	Unit 3	Unit 1A
Modern levee deposits		M: *** 90: ***	M: *** 90: ***	M:* 90:***	M:- 90:***	M:- 90:**	M:*** 90:-
Modern overbank deposits	M: *** 90: ***		M: *** 90: ***	M:- 90:-	M:** 90:-	M:- 90:-	M:*** 90:***
Modern channel and point bar deposits	M: *** 90: ***	M: *** 90: ***		M:*** 90:***	M:*** 90:***	M:*** 90:***	M:*** 90:***
Unit 5	M:* 90:***	M:- 90:-	M:*** 90:***		M:- 90:-	M:* 90:-	M:*** 90:***
Unit 5A	M:- 90:***	M:** 90:-	M:*** 90:***	M:- 90:-		M:- 90:-	M:*** 90:***
Unit 3	M:- 90:**	M:- 90:-	M:*** 90:***	M:* 90:-	M:- 90:-		M:- 90:**
Unit 1A	M:*** 90:-	M:*** 90:***	M:*** 90:***	M:*** 90:***	M:*** 90:***	M:- 90:**	

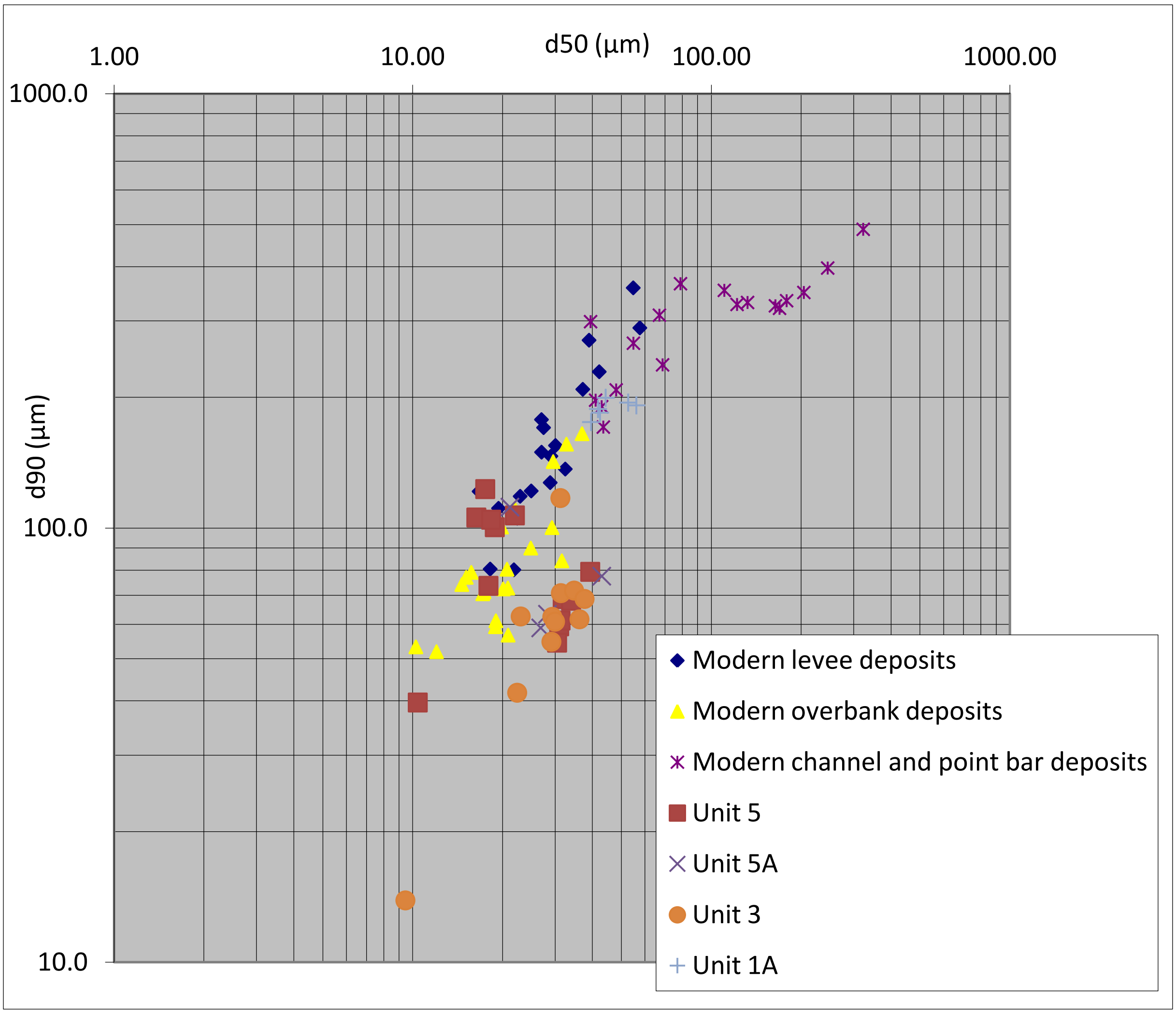

Figure 2.8. CM pattern for modern floodplain deposits (based on Broothaerts, 2008) and palaeo-floodplain deposits (based on Coenen, 2013), for study site Korbeek.

2.4.3 Radiocarbon ages and floodplain accumulation rates

Radiocarbon dating results (Appendix 1) were used to make an age-depth model for the study sites for which pollen data were gathered (Figure 2.9). These age-depth models were used to derive a chronostratigraphical framework for the whole pollen sequence and the floodplain changes for each study site. At two study sites, the age-depth model shows age-depth inversions. In Sint-Agatha-Rode, one radiocarbon age was removed from the age-depth model based on this stratigraphical inconsistency (Figure 2.9c). For Korbeek, three radiocarbon age are in an inconsistent order. Since it is not clear how to establish a good age-depth model based on the radiocarbon ages of this study site, two age-depth models were suggested, one including all radiocarbon ages (Figure 2.9e) and one excluding the three radiocarbon ages which are in an inconsistent order (Figure 2.9f).

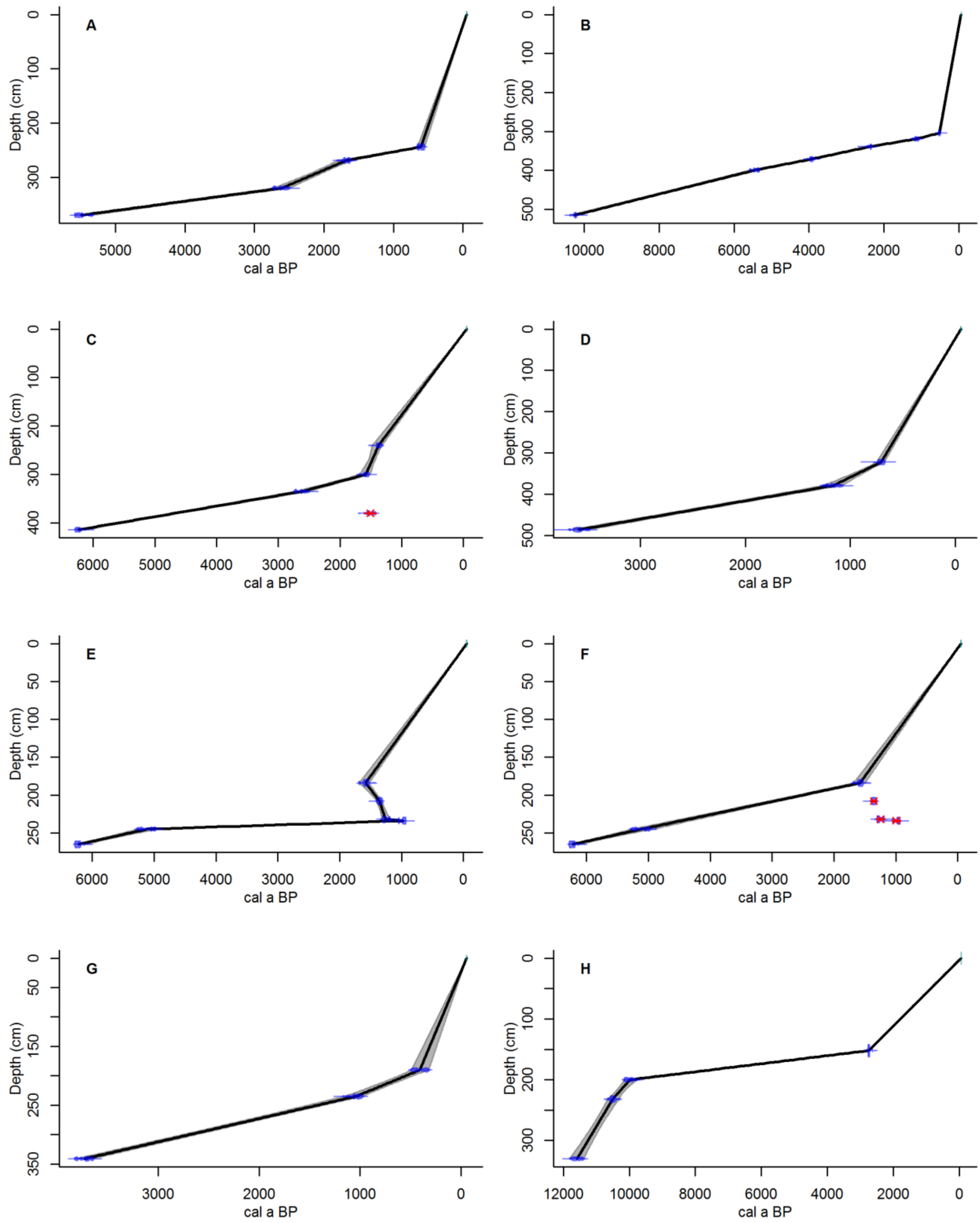

Figure 2.9. Calibrated AMS radiocarbon dating results (Appendix 1, indicated with an asterisk (*)) and age-depth models using linear interpolation between dated levels. Red dates indicate neglected age-depth inversions. (A) Cortil (n= 4), (B) Sclage (n=5), (C) Sint-Agatha-Rode (n=5), (D) Archennes (n=3), (E) Korbeek, including all dating results (n=6), (F) Korbeek, excluding age-depth inversions (n=3), (G) Loonbeek (n=3) and (H) Rotselaar (n=4).

Based on the radiocarbon dating results, floodplain accumulation rates were calculated for each study site (Figure 2.12). Results are rather consistent over the different study sites. Floodplain accumulation rates are constant at ca. 0.2 mm a^{-1} for the period with active peat formation, and increase once active peat formation halted to ca. 2 to 6 mm a^{-1}. Peat compaction was estimated between 40 and 60%, with average values of 50%, following Van Asselen (2011). Consequently, peat growth rates are ranging between 0.4 and 0.6 mm a^{-1} in the Dijle catchment. Brown (1988) found comparable Holocene peat growth rates, ranging between 0.2 and 0.5 mm a^{-1}, in floodplains in the West Midlands, United Kingdom. The observed rates in the Dijle catchment are also comparable with modern peat growth rates in Siberian peatlands (0.35 and 1.13 mm a^{-1} (Borren et al., 2004)), and in wetlands in Canada (0.1 and 0.9 mm a^{-1} (Ovenden, 1990)).

The change in relative accumulated sediment mass throughout the Holocene is similar for different study sites in the Dijle catchment (Figure 2.10). The obtained curves suffer from averaging effects and assume continuous sedimentation, and it is not possible to identify short term variations in sediment accumulation. Moreover, age-depth inversions are present in two study sites (Figures 2.9c and e). Nevertheless, the curves are very useful to discuss the general sedimentation trends. During Early and Middle Holocene, relative accumulated sediment mass in the floodplain was constant but low. Between 6000 cal a BP and 500 cal a BP, sediment accumulation in the floodplain increased. This increase did not occur at the same moment for all study sites (see chapter 3). However, sediment deposition in the floodplain mainly occurred in the last 1500 years. A detailed dated sediment core from study site Korbeek, dated by radiocarbon and OSL (optical stimulated luminescence) by Notebaert et al. (2011b), indicates that the sediment accumulation was rather constant in this period, with only a small decrease in the last 150 years. When the sediment input in the floodplain increased, the peat growth ceased and instead the floodplain deposits are characterized by clastic overbank deposits (e.g. see Notebaert et al., 2011b). In study site Rotselaar, the channel infill during the Late Glacial – Early Holocene period has been dated as well. When including this channel infill in the calculation of the relative accumulated sediment mass of this study site, a different trend appears (Figure 2.11), illustrating the high sediment input during the infill of the abandoned channel.

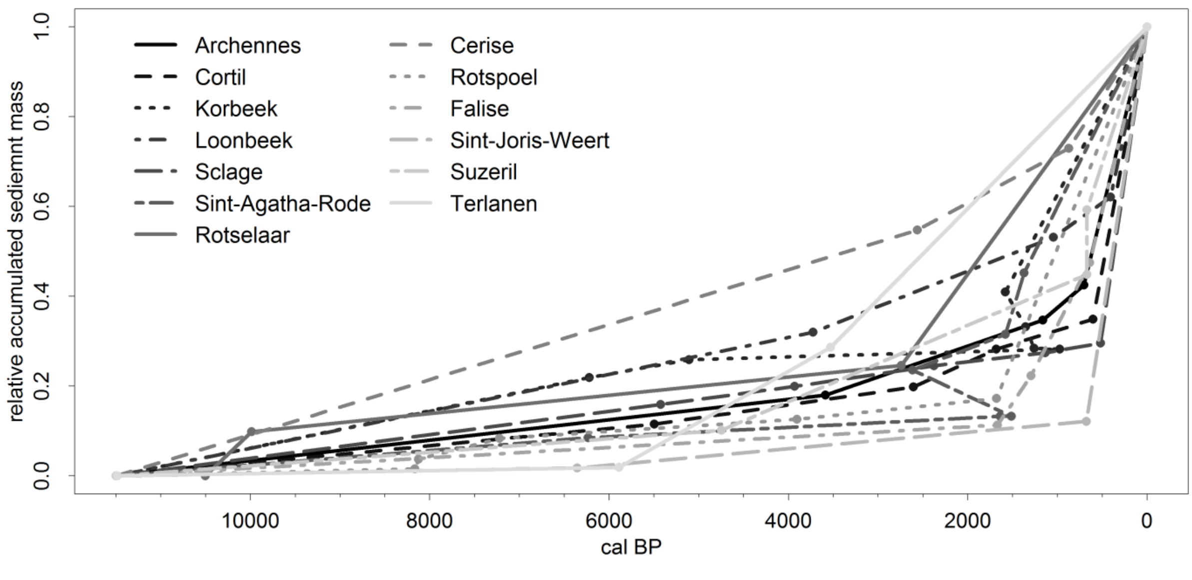

Figure 2.10. Age and relative accumulated sediment mass for different study sites in the Dijle catchment. Data from Rotspoel are obtained from De Smedt (1973), data from Cerise, Falise, Sint-Joris-Weert, Suzeril and Terlanen are obtained from Notebaert (2009).

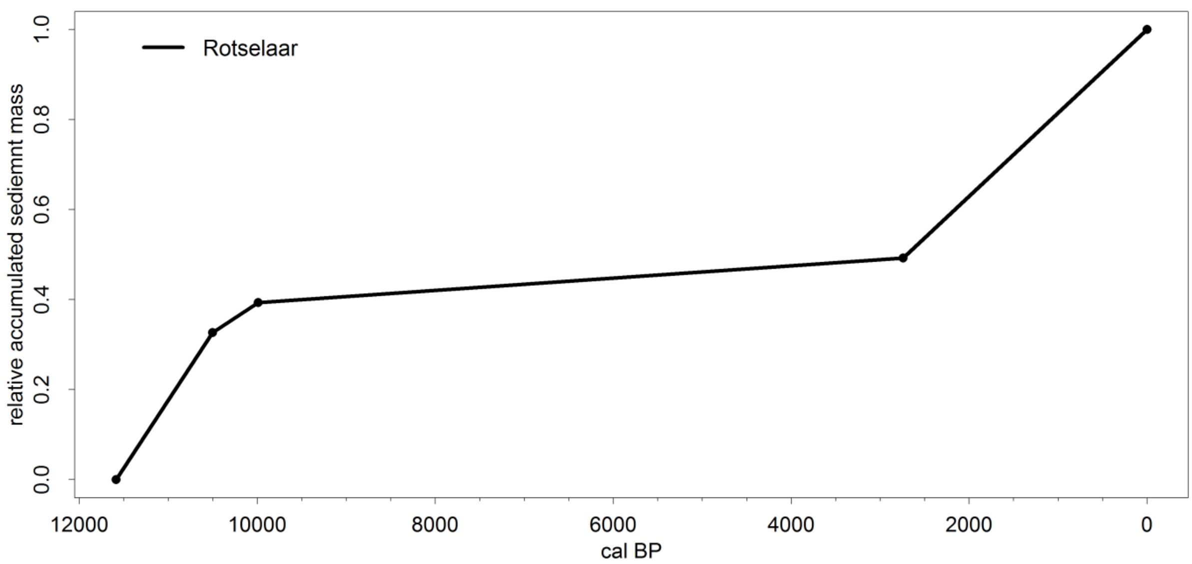

Figure 2.11. Age and relative accumulated sediment mass for Rotselaar.

2.4.4 Local floodplain vegetation

Since the focus in this chapter is on the changing floodplain geoecology, only the local vegetation will be discussed. Regional vegetation will be discussed in chapter 4. Raw pollen data can be found in Appendix 3. Local floodplain vegetation in the Dijle catchment has been reconstructed based on pollen data of six study sites (Figure 2.12). The local vegetation of the individual study sites was split up in different pollen zones, based on the cluster analysis (Appendix 4).

The local pollen signal of Cortil (Figure 2.12a) shows a variation between 2 clusters (Appendix 4A). Cluster 1 contains high values of Cyperaceae, while *Alnus* is almost absent. Cluster 2 contains mainly high values of *Alnus*, while Cyperaceae is almost absent. In cluster 2, also moderate values of *Salix*, *Polygonum bistorta* and Typhaceae are present.

The local pollen signal of Sclage (Figure 2.12b) can be split up in 3 major clusters (Appendix 4B). At the base and the top of the pollen diagram, cluster 3 is present. Cluster 3 contains moderate values of *Alnus* and moderate values of Cyperaceae. In the intermediate part of the pollen diagram, cluster 2 is present, characterised with high values of *Alnus* and low values of Cyperaceae and Typhaceae. Cluster 1 is present in the uppermost part of the pollen diagram and is characterized by low values of *Alnus*, moderate values of Cyperaceae and high values of Typhaceae.

The local pollen signal of Sint-Agatha-Rode (Figure 2.12c) can be split up in 2 major clusters (Appendix 4C). The pollen diagram is characterised by a variation between these 2 clusters. Cluster 1 contains low values of *Alnus* and high values of Cyperaceae. Cluster 1 contains high values of *Alnus* and moderate to low values of Cyperaceae and Typhaceae. Consequently the variation between cluster 1 and 2 represents a variation in high values of *Alnus* and high values of Cyperaceae.

The cluster analysis of Korbeek results in two major clusters (Figure 2.12d and Appendix 4D). Cluster 1 contains high values of *Alnus* and low to moderate values of Cyperaceae and Typhaceae. Cluster 2 contains low *Alnus* values, combined with high values of Cyperaceae and moderate values of Typhaceae. The local pollen signal of Korbeek (Figure 2.12d) is characterised by a variation between these 2 clusters, representing variation between high values of *Alnus* (cluster 1) and low values of *Alnus* (cluster 2).

The local pollen signal of Archennes (Figure 2.12e) can be split up in 3 major clusters (Appendix 4E). Cluster 1 contains only one pollen sample, and is characterised by high values of Typhaceae. Cluster 2 contains moderate values of *Alnus* and high values of Cyperaceae, and cluster 3 contains high values of *Alnus* and moderate values of Cyperaceae. Consequently, also the local pollen signal of Archennes is characterised by a variation between higher values of *Alnus* (cluster 3) and lower values of *Alnus* (cluster 1 and 2).

The local pollen signal of Loonbeek (Figure 2.12f) can be split up in 2 major clusters (Appendix 4F). The pollen diagram is characterised by a variation between these 2 clusters. Cluster 1 contains high values of Cyperaceae, low values of *Alnus* and Typhaceae and moderate values of Equisetum. Cluster 2 contains high values of Alnus, and moderate values of Cyperaceae and Equisetum.

Overall, it is clear that the cluster analysis of the local pollen signal mainly shows variations between clusters containing high values of Alnus and clusters containing high values of Cyperaceae and Typhaceae, indicating a more open vegetation.

The observed pollen signal of Rotselaar differences from the pollen signal of the study sites described above (Figure 2.13). Since study site Rotselaar will not be included in the analysis in the next chapters (results show Late Glacial and Early Holocene floodplain changes, see section 2.4.1 and Figure 2.9), we discuss here both the local and regional pollen signal at Rotselaar. Local vegetation in Rotselaar is rather constant over the investigated time frame. Cluster analysis shows that the distance between the different pollen samples are not so large (Appendix 4G), indicating that the local vegetation is similar in all pollen samples. Alnus is almost absent, local vegetation is mainly dominated by Cyperaceae. Only one sample, at 170 cm depth, differs from the other samples, with higher values of Cyperaceae. Regional vegetation in Rotselaar can be subdivided in two major clusters (Appendix 4 and Figure 2.13). Cluster 1 (175-150 cm) contains high values of arboreal pollen (AP), with especially high values of Corylus. Betula is absent and Pinus, Quercus and Ulmus are present in moderate values. Cluster 2A (215-175 cm) contains very high values of Pinus. Betula is absent also in this cluster, and Corylus and Quercus are present in low values. De Smedt (1973) found a similar vegetation zone in the Dijle-Demer confluence area and related this zone with the Boreal Period. Cluster 2Ba (288-215 cm) contains high values of Betula, moderate values of Pinus and low values of Corylus and Quercus. Finally, cluster 2Bb (324-288 cm) contains decreasing values of AP and increasing values of non-arboreal values (NAP), in particular increasing values of Poaceae. Values of Pinus and Betula are moderate in this cluster. De Smedt (1973) related similar vegetation zones as Cluster 2B with the Preboreal period.

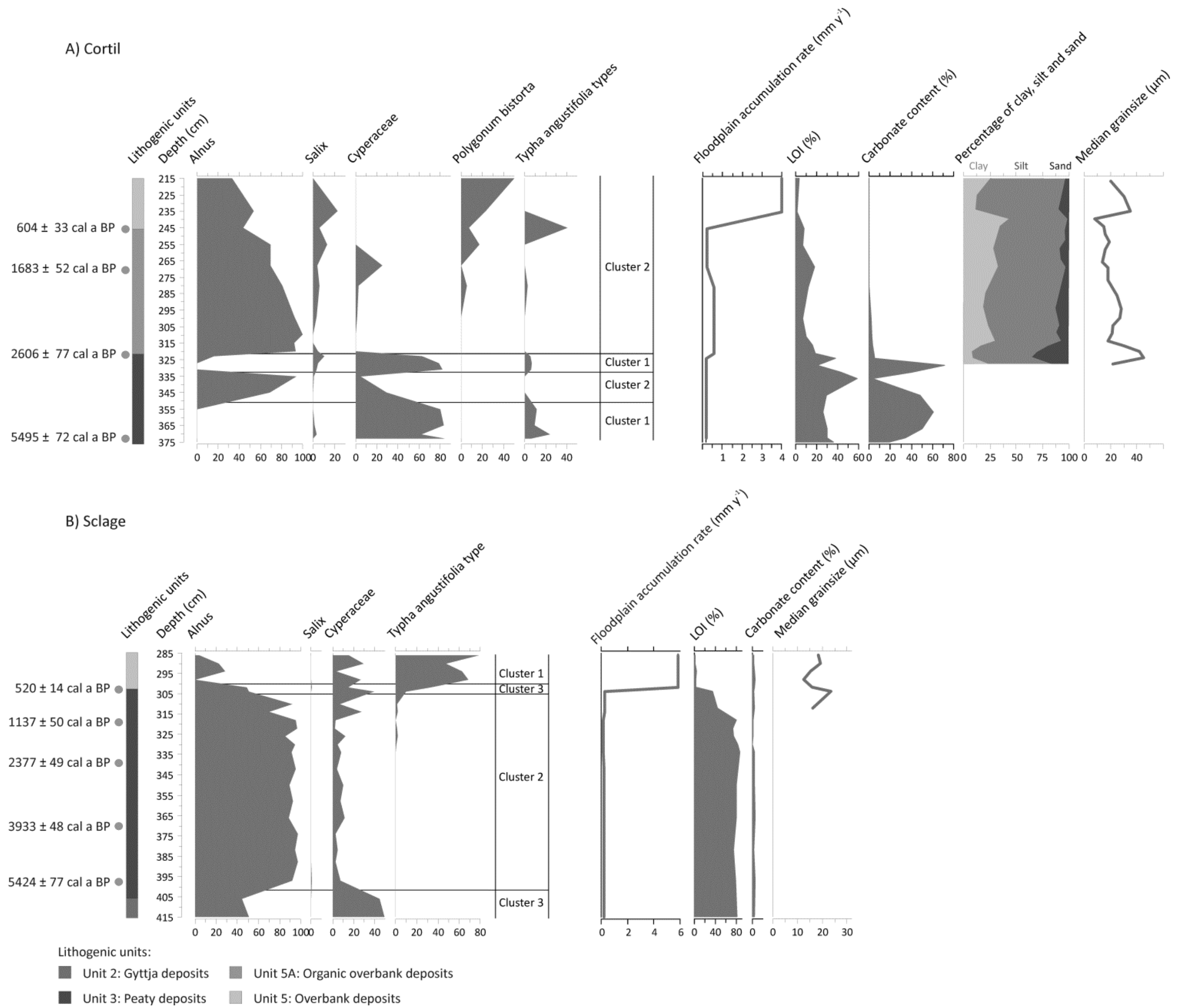

Figure 2.12. Simplified pollen diagrams from study sites (a) Cortil, (b) Sclage, (c) Sint-Agatha-Rode, (d) Korbeek, (e) Archennes and (f) Loonbeek; with indications of the different clusters. Also floodplain accumulation rates, organic matter and carbonate content, median grain size and volume percentage of clay, silt and sand are shown.

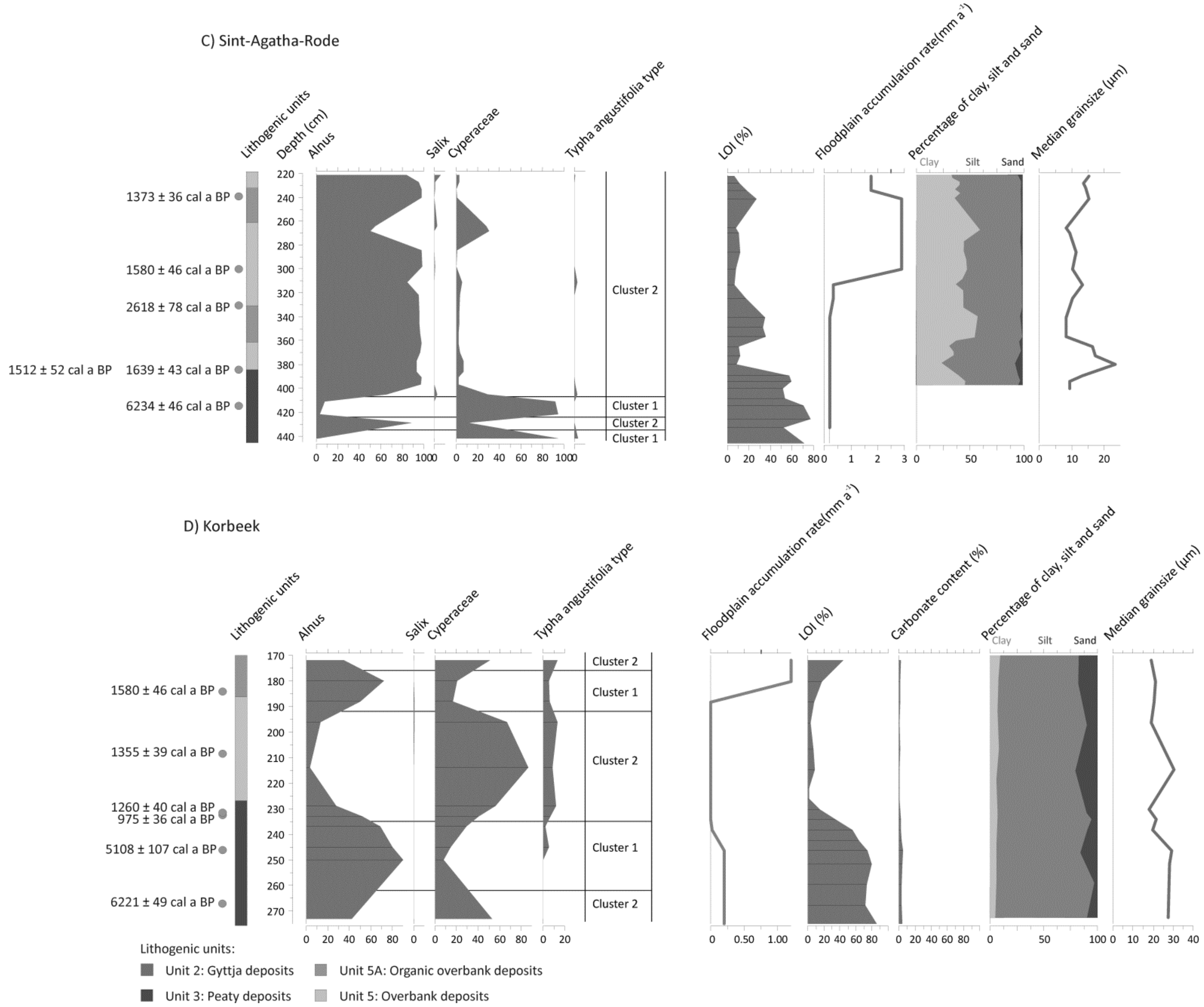

Figure 2.12. Cont.

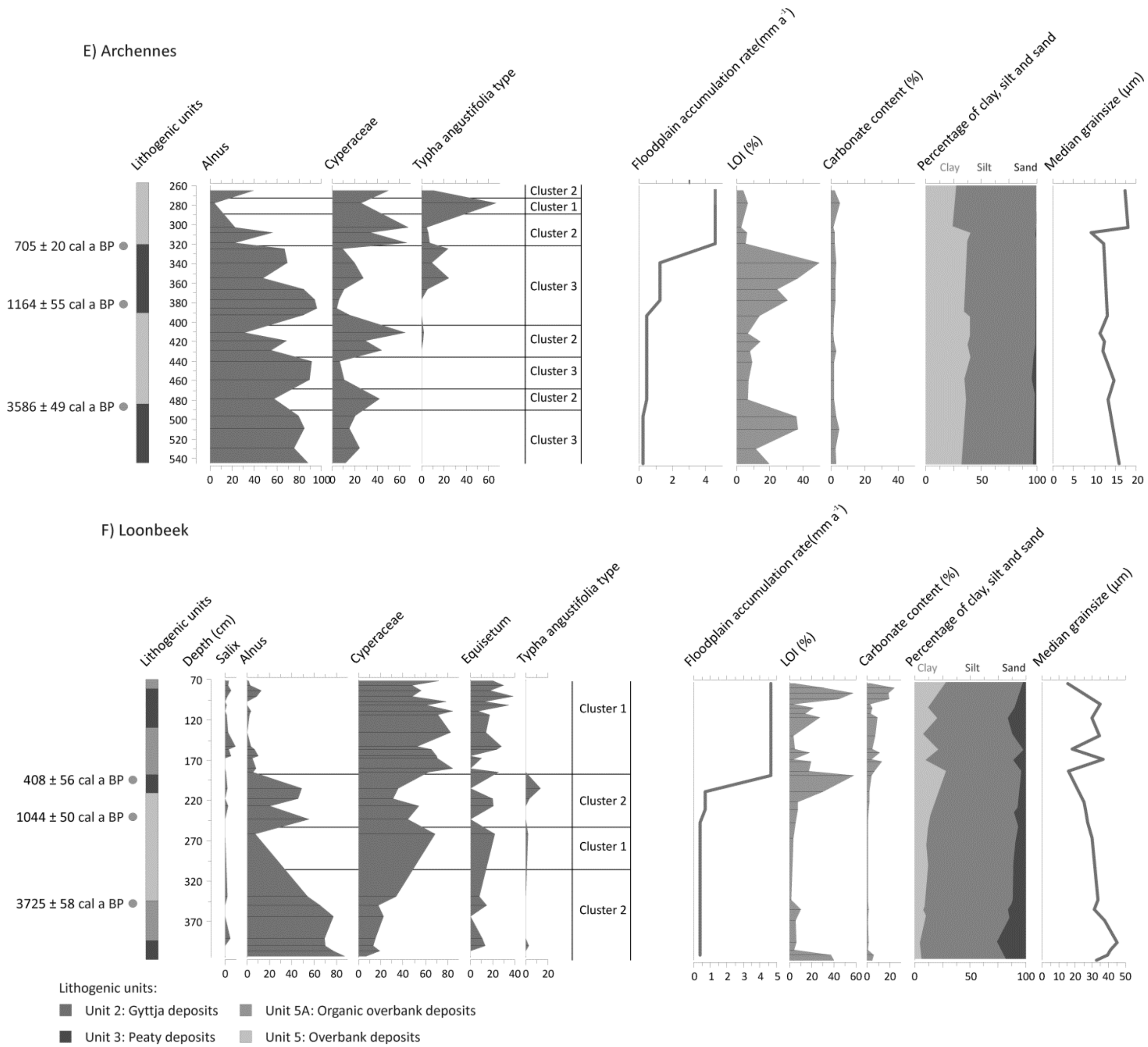

Figure 2.12. Cont.

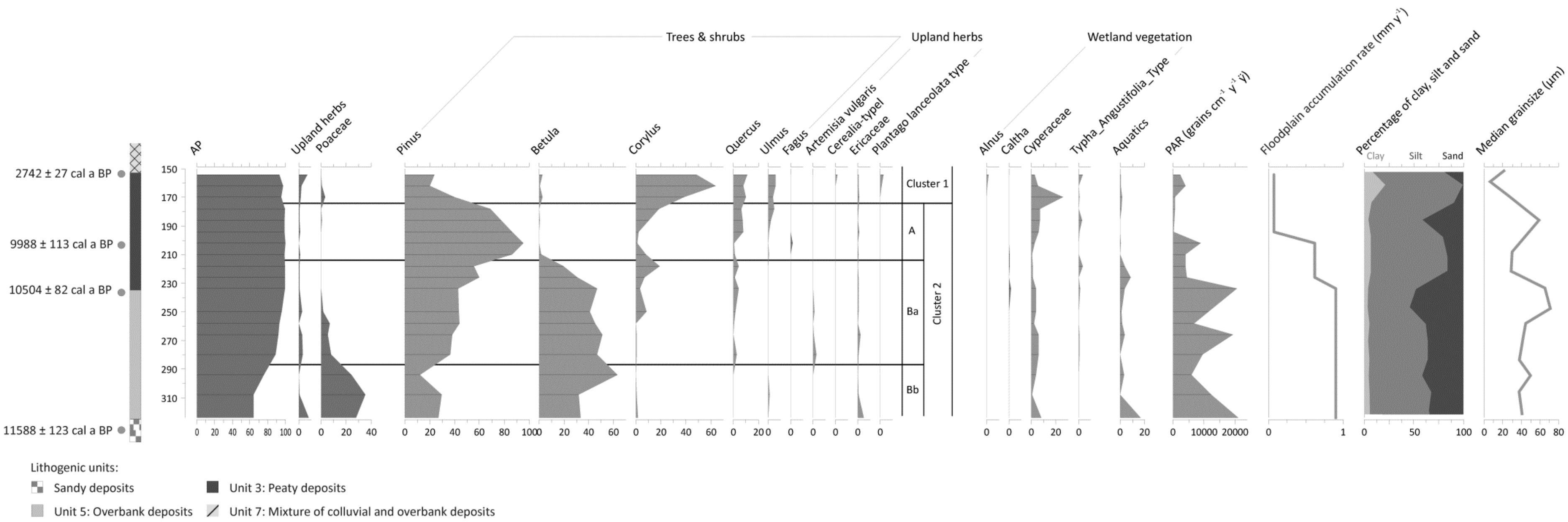

Figure 2.13. Simplified pollen diagram from study site Rotselaar; with indications of the different clusters. Also floodplain accumulation rates, organic matter and carbonate content and median grain size are shown.

2.5 Discussion

Based on the previous research in the Dijle catchment (Mullenders and Gullentops, 1957; Mullenders et al., 1966; Munaut, 1967; De Smedt, 1973; Rommens et al., 2006; Notebaert, 2009) and new data presented here, the changing floodplain geoecology in the Dijle catchment can be reconstructed. This shows that, from the beginning of the Holocene onwards, the floodplain was a stable environment (Appendix 1 and 2) – sediment discharge and sediment deposition in the floodplain were low (Figure 2.10). This resulted in peat and gyttja accumulation. At this stage, no clear river channel was present in the floodplain. We suggest, following De Smedt (1973) and Notebaert et al. (2011a), that during this period, the floodplain consisted of a marshy environment with a diffuse water transport without a clearly developed river channel (Figure 2.14), as indicated by the limited sediment mass accumulation (Figure 2.10) and the absence of large channel deposits from this period (Appendix 2). At some places the floodplain was an open water system, i.e. shallow floodplain lakes related to groundwater seepage in the floodplain, resulting in gyttja and carbonate-rich deposits (units 2 and 4). Peat growth rates are ranging between 0.4 and 0.6 mm a^{-1} during this period. Vegetation in most floodplains of the Dijle catchment was mainly dominated by a wet alder carr forest (*Alnion glutinosae*). This resulted in most study sites in woody peat deposits.

Throughout the Holocene, the floodplain morphology and ecology in the Dijle catchment changed, coinciding with the increasing accumulated sediment mass in the floodplain (Appendix 2 and Figure 2.12). This change differs for the different study sites. In Sclage, the alder carr forest disappeared around 500 cal a BP, coinciding with the increasing accumulated sediment mass in the floodplain (Figure 2.10) – floodplain accumulation rates increased from ca. 0.4 to ca. 6 mm a^{-1} around 500 cal a BP (Figure 2.12) (for details, see chapter 3). The alder carr forest was replaced by a more open floodplain vegetation, dominated by Cyperaceae and Typhaceae (Figure 2.12). On the illustrative *de Ferraris* map (ca. 1775), wet meadows are indicated on these floodplains. In Cortil and Sint-Agatha-Rode, the floodplain vegetation shows a variation between an open floodplain, dominated by e.g. Cyperaceae on the one hand, and *Alnion glutinosae* on the other hand (Figure 2.12). This alternation can be related to changes in wetter and dryer conditions in the floodplain, illustrated by the changing $CaCO_3$ content (Figure 2.12) due to changes in the input of calcareous rich groundwater seepage. During wetter stages the floodplain was more open and dominated by Cyperaceae and Typhaceae, whereas during drier stages the floodplain was dominated by alder carr forest. These variations did not occur at the same moment for the two study sites. In Cortil, they occurred between ca. 6000 and 2500 cal a BP, in Sint-Agatha-Rode, between ca. 7500 and 5500 cal a BP. In both study sites, the floodplain remained stable during these variations with limited sediment deposition, resulting in gyttja and peat accumulation. In Cortil, small diffuse channels were present in the floodplain during the formation of these peat and gyttja deposits (Appendix 2). From ca. 600 cal a BP in Cortil, and from ca. 1600 cal a BP in Sint-Agatha-Rode, peat accumulation stopped and was overlain by clastic deposits. Floodplain accumulation rate increased to ca. 4 mm a^{-1} (Figure 2.12). In Sint-Agatha-Rode, an expansion of the alder carr forest can be observed, dated around ca. 1370 cal a BP. This expansion of the alder carr forest coincides with organic overbank deposition, indicating a new stable phase in the floodplain. In Korbeek, the alder carr forest disappeared, coinciding with the start in clastic overbank deposits. The timing of this transition will be discussed in detail in chapter 3. Around 1500 cal a BP, a stable phase can be observed in the floodplain, with a regrowth of the alder carr forest and deposition of organic overbank deposits (Figure 2.12). A similar pattern can be observed in

Archennes. In Loonbeek, peat formation stopped around 3700 cal a BP, whereas the increase in floodplain accumulation rate and disappearance of the alder carr forest is only observed from ca. 400 cal a BP onwards. The alder carr forest is replaced by a more open vegetation, dominated with Cyperaceae.

Overall, we observe that the floodplains in the Dijle catchment changed from a strongly vegetated (dominated by an alder carr forest) and stable environment (i.e. an environment with limited sediment discharge and sediment deposition) resulting in peat accumulation, towards a floodplain with open vegetation, the creation of a single channel river and the dominance of minerogenic overbank sedimentation (Figure 2.14). The exact evolution between these two stages differs between the study sites. Only a few study sites differ from this general pattern of floodplain changes. At study site Thy (Appendix 2H) and in the Nethen valley (Rommens et al., 2006), gyttja deposits are overlain by calcium carbonate rich deposits, which are in turn overlain by clastic overbank deposits. Similar organic layers with a large amount of calcium carbonates – with even formation of travertine at some places – can be found in the Train river (Geurts, 1976; Notebaert, 2009). Nevertheless, the reconstruction presented here remained limited since it only includes the main geomorphological and vegetation changes. To attain a more detailed and comprehensive understanding of the aquatic and terrestrial ecological changes, a multi-proxy analysis should be used, including not only analysis of pollen but also the analysis of macro remains (seeds, fruits and wood remains), molluscs, diatoms and vertebrate remains (e.g. Deforce et al., 2014). Moreover, such a detailed, multi-proxy reconstruction could allow a discussion on e.g. the spatial variation of habitats along a floodplain transect, and could provide a more detailed understanding of the interaction between changing floodplain geomorphology and vegetation (e.g. Hughes, 1997). Also the temporal resolution is limited and does not allow, for instance, an identification on the influence of short-term climatic variations. Beside these limitations, our reconstruction of the floodplain geoecology remained detailed enough to achieve the objectives of this study, and to study the timing, nature and extent of human impact on the floodplain geoecology.

Similar sedimentation patterns and changes in geomorphology and environmental conditions of floodplains were observed in other catchments in Belgium, such as the Scheldt basin (e.g. Meylemans et al., 2013), Mark catchment (Huybrechts, 1999) and the Geul catchment (e.g. De Moor et al., 2008; De Moor and Verstraeten, 2008). Also in other parts of West and Central Europe similar floodplain changes were observed, e.g. in Germany (e.g. Lang and Nolte, 1999; Rittweger, 2000; Kalis et al., 2003; Houben, 2007), France (e.g. Pastre et al., 2002; Lespez et al., 2008) and United Kingdom (e.g. Foulds and Macklin, 2006; Chiverrell et al., 2009; Macklin et al., 2010). A clear overview of the floodplain changes and sediment dynamics in West and Central Europe throughout the Holocene is provided by Notebaert and Verstraeten (2010).

The study site near Rotselaar shows the evolution of the fluvial system of the Dijle river downstream Leuven during the Late Glacial and Early Holocene period. Floodplain transects and radiocarbon ages indicate that the Dijle River consisted of a meandering system, which was active during the Younger Dryas (Figure 2.13 and De Smedt (1973)). Also the Scheldt River was meandering during the Late Glacial period (Meylemans et al., 2013). At the beginning of the Holocene, several meanders were cut off from the river (De Smedt, 1973), including the meander investigated in this study, and started to infill with loamy sediments (Appendix 2J). After infilling of the palaeo-channel, the floodplain became dominated by peaty deposits (Appendix 2J). De Smedt (1973) interpreted this peaty unit to be deposited in a marshy environment, with diffuse water transport. The floodplain transect near Rotselaar (Appendix 2J) shows a hiatus at the top of this peaty layer. Pollen samples until 10 cm below the top of the peat layer can be interpreted as dating from the Boreal period, whereas the pollen sample at the top of the peat layer contains higher values of upland herbs, including anthropogenic indicators such as *Plantago lanceolata* and Cereal-type. This sample has been dated at 2742 ± 27 cal a BP, which indicates a hiatus or a very slow peat growth rate at the top of the peat layer. Consequently, the study of the transition from peaty deposits towards clastic overbank deposits is difficult and incomplete. Therefore, this study site Rotselaar is not included in the analysis in the next chapters.

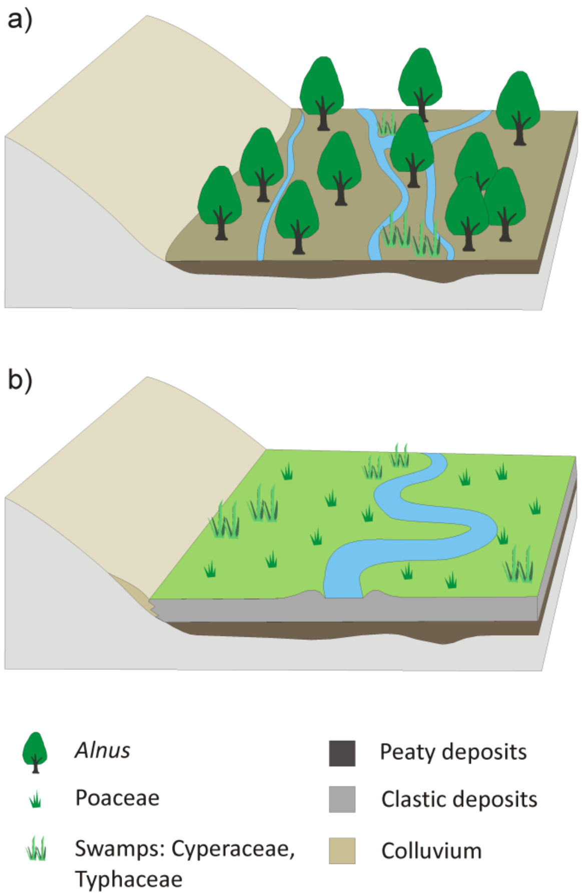

Figure 2.14. Schematic reconstruction of the Dijle floodplain, (a) around 5000 cal a BP and (b) around 1000 cal a BP.

2.6 Conclusions

In this study the fluvial architecture in the Dijle catchment was studied and local floodplain vegetation was reconstructed. These data were combined with radiocarbon dating results to reconstruct the changing floodplain geoecology in the Dijle catchment throughout the Holocene. During the Middle Holocene, the floodplain mainly consisted of a strongly vegetated marshy environment (dominated by an alder carr forest) which resulted in peat accumulation. The floodplain was a relative stable environment, with limited sediment discharge and sediment deposition.

Throughout the Holocene, floodplain geoecology changed with clearing of the alder carr forest, the creation of a single channel river and the dominance of minerogenic overbank sedimentation. Floodplain vegetation became more open, dominated by Cyperaceae and Typhaceae. Floodplain accumulation rates increased mainly in the last 1500 years, from ca. 0.2 mm a^{-1} for the period with active peat formation, to ca. 2 to 6 mm a^{-1} once active peat growth halted. The exact evolution between these two floodplain stages differs between the study sites. Moreover, the timing of the onset of these changes differs among the different study sites and needs more detailed analysis (see chapter 3).

The contemporary morphology of the floodplains in the Dijle catchment, with a meandering river and mineral overbank deposits, contrast strongly with the Middle Holocene floodplains which were dominated by peat formation in marshes and gyttja deposition in floodplain lakes, and which lack evidence of a well developed main channel. More research is needed to understand the driving forces for these changes and to understand to which extent human impact has altered the floodplain geoecology.

Chapter 3 Non-uniform and diachronous changes in Holocene floodplain evolution

This chapter is published as: Broothaerts N, Notebaert B, Verstraeten G, Kasse C, Bohncke S and Vandenberghe J (2014a) Non-uniform and diachronous Holocene floodplain evolution: a case study from the Dijle catchment, Belgium. *Journal of Quaternary Science* 29: 351-360.

3.1 Introduction

Floodplain deposition rates have increased intensively under influence of increasing human impact throughout the Late Holocene in many West and Central European catchments (Notebaert and Verstraeten, 2010). This increase in sedimentation rates has changed the geomorphology and environmental conditions of many floodplains in e.g. Germany (e.g. Rittweger, 2000; Kalis et al., 2003; Houben, 2007), France (e.g. Pastre et al., 2002; Lespez et al., 2008) and Belgium (Vandenberghe and De Smedt, 1979; De Moor and Verstraeten, 2008). Also in the Dijle catchment, the floodplain geoecology underwent important changes (chapter 2 and Rommens et al., 2006; Notebaert et al., 2011b). Floodplains changed from stable, wet environments with limited floodplain aggradation – resulting in peat and soil formation – towards single-channel meandering rivers dominated by clastic overbank deposition. This transition from peat formation towards clastic deposition, which is common in small river catchments across West and Central Europe, can be attributed, at least in part, to increasing agricultural activities in the catchment. Contemporary meandering of rivers in West and Central Europe is thus the indirect result of increased human impact in the catchment.

Although the overall influence of anthropogenic land cover change on floodplain geomorphology is well established now, we lack a detailed reconstruction or model of the impact-response relationships that is needed to fully grasp how, when and to what extent humans have reshaped fluvial systems (see chapter 1). We do not know, for instance, specific thresholds which human impact must cross to completely alter the floodplain morphology. Nor do we know whether these man-induced fluvial changes took place gradually or abruptly, both in time and in space. If temporal differences between subcatchments exist, the question remains whether these differences can be attributed to heterogeneity in the timing and nature of the external forcings, or to differences in intrinsic sensitivity towards the same environmental disturbances – which can indicate a non-linearity in the process-response relationship. To solve these questions, a more robust chronology of these floodplain changes is necessary to identify their relationship to land use changes, and separate the potential driving forces and processes involved (e.g. Verstraeten et al., 2009a). Nevertheless, past studies have often been based on limited dating evidence for individual catchments (e.g. see Notebaert and Verstraeten, 2010), frequently due to the unavailability of datable material in floodplain deposits or to financial restrictions. Consequently, these studies suffer from averaging effects, leading to a rather low temporal resolution. The lack of a detailed chronology makes it hard to retrieve unambiguous information on the driving forces for the observed sediment dynamics and floodplain changes.

The objective of this chapter is to understand the temporal changes in floodplain morphology and sedimentation patterns by means of a detailed chronology. We show the importance of a detailed chronology at the catchment scale, with an example from the Dijle catchment located in the Belgian loess belt. For the 758 km² Dijle catchment detailed insights in the sediment dynamics is already provided by previous studies (e.g. Rommens et al., 2006; Verstraeten et al., 2009b; Notebaert et al., 2011b). Chronological information on changes in floodplain geomorphology is retrieved from previous studies and from newly obtained radiocarbon dating results providing one of the most detailed databases on Holocene floodplain changes for such a small river catchment.

3.2 Study area

This study focuses on the Dijle catchment south of Leuven (758 km²) (Figure 3.1), which is part of the Scheldt catchment (ca. 20 000 km²). The Dijle catchment is located in the central Belgium loess belt and is characterized by an undulating plateau in which several rivers are incised. Height in the catchment varies between 165 m a.s.l. in the south to 25 m a.s.l. near the outlet of the studied catchment. The soils of the catchment are mainly Luvisols, developed in the loess deposits. Palynological studies in the Dijle catchment show that the catchment was mainly forested during the first half of the Holocene (Mullenders and Gullentops, 1957; Mullenders et al., 1966; De Smedt, 1973). The oldest known Neolithic settlements near the Dijle catchment dated from ca. 6200 cal a BP (Crombé and Vanmontfort, 2007; Vanmontfort, 2007). Anthropogenic disturbances in the landscape became evident in the pollen assemblages from ca. 2500 cal a BP (Mullenders and Gullentops, 1957; Mullenders et al., 1966), although these palynological data had a poor chronological control. Current land use is dominated by cropland, except for some large plantation forests in the northeast and northwest of the catchment. The floodplain is currently used as forest or grassland. A detailed description of the study area can be found in chapter 2.

Holocene floodplain changes in the Dijle catchment were previously reconstructed by e.g. Rommens et al. (2006), Notebaert et al. (2011b) and were discussed in chapter 2. During the Early and Middle Holocene, the Dijle floodplain was stable and consisted of a marshy environment where organic material accumulated, resulting in peat formation. Throughout the Holocene, floodplain geomorphology changed to a single-channel river with clastic overbank sedimentation, resulting in a clear boundary between peaty and clastic deposits (see chapter 2 and Appendix 2). No clear indications for erosion of the top of the peat layer are present (chapter 2). Although this stratigraphic transition had been dated for individual study sites, the general temporal pattern of this boundary at the catchment scale is still not clear.

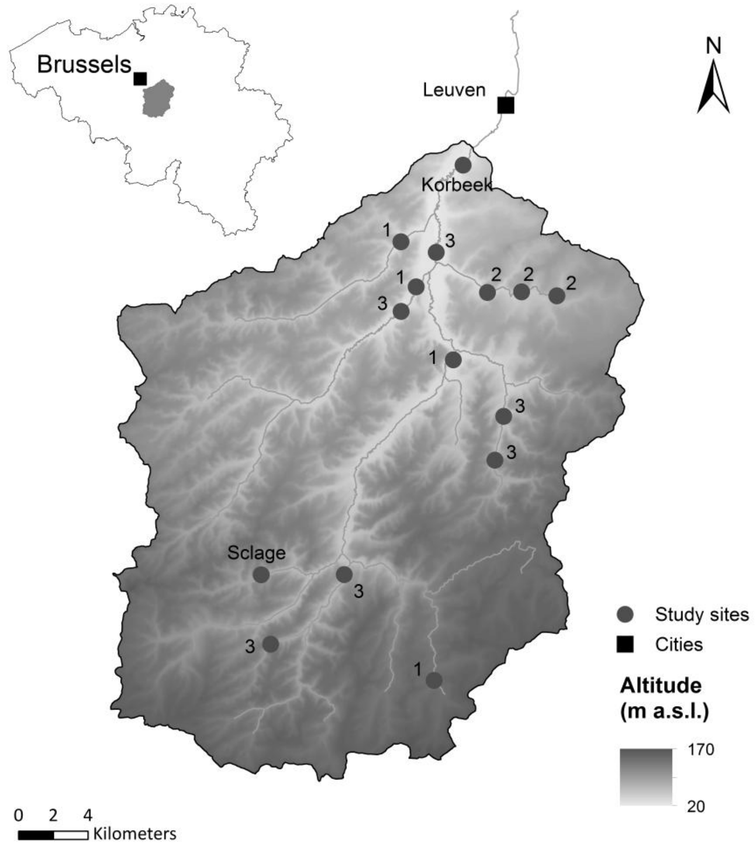

Figure 3.1. Location of the Dijle catchment in Belgium and study sites for which radiocarbon dating results are available (15 sites). Sources: 1: this study, 2: Rommens et al. (2006), 3: Notebaert et al. (2011b). Two study sites were studied in detail: Korbeek (this study + Notebaert et al. (2011b)) and Sclage (this study + Notebaert et al. (2011b).

3.3 Material and Methods

3.3.1 AMS radiocarbon dating

AMS (accelerator mass spectrometry) radiocarbon dating results for the Dijle catchment are available from studies by Rommens et al. (2006) and Notebaert et al. (2011b). To provide a more representative database regarding the morphological changes in the floodplain, four extra study sites and 20 new radiocarbon dates have been added. These 20 dates include 8 samples from the base and 12 samples from the top 5 cm of the peat layer (Appendix 1). Two study sites were selected to be studied in detail (Figure 3.1). The first study site (Sclage) is located in the headwaters of the catchment along the Cala River, a small tributary of the Dijle River (Figure 2.4). A second study site (Korbeek) is located in the main trunk valley of the Dijle River (Figure 2.5). The upstream area of these two study sites is 13 km² and 750 km² respectively; floodplain width 90 m and 1100 m respectively. For these study sites radiocarbon dating results were obtained to establish insight in the lateral variation (perpendicular to the valley axis) of the age of the top of the peat layer (Appendix 2B and 2D). Each sample was sieved at 250 µm and datable material was extracted by hand. Terrestrial plant and wood remains were selected to avoid hard-water effects, reservoir effect or incorporation of older organic material (e.g. Törnqvist et al., 1992). Dating reworked wood remains was avoided by selecting samples from the top 5 cm of the peat layer. Since river channels were absent during the deposition of the peat layer (chapter 2), the presence of reworked wood remains in the peat layer is highly unlikely. In total, 45 AMS radiocarbon dates (Appendix 1) from 15 alluvial sites within the Dijle catchment (Figure 3.1) are available in this study, including 16 samples from the base of the peat layer and 29 samples from the top of the peat layer. Obtained conventional radiocarbon ages (BP) were calibrated using Oxcal 4.2 (Ramsey, 2009) and the IntCal13 calibration curve (Reimer et al., 2013).

3.3.2 Cumulative probability functions

Cumulative probability functions (CPFs) have been used frequently to analyze chronological databases of fluvial activity, e.g. in Britain (Macklin and Lewin, 2003; Lewin et al., 2005; Macklin et al., 2010), Spain (Thorndycraft and Benito, 2006a; Thorndycraft and Benito, 2006b), Germany (Hoffmann et al., 2008; Hoffmann et al., 2009), and Belgium (Notebaert et al., 2011b). In this study, CPFs were used to get more insights in the timing of the floodplain changes in the Dijle catchment. CPFs were made by the addition of the probability functions of the individual calibrated radiocarbon ages. A CPF was made of all available radiocarbon ages from the top of the peat layer (n=29, 12 study sites) and the base of the peat layer (n=16, 6 study sites). To study the lateral variations along a floodplain transect perpendicular to the valley axis, a CPF was made of the radiocarbon ages from the top of the peat layer for study sites Sclage (n=6) and Korbeek (n=10) separately.

Despite the advantages, several problems are related with CPFs (e.g. Chiverrell et al., 2011). One of the issues is the problematic influence of the shape of the calibration curve on the CPFs (Hoffmann et al., 2008; Chiverrell et al., 2011). To remove the calibration curve structure, the calculated CPFs were divided in this study by a CPF of 100 equally spaced ages with a standard deviation of 35 years (following Hoffman et al. (2008)). The standard deviation used of 35 years equals the average uncalibrated standard deviation of the radiocarbon ages in the dataset. A second problem associated with CPFs is that it may not be valid to assume that each radiocarbon measurement is a true age estimate for a point in time (Chiverrell et al., 2011). This problem was countered in this study by avoiding conclusions based on individual peaks in the CPFs. Thirdly, the temporal relationship between the dated material and the likely dated event is not always straightforward (Hoffmann et al., 2008; Chiverrell et al., 2011), e.g. the obtained radiocarbon age from the top of the peat layer does not always represent the end of peat growth due to erosion of the top of the peat layer or a period of no or very slow peat growth. In the Dijle catchment no clear indications of erosion of the top of the peat layer are present (see chapter 2), partly avoiding this third problem. Fourthly, chronometric data that were not tested for their robustness should not be included in a CPF analysis, such as data from stratigraphies with temporal inversions (Chiverrell et al., 2011). These problems are all valid when CPFs are used to study events of a relative short duration, e.g. flood events. In this study however, the aim is to investigate the general pattern of floodplain changes, rather than establishing a very detailed chronology of individual events (cf. Macklin et al., 2011). Moreover, the nature of this study partially avoids these problems, as its local scale and detailed focus allows a strict selection of dated material and a profound understanding of local geomorphology. A final problem associated with the obtained CPFs in this study is the possible bias caused by the sampling strategy. Only a limited number of radiocarbon ages (45 in total) from a limited number of study sites (15 in total) are available. These study sites are not equally distributed over the catchment (Figure 3.1), but their location depends on the accessibility, the degree of recent disturbance of the floodplain area and the availability of previous research. Moreover, the radiocarbon ages are not equally distributed over the study sites. This problem is countered by correcting the CPFs for the number of available radiocarbon ages per study site.

The cumulative probability of a given set of radiocarbon ages can be calculated at each time step (*t*), by the addition of the probability functions of the individual calibrated radiocarbon ages at this time step. This can then be summed over a certain time period (*k*):

$$\sum_{t=t0}^{k} CP\_bottom_t \qquad \text{Equation (3.1)}$$

With CP_bottom_t the cumulative probability of the available radiocarbon ages of the base of the peat layer, at time *t*; and t_0 the oldest available radiocarbon age of the base of the peat layer. This can be made relative to the total cumulative probability of all available radiocarbon ages of the base of the peat layer:

$$\left[\frac{\sum_{t=t0}^{k} CP\_bottom_t}{\sum_{t=t0}^{tend} CP\_bottom_t}\right] \qquad \text{Equation (3.2)}$$

With t_{end} the youngest available radiocarbon age of the base of the peat layer. The same can be done with the available radiocarbon ages of the top of the peat layer. By combining these relative CPFs of the base and the top of the peat layer, the evolution of peat growth in the catchment over time can be reconstructed, using:

$$SPI_k = \left[\frac{\sum_{t=t0}^{k} CP\_bottom_t}{\sum_{t=t0}^{tend} CP\_bottom_t}\right] - \left[\frac{\sum_{t=t0}^{k} CP\_top_t}{\sum_{t=t0}^{t=tend} CP\_top_t}\right] \qquad \text{Equation (3.3)}$$

With SPI_k the Surface Peat Index at time *k*; t_0 the oldest radiocarbon age of peat in the catchment; t_{end} the youngest radiocarbon age of peat in the catchment; and CP_bottom_t and CP_top_t the cumulative probability of the available radiocarbon ages of the base and top of the peat layer respectively, at time *t*. The probabilities of the available ages were weighted according to the floodplain width of the respective study site. Consequently, SPI_k is a measure for the proportion of floodplain area in the catchment with active peat growth at time *k*, varying between 0 (no floodplain area with active peat growth) and 1 (all floodplains with active peat growth). This proportion can be plotted in function of time, to provide more insights in the evolution of peat growth in the catchment throughout the Holocene.

3.4 Results

3.4.1 Temporal pattern of floodplain changes at the catchment scale

The CPF of the lower part of the peat layer provides information regarding the onset of peat formation in the Dijle catchment (Figure 3.2). Most peaks are located between 11500 and 9500 cal a BP, indicating that peat growth in the floodplain started at the beginning of the Holocene.

The CPF of the top of the peat layer shows a more diffusive pattern (Figure 3.3). The observed shift from marshy environment with peat accumulation towards clastic deposits did not occur at the same moment at a catchment scale: while some parts of the catchment are prone to clastic floodplain aggradation, floodplains in other parts remained stable and peat growth continued. Oldest dates from the top of the peat layer are situated around 6500 cal a BP. However, most dates are situated between 2000 and 500 cal a BP, indicating that in most study sites, the peat growth ceased in this period.

This is also clear from the changes in the proportion of floodplain area with peat growth (Figure 3.4). The stepwise pattern is a consequence of the limited number of available radiocarbon ages. Nevertheless, the overall pattern of the proportion of floodplain area with peat growth in the Dijle catchment shows a clear trend. Peat growth started at the beginning of the Holocene onwards. The peat growth expanded over (almost) all floodplain sites by 9500 cal a BP. From ca. 9500 until ca. 6500 cal a BP most floodplains remained stable and peat growth dominated. From ca. 6500 cal a BP onwards, peat gradually disappeared in some of the study sites. The decrease in active peat forming areas accelerated from 2000 cal a BP onwards.

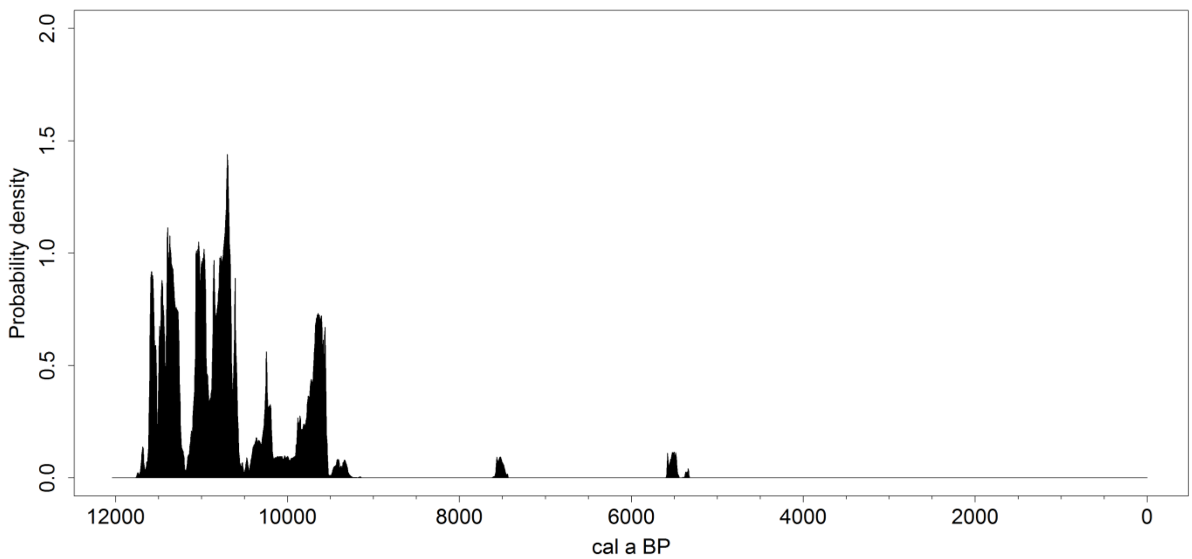

Figure 3.2. CPF of all radiocarbon ages of the base of the peat layer (n=16, 6 study sites). Probabilities were divided by the probability of equally spaced ages, and corrected for the number of radiocarbon ages per study site.

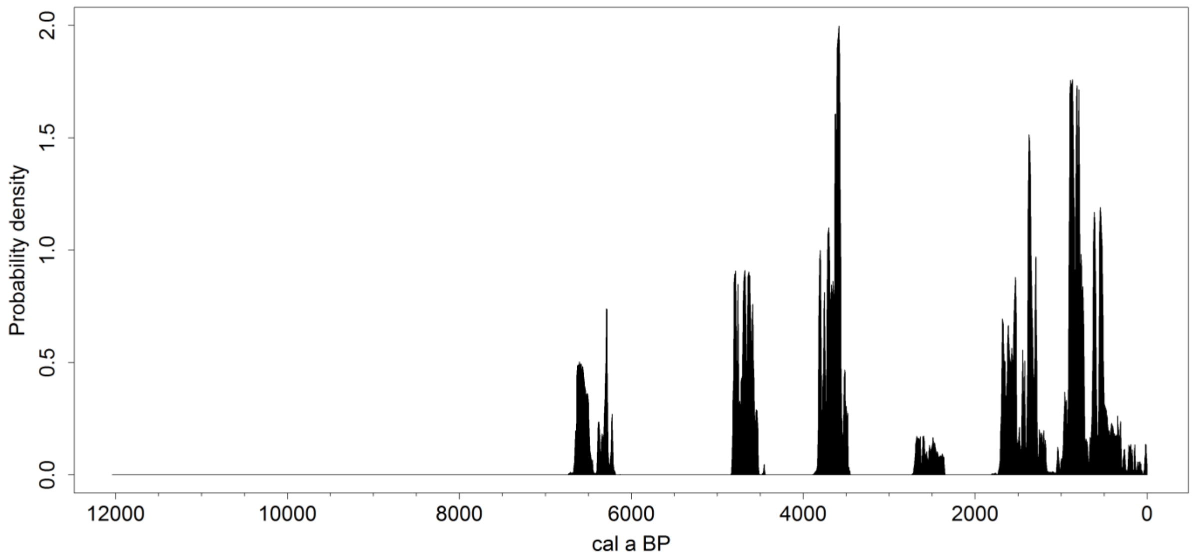

Figure 3.3. CPF of all radiocarbon ages of the top of the peat layer (n=29, 12 study sites). Probabilities were divided by the probability of equally spaced ages, and corrected for the number of radiocarbon ages per study site.

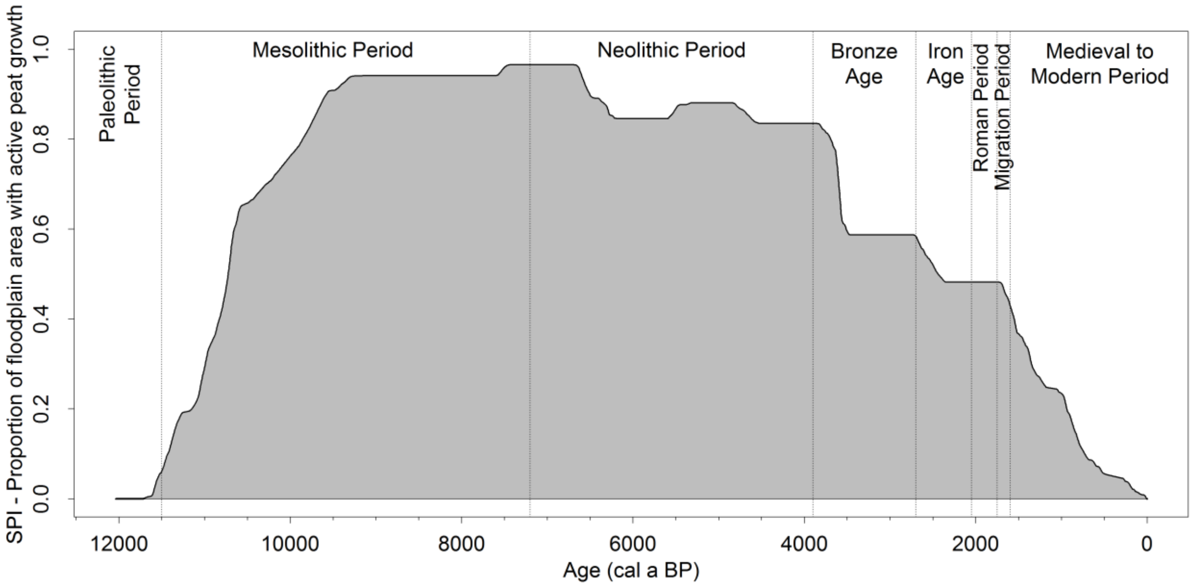

Figure 3.4. Proportion of floodplain area under active peat growth in the Dijle catchment (SPI) (n=45, 15 study sites), using equation (3.3), with indication of the different archaeological periods in the Belgian loess belt. Probabilities were divided by the probability of equally spaced ages, corrected for the number of radiocarbon ages per study site, and weighted according to the floodplain width.

3.4.2 Temporal pattern of the floodplain changes within cross-sections

The termination of peat growth not only varied between sites in the Dijle catchment, but also within a single floodplain cross-section. This within cross-section variability seems to be higher for sites where the floodplain is wider. For the 90 m wide floodplain at Sclage (Figure 3.1 and Appendix 2B), the transition from peat formation to deposition of clastic overbank deposition is rather abrupt (Figure 3.5). The end of peat accumulation ranges between 660 and 310 cal a BP, with a clear peak around 510 cal a BP.

For the 1100 m wide main trunk valley at Korbeek (Figure 3.1 and Appendix 2D), the transition from peat formation towards clastic deposition is diachronic (Figure 3.6). The top of the peat layer is dated between 2800 and 150 cal a BP, indicating that for a wide floodplain located in the downstream part of the catchment the transition from peat formation towards clastic sedimentation was diachronous.

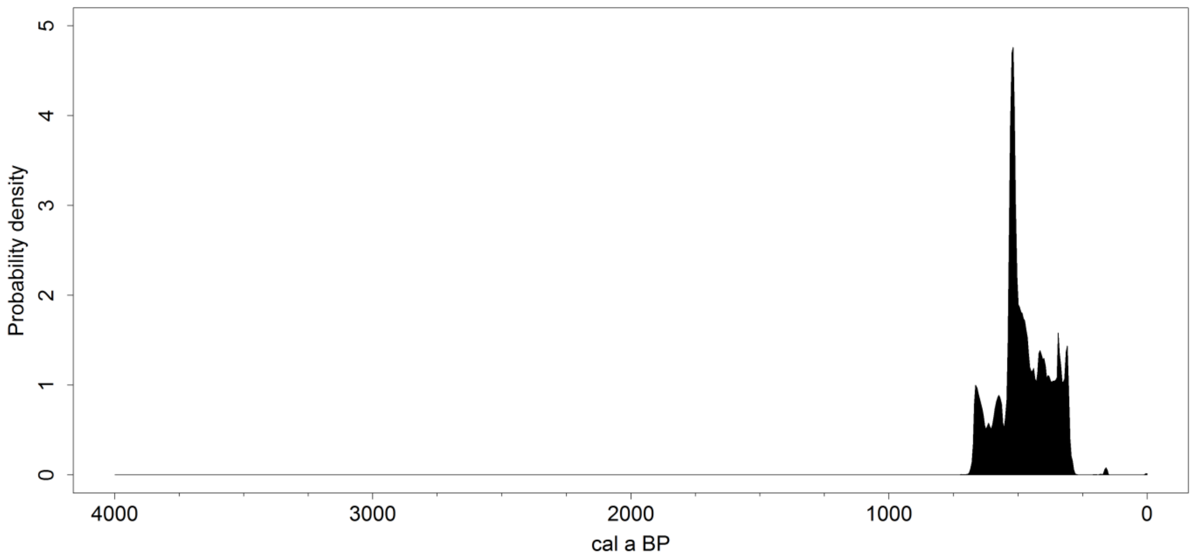

Figure 3.5. CPF of all radiocarbon ages of the top of the peat layer at Sclage, located in the headwaters of the catchment (n=6, 1 study site). Probabilities were divided by the probability of equally spaced ages.

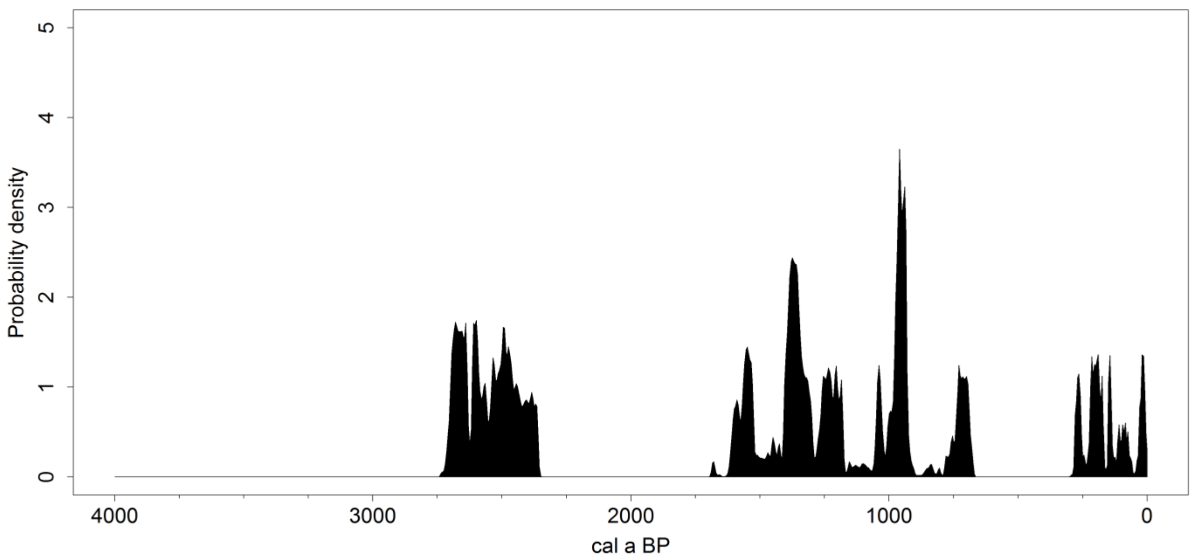

Figure 3.6. CPF of all radiocarbon ages of the top of the peat layer at Korbeek, located in the main trunk valley (n=10, 1 study site). Probabilities were divided by the probability of equally spaced ages.

3.5 Discussion

3.5.1 Catchment scale evolution

Peat growth in the floodplains of the Dijle catchment started abruptly at the beginning of the Holocene for all dated sites (Figure 3.2), which is explained by the warmer and wetter climate, vegetation development and related landscape stability during that period. Peat growth started in the lowest parts of the floodplain – typically depressions of pre-Holocene channel systems – and gradually expanded toward the edges of the floodplain with increasing filling of these depressions (e.g. Bohncke and Vandenberghe, 1991; Gibbard and Lewin, 2002). Around 9500 cal a BP, most of the contemporary floodplain areas in the Dijle catchment were under active peat growth (Figure 3.4). Between c. 9500 and 6500 cal a BP, peat growth dominated the floodplains of the Dijle catchment. During this period the floodplain was a stable marshy environment in which organic material accumulated. A well developed river channel was absent (see chapter 2 and De Smedt, 1973). Such a stable phase is reported for different catchments in West and Central Europe (e.g. see Notebaert and Verstraeten, 2010), with the exception of some large catchments (>10^4 km²) like the Rhine catchment (e.g. Hoffmann et al., 2007; Erkens, 2009). This stable phase, however, does not always correspond with peat formation, e.g. in Germany often black floodplain soils are formed during this phase (e.g. Rittweger, 2000; Houben et al., 2001).

From ca. 6500 cal a BP onwards the proportion of floodplain area with peat growth in the Dijle catchment decreases slightly in a gradual way (Figure 3.4). This period coincides with the oldest known Neolithic settlements in the region, dated around 6200 cal a BP (Crombé and Vanmontfort, 2007; Vanmontfort, 2007). At ca. 3500 cal a BP peat growth further declines, coinciding with the beginning of the Bronze Age. From ca. 2000 cal a BP (Roman Period) the decrease in peat growth is accelerating. Consequently the top of the peat layer in the Dijle catchment is clearly diachronic at the catchment scale, ranging between 6500 to 500 cal a BP (Figure 3.3). Such variations in timing of the onset of human-induced deposition have been observed in other catchments (e.g. Lang and Nolte, 1999; Kalicki, 2008; Houben et al., 2013), between closely related catchments (e.g. Brown et al., 2013) and at regional and continental scales (e.g. Notebaert and Verstraeten, 2010; Brown et al., 2013).

At present a limited part of the floodplain area in the Dijle catchment is still under active peat growth, especially in the distal parts of the wide floodplains. Given the design of SPI (equation 3.3), this recent peat formation is not included in the index. In addition there is a sampling bias, as sampling is concentrated on peat layers older than ca. 300 cal a BP.

3.5.2 Site-specific variability

The diachronic top of the peat layer in the wide floodplain (width ca. 1000 m) of the main trunk valley at Korbeek (Figure 3.6) indicates that the transition from the peat layer towards clastic deposition is not occurring at the same moment within one cross-section. While clastic sedimentation occurred close to the stream channel(s), the distal parts of the floodplain were still under active peat growth (Figure 3.7, 2500 and 1500 cal a BP panel). At the distal parts of the floodplain, peat growth could even continue until present. These observations show that the sediment supply in the floodplain gradually increased, hampering peat growth near the channel(s) by the formation of levees. Later on, when sediment input further increased, the distal parts of the floodplain were affected and the entire floodplain was dominated by the deposition of clastic sediment (Figure 3.7, >500 cal a BP panel). Consequently, the diachronic pattern of floodplain changes at the catchment scale (Figure 3.3) is at least partly caused by this diachronic top of the peat layer in the wide floodplains.

This development is different for narrow floodplains (width <100 m) located in the headwaters of the catchment. Here, the change from peat growth to clastic deposition is more abrupt (Figure 3.5), indicating that the increase in sediment input into the floodplain is high enough to trigger floodplain changes at more or less the same moment for the entire floodplain width (Figure 3.7). Radiocarbon ages are slightly older at the southern side of the floodplain (Appendix 1 and 2B), indicating that floodplain changes started at this side of the floodplain and moved rapidly to the northern side. The observed pattern of radiocarbon ages suggests that the dated terrestrial plant and wood remains are not reworked – which would cause a more random pattern. Moreover, the vertical chronology of this and other study sites in the Dijle catchment shows a logical pattern (Figure 2.9 and Notebaert et al., 2011b), suggesting the reliability of the radiocarbon ages.

3.5.3 Within catchment variability

The onset of peat growth at the beginning of the Holocene is rather consistent over the Dijle catchment (Figure 3.2 and Figure 3.8). Both in narrow and wide floodplains peat growth started from the beginning of the Holocene onwards. However, in wide floodplains in the main trunk valley, the first peat growth was confined to the incised palaeochannels and it took longer before the floodplain areas were covered by active peat growth (Figure 3.7 and Figure 3.8). Comparable results are found for the downstream part of the Scheldt catchment, where peat growth in the palaeochannels started in the same period (Meylemans et al., 2013). In the lower Scheldt valley, however, peat growth was confined to these incised palaeochannels for much longer, and only around 8000 to 5000 cal a BP did it start to spread over larger areas (Meylemans et al., 2013) (Figure 3.8).

For narrow floodplains in the headwaters of the Dijle catchment, the proportion of floodplain area with active peat growth decreases abruptly. The timing of this abrupt decrease in peat growth is different for each subcatchment, depending on the first moment of sediment input in the floodplain (Figure 3.8). For the main trunk valley, in the downstream part of the Dijle catchment, this decrease in peat growth is more gradual, due to the gradual increase of sediment in the floodplain (see above and Figure 3.7). The end of peat growth in the lower Scheldt catchment is dated between ca. 4900 and 1600 cal a BP (Meylemans et al., 2013), earlier than for the Dijle catchment (Figure 3.8). Consequently, the timing of floodplain changes depends upon location within the catchment.

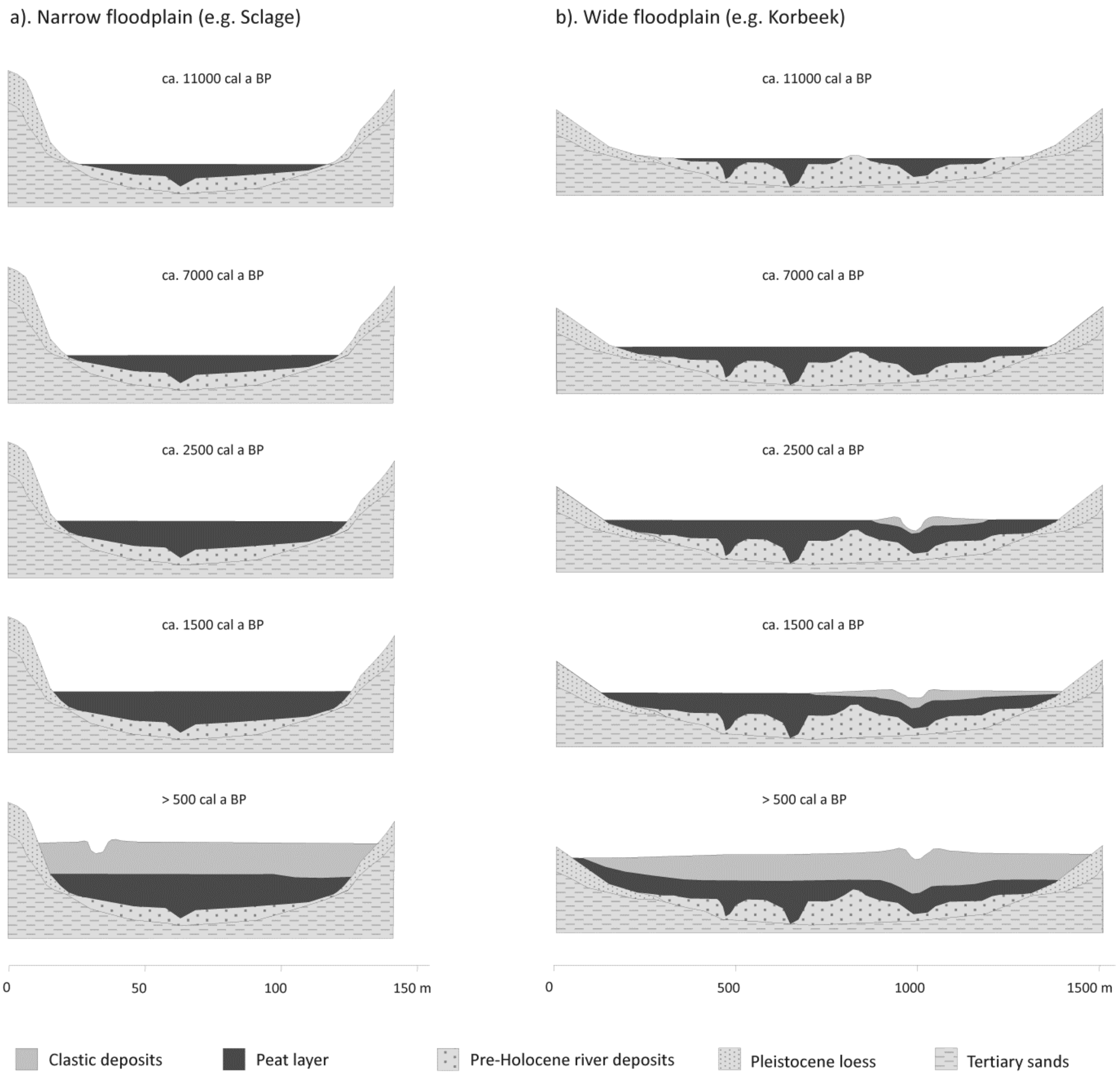

Figure 3.7. Schematic reconstruction of the peat growth and floodplain changes in a) a narrow floodplain in the headwaters of the Dijle catchment (e.g. Sclage) and b) a wide floodplain in the main trunk valley of the Dijle catchment (e.g. Korbeek).

3.5.4 The role of human impact

The gradual decrease of floodplain area with active peat growth contrasts with the abrupt climatic-driven onset of the peat growth at the beginning of the Holocene (Figure 3.4). Topography, soil properties and climate are rather homogenous in the Dijle catchment (e.g. Notebaert et al., 2011c). At the scale of small tributaries (up to 20 km²) differences in hillslope-floodplain connectivity exist, depending on site-specific geomorphologic conditions. For example, while the steep valley slopes remained under forest and could trap the majority of sediments, low-angle slopes facilitated the human exploitation of the entire floodplain-slope catena. However, at the scale of the entire catchment topography is more or less homogenous. The gradual and spatially heterogeneous decrease in peat growth (Figure 3.4) can not be entirely attributed to such topographic differences but it is hypothesized that it is mainly a consequence of the heterogeneous and gradual nature of human impact in the catchment (see section 6.2.3 and Notebaert et al., 2011c). Although the archaeological record is fragmentary, it shows that there is spatial variation in human occupation at the catchment scale, e.g. for the Neolithic and Roman Period (Crombé and Vanmontfort, 2007; Vanmontfort, 2007; Notebaert, 2009), indicating a different land cover history for different subcatchments. Consequently, the increased sediment input in the floodplain does not occur at the same instance for the different small subcatchments (Figure 2.10), initiating floodplain changes at different moments. Downstream in the catchment the human-induced increases in sediment supply accumulated and peat formation started to diminish earlier (Figure 3.7 and Figure 3.8). When human impact reached high levels in all parts of the catchment from 1500 cal a BP onwards (Notebaert et al., 2011b) active peat growth decelerated (Figure 3.4), and the entire floodplain became dominated by clastic overbank deposition (Figure 3.7). However, a more detailed archeological record and detailed and spatially integrated data on vegetation changes are necessary to fully understand the role of human impact in the observed diachronous cessation of peat growth.

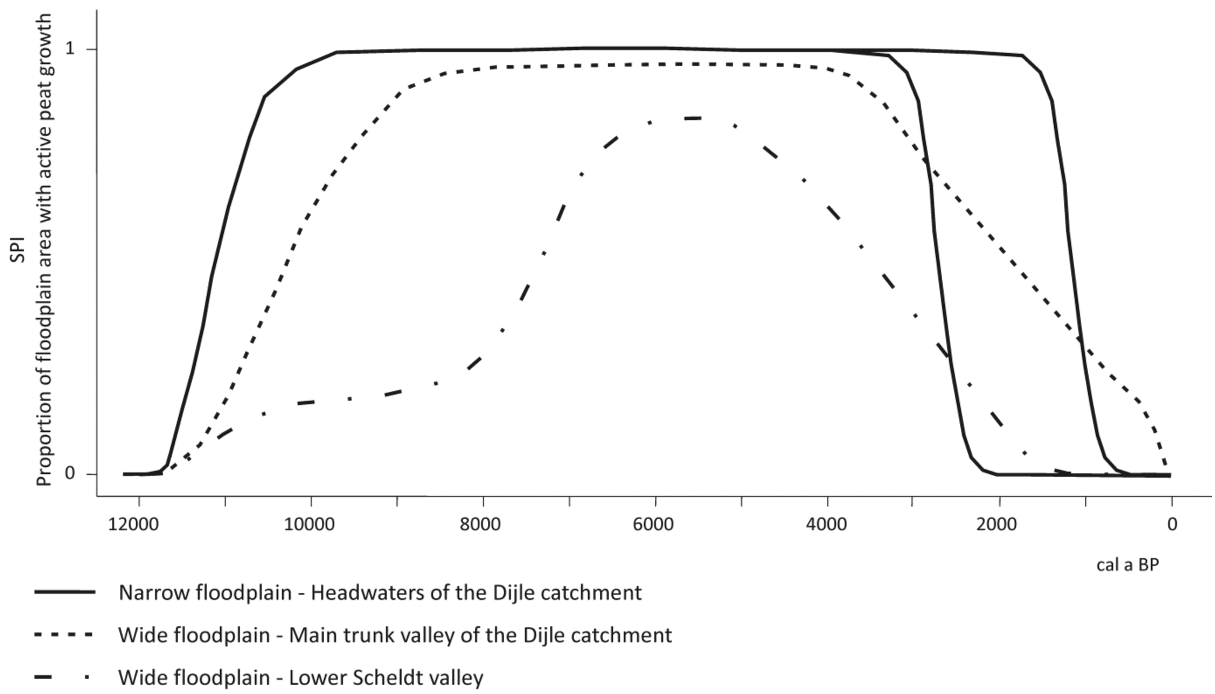

Figure 3.8. Schematic overview of the proportion of floodplain area with active peat growth for floodplains in the headwaters and main trunk valley of the Dijle catchment and the lower Scheldt valley. Data of the Scheldt valley is based on Meylemans et al. (2013).

3.5.5 Implications for palaeo-environmental studies

Dating floodplain sediments of large catchments is often based on linear extrapolations of radiocarbon ages of smaller subcatchments (e.g. see Notebaert and Verstraeten, 2010), frequently due to technical (availability of datable material), financial and time constraints. Results from the Dijle catchment show that there is spatial and temporal heterogeneity in floodplain changes, related to a heterogeneity in the driving forces (anthropogenic land use changes), but also in system properties like topography, hillslope connectivity, catchment size and floodplain characteristics. As a result, extrapolation of local dating results to the whole catchment is not justified. For example, the well dated study site near Sclage suggests an abrupt end of the peat growth around 500 cal a BP (Figure 3.5), but this study site is not representative for the changes at a catchment scale (Figure 3.3). The temporal variation within the cross-section of a wide floodplain (Figure 3.6) even shows that single core dates are insufficient to precisely date the human-induced transition at cross-section scale. Such a transition from a peaty layer to clastic deposits is often recorded in West and Central European catchments (Pastre et al., 2002; Kalis et al., 2003; Houben, 2007; Lespez et al., 2008; Notebaert et al., 2011b) and is even suggested as a boundary for the beginning of the Anthropocene Period (Brown et al., 2013). The results of this study show that there is temporal and spatial variability in this transition, at a scale of only 758 km². Multiple dated corings within one cross-section and dating results for different study sites are necessary to get full insight in the timing of this change. Interpretations based on single radiocarbon ages or based on a few study sites should be handled with caution. Detailed and spatially integrated core data and radiocarbon ages are necessary.

3.6 Conclusions

This study demonstrates that floodplain changes in the Dijle catchment are diachronous. The transition from peat formation toward clastic overbank deposition does not occur at the same moment at the catchment scale, but ranges between 6500 to 500 cal a BP. The diachronic pattern at catchment scale can partly be attributed to differences in the hillslope-floodplain connectivity and the location of the floodplain in the catchment, but it is hypothesized that it is mainly a consequence of differences in the timing and intensity of agricultural activities at catchment scale. Moreover, a well-dated cross-section of a wide floodplain suggests that floodplain changes are asynchronous at cross-section scale, caused by a gradual increasing sediment input in the floodplain that first affects the near-channel parts.

These results show that the transition from natural peaty floodplain marshes towards clastic overbank deposition is asynchronous on a catchment scale and even on the scale of single floodplain transects. Therefore, interpretations of past floodplain changes should be based on coring transects in upstream and downstream parts of the catchment in combination with a multi-core dating approach. Detailed dating results combined with detailed and spatially integrated data on the land cover history and floodplain changes are necessary to fully understand all involved driving factors.

3.7 Acknowledgements

This research has partly been funded by the Interuniversity Attraction Poles Programme IAP 07/09, initiated by the Belgian Science Policy Office. Their support is gratefully acknowledged. The authors would also like to thank Rick Assendelft, Maartje Buijs and Jesper van Schilt for their assistance during fieldwork, and Elena Marinova for the help with the identification of the datable material.

Chapter 4 Reconstruction and semi-quantification of human impact in the Dijle catchment: a palynological and statistical approach

This chapter is published as: Broothaerts N, Verstraeten G, Kasse C, Bohncke S, Notebaert B, Vandenberghe J (2014b) Reconstruction and semi-quantification of human impact in the Dijle catchment, central Belgium: a palynological and statistical approach. *Quaternary Science Reviews* 102, 96-110.

4.1 Introduction

From the Neolithic period onwards, human impact increased in many catchments in West and Central Europe through deforestation and the development of agriculture (e.g. Kalis et al., 2003; Dotterweich, 2008). As one specific result, sediment fluxes within the landscape changed (for an overview, see e.g. Notebaert and Verstraeten, 2010), and sediment supply from the hill slopes to the river systems increased and floodplain geomorphology and ecology changed (e.g. Kalis et al., 2003; Houben, 2007; De Moor and Verstraeten, 2008; Lespez et al., 2008).

this general framework of changes in sediment fluxes in relation to anthropogenic land cover changes during the Holocene is now established. Nevertheless, many uncertainties still exist. For instance, we still lack a detailed insight on the impact-response relation to fully grasp how, when and to what extent humans have changed sediment fluxes (see also chapter 1). It is for instance still uncertain which threshold levels of human impact need to be reached to increase sediment supply from hill slopes to the river system and completely alter the floodplain morphology. To identify such threshold levels and fully understand the role human impact has played to change sediment fluxes, an accurate reconstruction of the vegetation changes and quantitative measures of human impact on the landscape during the Holocene are needed (see chapter 1). Moreover such a reconstruction is necessary at a catchment scale to understand whether differences between subcatchments can be attributed to heterogeneity in the timing and nature of the driving forces or to a different response of floodplains to the same driving forces, indicating a non-linearity in the process-response relationship.

Data on land cover history can be reconstructed based on archaeological and palynological records. Traditionally, human impact has been reconstructed in pollen diagrams based on specific anthropogenic indicators in the pollen diagrams (e.g. Behre, 1981), or by changes in the vegetation composition (e.g. non-arboreal/arboreal pollen ratio) (e.g. Faegri and Iversen, 1989). These traditional interpretations of pollen data are mainly qualitative approaches, and detailed determination of causal factors or detailed comparisons of different study sites are difficult. Recently, advances in pollen studies have been made and new approaches are proposed to (semi-)quantify vegetation cover based on pollen data, such as the Multiple Scenario Approach (MSA; Bunting and Middleton, 2009) and the Landscape Reconstruction Algorithm (LRA; Sugita, 2007b; Sugita, 2007a). Although these models have been validated and successfully applied in several studies (e.g. Hellman et al., 2008; Soepboer et al., 2010), several restrictions are associated with them, limiting their use. For instance, both models rely on good approximations of pollen productivity which are not available for many regions (e.g. Brostrom et al., 1998) and the LRA is only validated for pollen data from large lakes. Alternatively, statistical analysis of pollen data has recently been used to characterize vegetation changes and to extract (semi-) quantitative data on human impact based on the entire pollen signal (e.g. Birks, 1985; Kerig and Lechterbeck, 2004; Lechterbeck et al., 2009; Lopez-Merino et al., 2012). Although these statistical techniques allow a comparison over different study sites (Lechterbeck et al., 2009), these techniques have not yet been used at the scale of an entire catchment. Reconstructing human impact at a catchment scale will help to understand (non-)linearity in the process-response relationship.

In this chapter we present a reconstruction of vegetation changes in the Dijle catchment throughout the Holocene based on palynological data of six study sites. We aim to reconstruct and semi-quantify human impact in the catchment based on statistical analyses (cluster analysis and non-metric multidimensional scaling (NMDS)) of the pollen records. NMDS is used to compare vegetation changes through time in different subcatchments of the Dijle catchment.

4.2 Study area

This study focuses on the Dijle catchment south of Leuven (758 km²), located in the central Belgium loess belt (Figure 4.1). The Dijle catchment is characterized by an undulating plateau in which several rivers are incised. The soils of the catchment are mainly Luvisols, developed in the loess deposits. Previous palynological studies in the Dijle catchment show that the catchment was mainly forested during the first half of the Holocene (Mullenders and Gullentops, 1957; Mullenders et al., 1966; De Smedt, 1973). The Linearbandkeramik arrived in the Belgian loess belt around 7200 cal a BP, however, no indications of the presence of this culture in the Dijle catchment are present (Vanmontfort, 2007). The Neolithic Period in the Belgian loess belt lasted from ca. 7200 to 3900 cal a BP (Table 2.1; CAI, 2014). The oldest known Neolithic settlement in the Dijle catchment ('Ottenburg'), located nearby study site Archennes (Figure 4.1), dates from ca. 6200 cal a BP (Crombé and Vanmontfort, 2007; Vanmontfort, 2007). The impact of the Neolithic activities in the Belgian loess belt was limited to local-scale deforestation. Neolithic clearances were small and only used for a few decades (Crombé and Vanmontfort, 2007; Vanmontfort, 2007). The Bronze Age in the Belgian loess belt lasted from ca. 3900 to 2700 cal a BP, the Iron Age from ca. 2700 to 2050 cal a BP (CAI, 2014). According to Mullenders and Gullentops (1957) and Mullenders et al. (1966), anthropogenic disturbances in the landscape became evident in the pollen assemblages from 2500 cal a BP, but these palynological data had a poor chronological control. Archaeological data for the Dijle catchment is fragmented. For the Flemish part of the catchment, an extensive database is available

(*Centrale Archeologische Inventaris* (CAI, 2014)). For the Walloon part, such a detailed database is still missing. Consequently, the archaeological data for the Walloon part is limited to overviews provided by Rommens (2006) and Notebaert (2009) (Figure 4.1). Current land use in the Dijle catchment is dominated by cropland. Half of the cropland area is used for cereal cultivation (mainly wheat; *Triticum aestivum*), half of it is used for cultivation of other crops such as Beet (*Beta vulgaris*), Maize (*Zea mays*) and Potato (*Solanum tuberosum*). In the northeast (Meerdaal Forest) and northwest (Zonien Forest) of the Dijle catchment, large deciduous plantation forests are present, dominated by *Fagus*. Historical documents indicate that these forests remained forested for several centuries, the Meerdaal Forest at least since the 14th century (Vanwalleghem et al., 2005), and the Zonien Forest at least since the 12th century (Langohr, 2001). No agricultural activities took place in these forests since the 14th century (Vanwalleghem et al., 2005). The floodplain is currently used as forest (dominated by *Alnus*) or grassland.

Within this study, six alluvial study sites were selected in the Dijle catchment (Figure 4.1). These sites are selected based on the availability of previous research and their accessibility, but mainly on their location within the catchment. Two of them (Sclage and Cortil) are located in the headwaters of the catchment. Two study sites (Archennes and Korbeek) are located in the main valley of the Dijle River, and two study sites (Sint-Agatha-Rode and Loonbeek) are located along important tributaries of the Dijle River. A more detailed description of the study area can be found in chapter 2.

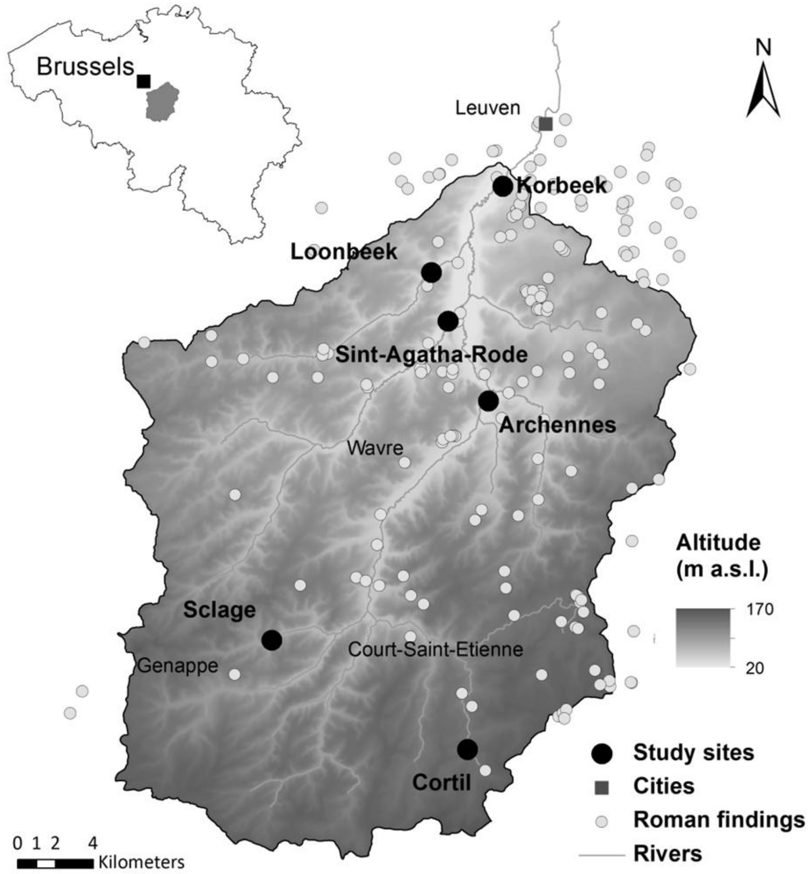

Figure 4.1. Location of the study sites in the Dijle catchment and in Belgium, with indications of Roman findings (including artefacts, remains of villas and tumuli) in and near the Dijle catchment (location of the Roman archaeological findings are based on Notebaert (2009)).

4.3 Material and Methods

4.3.1 Palynological analysis

For each alluvial study site a sediment core was collected using a gouge auger (100 cm long and a diameter of 6 cm), and a palynological analysis was performed for a selected depth range of this sediment core. Pollen samples were extracted from the sediment using a sampler of defined volume (100 mm^3 for organic rich sediments, 200 mm^3 for minorgenic sediments), and were prepared following the standard techniques of Faegri and Iversen (1989). A known quantity of *Lycopodium* spores was added. Samples were studied under a 630x and 1000x magnification using oil immersion. Nomenclature follows the keys of Moore et al. (1991), Beug (2004) and a modern reference collection were used for the identification of the pollen types. Pollen data are expressed as relative frequencies (percentages) of the pollen sum, containing the regional pollen signal. This regional pollen signal includes upland herbs, Poaceae and trees and shrubs. Wetland vegetation (e.g. *Alnus*, *Salix*, Cyperaceae and Typhaceae) and aquatics are interpreted as local vegetation and were excluded from the pollen sum. Percentage diagrams were divided into regional and local components and constructed using C2 computer program (Juggins, 2007).

4.3.2 AMS radiocarbon dating and age-depth modelling

AMS (accelerator mass spectrometry) radiocarbon dating results (Appendix 1, indicated with an asterisk) were used to provide a chronostratigraphical framework for the pollen assemblages. Each sample was sieved at 250 µm and datable material was handpicked and identified for dating. Terrestrial plant and wood remains were selected to avoid hard-water effects, reservoir effects and/or incorporation of older organic material (e.g. Törnqvist et al., 1992). Ages were calibrated using the IntCal13 calibration curve (Reimer et al., 2013) and *Oxcal 4.2* software (Ramsey, 2009). An age-depth model was established for each study site using the *clam.R* package version 2.2 (Blaauw, 2010), based on the obtained ages from the sediment core of each study site (Appendix 1). Ages obtained from other cores in the same study site were not included since floodplain evolution can be diachronous at cross-section scale (Figure 3.6). The age-depth model was established using linear interpolation between the dated levels for all six sites (Figure 2.9). These age-depth models were used to derive a timescale for the whole pollen sequence for each study site. At two study sites, the age-depth model shows age-depth inversions. In Sint-Agatha-Rode, one radiocarbon age was removed from the age-depth model based on this stratigraphical inconsistency (Figure 2.9c). For Korbeek, three radiocarbon age are in an inconsistent order. Since it is not clear how to establish a good age-depth model based on the radiocarbon ages of this study site, two age-depth models were constructed, one including all radiocarbon ages (Figure 2.9e) and one excluding the three radiocarbon ages which are in an inconsistent order (Figure 2.9f). However, also different intermediate age-depth models are possible.

4.3.3 Statistical analysis

To provide more insight in the pollen signal of the study sites and to define regional palynological zones, a hierarchical cluster analysis was applied. The regional pollen signal of all study sites were included in the cluster analysis, and percentage pollen values were used. All taxa that occurred in more than 5% of the samples were included in the cluster analysis. Pollen samples that contain a similar pollen signal were grouped together (Hammer and Harper, 2006; Birks et al., 2012). The used clustering method was 'average linkage clustering', where the distance between clusters is defined as the average of all possible distances between members of the clusters (McCune and Grace, 2002; Hammer and Harper, 2006). The distance between two clusters was defined as the Euclidean distance. To preserve the hierarchy of the clusters, the resulting cluster tree was first split into a set of larger groups (indicated with numbers), and thereafter subdivided into smaller clusters (indicated with letters).

Non-metric multidimensional scaling (NMDS) was used to gain more insights into the changes in the pollen records through time and to compare the pollen record over the different study sites. NMDS is an unconstrained ordination technique which is useful to provide views into a high-dimensional dataset. The technique was developed by Shepard (Shepard, 1962a; Shepard, 1962b) and Kruskal (1964) and has successfully been applied to pollen data in previous studies (e.g. Oswald et al., 2007; Ghilardi and O'Connell, 2013). Full explanation of the application of NMDS is provided by Legendre and Legendre (1983) and McCune and Grace (2002). NMDS has several advantages compared with other ordination techniques applied to pollen data such as principal components analysis (PCA; e.g. Lopez-Merino et al., 2012; Etienne et al., 2013) and canonical correspondence analysis (CCA; e.g. Lechterbeck et al., 2009). According to Minchin (1987) NMDS is the most robust unconstrained ordination method in ecology. NMDS avoids the assumption of a linear response model (like PCA) or a unimodal response model (like CCA) between the pollen-types and the underlying environmental gradients, and avoids the requirement of normality of data. Moreover, since in NMDS a limited number of axes are chosen prior to the analysis, there are no hidden axes of variation unlike other ordination techniques (Legendre and Legendre, 1983; McCune and Grace, 2002). In this study, NMDS was performed in *R* software using package *vegan* (Oksanen et al., 2012). Bray-Curtis dissimilarity was used to calculate the distance matrix for ordination. The analysis included all regional pollen samples from all study sites. All taxa that occurred in more than 5% of the samples were included. Percentage pollen values were used. If the pollen values were larger than common abundance class scales, a Wisconsin double standardization and a square-root transformation were performed in *vegan*. An appropriate number of dimensions was determined by plotting final stress (an inverse measure of fit to the data; McCune and Grace, 2002) versus the number of dimensions, in a so-called scree plot (Figure 4.2). The obtained scree plot (Figure 4.2) shows that two axes provide a greater reduction in stress than higher number of axes, which illustrates that a two dimensional solution is best for this dataset. The two dimensional solution corresponds with a stress value of 14. According to Kruskal (1964) and McCune and Grace (2002), a stress value between 10 and 15 is satisfactory and will result in a usable ordination. Therefore, a two dimensional ordination was performed in this study. The scores of the NMDS were plotted in function of time, using the timescale constructed for each pollen sequence. For the time frame for which data of at least 2 study sites are available, average NMDS scores and standard deviation were calculated based on the scores of all study sites, except Korbeek, with a time step of 200 year. Korbeek was left out since this study site has a poor chronological control. The standard error of the mean was estimated by dividing the standard deviation by the square root of the sample size.

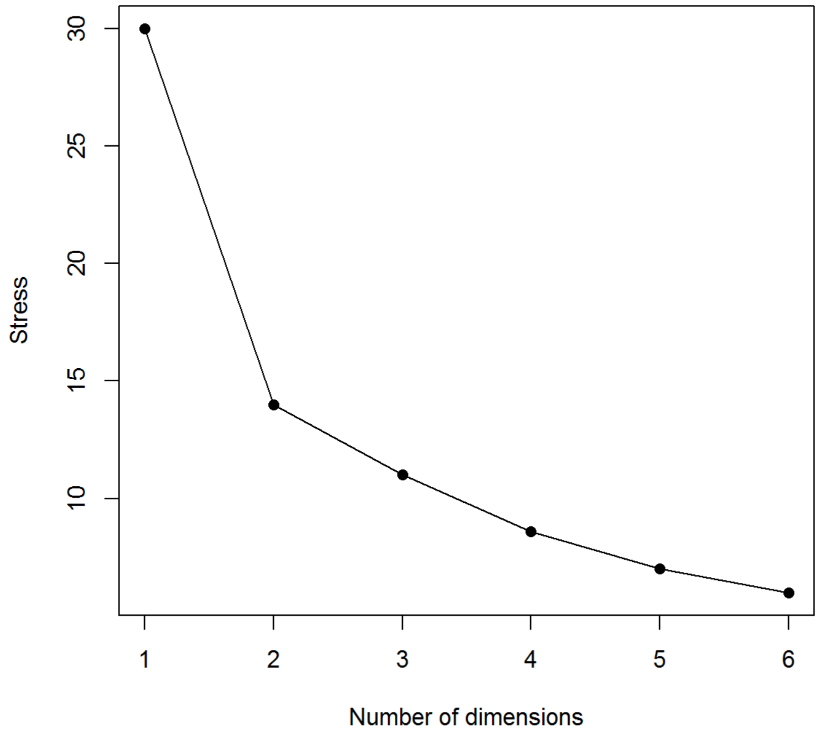

Figure 4.2. Scree plot, showing stress (an inverse measure of fit to the data) as a function of the number of dimensions.

4.4 Results

4.4.1 Regional vegetation in the Dijle catchment

The regional pollen signal for all study sites can be split in four major clusters (Figures 4.3 and 4.4). Cluster 1 contains low values of arboreal pollen (AP) and high values of non-arboreal pollen (NAP) including high values of Poaceae, upland herbs and anthropogenic indicators (which are pollen of cultivated plants, e.g. Cereal-type, or plants which are supported by human activities, e.g. *Centaurea cyanus* and *Plantago lanceolata*). This first cluster can be split in three subclusters A, B and C. Cluster 1B contains highest values of NAP and lowest values of AP, and is found in the most recent phases of the pollen diagrams (Figure 4.3). In cluster 1A, values of NAP are relatively lower and values of AP are relatively higher (dominated by *Quercus* and *Corylus*). Cluster 1C is characterized by especially high values of Asteraceae (> 50%; relative frequencies of the regional pollen sum), consequently also NAP values are very high (> 70%). This cluster 1C is less important as it only contains 3 pollen samples (Figure 4.4). CHAR, PAR and floodplain accumulation rates are mainly increasing from the beginning of cluster 1 onwards (Figure 4.3). Cluster 2 contains low values of NAP and high values of AP, especially high values of *Quercus*, *Corylus* and *Tilia*. This cluster is mainly present in the oldest parts of the pollen diagrams (Figure 4.3). Cluster 3 is characterized by high values of Poaceae, *Pinus* and *Betula*. Most other pollen types are low in this cluster 3. Finally, cluster 4 contains very high values of *Pinus* (> 80 %). This cluster is only present in the study site Sint-Agatha-Rode (Figure 4.3).

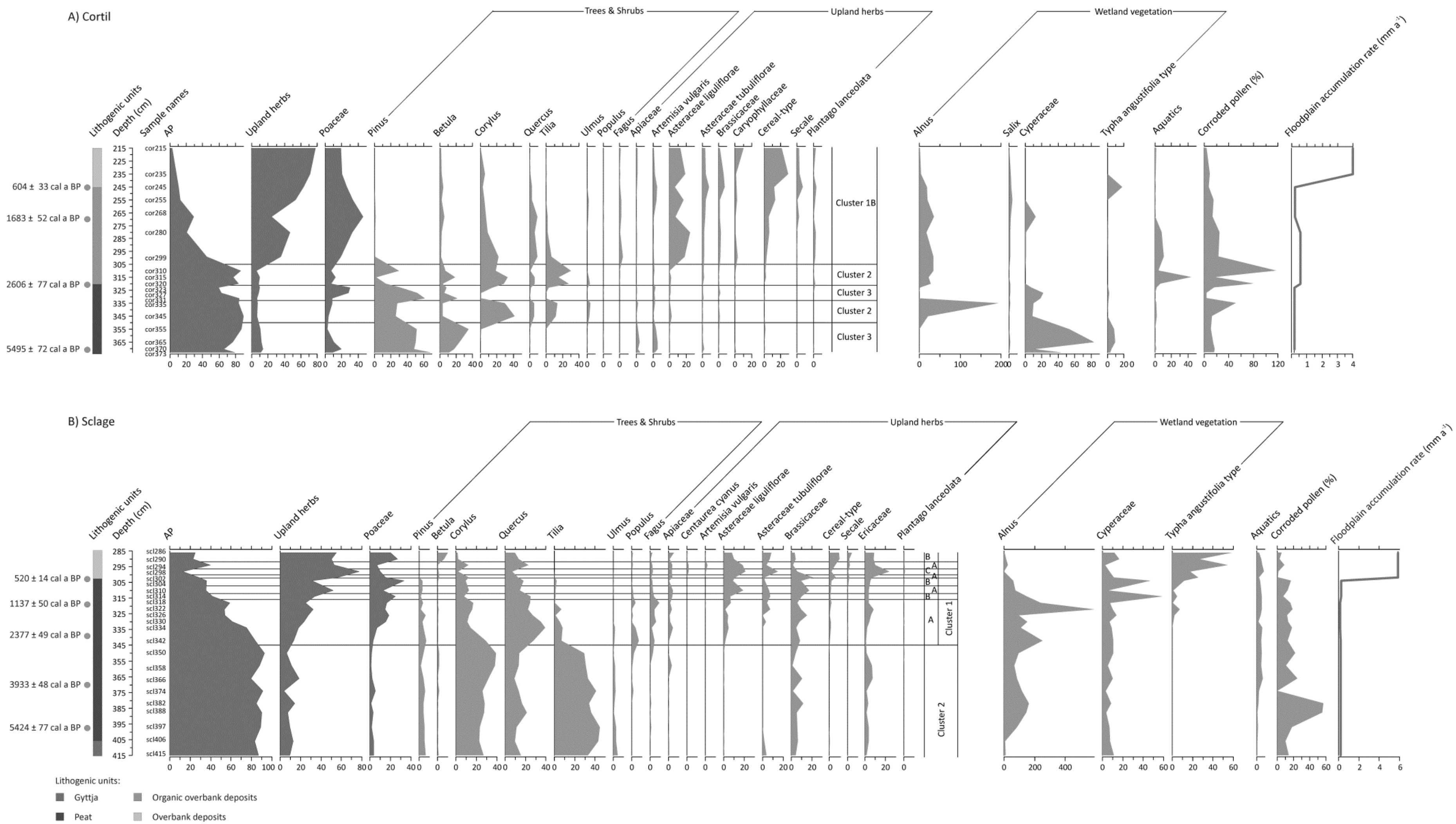

Figure 4.3. Simplified pollen diagrams from study sites (a) Cortil, (b) Sclage, (c) Sint-Agatha-Rode, (d) Korbeek, (e) Archennes and (f) Loonbeek; with indications of the different clusters (Figure 4.4). Pollen data are expressed as relative frequencies (percentages) of the regional pollen sum (including upland herbs, Poaceae and trees and shrubs).

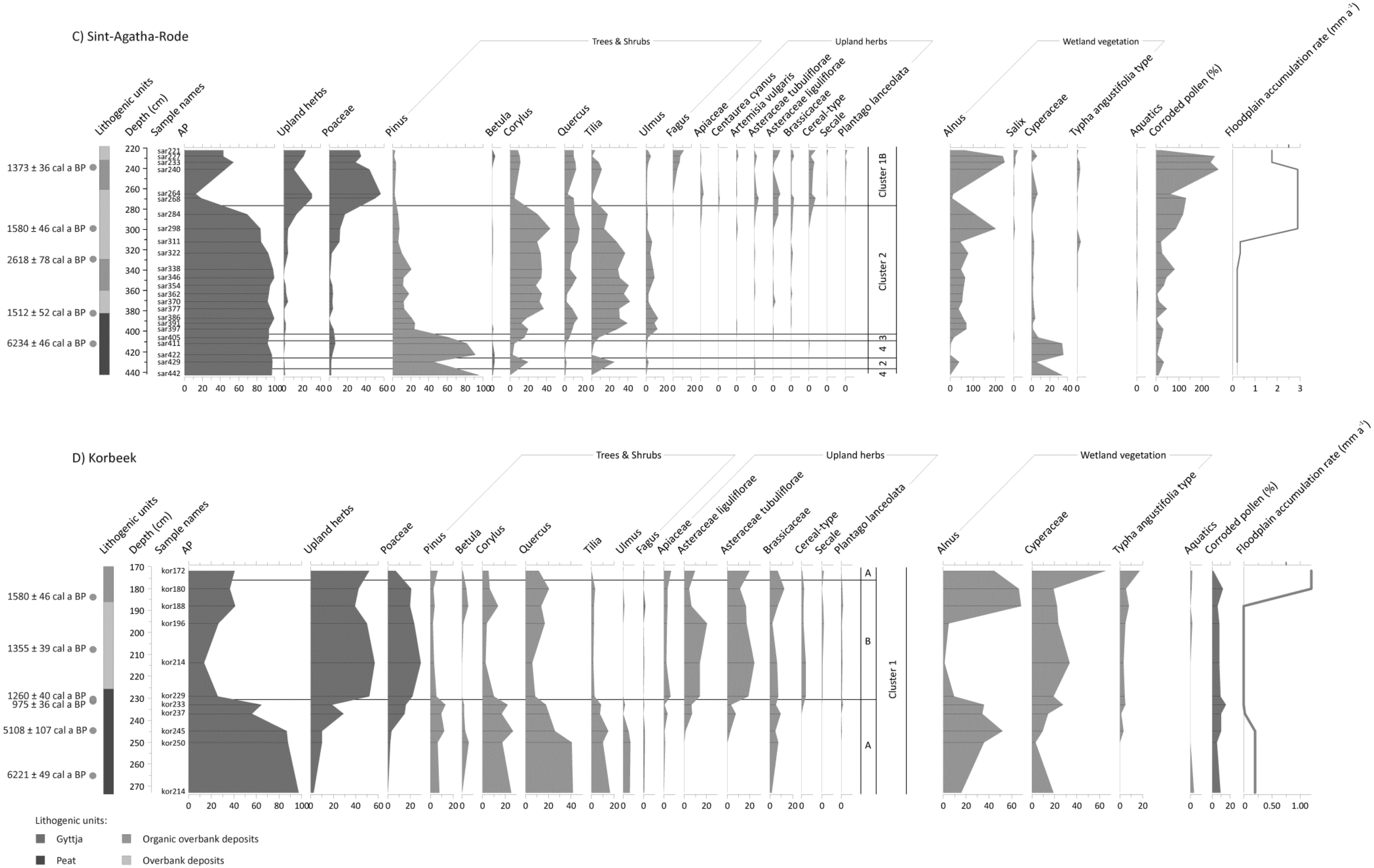

Figure 4.3. Cont.

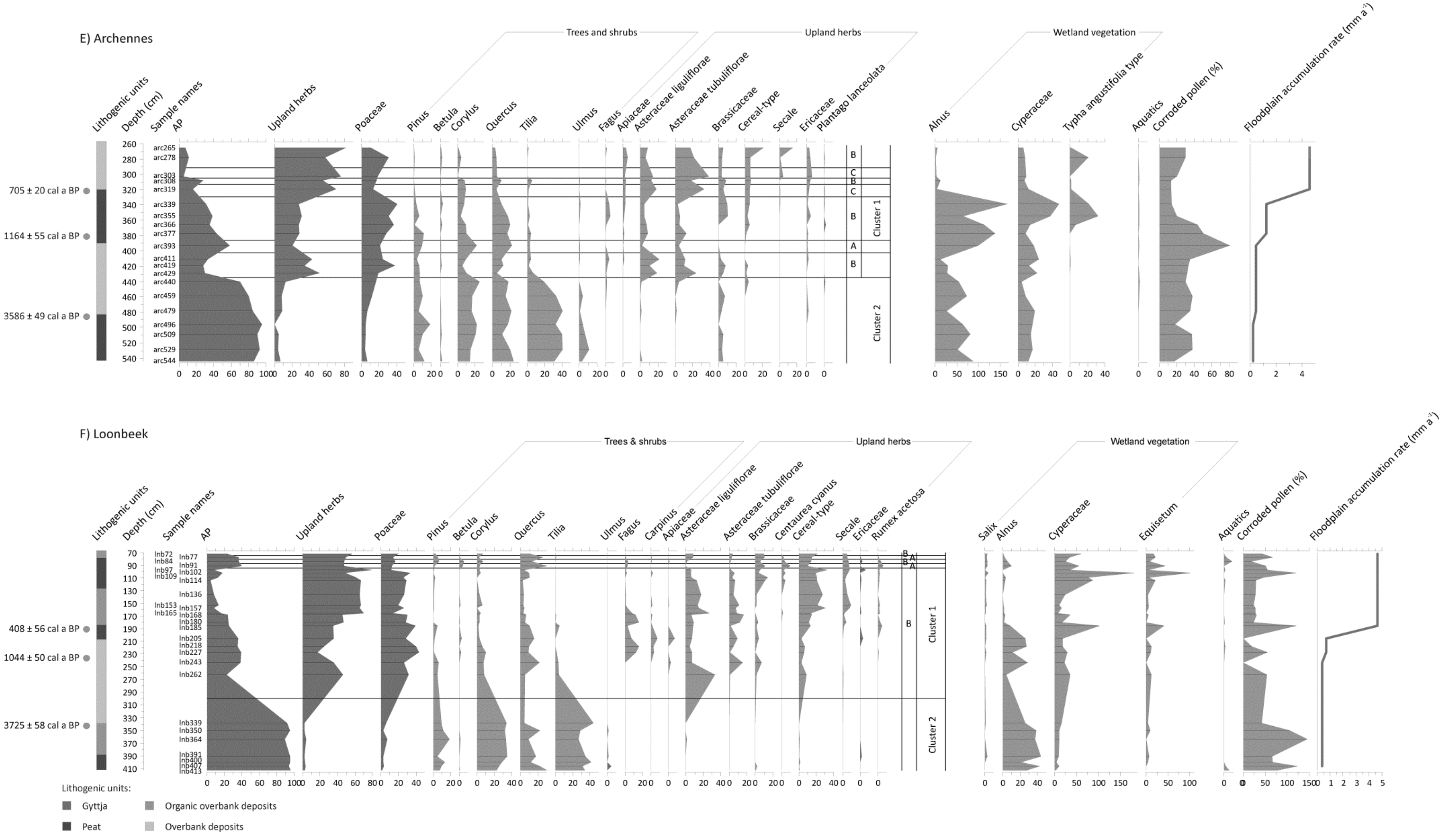

Figure 4.3. Cont.

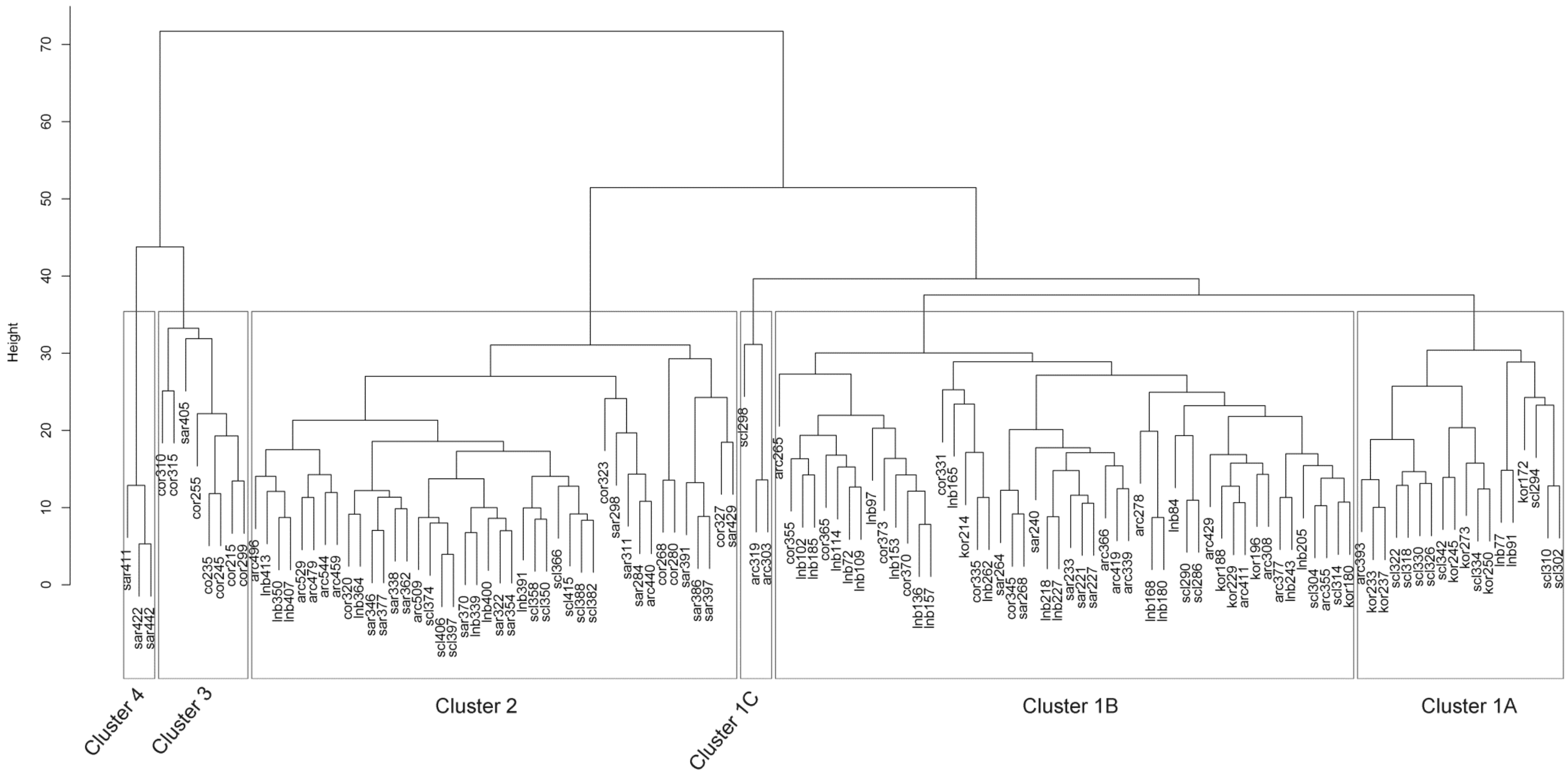

Figure 4.4. Clustering tree for the regional pollen signal from all study sites. Sample names are indicated by the name of the study site and the sample depth (see Figure 4.3). The height of each branch represents the distance between the two objects being connected.

4.4.2 Non-metric multidimensional scaling of the pollen data

A detailed view on the scores on axis 1 (Figure 4.5 and 4.6a) shows that most tree pollen-types, such as *Ulmus*, *Tilia*, *Corylus*, *Pinus*, *Acer* and *Quercus*, have low negative scores on axis 1. *Betula*, *Fraxinus* and *Populus*, possibly related to riparian environments, have scores close to zero. Only *Fagus* has a high positive score. *Fagus* has previously been reported to profit from clearing activities as it is a shade tolerant tree, and the Holocene expansion of *Fagus* has often been associated with human activities (see e.g. Kalis et al., 2003; Tinner and Lotter, 2006; Bradshaw, 2008). On the other hand, all non-arboreal pollen-types have positive scores. Cultural indicators, such as *Centaurea cyanus*, *Secale*, *Plantago lanceolata* and Cereal-type, have the highest scores on axis 1. Consequently, negative scores on axis 1 indicate forested landscapes while positive scores indicate deforested landscapes, related with human activities. We assume therefore that the scores on axis 1 can be seen as an indicator for human impact. High scores on axis 1 represent high human impact, and low scores on axis 1 represent low human impact.

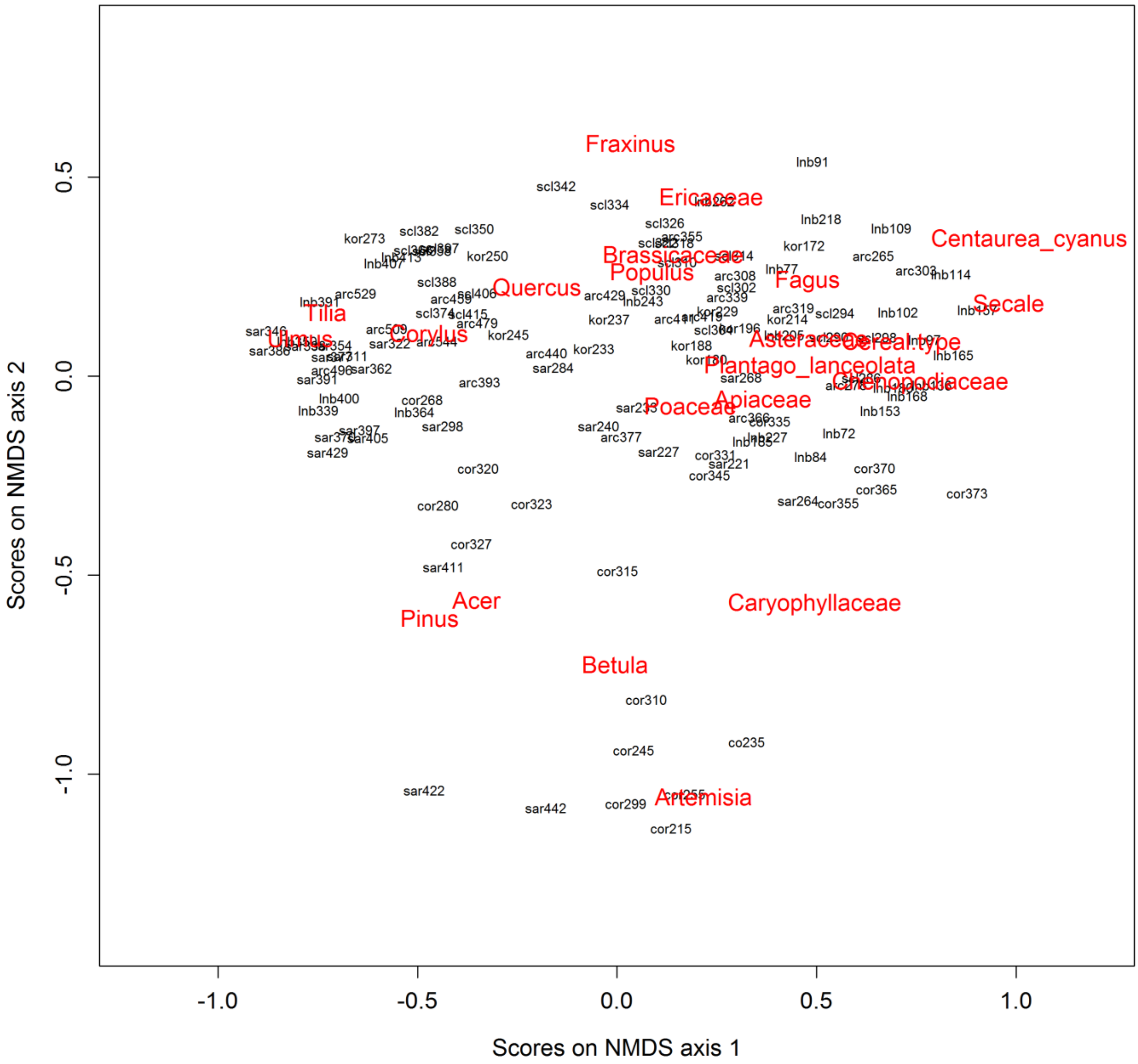

Figure 4.5. Non-metric multidimensional scaling of pollen types (red text) and pollen samples (black numbers) from all six study sites. Samples names are indicated by the name of the study site and the sample depth (see Figure 4.3).

A detailed view on the scores on axis 2 (Figure 4.5 and 4.6b) shows a less obvious pattern. Nevertheless, some trends are present. *Betula, Acer* and *Pinus* have low negative scores, while *Fraxinus*, *Fagus*, *Populus*, *Quercus*, *Tilia* and *Corylus* have high positive scores. This suggests that the scores on axis 2 can be seen as an indicator for variations in forest composition.

Consequently, some pollen types are grouped and plotted together in the NMDS ordination plot (Figure 4.5). First, deciduous forest types such as *Ulmus*, *Tilia*, *Corylus* and *Quercus* are plotted together. They have low scores on NMDS axis 1, and scores closed to zero on axis 2. Second, anthropogenic indicators such as *Centaurea cyanus*, *Secale* and Cereal-type have high scores on axis 1 and are consequently plotted at the other side of the ordination space. Poaceae, Asteraceae, and *Plantago lanceolata*, all related with grassland, are also plotted together, in the middle of the ordination plot. *Betula*, *Pinus, Acer* and *Artemisia* on the other hand, have all low scores on axis 2 and are plotted together.

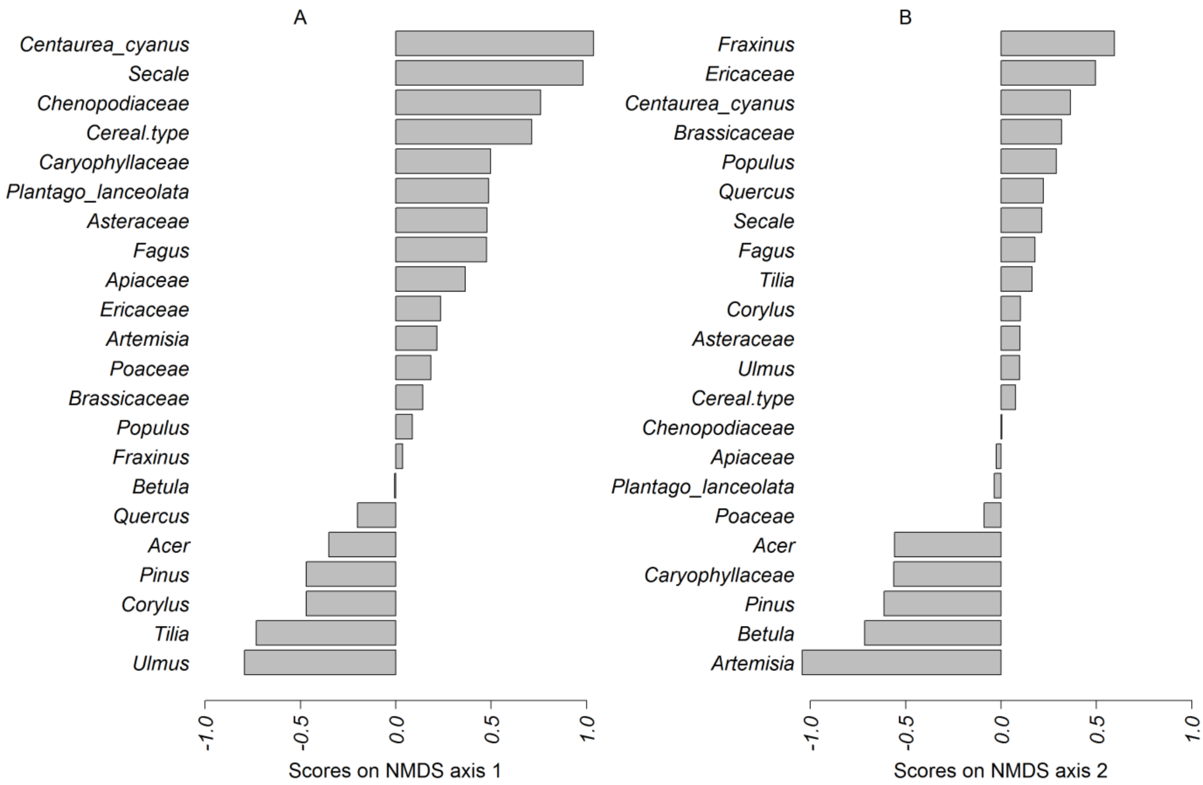

Figure 4.6. Scores on (A) NMDS axis 1 and (B) NMDS axis 2 for pollen types of all study sites.

The trajectories of pollen records through time illustrate the shift in the vegetation composition through time in the different study sites (Figure 4.7). The study sites Sclage, Korbeek, Archennes and Loonbeek show similar trajectories (Figure 4.7), suggesting that these sites also experienced similar vegetation changes. These study sites evolve from low scores on axis 1 (where *Quercus*, *Corylus*, *Tilia* and *Ulmus* are positioned) to high scores on axis 1 (where anthropogenic indicators are positioned). The study sites near Cortil and Sint-Agatha-Rode show different vegetation changes (Figure 4.3). Their trajectories (Figure 4.7) first fluctuate between low scores on axis 1 (*Quercus*, *Corylus*, etc.) and low negative scores on axis 2 (where *Pinus* and *Betula* are positioned). Afterwards, they show the same trajectory as the other study sites and they shift towards high scores on axis 1 (Figure 4.7).

The scores on NMDS axis 1 are plotted in function of time (Figure 4.8), based on the age-depth models (Figure 2.9). Since the scores on the first axis can be seen as an indicator for human impact (Figure 4.6a), plotting the scores on NMDS axis 1 in function of time can be used to study the evolution of human impact through time. The average score over all study sites (Figure 4.8g) shows lowest values on axis 1 between ca. 6500 and 3800 cal a BP. From ca. 3800 cal a BP, this average score is increasing, coinciding with the beginning of the Bronze Age. This increase continues through the Iron Age and the Early Roman period. After the Roman period, between ca. 1900 and 1600 cal a BP, the average score stagnates. Finally, a strong increase in the average score is occurring from ca. 1600 cal a BP onwards, and reaches highest levels at the end of the pollen analysis, around 500 cal a BP. The scores of the individual study sites show more or less the same trends, although some site-specific variations are present. The variation between the study sites is indicated by the standard deviation (Figure 4.8g), which is large between 5500 and 1500 cal a BP, and lower between 1500 and 500 cal a BP. The trend of study site Sclage is rather similar to the average trend (Figure 4.8), however the first increase in scores on axis 1 occurred around 2700 cal a BP, later than the average trend. At study site Cortil, variations in the scores on axis 1 are present between 6000 and 2500 cal a BP (Figure 4.8a). The long-term increase in scores on axis 1 occurs around 2300 cal a BP at Cortil. Next, also study sites Archennes and Loonbeek show similar trends (Figure 4.8e and f). In Archennes scores on axis 1 are lower than the average during the Neolithic Period. A first increase in scores is observed from 3800 cal a BP onward. Between 1900 and 1600 cal a BP, a remarkable decrease in scores is observed. Loonbeek shows the same trends, but the timing of the increase in scores is less known due to a gap in the pollen data, leading to a gap in the vegetation reconstruction for the time-range 3500 to 2000 cal a BP. In Sint-Agatha-Rode, the start of the increase in scores on axis 1 occurs late, only around 1600 cal a BP (Figure 4.8c). In Korbeek, this increase is less well dated. The two age-depth models which have been constructed (see Figure 2.9e and f), resulted in two different curves (Figure 4.8a). It is uncertain which curve is the best, due to the uncertainties on the age-depth model of Korbeek. Moreover, different intermediate curves are also possible. Consequently, the timing of the increase in scores on NMDS axis 1 is uncertain, and ranges between 4500 and 1500 cal a BP.

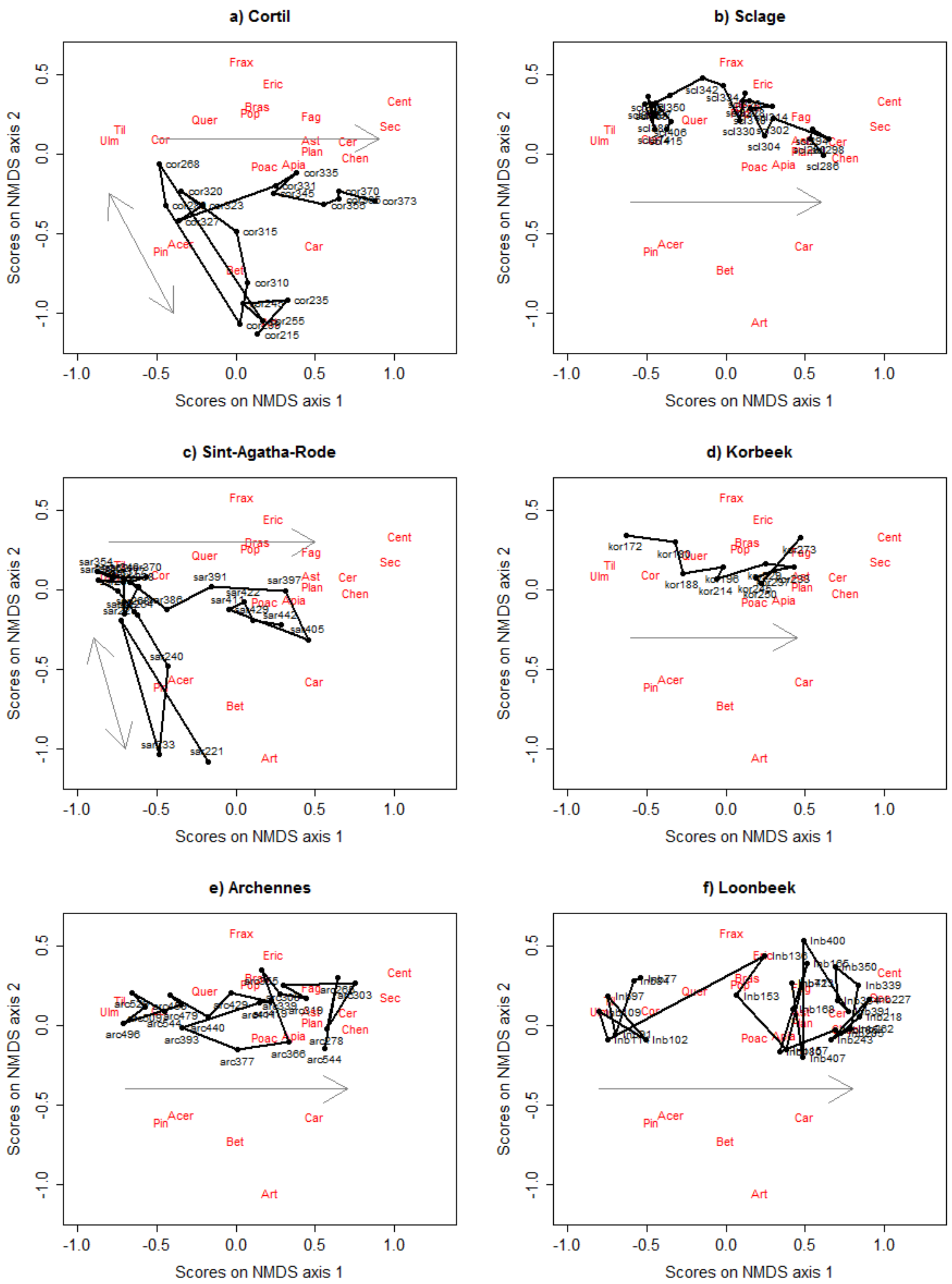

Figure 4.7. Non-metric multidimensional scaling of pollen types (red text) and pollen samples (black dots) of the different study sites. Sample names are indicated by the name of the study site and the sample depth (see Figure 4.3). Arrows illustrate the trajectories of the pollen samples through time.

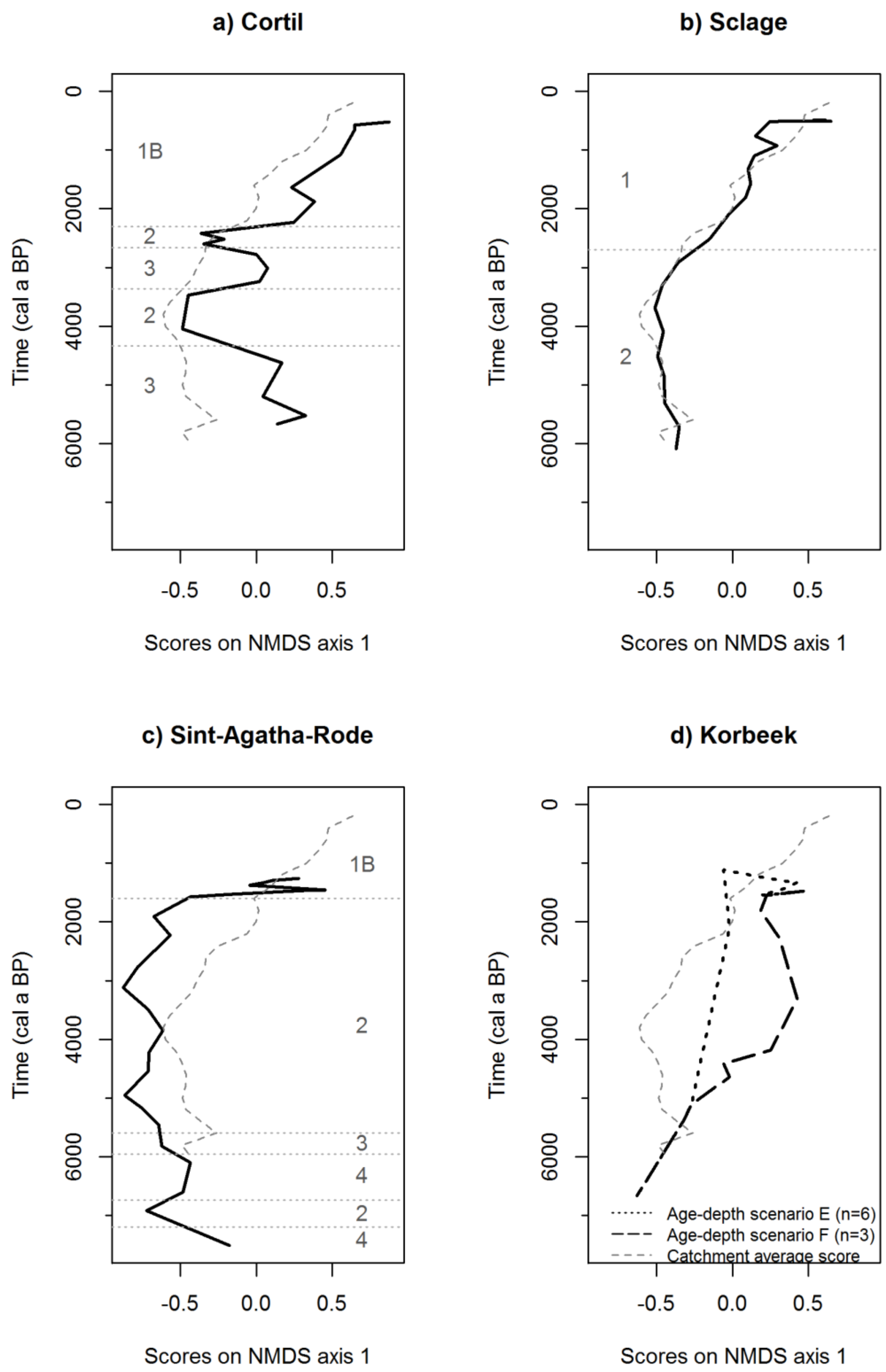

Figure 4.8. Scores on NMDS axis 1 plotted against time for (a – f) the 6 study sites with indication of the different clusters (Figure 4.4) and (g) the catchment average score for the five study sites (Korbeek was left out), standard error of the mean and standard deviation, with indication of the different archaeological periods in the Belgian loess belt. In (d) Korbeek, two scenarios are shown, based on two age-depth scenarios: E, including all dating results (n=6); and F, excluding age-depth inversions (n=3) (see Figure 2.9). The dotted grey line in (a – f) represents the average score

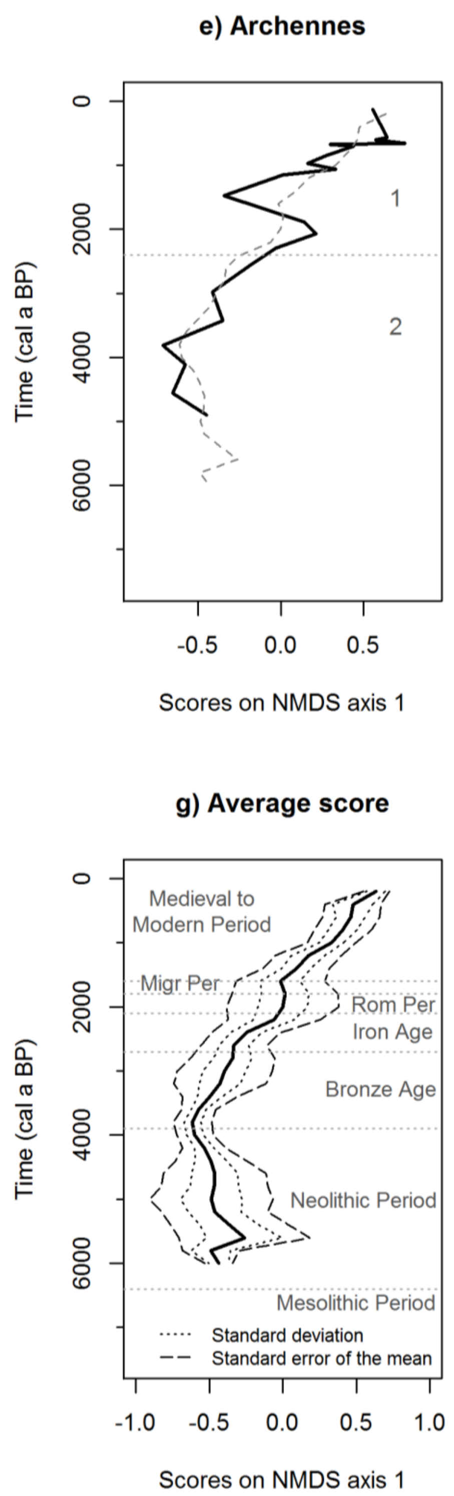

Figure 4.8. Cont.

4.5 Discussion

4.5.1 Vegetation changes in the Dijle catchment

The reconstruction of the vegetation changes in the Dijle catchment dates back to ca. 6500 cal a BP. The pollen diagrams and cluster analysis (Figure 4.3) and the NMDS (Figure 4.7) show that the vegetation changes for the different study sites were rather similar in pattern. During the Middle Holocene the Dijle catchment was mainly covered by deciduous forest, dominated by *Corylus*, *Tilia* and *Quercus* (Cluster 2) (Figure 4.3). Anthropogenic indicators were absent or present in only very low quantities, resulting in low scores on NMDS axis 1 (Figure 4.5 and 4.6) indicating that human impact in the landscape was limited or only affecting the vegetation at a small scale. The vegetation in the different study sites changed gradually from the deciduous forest (cluster 2) towards an intensively cultivated landscape (cluster 1) (Figure 4.3). The AP fraction decreased and more upland herbs, Poaceae and anthropogenic indicators appeared. This resulted in high scores on NMDS axis 1, indicating high human impact during that period (Figures 4.5 and 4.6).

Beside these general vegetation changes, some variations among the different study sites existed. First, in Cortil a variation was present between high values of *Pinus*, *Betula* and Poaceae (cluster 3) and high values of *Quercus*, *Corylus* and *Tilia* (cluster 2) (Figure 4.3a and 4.7a). This resulted in variations in the human-impact curves, dated between ca. 6000 and 2500 cal a BP (Figure 4.8a). This can be interpreted as variations in forest composition, possibly caused by human-induced forest clearance during cluster 3 and forest regrowth during cluster 2. Similar patterns are observed in Sint-Agatha-Rode, with variations between cluster 2 and cluster 3 and 4 (very high values of *Pinus*) (Figures 4.3c and 4.7c). Next, in Korbeek cluster 2 was not present. Instead, a variation can be observed between cluster 1A, representing moderate human impact, and cluster 1B, representing very high human impact (Figure 4.3d). Also in other study sites variations between cluster 1A and cluster 1B can be observed, representing variations in human impact (Figure 4.3).

4.5.2 Increasing human impact in the Dijle catchment: chronology and intensity

The overall pattern of the changing human impact through time (Figure 4.8g) shows that the pollen records and the NMDS analysis do not detect Mesolithic or Neolithic human activities in the Dijle catchment. This can be seen as a confirmation of the absence of wide-scale settlements or clearings during the Neolithic Period and the absence of Linearbandkeramik communities in the Dijle catchment. The Neolithic human activities could, however, have been localized and limited to local-scale clearings (e.g. Crombé and Vanmontfort, 2007; Vanmontfort, 2007; Bakels, 2009), since such local disturbances were hardly connected with the fluvial system (e.g. Notebaert et al., 2011b; Houben et al., 2013) and pollen of e.g. anthropogenic indicators are not easily represented in pollen records from alluvial study sites. Consequently, pollen records from alluvial sites are not always an appropriate tool to detect Neolithic human activities (see e.g. Kalis et al., 2003). Quantitative and spatially distributed data of archeological findings for the entire Belgian loess belt is still lacking. However, our data can be compared with radiocarbon databases of the nearby Paris basin and the lower Rhineland-Hesse region, indicating low population density at the end of the six millennium and most of the fifth millennium (between ca. 6500 and 4000 cal a BP) (Shennan et al., 2013), which is the same period which shows low human impact in the Dijle catchment (Figure 4.8g). Beside the general trend of low human impact during the Mesolithic and Neolithic Period, some small variations are present in the average pattern (Figure 4.8g). The peak in the average score around 5500 cal a BP is caused by higher scores in Cortil (Figure 4.8a), related with variations in forest composition.

From ca. 3900 cal a BP onwards, the beginning of the Bronze Age in the Belgian loess belt, the pollen records show decreasing AP values, increasing values of anthropogenic indicators (Figure 4.3) and consequently increasing NMDS scores representing increasing human impact (Figure 4.8). Population densities in central Europe increased from the Bronze Age onwards (Zimmermann et al., 2009). Also archeological findings in the Dijle catchment from this period are more common (Rommens, 2006). Time-differentiated sediment budgets for the Dijle (Notebaert et al., 2011b) and Nethen catchment (Verstraeten et al., 2009b) indicated an increase in anthropogenic erosion and colluviation from the Bronze Age onwards. The increasing human impact (Figure 4.8) continued through the Iron Age and the Early Roman period, beside a stabilization in human impact around the transition from Bronze Age to Iron Age (ca. 2800 – 2600 cal a BP). At this transition, population densities in central Europe were decreasing (Zimmermann et al., 2009) and fewer archaeological findings in the Dijle catchment are reported (CAI, 2014). Similar trends in increasing human impact from the Bronze Age onwards are observed from pollen diagrams in other areas in West and Central Europe, e.g. in Germany (Kalis et al., 2003; Kerig and Lechterbeck, 2004) and in France (Pastre et al., 2002).

Between ca. 1900 and 1600 cal a BP, human impact in the catchment stagnated (Figure 4.8) which can possibly be related to a decreased population density and human impact in Europe during the Migration Period (Dotterweich, 2008; Zimmermann et al., 2009), dated between ca. 1750 and 1600 cal a BP (Buntgen et al., 2011). This stagnation in human impact is visible in all study sites, and is even represented by a sharp decrease in scores on axis 1 in e.g. Archennes and Loonbeek (Figures 4.8e and f). A similar drop in human impact during the Migration Period is observed in pollen records from the Loess area in Germany (Lechterbeck et al., 2009). Finally, a larger increase in human impact occurred from ca. 1600 cal a BP onwards during the Medieval Period, and reached its highest levels at the end of the pollen analysis, around 500 cal a BP (Figure 4.8).

The individual study sites differ at some points from this general pattern of increasing human impact in the catchment (Figure 4.8). In the headwaters (Sclage and Cortil), the increase in human impact occurred later than the average of the catchment, around 2700 cal a BP at Sclage and around 2300 cal a BP at Cortil (Figure 4.8a and b and Table 4.1). Also differences in intensity of human impact can be observed between these two study sites. Human impact in the last 2500 years is higher in Cortil than in Sclage (Figure 4.8a and b). This is in agreement with the higher concentration of archaeological findings from the Roman Period in the surroundings of Cortil (Figure 4.1), although the archeological record for the Dijle catchment is fragmentary. The evolution of human impact in Archennes and in Loonbeek is comparable and shows similar trends as the average of the catchment (Figure 4.8e and f). The changes in vegetation and increase in human impact is dated around 2400 cal a BP in Archennes (Table 4.1). For Loonbeek, the timing is less clear due to a gap in the vegetation reconstruction and the increase in human impact ranges between 3500 to 2000 cal a BP. In Loonbeek, a decrease in human impact is observed in the last 300 years, which can possibly be related to the reforestation in the Zonien forest, a large deciduous plantation forest in the subcatchment of this study site. The late increase in human impact in study site Sint-Agatha-Rode (around 1600 cal a BP; Table 4.1), which is closely located to study sites Archennes and Loonbeek (Figure 4.1), cannot be explained by the specific geomorphological conditions at this study site as the geomorphology is homogenous at the scale of the Dijle catchment. Nor it can be explained with our current knowledge of the archaeological record; it cannot be related to differences in occupation history (Figure 4.1). However, the toponym 'Rode' can indicate a late deforestation phase. Finally, in Korbeek, two different scenarios are proposed for the increase in human impact, due to the absence of a precise chronostratigraphical framework. When including all available radiocarbon ages in the age-depth model, human impact remained stable during the largest part of the investigated period. Only around 1500 cal a BP, human impact clearly increased. When excluding three radiocarbon ages which are in an inconsistent order (Figure 2.9), human impact in Korbeek Dijle increased from 4500 cal a BP onwards. Consequently, the timing of the change in vegetation and increase in human impact ranges between 4500 and 1500 cal a BP (Table 4.1).

Overall, the increase in human impact seems to have been gradual, as can be observed from the pollen data (Figure 4.3), and the human-impact curves (Figure 4.8). The general vegetation changes are similar among the different subcatchments, although some variations are present. Especially between 5500 and 1500 cal a BP, this variation is large (Figure 4.8g), indicating that the intensity and timing of the increasing human impact differ between the study sites in this period (Table 4.1). In order to relate these differences to the archeological record (including quantification of occupation history), a more extensive database of archeological findings for the Dijle catchment and the entire Belgian loess belt is necessary.

NMDS seems to be an appropriate tool to obtain information on human impact, and allows a comparison of different study sites. However, NMDS as an indicator for human impact still remains a semi-quantitative technique and cannot be considered as an absolute quantification of this impact. The scores on the two NMDS-axes are dimensionless and it is not possible to couple them with absolute numbers of settlements or area under human impact (see also Lechterbeck et al., 2009). Moreover, the exact interpretation of the observed increase in human impact – e.g. more deforestation, intensification of ploughing or a different organization of the cropland – remains uncertain. Further research and an integration of data from both environmental sciences and humanities is needed to solve this issue.

Table 4.1. Approximate timing of the vegetation transition from cluster 2 (representing natural deciduous forest) towards cluster 1 (representing anthropogenic landscape), corresponding with the increase in human impact (Figure 4.8).

Study site	**Timing of vegetation transition (cal a BP)**
Cortil	ca. 2300 cal a BP
Sclage	ca. 2700 cal a BP
Sint-Agatha-Rode	ca. 1600 cal a BP
Korbeek	ca. 4500 - 1500 cal a BP
Archennes	ca. 2400 cal a BP
Loonbeek	ca. 3500 - 2000 cal a BP

4.6 Conclusions

This study shows a reconstruction of vegetation changes in the Dijle catchment throughout the Holocene, based on palynological data of six study sites, cluster analysis and non-metric multidimensional scaling (NMDS). Until ca. 3800 cal a BP, the beginning of the Bronze Age, human impact in the catchment was limited to local disturbances and small-scale forest clearances, wide-scale impact was absent. The Dijle catchment was covered by deciduous forest, dominated by *Quercus*, *Corylus* and *Tilia*, the natural vegetation for the catchment. From ca. 3800 cal a BP vegetation gradually changed (decreasing forest cover and increasing amount of grasses and anthropogenic indicators) under influence of the gradually increasing human impact in the catchment. Human impact further increased during the Iron Age and Roman Period. A remarkable stagnation in human impact was observed between ca. 1900 and 1600 cal a BP, possibly coupled with the Migration Period in Europe. Further increase in human impact is observed during the Medieval and Modern Period. The vegetation patterns and increasing human impact are rather consistent at the catchment scale, beside some local variations in timing and intensity of the vegetation changes between the different subcatchments. The applied methodology, cluster analysis and NMDS, has proved to be a useful tool to provide more insights in the temporal and spatial vegetation changes related to increasing human impact. NMDS enables to compare semi-quantitatively the timing and intensity of human impact between different study sites in the Dijle catchment.

4.7 Acknowledgements

This research has partly been funded by the Interuniversity Attraction Poles Programme IAP 07/09, initiated by the Belgian Science Policy Office. Their support is gratefully acknowledged. Part of the pollen analyses were performed by Rick Assendelft, Maartje Buijs and Jesper van Schilt (MSc students Earth Sciences at Vrije Universiteit Amsterdam). Their help is gratefully acknowledged by the authors. We are also grateful to Martin Hermy for his comments and advice on the statistical analysis, and to Elena Marinova for the help with the identification of the datable material.

4.8 Annex: pollen-vegetation relationships

4.8.1 Introduction

As shown in chapter 4, the cluster analysis and non-metric multidimensional scaling (NMDS) has proved to be an objective tool to provide more insights into the temporal and spatial vegetation changes related to human impact. NMDS enables to compare semi-quantitatively the timing and intensity of human impact between different study sites in a catchment, such as the Dijle catchment. However, NMDS still remains a semi-quantitative technique and cannot be considered as an absolute quantification of human impact. The scores on the two NMDS-axes are dimensionless and it is not possible to couple them with percentages of deforestation, area under cultivation or absolute numbers of settlements (see chapter 4). Information on the relation between pollen deposited in the floodplain and vegetation abundance in the surroundings of the sampling site, necessary to achieve this, is still missing. A quantification of human impact is, however, a crucial step to understand the role humans have played in changing the sediment fluxes in the landscapes (see e.g. Verstraeten et al., 2009a) and more specific in changing the floodplain geoecology (see chapter 1).

As discussed in chapter 1, different approaches have previously been proposed to translate pollen data into measures of land cover. In chapter 4, statistical analysis (NMDS and cluster analysis) of pollen diagrams has been used to characterize vegetation changes and to extract data on human impact. Other recently developed techniques are the model-based correction approaches, which are based on the empirical understanding of the relationship between pollen values and vegetation cover for individual pollen taxa (e.g. Gaillard et al., 2008), such as the Landscape Reconstruction Algorithm (LRA; Sugita, 2007b; Sugita, 2007a) and the Multiple Scenario Approach (MSA; Bunting and Middleton, 2009). The MSA of Bunting and Middleton (2009) starts with generating possible vegetation maps, based on rules of plant requirements and ecological processes combined with environmental parameters such as topography. The HUMPOL software suite (i.e. a pollen dispersal and deposition model; Bunting and Middleton, 2005) is then used to simulate the pollen assemblage at a known sampling point in the landscape for each possible map. These simulated pollen assemblages are then compared with known pollen data from the same location to select which of those maps can be considered as the most likely reconstruction of past vegetation (Bunting and Middleton, 2009). Although the MSA approach and the HUMPOL software have been successfully applied in different areas, it is still uncertain if these pollen dispersal and deposition models will work in other areas and under different circumstances. For instance, various studies have indicated that the pollen source area of the aerial component used in these models, is a poor starting point, since pollen influx in lakes is often dominated by waterborne pollen (e.g. Bonny, 1978; Xu et al., 2012). Also in alluvial sites, investigated in our study (chapter 2 and 4), one can expect that waterborne pollen are an important contributor to the pollen influx (Brown et al., 2007).

Therefore, the aim of this study is to explore if the HUMPOL software suite (Bunting and Middleton, 2005) is applicable in the Dijle catchment. This will be tested based on pollen samples from modern floodplain deposits. If this is the case, we will investigate if the Multiple Scenario Approach (MSA; Bunting and Middleton, 2009) is a suitable approach to reconstruct probable past vegetation maps based on the fossil pollen data from alluvial study sites in the Dijle catchment.

4.8.2 Material and Methods

4.8.2.1 Study sites

Twelve alluvial study sites were selected in the Dijle catchment based on the local vegetation cover and the vegetation in the catchment of the sampled sites (Figure 4.8). They include the six study sites from which fossil pollen data are available (see previous chapters) and six additional sites.

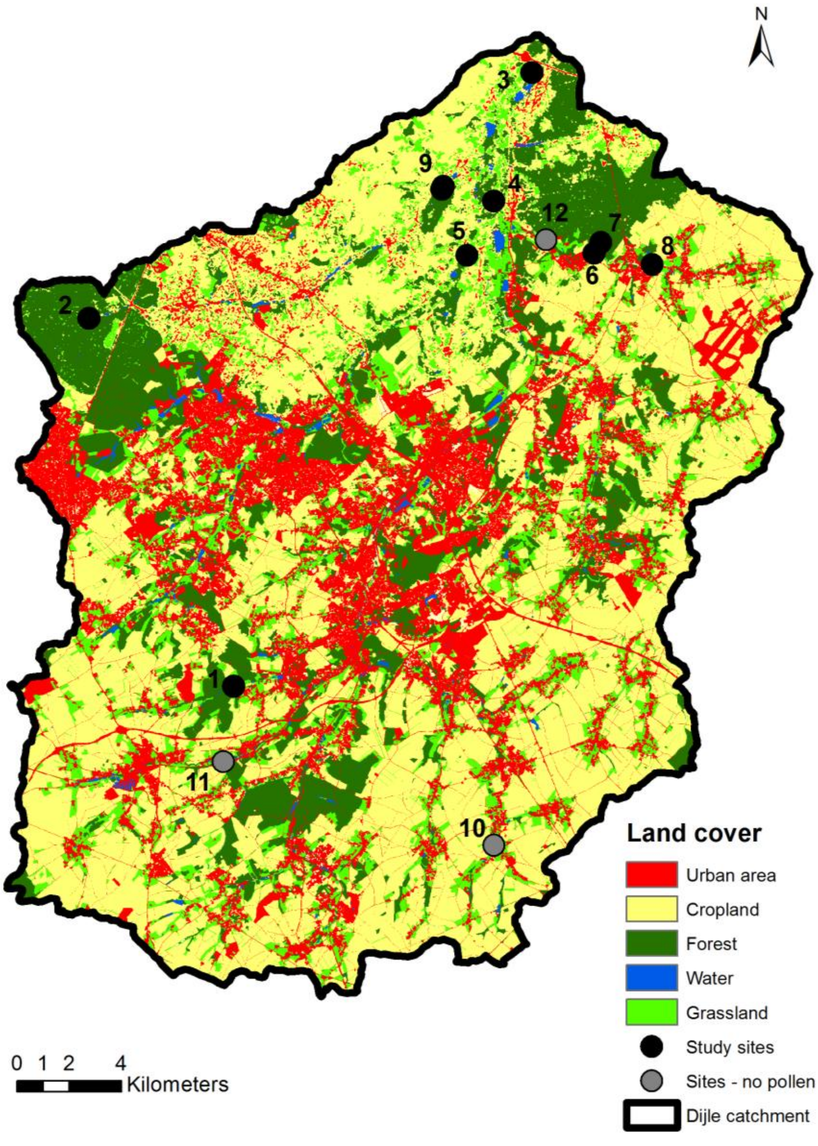

Figure 4.9. Location of the 12 study sites in the Dijle catchment, with indication of the contemporary land cover classes (based on CORINE land cover maps, see section 4.8.2.3). 1: Sclage; 2: Groenendaal; 3: Korbeek; 4: Sint-Joris-Weert; 5: Sint-Agatha-Rode; 6: Le Wez; 7: Warande; 8: Hamme-Mille; 9: Loonbeek; 10: Cortil; 11: Thy, 12: Nethen. Large forested area in the NW is the Zonien Forest, in the NE the Meerdaal Forest.

4.8.2.2 Modern pollen data

At each study site, samples for pollen analysis were taken from the upper floodplain deposits (first 2-4 cm). Pollen samples were extracted from the sediment using a sampler of defined volume (200 mm³), following the standard techniques of Faegri and Iversen (1989) (see also chapter 2 and 4).

Pollen data were expressed as relative frequencies (percentages) of the pollen sum. Two different pollen sums were defined. First, in order to study the regional pollen signal and to be able to compare this with the results from chapter 4, a regional pollen sum was defined. This regional pollen sum includes upland herbs, Poaceae and trees and shrubs. Wetland vegetation (e.g. *Alnus*, *Salix*, Cyperaceae and Typhaceae) and aquatics were interpreted as local vegetation and were excluded from the regional pollen sum. Second, in order to compare modern local floodplain vegetation with the past floodplain vegetation (chapter 2), also a local pollen sum was defined, containing the local pollen signal (e.g. *Alnus*, *Salix*, Cyperaceae and Typhaceae). Percentage diagrams were constructed using *C2* computer program (Juggins, 2007).

4.8.2.3 Land use data

Vegetation maps were based on 'La Cart d'Occupation du Sol de Wallonie' (COSW; survey 2005) for the Walloon part, and 'Bodemgebruiksbestand' (survey 2001) for the Flemish part of the catchment. Both are based on the CORINE 2000 land cover maps of the European Environment Agency (http://www.eea.eu.int), and have a resolution of 15 m. These maps were reclassed to obtain five simplified land cover classes, i.e. urban area, cropland, forest, grassland and water (Table 4.2).

4.8.2.4 HUMPOL simulations

Pollen loadings at each sampling place were simulated using POLFLOW, a part of the HUMPOL software suite (Bunting and Middleton, 2005). HUMPOL is a software suite for modelling pollen dispersal and deposition. The suite uses a standard algorithm, the Prentice-Sugita model (Prentice, 1985; Sugita, 1994), to model pollen dispersal from vegetation sources and pollen deposition at a sampling location. The Prentice-Sugita model requires data on the relative pollen productivity and fall speed for all modelled pollen types. The pollen type parameters used for the Dijle catchment (Table 4.3) were based on the standardised set of Mazier et al. (2012). Pollen productivity estimate (PPE) of Cereal-type was defined at 1.27, following the PPE defined for Denmark (Nielsen 2003). According to Broström et al. (2008), the Danish PPE is a better value to use in areas where cereals are dominated by types other than Secale, such as in the Dijle catchment. Dominant wind direction is defined as from south west, i.e. the dominant wind direction in Belgium.

Land cover in the Dijle catchment, used as input in the HUMPOL software, was based on the reclassed CORINE land cover maps (see section 4.8.2.3). For each land cover class, associated pollen types were defined (Table 4.2), to specify how the land cover classes relate to the different modelled pollen types. Urban area was defined to be not related to a pollen type. Cropland in the Dijle catchment is mostly related to cereal pollen types, but is not exclusively used for cereal cultivation. Half of the cropland area is used for the cultivation of other crops such as Beet (*Beta vulgaris*) and Potato (*Solanum tuberosum*) (FODEconomie, 2013). Forest in the Dijle catchment was associated with *Fagus*, *Quercus*, *Corylus* and *Pinus*. At the margins of the areas classified as water (e.g. rivers, ponds and lakes), Poaceae and *Betula* can be found. Finally, grassland was defined as dominated by Poaceae.

Table 4.2. Land cover classes, the associated pollen types, and their relative abundance in each land cover type; for the Dijle catchment.

Land cover class	Associated pollen types	Estimated relative abundance
Urban area	/	/
Cropland	Cereal-type	50%
Forest	*Fagus*	70%
	Quercus	10%
	Corylus	10%
	Pinus	10%
Water	Poaceae	20%
	Betula	5%
Grassland	Poaceae	100%

Table 4.3. Fall speed of pollen (FSP; m s^{-1}) and pollen productivity estimate (PPE) from standardised sets of Mazier et al. (2012). PPE of Cereal-type is based on Nielsen (2003).

Pollen type	FSP (m s^{-1})	PPE
Quercus	0.031	5.83
Corylus	0.025	1.99
Tilia	0.032	0.8
Betula	0.024	3.09
Poaceae	0.035	1
Cereal-type	0.06	1.27
Fagus	0.057	2.35
Pinus	0.031	6.38

4.8.3 Results and discussion

4.8.3.1 Pollen data

In the floodplain samples of three study sites, Cortil, Thy and Nethen, no pollen were present. Probably, all pollen in the sediments were degraded and corroded. Consequently results are available for only nine study sites. When expressing the pollen data as relative frequencies of the regional pollen sum, it is clear that the different study sites show a different pollen signal (Figure 4.9). Study sites Groenendaal, Le Wez and Warande have high values of arboreal pollen (AP; >70%), and low values of non-arboreal pollen (NAP). These study sites are located in, or close to, the Meerdaal Forest and Zonien Forest (Figure 4.8). In the other study sites, the AP values are low and the NAP values (e.g. Asteraceae and Poaceae) are high.

Absolute pollen frequencies (APF) of the individual study sites are shown in Figure 4.10. APF differ between the different study sites and ranges between 20 000 and 500 000 grains cm^{-3} (Figure 4.10), which is in the same order as the fossil pollen samples (ranging between 10 000 and 200 000 grains cm^{-3}).

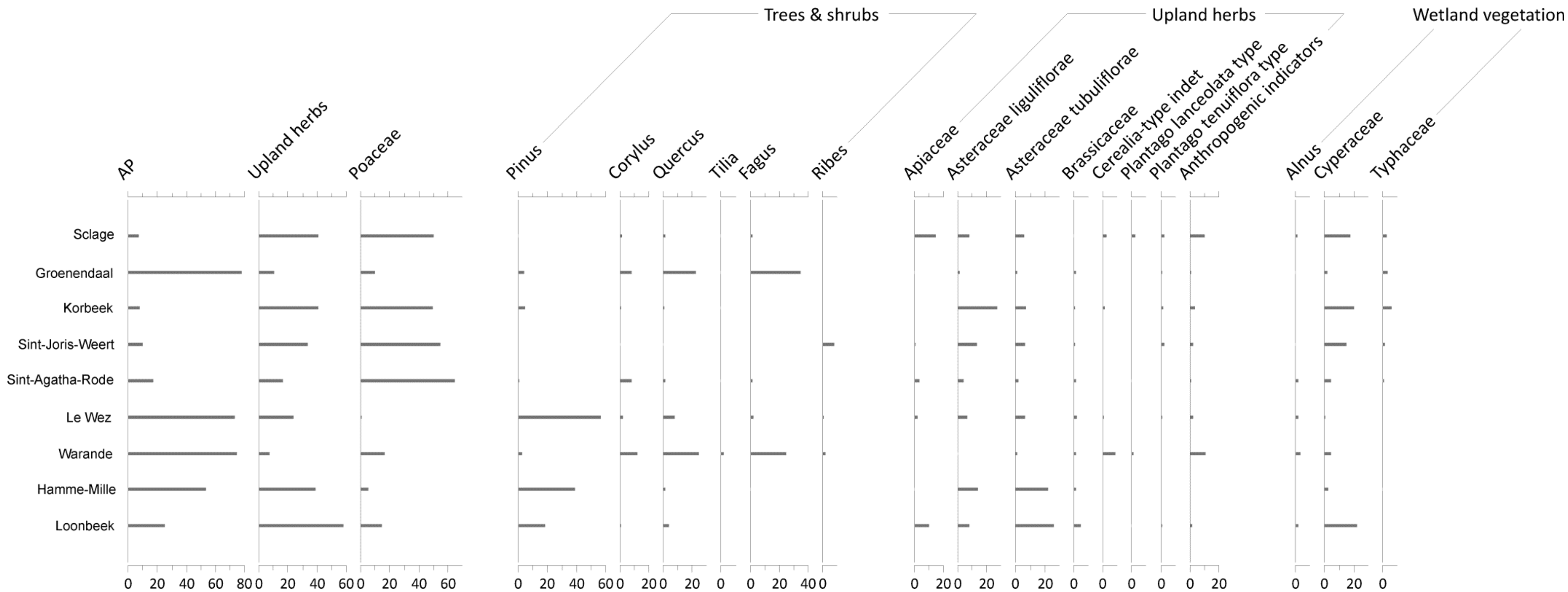

Figure 4.10. Simplified pollen diagram of the modern floodplain deposits, from Sclage, Groenendaal, Korbeek, Sint-Joris-Weert, Sint-Agatha-Rode, Le Wez, Warande, Hamme-Mille and Loonbeek.

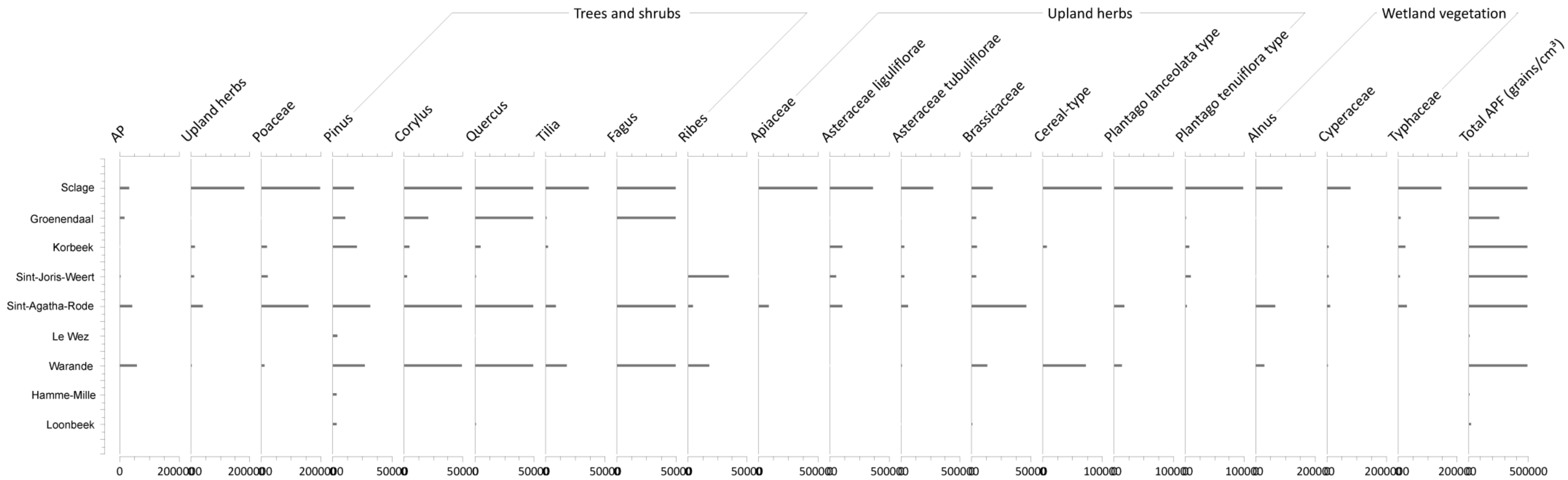

Figure 4.11. Absolute pollen frequencies (grains cm^{-3}) of the modern floodplain deposits, from Sclage, Groenendaal, Korbeek, Sint-Joris-Weert, Sint-Agatha-Rode, Le Wez, Warande, Hamme-Mille and Loonbeek.

4.8.3.2 Non-metric multidimensional scaling (NMDS)

The pollen data from the modern floodplain deposits can be compared with the fossil pollen data (chapter 4). The modern pollen samples of Sclage, Korbeek, Loonbeek and Sint-Agatha-Rode were included in the NMDS (full explanation on NMDS can be found in section 4.3.3). The modern pollen have all high scores on NMDS axis 1 (Figure 4.11), indicating high human impact. Nevertheless, for three out of four study sites, scores on the first axis of the modern pollen are lower than the scores of the most recent fossil pollen signal (Figures 4.11a, c and d), which is in line with the observed (limited) reforestation in the Dijle catchment in the last two centuries (e.g. Notebaert, 2009). Beside these similarities on axis 1, the scores on axis 2 of the modern pollen are different from the fossil pollen signal, for Sclage and Korbeek (Figure 4.11 a and b). Scores on axis 2 can be seen as an indicator for variations in forest composition (chapter 4, Figure 4.5). Indeed, due to high values of *Pinus* (Figure 4.9), the modern pollen signal plot at a different place compared to the fossil pollen. This can indicate that the vegetation in the surroundings of the study sites has changed, with especially a change in forest composition. But it can also indicate that the modern pollen signal does provide a different representation of the vegetation in the surroundings of the sampling place, compared with the fossil pollen signal, e.g. due to different pollen transport and deposition mechanisms.

4.8.3.3 Modern floodplain vegetation versus past floodplain vegetation

The current local floodplain vegetation, as derived from the modern pollen samples, was plotted together with the fossil local floodplain vegetation (chapter 2) for the four study sites for which both pollen data are available (Figure 4.12). The modern pollen samples indicate an open floodplain vegetation, dominated by Cyperaceae. *Alnus* values are very low. This open floodplain vegetation differs from the Middle-Holocene floodplains, which were dominated by an Alder carr forest, but resembles largely the pollen samples from the Medieval Period (Figure 4.12).

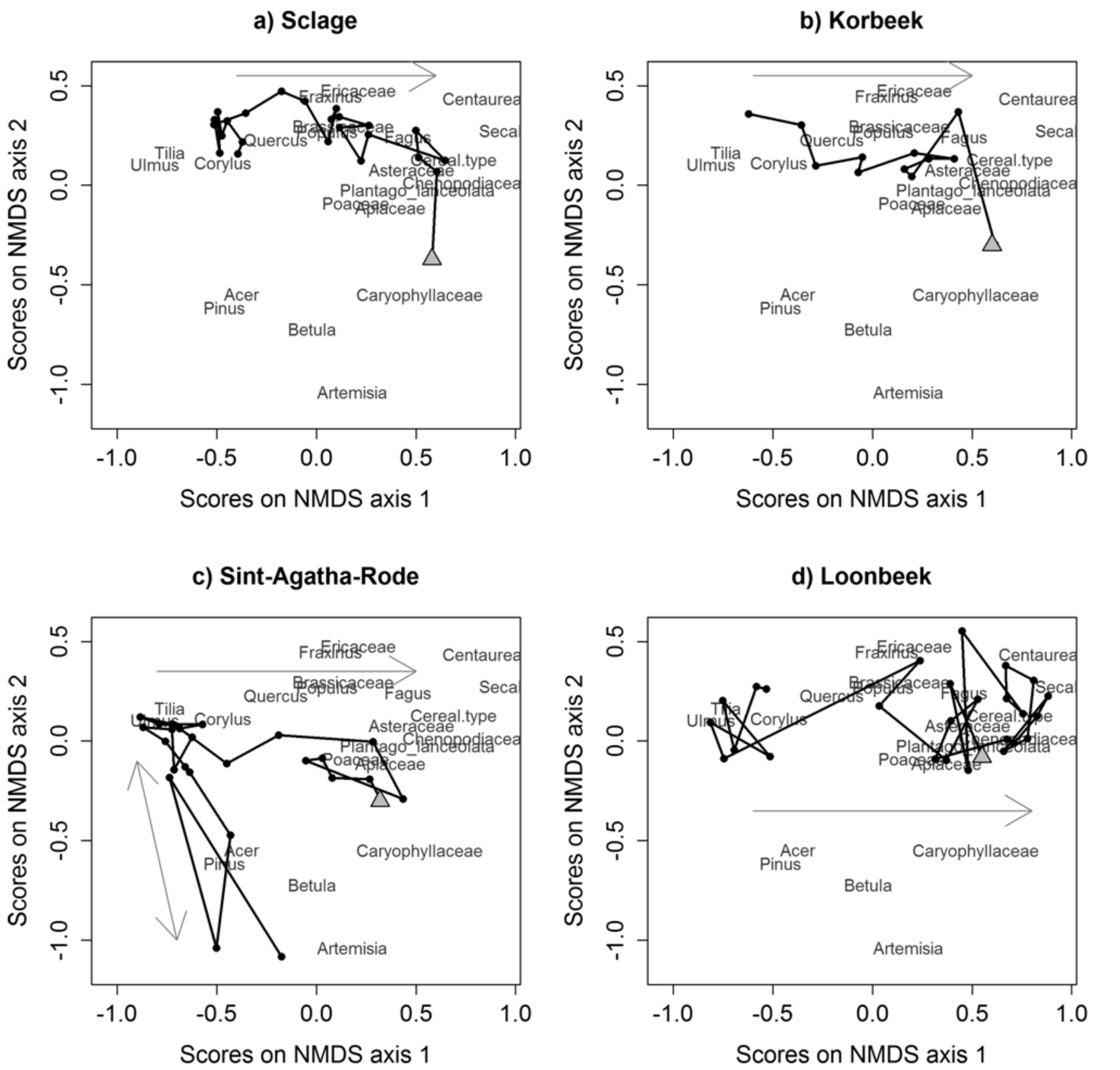

Figure 4.12 Non-metric multidimensional scaling of pollen types and fossil pollen samples (black dots; chapter 4) of the different study sites. Grey triangles indicate the location of the modern pollen samples. Arrows indicate the trajectories of the pollen samples through time. For a) Sclage; b) Korbeek, c) Sint-Agatha-Rode and d) Loonbeek.

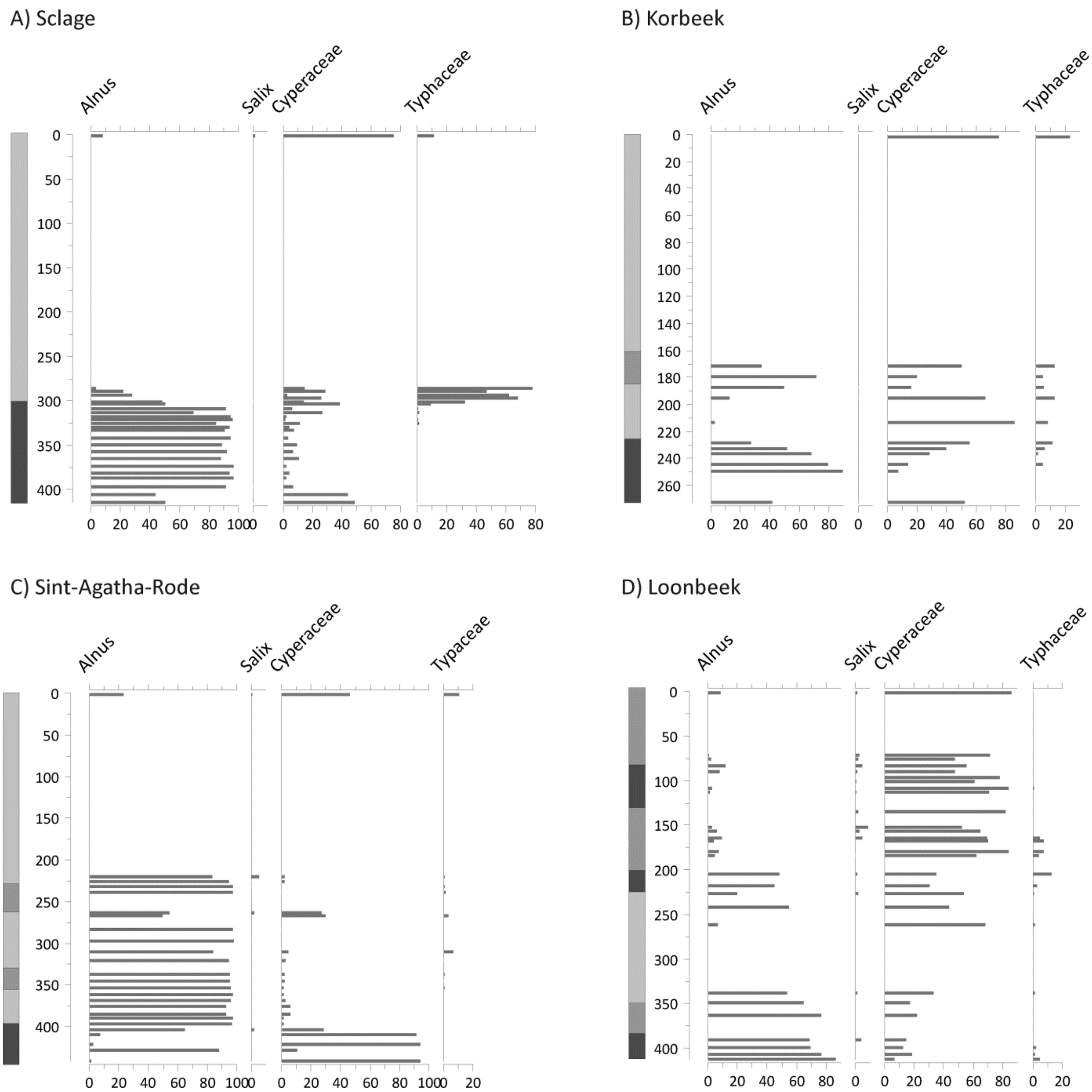

Figure 4.13. Local floodplain vegetation in Sclage, Korbeek, Sint-Agatha-Rode and Loonbeek; based on samples from modern and fossil floodplain deposits. Level 0 represents the modern pollen assemblages.

4.8.3.4 HUMPOL simulations

Pollen deposition at the nine study sites was simulated using POLFLOW, a part of the HUMPOL software suite. The simulated pollen signal is not perfectly comparable with the observed pollen signal, but the trends are similar (Table 4.4). In most study sites, the cropland area is slightly overestimated in the HUMPOL simulations (Korbeek, Sint-Agatha-Rode, Loonbeek, Sint-Joris-Weert, Le Wez and Hamme-Mille), grassland is underestimated (Sclage, Korbeek, Sint-Agatha-Rode, Groenendaal, Sint-Joris-Weert and Warande), and forest is overestimated (study sites Sclage, Korbeek, Sint-Joris-Weert and Warande).

These over- and underestimations can be due to different reasons. First, PPE and FSP are not calibrated for the Dijle catchment. Pollen type parameters of other areas in Europe (Denmark and Sweden) were used, but estimations of pollen productivity depend on local or regional environmental characteristics, and the calibration of PPEs of the analyzed plant taxa for each landscape is necessary. Especially a large range in PPEs for Cereal-type exist among different study sites (Broström et al., 2008). The overrepresentation of the cropland area in the simulations for the Dijle catchment indicate that the PPE of Cereal-type will be lower than the used value of 1.27. Second, vegetation maps were limited to the CORINE land cover maps. However, such regional, low resolution maps should be combined with high resolution maps of the vicinity of the target sampling points (Bunting and Middleton, 2005). Thirdly, we used simplified communities associated with each land cover type (Table 4.2). These communities need more detail to provide more detailed simulations. Next to these problems associated with the model input and model specifications, also reworking (e.g. Brown et al., 2007; Paus, 2013) and selective corrosion and selective preservation (e.g. Wilmshurst and McGlone, 2005) of pollen in the top sediments in the floodplain can result in differences between the simulated and observed pollen signal. In the last decades, the Dijle floodplain became dryer, probably due to the recent incision of the Dijle floodplain (Notebaert, 2009). Consequently, the top floodplain sediments underwent wet-dry cycles throughout the year, and could even dry out completely during summer. Pollen degrade during such wet-dry cycles and complete dry phases (Campbell and Campbell, 1994). Some pollen types are more vulnerable to such degradation and consequently the pollen signal will not be complete. Over-representation of robust pollen types can have the potential to affect the accuracy of quantitative vegetation reconstructions (e.g. Wilmshurst and McGlone, 2005). Such selective corrosion and selective preservation of pollen could have caused the discrepancies in study site Hamme-Mille and Le Wez (Figure 4.13).

Although the correlation between the observed and simulated pollen signal is not perfect, the overlap is better than when the observed pollen are compared with vegetation in the catchment of the sampling sites (Figure 4.13). First, in the catchment vegetation of most study site, a large part is cropland. This high percentage of cropland area is not represented in the modern pollen signal, probably due to the fact that these croplands are located on the plateaus at some distance from the floodplains. Consequently, cereal-type pollen will not easily be transported to the alluvial study sites. The HUMPOL simulations take the location of the cropland area into account and provide therefore a better similarity to the observed pollen signal. Second, only a small part of the catchment is classified as grassland, but this grassland is mainly located in the floodplains, close to the pollen sampling sites. The HUMPOL simulations take the location of the grassland into account and provide therefore a better overlap with the observed pollen signal.

These results indicate that the modern pollen signal from alluvial study sites can not directly be translated in vegetation abundance in the catchment of the sampling site. Instead, model simulations, such as HUMPOL, are necessary. Our results shows that the HUMPOL simulations work well for modern pollen deposited in the Dijle floodplain.

Table 4.4. Observed versus simulated pollen assemblage (%) for 9 study sites in the Dijle catchment. Observed pollen data are gathered from top floodplain deposits, simulation were done in HUMPOL, using the CORINE land cover maps and PPEs and FSP from Mazier et al. (2012) as input.

	Sclage		**Korbeek**		**St-Agatha-R**		**Loonbeek**		**Groenendaal**		**St-Joris-W**		**Le Wez**		**Warande**		**Hamme-Mille**	
	obs	sim	obs	sim	obs	sim	obs	sim	obs	sim	obs	sim	obs	sim	obs	sim	obs	sim
Pinus	1	11	9	7	2	7	47	10	6	27	0	9	75	13	4	26	80	11
Betula	2	0	0	3	2	1	0	0	2	0	1	1	2	1	1	0	3	5
Corylus	3	4	2	2	11	3	3	4	10	9	1	3	4	5	15	9	0	4
Quercus	3	9	2	5	3	6	12	8	28	23	1	7	11	11	30	22	3	9
Fagus	3	13	0	6	3	6	0	11	42	39	0	9	4	13	30	40	2	13
Poaceae	83	60	84	72	80	72	38	60	12	1	97	66	2	51	20	2	12	48
Cerealia	5	2	3	5	0	6	0	8	0	0	0	4	2	7	0	1	0	11

forest	12	38	13	24	20	22	62	32	88	98	3	30	96	43	80	97	88	41
grassland	83	60	84	72	80	72	38	60	12	1	97	66	2	51	20	2	12	48
cropland	5	2	3	5	0	6	0	8	0	0	0	4	2	7	0	1	0	11

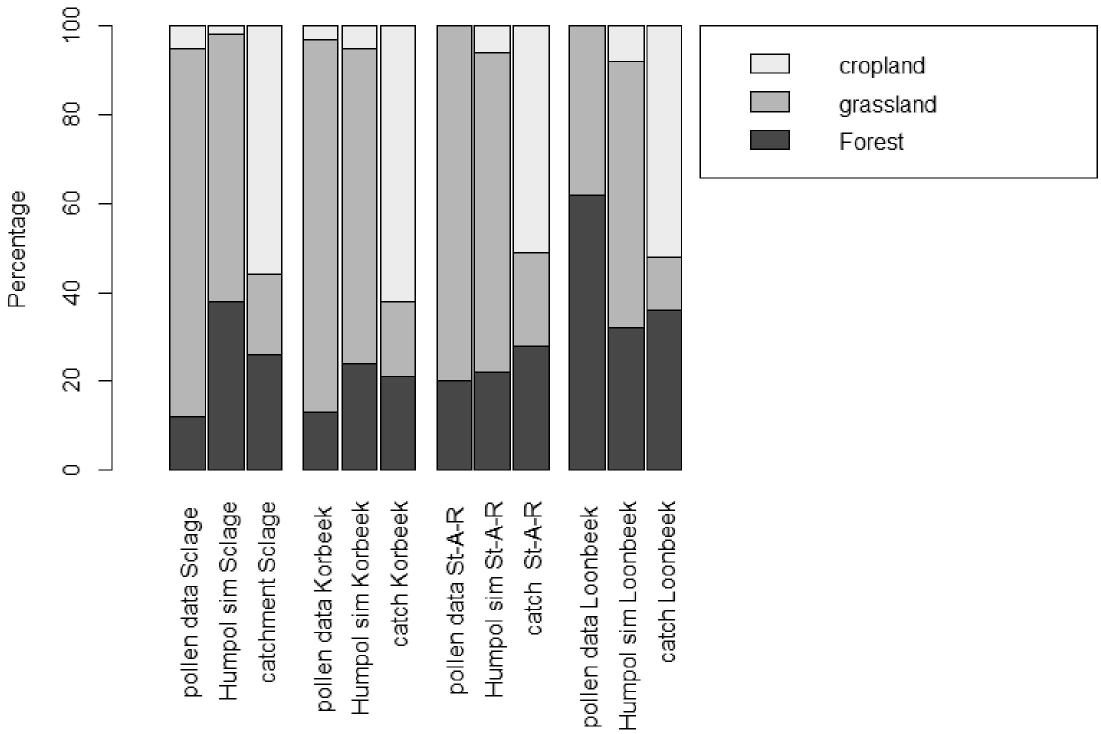

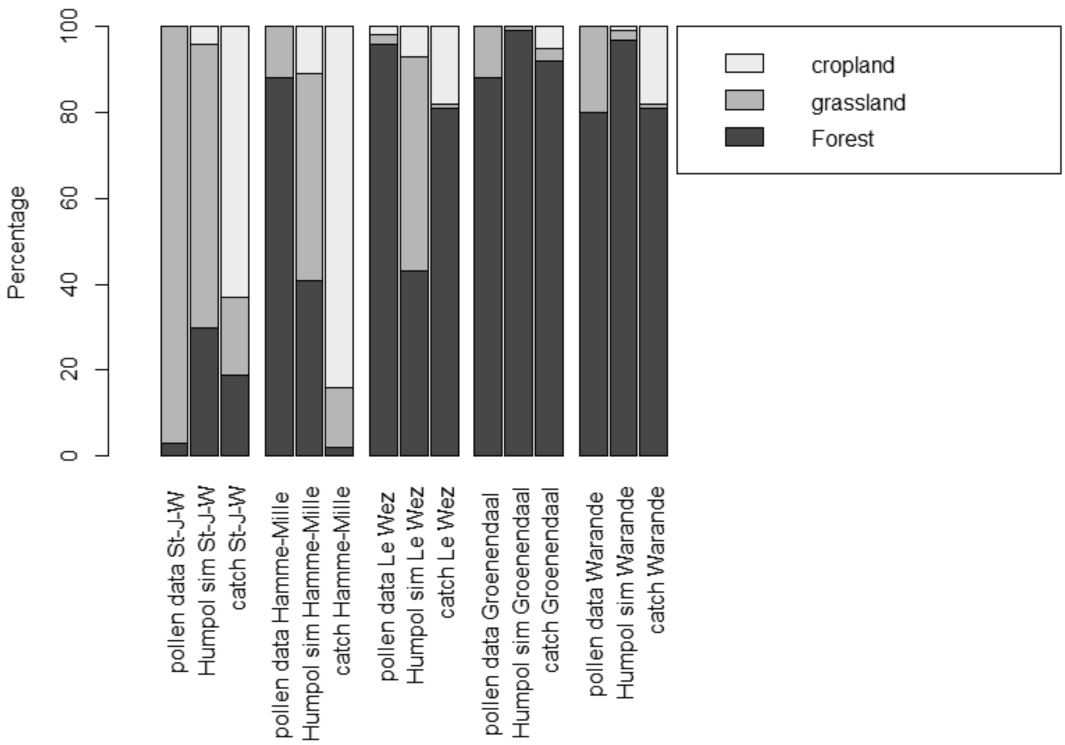

Figure 4.14. Observed and simulated pollen signal (using HUMPOL) grouped in land cover classes, and percentage of land cover type in the catchment of the sampling site. For Sclage, Sint-Joris-Weert, Korbeek, Warande, Le Wez, Sint-Agatha-Rode, Loonbeek, Hamme-Mille and Groenendaal.

4.8.3.5 Scope for further research

From the above results, it is clear that the HUMPOL simulations provide a better similarity to the observed pollen signal, than when the observed pollen signal is compared with the vegetation in the catchment of the sampling sites (Fig 4.13). However, some points need more research such as the calibration of PPEs for the Belgian loess belt and detailed vegetation surveys. If the HUMPOL software is applicable, the multiple scenario approach (MSA) can be used to create multiple past vegetation maps and select the most probable maps based on the comparison of simulated and observed fossil pollen assemblages, following Bunting and Middleton (2009) (see also section 4.8.1). However, extrapolating the results presented above to the past situation should only be undertaken with careful considerations, since the relative importance of fluvial transported pollen in the past situation is still unknown. If this fluvial pollen transport is very important, the pollen source area of the aerial component, used in the MSA, is a poor starting point and the MSA will not be able to simulate the most probable past vegetation map.

Several indications suggest that fluvial pollen transport was more important in the Dijle catchment in the past compared to the present situation. First of all, floods and deposition of sediments – and fluvial transported pollen – in the Dijle floodplain are relatively rare the last decades. For instance, comparison of topographic field survey data from 1969 and 2008 show that no detectable height change at the channel banks took place, suggesting limited recent sedimentation (Notebaert, 2009). Consequently, fluvial transported pollen are expected to be relatively less important, compared to the aerial transported pollen, for the pollen assemblages in the top floodplain deposits (used in the analysis in this annex). The aerial transported pollen can be mixed in the floodplain sediments by bioturbation or percolation (Dimbleby, 1957; Faegri and Iversen, 1989). In contrast, in the past situation, floods – and fluvial transported pollen – are expected to be more important, indicated e.g. by the high sediment mass accumulation (Figure 2.10) and the high pollen accumulation rates (chapter 4) (e.g. Van der Woude, 1983).

The relative importance of fluvial pollen transport, for pollen deposited in the floodplain, needs more research.More information on the importance of fluvial pollen transport is needed to correctly interpret the outcome of the MSA, applied to fossil pollen assemblages from alluvial sites and to select the most likely reconstruction of past vegetation. This will allow us to translate fossil pollen data into quantitative estimates of past land cover changes.

4.8.4 Conclusions

Our results indicate that the HUMPOL simulations provide a better similarity to the observed pollen signal, than the observed pollen and the vegetation in the catchment of the sampling sites. It is clear that such model simulations are needed to translate the modern pollen signal from alluvial sites into vegetation abundance in the surroundings of the sampling place. We argue that more insights in the importance of fluvial transported pollen for pollen deposited in the floodplain are needed to apply the multiple scenario approach (MSA) to the fossil pollen data. The importance of fluvial pollen transport in the current and past situation is still uncertain. Due to these uncertainties, the MSA has not yet been applied to the fossil pollen data in this study. Consequently, a translation of the fossil pollen data from the alluvial sites in the Dijle catchment into quantitative estimations of deforestation or area under cultivation, is still not available.

Chapter 5 Sensitivity of floodplain geoecology to human impact. Headwaters

This chapter is based on: Broothaerts N, Verstraeten G, Notebaert B, Assendelft R, Kasse C, Bohncke S, Vandenberghe J (2013) Sensitivity of floodplain geoecology to human impact – A Holocene perspective for the headwaters of the Dijle catchment, Central Belgium. *The Holocene* 23, 1403-1414.

5.1 Introductory remarks

To provide an answer to the research questions proposed in chapter 1 and to attain a better understanding of the sensitivity of floodplain geoecology to human impact in the landscape, our observations on floodplain changes from chapter 2 and 3 will be evaluated against the reconstruction of human impact (chapter 4). In this chapter 5, this integrating approach will be applied to the headwaters of the Dijle catchment. Only data from the study sites in the headwaters will be presented and conclusions made are applied on this small part of the catchment only.

This chapter has been published as a paper and is presented here as such, with addition of the soil erosion and sediment redistribution modelling. The paper repeats some parts of the other chapters with a detailed focus on the headwaters of the Dijle catchment, so some overlap with the different chapters is present. Also, some small differences in methodology compared with the other chapters are present here. First, a different statistical method to gain more insights into the pollen records is used. Here canonical correspondence analysis is used, instead of non-metric multidimensional scaling used in chapter 4 and 6. In the annex of this chapter, we shortly compare both methods and show that the trends are similar, beside some small differences. Second, the cluster analysis used in this chapter was performed for each study site and for both the regional and local pollen signal separately. Third, the sediments were grouped in lithogenetic units, only taking into account the two cross-sections of the headwaters of the Dijle catchment. Consequently, in this chapter, fewer units are distinguished compared with chapter 2.

5.2 Introduction

During the Early and Middle Holocene, most floodplains in the West and Central European lowlands were rather stable with limited floodplain aggradation resulting in peat formation e.g. in central Belgium (e.g. De Smedt, 1973; Vandenberghe and De Smedt, 1979; Notebaert et al., 2009b;

Notebaert and Verstraeten, 2010) and in the Paris Basin (e.g. Pastre et al., 2002), or resulting in the development of black floodplain soils in e.g. Germany (e.g. Rittweger, 2000; Kalis et al., 2003; Houben, 2007). During these times floodplains consisted mainly of large marshes where peat accumulated and river channels were absent or small (e.g. De Smedt, 1973; Vandenberghe and De Smedt, 1979). Sediment supply from the slopes to the river valleys increased with increasing human impact through deforestation and the development of agriculture from the Neolithic period onwards (e.g. Notebaert and Verstraeten, 2010). As a result, the floodplain geomorphology and ecology (hereafter called 'geoecology') changed (e.g. Zolitschka, 2003; Houben, 2007; Notebaert and Verstraeten, 2010). The present-day meandering small river channels in West and Central Europe are thus the indirect result of anthropogenic activities, i.e. land use change. Similar changes in floodplain morphology have been demonstrated for the eastern US, where 19th century human impact through mill dam construction following European colonization is seen as the main trigger (Walter and Merritts, 2008). Although this general framework of changes in river geoecology in relation to the growing impact of humans during the Holocene is now established, many uncertainties on the exact timing and nature of this relation still exist. First, it remains a question whether the floodplain geoecology gradually changed, coinciding with the gradually increasing human impact in the catchment (e.g. Kalis et al., 2003; Dotterweich, 2008), or that changes in floodplain geoecology were abrupt and only occurring when a certain threshold in human impact has been reached (e.g. Kalicki, 2008; Lespez et al., 2008; Notebaert et al., 2011b; Houben et al., 2012). Related to this, it is unclear when exactly these changes in river geoecology occurred, and whether these changes occurred simultaneously in the entire catchment. If not, the question remains if these differences in sub-catchments can be attributed to the difference in sensitivity towards environmental disturbances, which in turn can indicate a non-linearity in the process-response relation. Due to these uncertainties, it is still a question what exactly the natural state of a floodplain of lowland rivers in West and Central Europe was, and to which extent human impact has altered the floodplain geoecology (e.g. Brown, 2002; Buijse et al., 2002; Tockner and Stanford, 2002). Such information on the natural reference situation – before significant catchment deforestation and management of floodplain systems (e.g. Brown, 2002) – and the behavior of floodplains under changing human impact is very useful for river management and river restoration (e.g. Wohl et al., 2005; Newson and Large, 2006). Due to the strong human impact in West and Central Europe, however, at present no lowland rivers are in a natural state (e.g. Tockner and Stanford, 2002) and therefore the study of past river systems during times that human impact was limited is necessary. In this paper we consider a natural river as a river for which all components are still in a pristine situation, including the non-direct impact e.g. through changes in water or sediment fluxes.

Here, we aim to provide insights in the spatial and temporal relation between human impact and changing floodplain geoecology. We present a detailed reconstruction of the floodplain geoecology for two upland tributary rivers in the Dijle catchment, central Belgium. Information on changes in river geomorphology was gathered through detailed field-based sediment coring. For reconstructing local and regional vegetation changes, palynological data were used. Time control was facilitated by radiocarbon dates of crucial lithological and/or palynological transitions. The reconstruction of changing regional vegetation and the reconstruction of the floodplain response for the two study sites was evaluated using a soil erosion and sediment redistribution model (WaTEM/SEDEM model). Modelling soil erosion and sediment redistribution for several scenarios of past land use can help to test hypothesis on the different floodplain response between two study sites. Here, the reconstruction of the regional vegetation and the floodplain changes was confronted with results of the modelling approach.

5.3 Material and Methods

5.3.1 Study area

This study focuses on the Dijle catchment upstream of Leuven (758 km²), situated in the central Belgian loess belt (Figure 5.1). The topography of the Dijle catchment consists of an undulating plateau in which several rivers are incised. The geology is dominated by alternating Paleogene sands and clays dipping towards the north, which are covered with Pleistocene loess. In the incised river valleys in the southern part of the catchment, Palaeozoic basement rocks crop out. The soils of the catchment are mainly Luvisols developed in the loess deposits. Locally, loess has been eroded resulting in sandy outcrops. During the first half of the Holocene, the Dijle catchment was mainly forested, as indicated by previous palynological research in the Dijle catchment (e.g. Mullenders and Gullentops, 1957; Mullenders et al., 1966; De Smedt, 1973). The oldest known Neolithic settlement near the Dijle catchment dates from ca. 6200 cal a BP (Crombé and Vanmontfort, 2007). According to Mullenders et al. (1966) first palynological traces of agriculture (e.g. Cereal-type grasses) date back to ca. 5000 cal a BP (Mullenders et al., 1966), but previous palynological data had a poor chronological control. Anthropogenic disturbances in the landscape became more evident in the pollen assemblages from 2500 cal a BP on, with up to 60% of upland herbs and 10% of Cereal-type pollen (Mullenders and Gullentops, 1957; Mullenders et al., 1966), and peaked during the Roman Period (ca. 2050-1600 cal a BP) and from the Medieval Period onwards (e.g. Van Hove et al., 2005). At present, land use is dominated by cropland, except for some large deciduous plantation forests in the northeast and northwest of the catchment. The floodplain is currently mainly used as forest or grassland.

For the Dijle river and tributaries, insights in the Holocene sediment dynamics were already provided by different studies (e.g. Rommens et al., 2005; Rommens et al., 2006; Notebaert et al., 2009b; Verstraeten et al., 2009b; Notebaert et al., 2011a; Notebaert et al., 2011b). A time-differentiated sediment budget constructed for the Dijle catchment by Notebaert et al. (2011b) shed light on the changing sediment dynamics in the catchment. First colluvial deposition is reported from ca. 4000 cal a BP and became more important between ca. 2000 and 700 cal a BP. The increase in alluvial deposition in the Dijle catchment occurred later than the increase in colluvial deposition, with the major part of floodplain sedimentation since ca. 1000 cal a BP. The increasing colluvial and alluvial deposition coincided with the increasing intensity in agricultural activities in the catchment, whereas little evidence exists for the influence of climate variability on the colluvial and alluvial deposition pattern (Notebaert et al., 2011b).

In this study, we consider the headwaters of the Dijle catchment, where a strong connection between sediment sources (i.e. hill slopes and loess plateau) and floodplains is expected. Two study sites in the headwaters are selected, one near the village of Sclage along the Cala River, and one near the village of Cortil along the Orne River (Figure 5.1). Both rivers are tributaries of the main Dijle River. The upstream area of both sites is ca. 13 km². The width of the floodplain in Sclage is ca. 90 m compared to ca. 70 m in Cortil. These sites were selected based on their accessibility, availability of previous research and mainly on their differences in slope morphology and land cover history. The difference in slope morphology is related to differences in geology. The Cala River has cut through the sandy Tertiary deposits, resulting in outcrops of more resistant Palaeozoic rocks. Consequently, the slopes along the axes of the Cala River are steeper (up to 40%) compared to slopes along the Orne River (less than 5%), which has not cut through the sandy Tertiary deposits. The Cala floodplain at Sclage is consequently surrounded by steep slopes, whereas the Orne floodplain at Cortil is more open (Figure 5.1). The south-western part of the Dijle catchment (where the site of Sclage is located) lacks archaeological findings from the Roman Period, whereas in the surroundings of the site of Cortil a cluster of Roman findings can be identified (Figure 5.1) (Notebaert, 2009). Although the archaeological record is incomplete, this could suggest a difference in land cover history between both sites.

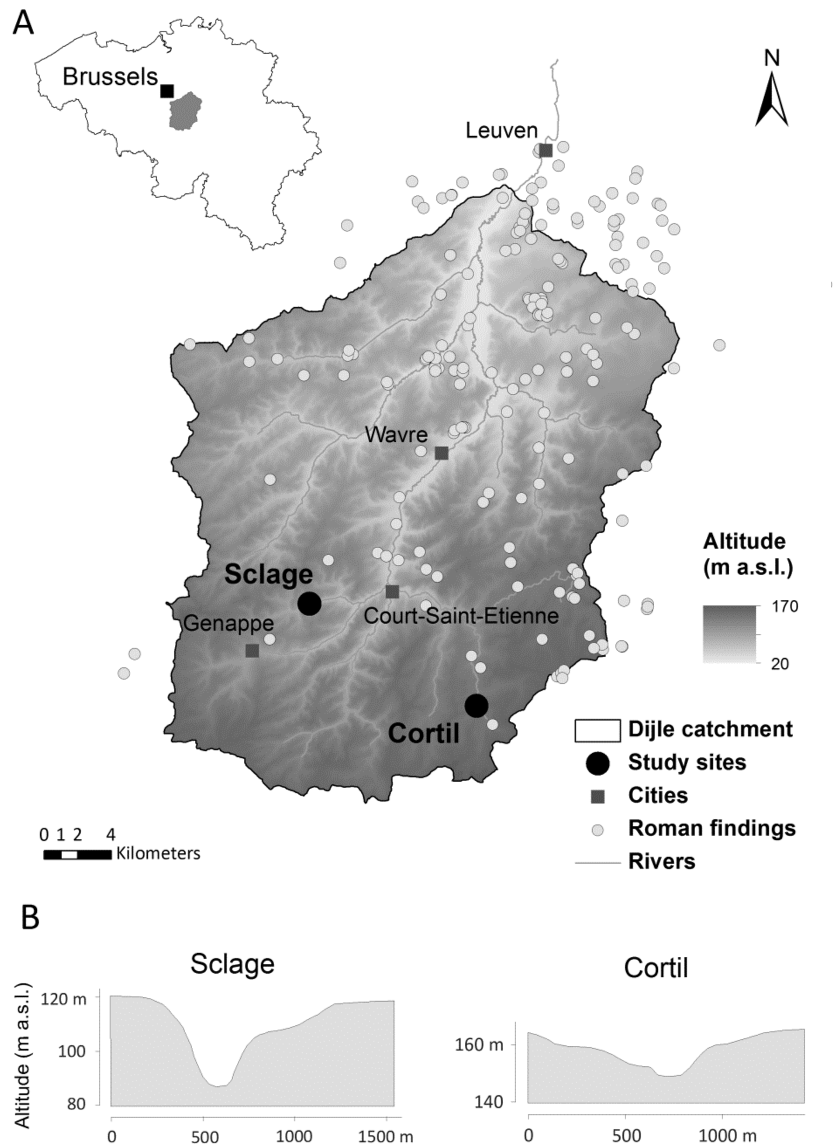

Figure 5.1. (A) Location of the study sites Sclage and Cortil in the Dijle catchment and in Belgium, with indications of Roman findings in and near the Dijle catchment (location of archeological findings based on Notebaert (2009)); (B) cross-section from the loess plateau towards the floodplain for both study sites.

5.3.2 Coring and sediment analysis

Information for the reconstruction of the floodplain morphology is retrieved from coring data, grouped in transects across the floodplain, one at both study sites. The coring transect at Sclage contains 11 cores with a coring spacing of 5 to 15 m. At Cortil five cores were made with a spacing of 10 to 20 m. For each coring, a detailed sedimentologic field description was made with a vertical resolution of 5 cm, containing texture and sorting determined by palpation, colour description, and determining inclusions (such as gravel, plant material and artefacts). For each study site, one sediment core along the transect was collected for pollen analyses (Figure 5.3)3. The main focus of this study is the change in floodplain geoecology, especially the transition from peaty deposits towards minerogenic overbank deposits. Therefore the location of the pollen profiles on the transect was chosen based on a good preservation of this transition (e.g. no indications of erosion of the peat). For the same reason a specific depth range was selected around this transition in which pollen analyses and additional lab analyses were performed: for Sclage between 285 and 415 cm (Figure 5.3) and for Cortil between 215 and 370 cm depth (Figure 5.3). Thermo gravimetric analysis (loss on ignition, LOI) was performed to determine organic matter (OM) and carbonate content. Based on the analysis of the sediments, and taking into account the homologous contemporary deposition in the floodplain, the sediments are grouped in different facies representing different depositional environments, similar to Notebaert et al. (2011a).

5.3.3 Palynological analysis

For each study site a palynological analysis was performed for the selected depth range (Figure 5.3). Pollen samples were taken at a vertical resolution of ca. 4 cm around the transition from peaty deposits towards minerogenic deposits, and a vertical resolution of ca. 8 cm when no changes in sediment were observed. Pollen samples were extracted from the core using a sampler of defined volume (100 mm³ for organic rich sediment, 200 mm³ for minerogenic sediments), and were prepared following the standard technique of Faegri and Iversen (1989). A known quantity of *Lycopodium* spores was added, to allow the calculation of pollen accumulation rates (PAR) and charcoal accumulation rates (CHAR). The samples were studied under a 630x and 1000x magnification using oil immersion. Pollen types were identified using Moore et al. (1991), Beug (2004) and a modern reference collection; non-pollen palynomorphs by using Van Geel (1978). Pollen data are expressed as relative frequencies (percentages) of the pollen sum. The pollen sum includes the regional pollen signal, including upland herbs, Poaceae, trees and shrubs. Wetland vegetation (e.g. *Alnus*, *Salix*, Cyperaceae and Typhaceae) is interpreted as local vegetation and is left out of the pollen sum, as well as the aquatic species. Percentage diagrams were divided into regional and local components and constructed using *C2* computer program (Juggins, 2007). Pollen slide charcoal particles (50-200 µm) were counted and charcoal accumulation rates (CHAR, particles $cm^{-2}\ a^{-1}$) were calculated by taking into account the floodplain accumulation rate. Likewise, pollen accumulation rates (PAR, pollen $cm^{-2}\ a^{-1}$) were also calculated.

5.3.4 C14 analysis and floodplain accumulation rates

AMS radiocarbon dating of organic material embedded in organic or floodplain deposits was used to provide a chronostratigraphical framework for the pollen assemblages (Table 5.1). After sieving samples at 250 mm, terrestrial plant remains were handpicked, and identified for dating. Obtained ages were calibrated using the IntCal13 calibration curve (Reimer et al., 2013) and *Oxcal 4.2* software (Ramsey, 2009). An age-depth model was established for each site based on the *clam.R* package (Blaauw, 2010) using linear interpolation between the dated levels. Based on the age-depth model, a time-scale for the whole sequence was derived for each site. The age-depth model was used to estimate the dates of each transition in both the pollen diagram and floodplain architecture. Dating results were used to calculate floodplain accumulation rates (mm a^{-1}). Post-depositional compaction of peat and peaty deposits can lead to an underestimation of the peat growth rate and consequently to an underestimation of floodplain accumulation rates. Therefore the porosity-depth equation, developed by Sheldon and Retallack (2001) for nonmarine sediments, was used to estimate compaction of the peat deposits:

$$C = -S_i / [(F_0/e^{Dk}) - 1] \qquad \text{equation (5.1)}$$

Where C is the compaction as a fraction of the original thickness, S_i is the initial solidity, F_0 is the initial porosity ($1-S_i$), D is the burial depth and k is an empirically derived constant. Following Sheldon and Retallack (2001), $S_i = 0.06$, $F_0 = 0.94$ and $k = 2.09$ were used to incorporate peat compaction. Using these values, and assuming that the difference in peat compaction for peat layers with a LOI ranging between 40% and 60% is negligible, the compaction ratio (C) becomes e.g. 0.91 at 3 m and 0.85 at 5 m depth (91% and 85% respectively of the original thickness), which is used to make realistic estimates of floodplain accumulation rates.

5.3.5 Statistical analysis

In order to provide more objective insights into the pollen data, each pollen record was divided into different zones using a quantitative approach: samples are grouped by applying a hierarchical cluster analysis. A cluster analysis was performed for each study site and for both the regional and local pollen signal separately. The used clustering method is 'average linkage clustering', where the distance between two clusters is defined as the average of all possible distances between members of the two clusters. As a distance measure, one minus the cosine of the included angle between points has been used, as it is assumed that this provides the best results for ecological data (Hammer and Harper, 2006). The resulted cluster tree was firstly split in a set of larger groups (indicated with numbers), and secondly subdivided into smaller clusters (indicated with letters). In this way, the hierarchy of the clusters was preserved.

Canonical correspondence analysis (CCA) was performed to get more insights into the changes in the pollen record through time. Correspondence analysis (CA) is a mathematical tool for detecting structures, trends and gradients in large datasets. It displays high-dimensional data in a lower-dimensional space (such as the two-dimensional plane), while maintaining most of the original information. It has previously been applied to pollen data (e.g. Birks, 1985; Birks et al., 1988; Kerig and Lechterbeck, 2004; Lechterbeck et al., 2009). Full explanation of CA is provided by Shennan

(1997) and Hammer and Harper (2006). In canonical correspondence analysis, an independent variable is set to optimize the result so that variation correlates with the independent variable. We used the chronology as the independent variable such that the result is optimized to changes in the pollen record through time, which is an advantage compared to CA or principal component analysis (Ter Braak, 1986). Plotting the scores on the first CCA-axis as a function of time has previously been used as an indicator for human impact (e.g. Kerig and Lechterbeck, 2004; Lechterbeck et al., 2009). By analysing pollen data from different sites in one single step, the results can be directly compared over the sites (Lechterbeck et al., 2009). In this study, a CCA was applied on the regional pollen data of both study sites. Rare taxa were excluded from the CCA as these can cause statistical problems. Here rare taxa were defined as taxa that occurred in less than 7% of the samples.

Table 5.1. Radiocarbon dating results. Numbers refer to Figure 5.3.

nr	Sample ID	Lab-code	Conventional age (BP)	calibrated radiocarbon age (cal a BP) ± 1-σ error	location	depth (cm)	dated material	Stratigraphic position
1	SCL 4-2	Beta-257424	430 ± 40	470 ± 55	Sclage	230	wood remains	top peat layer
2	NB-SCL-50-9	Beta-297818	300 ± 40	376 ± 61	Sclage	270	wood remains	top peat layer
3	NB-SCL-50-17	Beta-297819	9080 ± 50	10247 ± 53	Sclage	515	wood remains	bottom gyttja layer
4	NB-SCL102-D1	Beta-302449	480 ± 30	520 ± 14	Sclage	304	wood remains	top peat layer
5	SCL-102-4-D5	Beta308870	1210 ± 30	1137 ± 50	Sclage	319	terrestrial plant remains	peat layer
6	NB-SCL102-D9	Beta-302450	2350 ± 30	2377 ± 49	Sclage	339	terrestrial plant remains	peat layer
7	SCL-102-4-15	Beta-308869	3620 ± 30	3933 ± 48	Sclage	371	terrestrial plant remains	peat layer
8	NB-SCL102-D12	Beta-302451	4700 ± 30	5424 ± 77	Sclage	399	terrestrial plant remains	peat layer
9	SCL 3-2	Beta250211	450 ± 40	494 ± 43	Sclage	330	wood remains	top peat layer
10	NB-SCL-53-9	Beta-297820	510 ± 40	543 ± 36	Sclage	340	wood remains	top peat layer
11	NB-SCL-53-17	Beta-297821	2230 ± 40	2237 ± 56	Sclage	490	terrestrial plant remains	bottom gyttja layer
12	SCL 2-1	Beta2577361	670 ± 40	620 ± 40	Sclage	320	terrestrial plant remains	top peat layer
13	SCL 2-7	Beta-257243	9870 ± 60	11304 ± 88	Sclage	500	wood remains	bottom peat layer
14	COR-103-D4	Beta-308864	620 ± 30	604 ± 33	Cortil	245	terrestrial plant remains	floodplain fines
15	COR-D12	Beta-323481	1770 ± 30	1683 ± 52	Cortil	269	ter. plant remains	floodplain fines
16	COR-103-D1	Beta-308862	2520 ± 30	2606 ± 77	Cortil	320	wood remains	top gyttja layer
17	COR-103-D3	Beta-308863	4760 ± 40	5495 ± 72	Cortil	370	ter. plant remains	gyttja layer

5.3.6 WaTEM/SEDEM model

To model past soil erosion and hillslope sediment delivery, the WaTEM/SEDEM model was used. Detailed description and explanation of the WaTEM/SEDEM model is provided by Van Oost et al. (2000), Van Rompaey et al. (2001) and Verstraeten et al. (2002). The model has previously been used to simulate sediment fluxes in the Dijle catchment (e.g. Notebaert et al., 2011c; De Brue and Verstraeten, 2014) and several other catchments (e.g. De Moor and Verstraeten, 2008; Ward et al., 2009). The model calculates soil erosion and sediment delivery to river channels. Processes within the fluvial system are however not modeled, and a distinction between sediment deposition in the floodplain and sediment export from the catchment is not possible. Within this study, the model was applied on a pixel resolution of 20 m. The model was applied for the two small subcatchments of study site Cortil and Sclage. Different land cover scenarios were constructed (Table 5.2 and Figure 5.2). Scenarios were developed for a pristine landscape (0% of arable land – scenario 1), and with 10, 20, 40, 60 and 80% of arable land (respectively scenario 2, 3, 4, 5 and 6). To allocate land cover, probability maps were made for arable land, based on the logistic regression analysis of Peeters (2007):

$$p(\text{arable}) = \frac{\exp(1.0729 - 0.1628 * S)}{1 + \exp(1.0729 - 0.1628 * S)} \qquad \text{equation (5.2)}$$

With *p(arable)* the probability for arable land, and *S* the slope gradient. In a next step, raster cells were ranked according to their suitability for arable land, and the necessary amount of raster cells were assigned to arable land, following the procedure of Notebaert (2009). For a second set of scenarios, it was assumed that the location of arable land depends on a threshold in slope gradient (<5%) and on the distance to rivers. In such a way, two scenarios with 15% of arable land were constructed, one with the arable land organized close to the rivers (scenario 7) and one with arable land further away from the rivers (scenario 8). Finally, scenario 9 was constructed with only forest on the slopes higher than 5%, and scenario 10 was based on the *de Ferraris* map (ca. 1775, scale 1:11 520). Two important tools to evaluate the sediment dynamics are the hillslope sediment delivery and the hillslope sediment delivery ratio (HSDR). The hillslope sediment delivery is the amount of sediment that is redistributed within the catchment from the hillslopes to the fluvial system per unit area. The HSDR is the fraction of sediment that is delivered by the hillslopes compared to the total soil erosion.

Table 5.2. Land cover scenarios.

Scenario	% forest	% arable land	remarks
1	100	0	arable land allocated using equation 5.2
2	90	10	arable land allocated using equation 5.2
3	80	20	arable land allocated using equation 5.2
4	60	40	arable land allocated using equation 5.2
5	40	60	arable land allocated using equation 5.2
6	20	80	arable land allocated using equation 5.2
7	85	15	arable land close to the rivers
8	85	15	arable land further away from the rivers
9			Forest on slopes > 5%
10			Based on Ferraris map

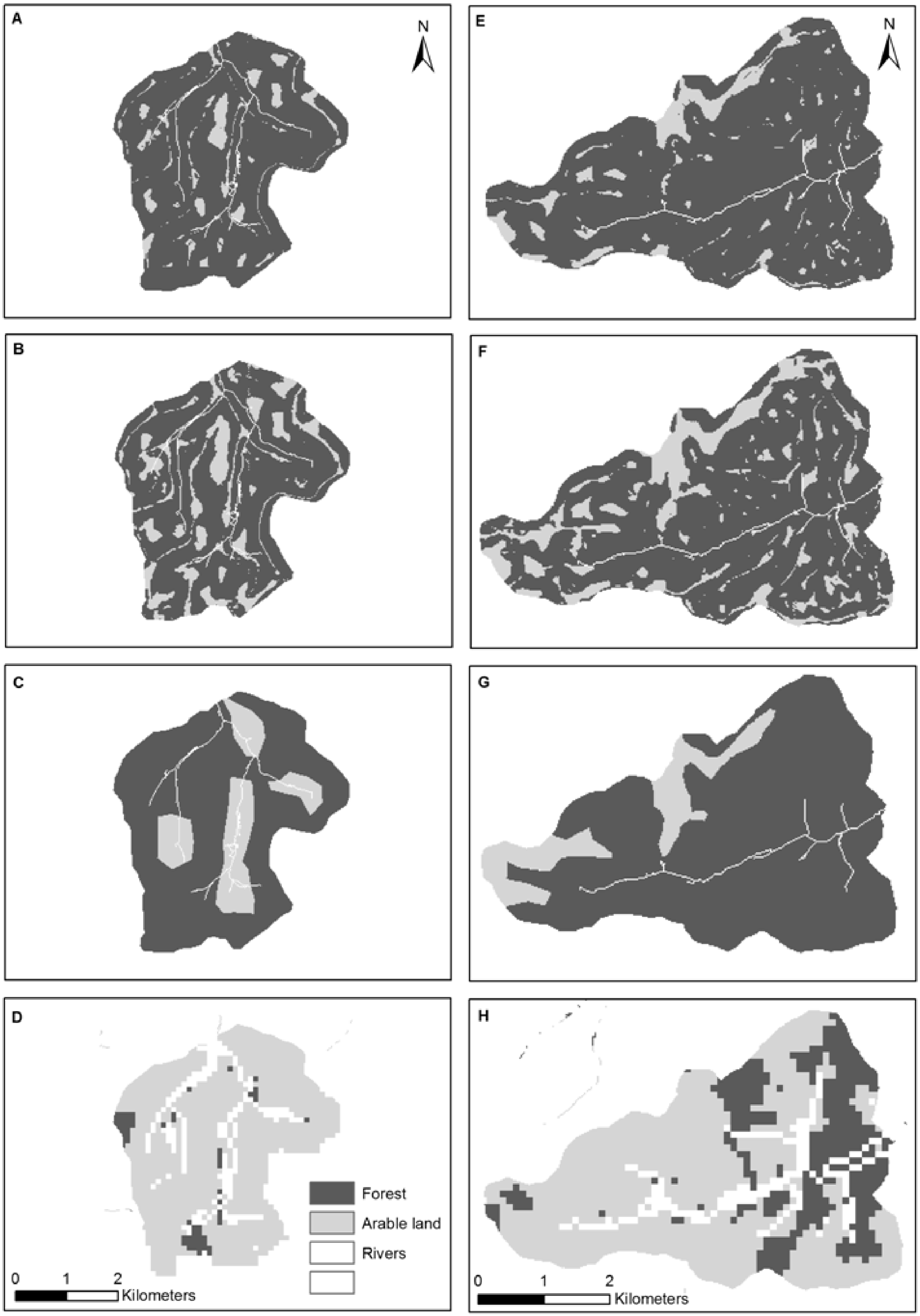

Figure 5.2. Selection of different simulated land cover scenarios (Table 5.2) for Cortil: A) Scenario 2; B) Scenario 3; C) scenario 7; D) Scenario 10; and Sclage: E) Scenario 2; F) Scenario 3; G) Scenario 8; H) Scenario 10.

5.4 Results

5.4.1 Floodplain architecture

Different sedimentary facies were identified in both sites (Table 5.3). Cross-sections of the floodplain in study site Sclage and Cortil are shown in Figure 5.3. Facies unit 1 consists of compact silty to loamy sediments with a low OM content, deposited at the base of the cross-sections. This unit is interpreted as Weichselian Late Glacial river deposits, or in-situ loess deposits (Notebaert et al., 2011a). Facies unit 2 are gyttja deposits: very organic sediments (LOI values above 40%) deposited in open water environment such as small ponds. Facies unit 3 is a peaty layer, containing mostly reed peat or woody peat (LOI values above 40%). Units 2 and 3 are overlain by silty to clayey overbank deposits with low OM content (LOI values below 10%) (unit 4). At some places unit 4 has slightly higher OM content (LOI values of ca. 15%), which is indicated as unit 4B. The transition between the peaty and gyttja deposits (unit 2 and 3), and the overbank deposits (unit 4) is abrupt but not erosive. Facies unit 5A consists of alternations of strong organic silty to clayey deposits and fine sandy layers, interpreted as multichannel deposits. Facies unit 5B consists of sandy sediments, without intermediate finer layers, and is interpreted as channel and point bar deposits because of their position and texture. Finally, facies unit 6 consists of silty clay loam to sandy deposits, arranged in layers and often containing brick fragments and is interpreted as a colluvial deposit. This unit covers unit 3, indicating that unit 6 is deposited after the formation of these organic rich layers. Similar facies were found by Notebaert et al. (2011a) in the entire Dijle catchment.

The base of units 2 and 3 is dated at ca. 10 ka cal a BP (Table 5.1). The top of the peaty deposits (unit 3) is slightly diachronic in Sclage, ranging between 376 ± 61 cal a BP and 620 ± 40 cal a BP. In Cortil, the top of unit 2 is dated at 2606 ± 72 cal a BP; the top of unit 4B at 604 ± 33 cal a BP. After around 400 cal a BP in Sclage and 600 cal a BP in Cortil, the entire floodplain is dominated by minerogenic overbank deposits with low OM content (unit 4). Based on the dating results (Table 5.1), an age-depth model was made for both sites (Figure 5.4). Results are rather similar for both sites. Floodplain accumulation rates are constant at ca. 0.2 mm a^{-1} until ca. 1650 cal a BP. At that moment, floodplain accumulation increases to ca. 0.6 mm a^{-1} for Cortil. From ca. 520 cal a BP onwards, sediment accumulation rates increased up to 6 mm a^{-1} at Sclage, and from ca. 604 cal a BP onwards it increases to 4 mm a^{-1} at Cortil. For both sites, this increase coincides with the transition from the organic floodplain deposits (unit 2 and 3) to the minerogenic floodplain deposits with very low OM content (unit 4). Radiocarbon dating results of the top of the peat layer at different locations along the transect in Sclage (Table 5.1) show that the floodplain accumulation rates increased to 2 mm a^{-1} around 520 cal a BP and further increased to 6 mm a^{-1} after 470 cal a BP.

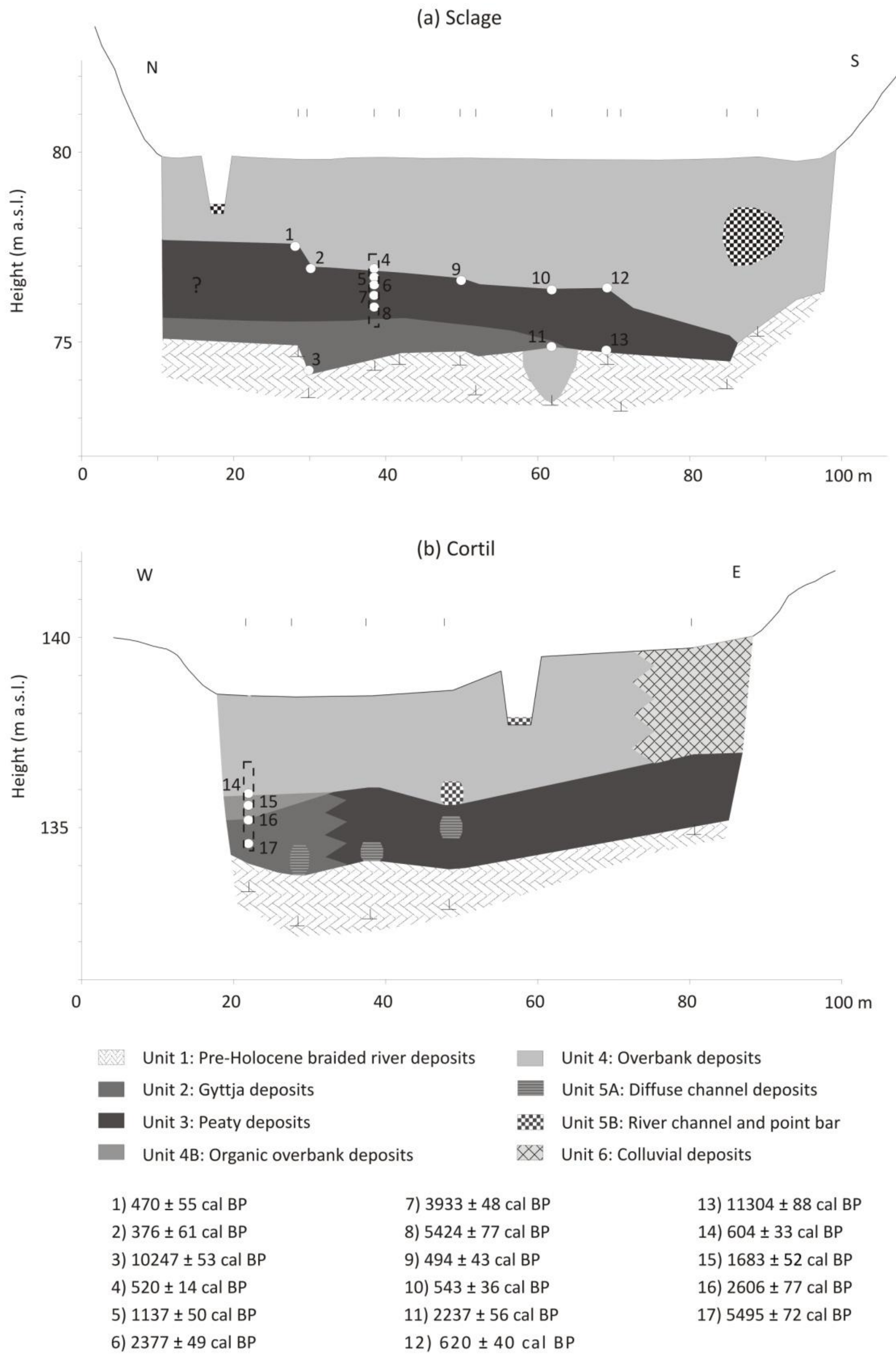

Figure 5.3. Cross-section of (A) the Cala floodplain near Sclage and (B) the Orne floodplain near Cortil (location, see Figure 5.1); with indication of the different lithogenetic units. Dotted rectangular indicates location of pollen profile, vertical lines indicate location and bottom of the individual corings.

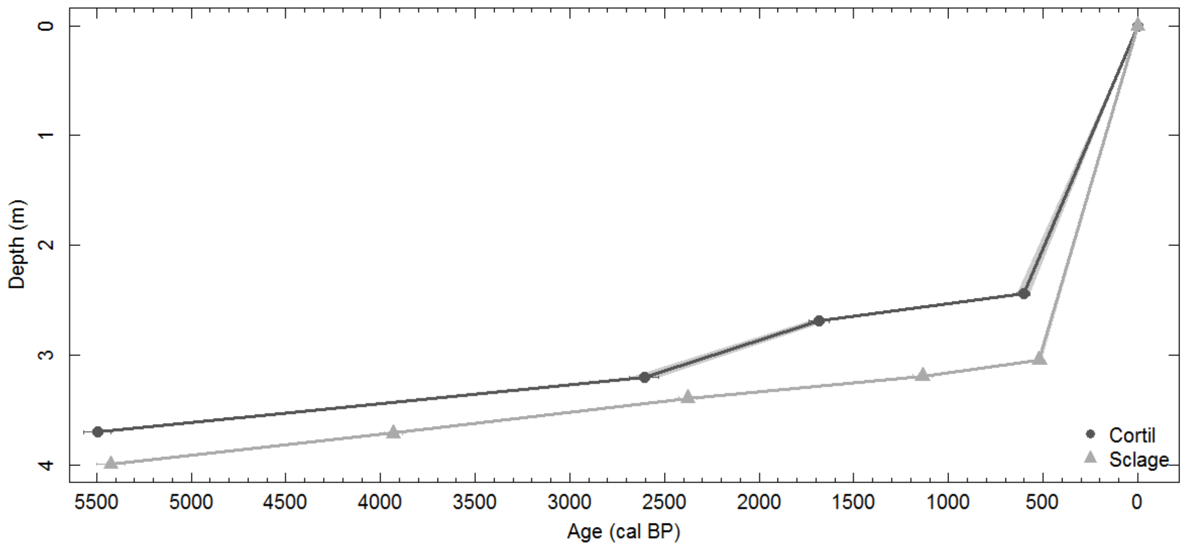

Figure 5.4. Calibrated AMS ^{14}C dating results and floodplain accumulation for the two study sites Sclage and Cortil.

Table 5.3. Lithogenetic units identified in both study sites. Similar units were found by Notebaert et al. (2011a) for the whole Dijle catchment.

Unit	Texture	Position	Interpreted deposition environment	Age
1	Compact silty to loamy sediments	Bottom of the floodplain deposits	Braided river deposits	Pre-Holocene
2	Gyttja deposits	Above unit 1, covered by unit 3 or 4	Open water deposits	From early Holocene to ca. 2500 cal a BP, depending on location
3	Peat to very organic silt and clays	Above unit 1 and 2, covered by unit 4	Marshy floodplain	From early Holocene to ca. 500 cal a BP, depending on location
4	Silty clay loam to loam	Top of floodplain	Overbank deposits	From ca. 600 cal a BP, depending on location
4B	Silty clay loam to silt loam, contains some organic material	Above unit 2, covered by unit 4	Overbank deposits	From ca. 2500 to 600 cal a BP
5A	Alterations of organic silty clay loam and fine sand deposits	Included in unit 2 and 3	Small diffuse channel deposits	From early Holocene to ca. 500 cal a BP, depending on location
5	Sandy loam and sands	Above unit 2, 3 and 4; sometimes included in unit 4	River channels and point bar deposits	After ca. 2500 cal a BP
6	Silty clay loam to sandy deposits, arranged in layers	At location of colluvial fans	Colluvial deposits	After ca. 2500 cal a BP

5.4.2 Local and regional vegetation

The regional pollen signal for the site of Sclage (Figure 5.5) can be split up in two major clusters (Figures 5.5 and 5.6). Cluster 1 (415-345 cm) contains high values of arboreal pollen (AP) (especially high values of *Corylus* and *Tilia*) and low values of non-arboreal pollen (NAP – containing Poaceae and upland herbs). Cluster 2 (345-286 cm) can be split in two sub clusters. Cluster 2A (345-303 cm) contains decreasing values of AP (decreasing values of *Corylus* and *Tilia*, but increasing values of *Quercus* and *Fagus*) and increasing values of NAP and anthropogenic indicators (e.g. Cereal-type and *Plantago lanceolata*). Cluster 2B (303-286 cm) contains low values of AP and high values of NAP, including Poaceae and other anthropogenic indicators. CHAR and floodplain accumulation rates are increasing from the beginning of cluster 2B upwards (Figure 5.5).

The cluster analysis of the local pollen signal of Sclage results in two major clusters (Figures 5.5 and 5.6). Cluster 1 (415-300 cm) is characterized by the absence of Typhaceae and low (cluster 1A, 415-400 cm) to high (cluster 1B, 400-300 cm) values of *Alnus*. Cluster 2 (300-286 cm) contains especially high values of Typhaceae.

The pollen diagram of the site Cortil is shown in Figure 5.5. The regional pollen signal can be divided in two major clusters (Figures 5.5 and 5.6). Cluster 1 (373-305 cm) contains mainly high AP values and low NAP values. This cluster can be split in Cluster 1A containing very high values of *Pinus* (up to 60%), and Cluster 1B containing high values of *Tilia* and *Corylus* and low values of *Pinus*. Cluster 2 (305-215 cm) contains low AP values and high NAP values including high values of Poaceae and anthropogenic indicators. CHAR and floodplain accumulation rates are increasing from 320 cm and are further increasing from 240 cm onwards.

The local pollen signal of Cortil can be divided in two major clusters (Figures 5.5 and 5.6). Cluster 1 contains high values of Cyperaceae, and low values of *Alnus*. This cluster coincides with cluster 1A of the regional signal. Cluster 2 contains mainly high values of *Alnus*, while Cyperaceae are almost absent. This cluster coincides with cluster 1B en cluster 2 of the regional signal.

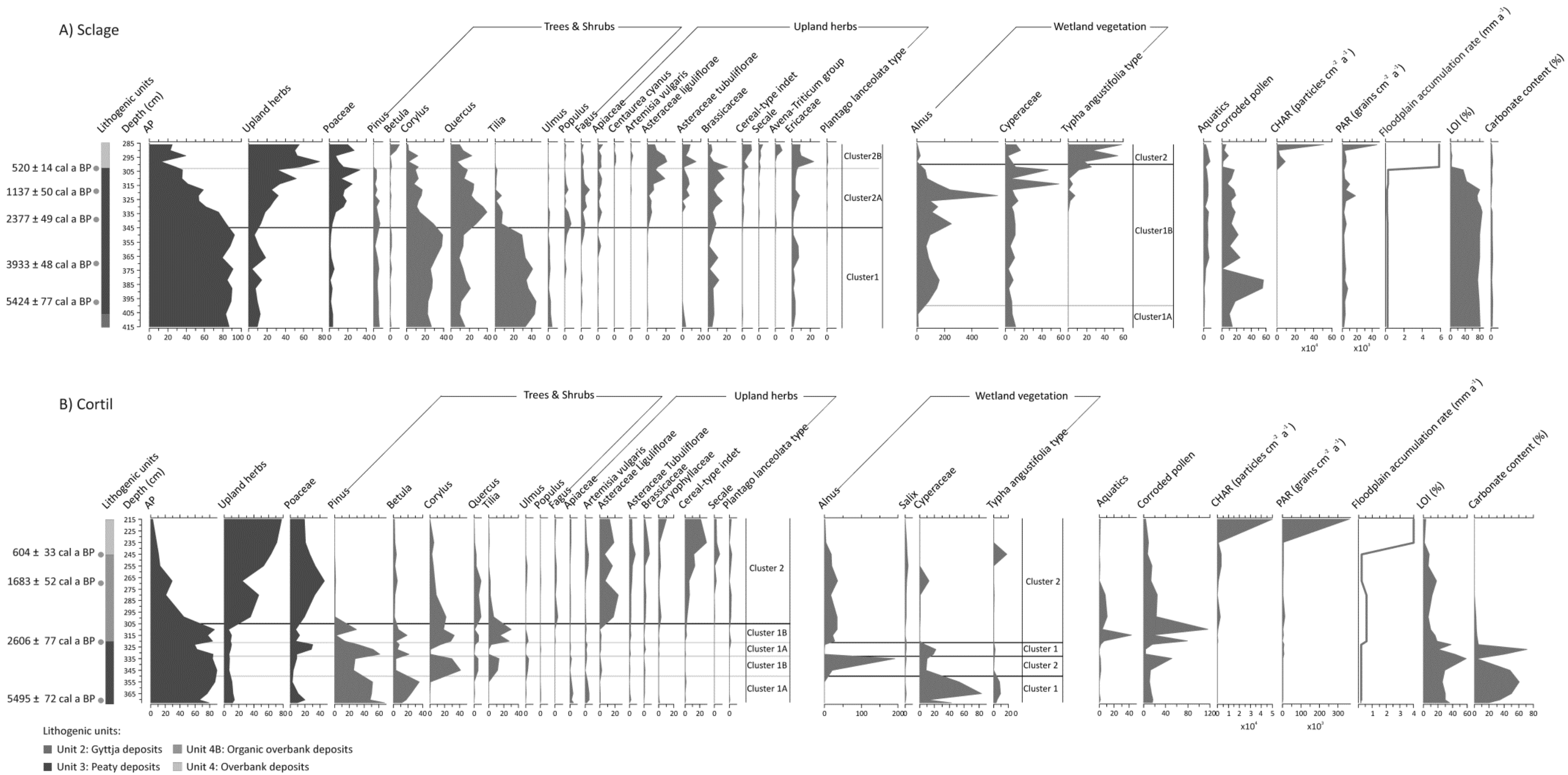

Figure 5.5. Simplified pollen diagram from site (A) Sclage and (B) Cortil; with indications of the different clusters.

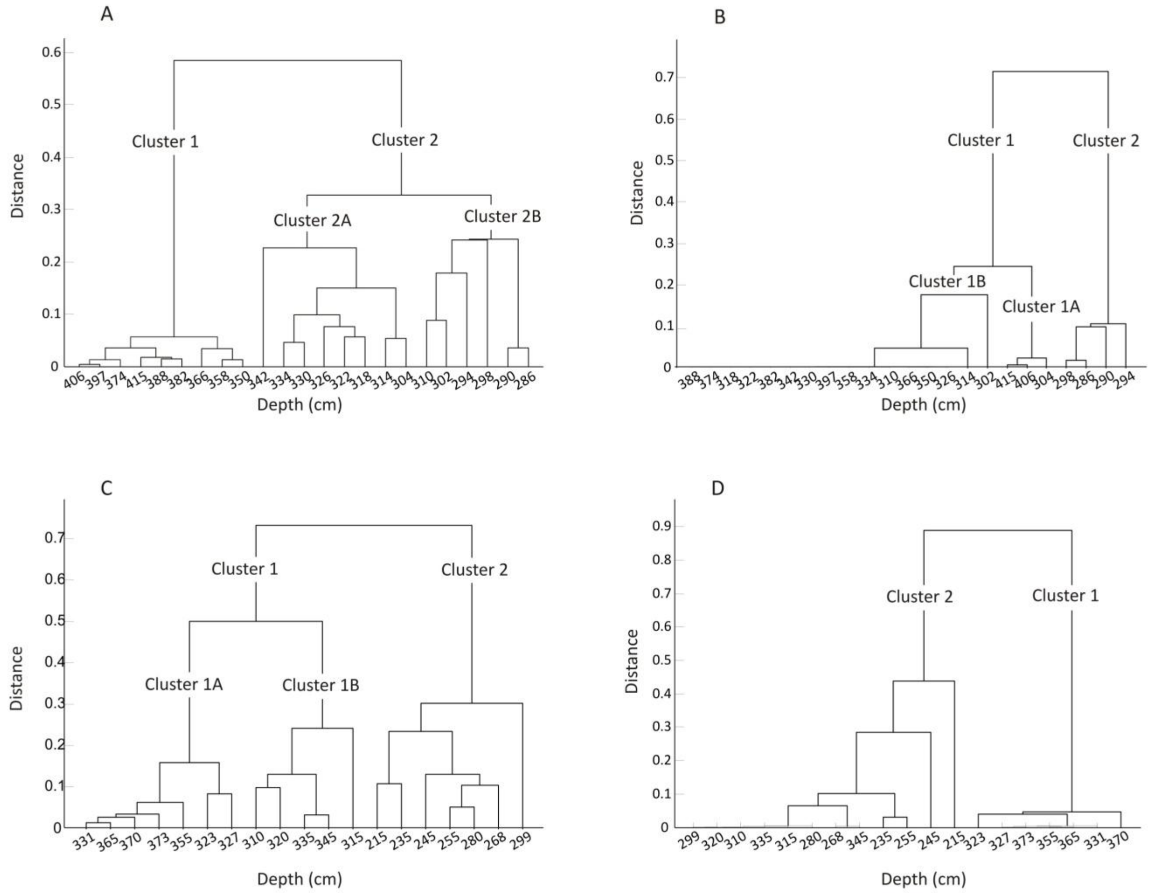

Figure 5.6. Clustering tree for (A) the regional pollen signal at Sclage; (B) the local pollen signal at Sclage; (C) the regional pollen signal at Cortil; (D) the local pollen signal at Cortil. The height of each branching point represents the distance between the two objects being connected.

5.4.3 Semi-quantification of human impact

The results of the CCA (Figure 5.7a) for both sites show that forest taxa have low scores on the first CCA-axis, whereas cultural indicators and all taxa associated with arable fields have high scores. Therefore, the scores on the first CCA-axis can be seen as an indicator for human impact. However, the scores are dimensionless and it is not possible to couple them with absolute numbers of settlements or area under human impact (e.g. Lechterbeck et al., 2009). When plotting the scores on the first CCA-axis in function of time (Figure 5.7b), an increase in human impact is suggested for both study sites. From ca. 6000 cal a BP until 2500 cal a BP human impact is at its lowest level in both sites. Within this time-span there is a small variation in human impact for Cortil, which can however not directly be linked with the alternation between cluster 1A and 1B (Figure 5.7). However, the significant increase in human impact starts more or less at the same time for both sites: around 2670 cal a BP at Sclage and 2340 cal a BP at Cortil. The increase in human impact in Sclage is rather gradual and reaches its highest level around 520 cal a BP. For Cortil, human impact increases to high levels in a shorter period (between ca. 2340 cal a BP and 2000 cal a BP), and reaches the highest level around 600 cal a BP.

A

Pollen type	score on 1st CCA axis	Ecotype	Cultural indicator
Pinus	-0.79425	Forest	
Tilia	-0.75771	Forest	
Ulmus	-0.6406	Forest	
Betula	-0.50766	Forest	
Corylus	-0.25983	Forest	
Artemisia vulgaris	-0.20902	Ruderal	CI
Acer	-0.08458	Forest	
Quercus	0.2011	Forest	
Apiaceae	0.22809	indiff	
Populus	0.26971	Forest	
Brassicaceae	0.34551	indiff	CI
Fraxinus	0.37384	Forest	
Poaceae	0.42184	Grassland	
Ericaceae	0.54698	Heath	
Plantago lanceolata	0.61195	Grassland	CI
Fagus	0.62814	Forest	
Caryophyllaceae	0.67501	indiff	
Asteraceae tubuliflorae	0.73247	indiff	
Asteraceae liguliflorae	0.83697	indiff	
Chenopodiaceae	0.95456	Ruderal	CI
Cerealia indet	0.96397	Arable fields	CI
Anthoceros	1.06	Arable fields	CI
Secale	1.07113	Arable fields	CI
Avena-Triticum group	1.14634	Arable fields	CI
Centaurea cyanus	1.15925	Arable fields	CI
Plantago major-media group	1.20022	Ruderal	CI

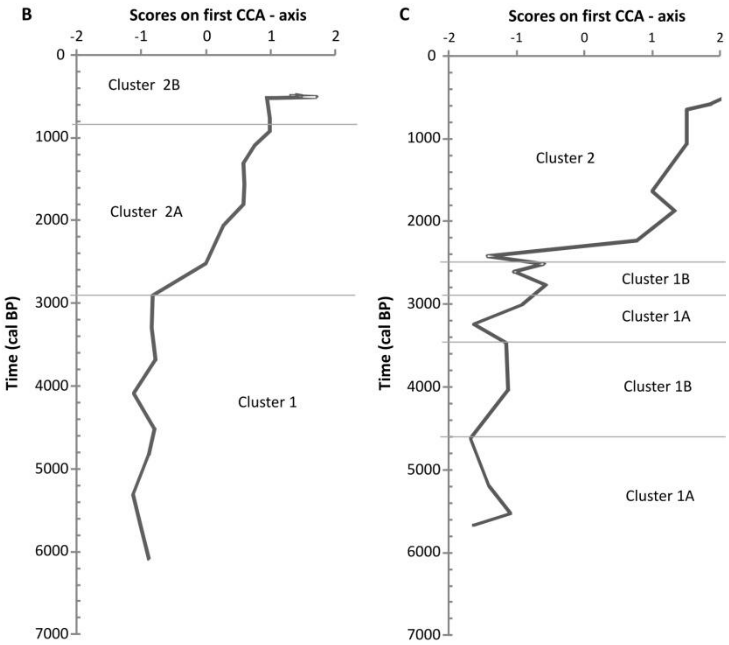

Figure 5.7. (A) Scores on the first CCA-axis for pollen types of both study sites Sclage and Cortil. Scores on the first CCA-axis plotted against time for (B) Sclage and (C) Cortil.

5.4.4 Modelling results

Soil erosion was modeled for the ten scenarios (Table 5.4 and Figure 5.8). Highest soil erosion amounts are predicted for the scenarios with high amount of cropland area, and for the scenarios were cropland is located close to the river system (Table 5.4). Sediment delivery is increasing with increasing fraction of cropland in the catchment, for both study sites (Figure 5.8).

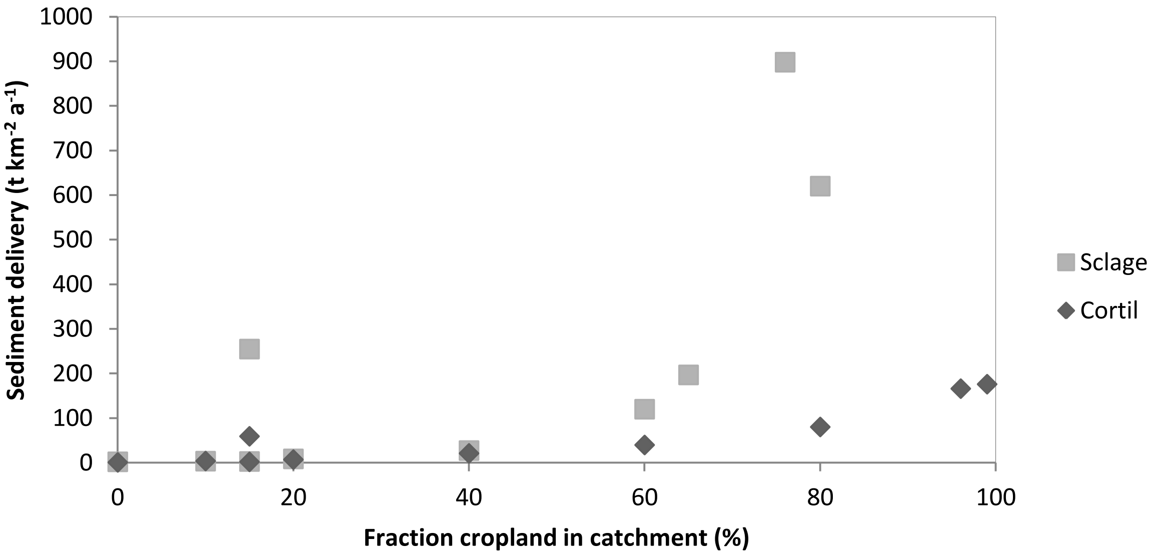

Figure 5.8. Sediment delivery (t km^{-2} a^{-1}) in function of the fraction of cropland in the catchment (%) for study site Cortil and Sclage.

Table 5.4. Results of the WaTEM/SEDEM modelling for different scenarios (see Table 5.2).

	Cortil (14km²)										Sclage (16 km²)									
scenario	1	2	3	4	5	6	7	8	9	10	1	2	3	4	5	6	7	8	9	10
% forest	100	90	80	60	40	20	85	85	1	4	100	90	80	60	40	20	85	85	35	24
% cropland	0	10	20	40	60	80	15	15	99	96	0	10	20	40	60	80	15	15	65	76
Sediment production (t a^{-1})	21	191	490	1549	3191	5622	1602	1745	9301	7486	68	272	907	3612	9106	20834	5638	1082	11607	21531
Sediment deposition (t a^{-1})	8	121	339	1105	2331	3861	752	1531	5798	4478	31	169	627	2576	5926	8475	1507	692	6851	5169
Sediment export (t a^{-1})	13	70	151	444	859	1760	850	214	3503	3008	38	103	279	1036	3180	12359	4132	389	4757	16362
River export (t a^{-1})	10	52	97	293	556	1121	828	26	2469	2327	32	55	136	435	1918	9920	4076	43	3149	14365
HSDR (%)	0.6	0.4	0.3	0.3	0.3	0.3	0.5	0.1	0.4	0.4	0.6	0.4	0.3	0.3	0.3	0.6	0.7	0.4	0.4	0.8
perc export (%)	47.6	27.2	19.8	18.9	17.4	19.9	51.7	1.5	26.5	31.1	47.1	20.2	15.0	12.0	21.1	47.6	72.3	4.0	27.1	66.7
sediment delivery (t km^{-2} a^{-1})	0.7	3.7	6.9	20.9	39.7	80.1	59.1	1.9	176	166.0	2.0	3.4	8.5	27.2	119.9	620.0	254.8	2.7	196.8	897.8

5.5 Discussion

5.5.1 Reconstruction of the floodplain geoecology

5.5.1.1 Sclage

Our data illustrate that from the beginning of the Holocene onwards the floodplain was a strongly vegetated and stable environment – i.e. an environment with limited sediment discharge and sediment deposition – resulting in peat and gyttja accumulation. Palynological data, used for the reconstruction of the floodplain ecology, were obtained for the period between ca. 6100 cal a BP and 520 cal a BP. The ecological reconstruction shows that from ca. 6100 cal a BP until 5460 cal a BP the floodplain was an open water system, resulting in gyttja deposits (Figures 5.3 and 5.5). These open water conditions are thought to be shallow lakes related to groundwater seepage in the floodplain. The sedimentological data shows limited sediment deposition (Figure 5.4), floodplain accumulation rate are of the order of 0.2 mm a^{-1}.

From ca. 5460 cal a BP until 520 cal a BP, the floodplain was dominated by Alder carr forests (*Alnion glutinosae*) (Figure 5.5). At this stage, no clear river channel was present in the floodplain. Instead the floodplain consisted of a marshy environment probably with a diffuse river pattern, as indicated by the limited sediment accumulation and the absence of channel deposits from this period (Figure 5.3). The *Alnion glutinosae* resulted in peat accumulation in the floodplain with an average peat accumulation rate of ca. 0.2 mm a^{-1}.

Around 520 cal a BP, the *Alnion glutinosae* disappeared and was replaced by an open floodplain dominated by Cyperaceae, Poaceae and Typhaceae (Figure 5.5). This transition occurred in a very short period (< 250 a), and is probably related to clearing of the *Alnus* forest and reclamation of the floodplain into wet meadows. At this transition, the sediment deposition increased from ca. 0.2 mm a^{-1} to ca. 6 mm a^{-1}. Consequently the peat accumulation stopped and was replaced by minerogenic overbank deposits. The top of the peat layer is slightly diachronic over the cross-section, ranging between 620 ± 40 cal a BP and 376 ± 61 cal a BP (Figure 5.3). We suggest that the diachronic transition between the two lithogenic units is due to the gradual built-up of levees that laterally expended over the backswamp areas when the sediment input increased. The build-up of the levees started at the southern side of the valley as suggested by the older dates, the lower elevation of the top of the peat and an old river channel at this side of the valley (Figure 5.3). After ca. 376 cal a BP, the entire floodplain was dominated by minerogenic sediment deposition, and had an open vegetation. This open floodplain vegetation is also visible on the illustrative *de Ferraris* map (ca. 1775, scale 1:11 520), and in the present floodplain.

5.5.1.2 Cortil

Also at Cortil the floodplain was vegetated and relatively stable with limited sediment deposition from the beginning of the Holocene onwards, resulting in peat and gyttja accumulation. Facies unit 5A indicate that small diffuse channels were present in the floodplain during the formation of these peat and gyttja deposits. The reconstruction of the floodplain ecology goes back from ca. 5495 cal a BP. Between ca. 5495 cal a BP and 2670 cal a BP, the vegetation in the floodplain shows an alternation between an open floodplain, dominated by Cyperaceae, Poaceae, Typhaceae and *Salix* on the one hand, and *Alnion glutinosae* on the other hand (Figure 5.5). This alternation is interpreted to be related to changes in wetter and dryer conditions in the floodplain, illustrated by the changing $CaCO_3$ content (Figure 5.5) due to changing input of groundwater seepage rich in $CaCo_3$. During dryer stages the floodplain is dominated by *Alnion glutinosae*; while during wetter stages the floodplain was more open and dominated by Cyperaceae, Poaceae and Typhaceae. During these alternations however, there was a constant low sediment deposition in the floodplain, resulting in organic (peaty and gyttja) deposits with an average floodplain accumulation rate of 0.2 mm a^{-1} (Figure 5.5).

From 2670 cal a BP to 620 cal a BP, the floodplain was dominated by *Alnion glutinosae*. Sediment accumulation was increasing, resulting in a cessation of peat accumulation. Instead, moderately organic (LOI values of ca. 10%) overbank deposits are found in the floodplain, with a sediment accumulation rate of 0.4 mm a^{-1} (Figure 5.5). This transition is rather gradual.

From 620 cal a BP onwards, the *Alnion glutinosae* disappeared and was replaced by wet meadows. This is also the land use type which is indicated on the *de Ferraris* map (ca. 1775). Sediment accumulation increases further to ca. 4 mm a^{-1}, and minerogenic overbank deposits with a low organic content (LOI values < 10%) are deposited (Figure 5.5).

5.5.2 The role of humans in changing the floodplain geoecology

Our reconstruction of the catchment vegetation and the human impact in the catchment dates back from ca. 6000 cal a BP. From ca. 6000 to 2500 cal a BP, the headwaters of the Dijle catchment were covered by deciduous forest, dominated by *Corylus*, *Tilia* and *Quercus* (Figure 5.9). Also Mullenders and Gullentops (1957), Mullenders et al. (1966) and De Smedt (1973) reported a deciduous forest in the Dijle catchment for this period. Anthropogenic indicators (e.g. Cereal-type and *Plantago lanceolata*) are present in low quantities in the pollen diagrams, resulting in low scores on first CCA-axis (Figure 5.7). This indicates that human impact was limited or only affecting geomorphology and ecology at a small scale. Consequently, in this period the investigated floodplains consist of a marshy environment with a multichannel river pattern. The floodplain was dominated by an *Alnion glutinosae* (Sclage); or characterised by an alternation between an open floodplain environment (dominated by Cyperaceae, Poaceae and Typhaceae) and an *Alnion glutinosae* (Cortil). This marshy environment with diffuse water transport seems to be the natural state of the floodplains of the headwaters of the Dijle catchment, which is also stated for locations further downstream in the Dijle-Demer confluence area by De Smedt (1973) and Vandenberghe and De Smedt (1979).

The *Pinus* pollen present in both diagrams are interpreted as a regional signal of a wider range. We suggest that the *Pinus* trees grew on the nutrient poor sandy deposits, which can be found north of the Belgian loess belt (De Smedt, 1973) and locally in the Dijle catchment where Paleogene sandy outcrops occur. The higher percentages for Cortil are explained by a better pollen trapping capacity for *Pinus* at this site due to more open water environments (gyttja deposition) and more gentle valley slopes. A poor trapping capacity at Sclage, due to the continuous dominance of *Alnus* in the floodplain and the forested steep slopes surrounding the floodplain of Sclage, resulted in low pollen values of *Pinus*. Pollen of a wider range are often removed from the pollen transport system before it is deposited at the sampling point, mainly via deposition on the vegetation (Bunting, 2007). Moreover, in the pollen diagram of Cortil (Figure 5.5), an alternation between high pollen values of

Pinus, *Betula* and Poaceae (cluster 1A) on the one hand and *Corylus*, *Ulmus*, *Tilia* and *Quercus* (cluster 1B) on the other hand is present. It is suggested that these variations are caused by human induced forest clearance during cluster 1A and forest regrowth during cluster 1B. However, cluster 1A has no significant higher scores on the first CCA-axis (Figure 5.7), suggesting that these clearances occurred only at a small scale and suggesting a limited coupling between these forest clearances and the floodplain. Nevertheless, we suggest that these alternations in forest clearance and regrowth can be related with the observed alternation in wetter and dryer conditions in the floodplain at Cortil (paragraph 4.1.2), as the early deforestation could cause increased infiltration on the slopes and seepage in the river valley and consequently caused wet conditions in the floodplain.

From ca. 2500 cal a BP onwards, both pollen diagrams reflect a clear increase in human impact (Figure 5.7). The AP fraction in the pollen diagrams decrease and more upland herbs, Poaceae and anthropogenic indicators appear (Figure 5.9). This happens earlier in Sclage (ca. 2670 cal a BP) compared to Cortil (ca. 2340 cal a BP). Also at other sites in the Dijle catchment, the presence of anthropogenic pollen indicators become significant around this time (Mullenders et al., 1966). Simultaneously with this decrease in forest cover, there is a change in the forest composition: whereas previously the forest was dominated by *Tilia* and *Corylus*, now *Quercus* becomes most dominant and *Fagus* appears (Figure 5.5). Previous research linked this *Tilia* decline with anthropogenic impact (e.g. Turner, 1962; Bradshaw, 2008). Also the slight increase in charcoal accumulation rate illustrates the increasing human impact in the catchment. This first significant increase in human impact in the catchment (around 2670 cal a BP) did not alter the floodplain morphology in Sclage, probably due to the limited connectivity between the cultivated areas and the fluvial system caused by the forested slopes and riparian vegetation surrounding the floodplains (e.g. Tabacchi et al., 1998; Houben et al., 2012) (Figure 5.9). The floodplain remained a marshy environment dominated by an *Alnion Glutinosae*, with a diffuse drainage network. In Cortil on the other hand, this increased human impact caused a small increase in sediment deposition in the floodplain, suggesting a better coupling between cultivated areas and floodplains as more and more cultivated areas are directly connected with the fluvial system (Figure 5.9). This resulted in a cessation of the peat accumulation and the start of the deposition of moderately organic minerogenic floodplain sediments.

During the Roman and Medieval Periods (from ca. 2000 cal a BP until 500 cal a BP) human impact continuously increased, indicated by a further decrease in forest cover and a further increase in Poaceae, upland herbs and anthropogenic indicators (Figure 5.9). Human impact appears to be higher in Cortil than in Sclage, as is illustrated by the higher scores on the first CCA-axis (Figure 5.7), which is in agreement with the higher concentrations of archaeological findings from the Roman Period in the surrounding of Cortil (Figure 5.1) (Notebaert, 2009). This continuous increase in human impact is only interrupted by a small increase in forest cover at Cortil around 1600 cal a BP, which can possibly be coupled with a decreased population density and human impact in Europe during the Migration Period (ca. 1750-1600 cal a BP) (Buntgen et al., 2011). From ca. 600 cal a BP (Cortil) and ca. 520 cal a BP (Sclage) onwards, human impact is at its highest level. This further increase in human impact from the Roman period onwards resulted in increased overland flow, soil erosion, and colluvial sediment deposition (unit 6 in Figure 5.3) (Notebaert et al., 2011b). Furthermore, there is a strong increase in floodplain accumulation rate (from ca. 0.2 mm a^{-1} to more than 4 mm a^{-1}). Similar trends in accumulation rate were found by Notebaert et al. (2011b) for other sites in the Dijle catchment. This increased sediment input in the river valley and formation of natural levees altered the river morphology towards a single channel river. Consequently, peat formation in the floodplain stopped, and the floodplain became dominated by minerogenic overbank deposits. Similar trends in floodplain accumulation rates and changes in river morphology are reported in other areas in West and Central Europe (e.g. Foulds and Macklin, 2006; Houben, 2007; Chiverrell et al., 2009; Macklin et al., 2010). Contrary to rivers in the Eastern US (e.g. Walter and Merritts, 2008) or in Germany (Houben et al., 2012), there is no evidence that these changes are related to direct human activities in the floodplain such as mill damming, but the floodplain geoecology changes are the indirect result of an intensification of agricultural activities in the catchment.

The abrupt change in floodplain geoecology in Sclage is in contrast to the gradual increase in human impact (Figure 5.7). This suggests a time-lag between the start of soil erosion and the start of alluvial deposition (e.g. Lang et al., 2003; Notebaert et al., 2011c; Houben et al., 2012), and illustrates that the changes in floodplain geoecology at Sclage are only occurring when a certain threshold has been reached. Quantifying this threshold in terms of area of arable land is, however, still not possible (e.g. Lechterbeck et al., 2009). At Cortil, the increase in human impact is more abrupt, and influences the floodplain geoecology earlier: from ca. 2500 cal a BP the increased human impact caused a slight increase in floodplain accumulation rate. However, only after circa 600 cal a BP, when human impact is at its highest level the threshold towards floodplain morphology changes was reached. The differences between the two study sites can be attributed to a stronger connectivity between the cultivated and eroding uplands and floodplains at Cortil compared to the lower degree of connectivity at Sclage. Indeed, in Cortil, the gentle transition from the valley bottom to the low-angle slopes facilitated the continuous exploitation of the entire floodplain-slope catena, whereas in Sclage the steep valley-side slopes remained under forest and thus trapped the majority of sediment that was produced on the more gentle hillslopes higher up (Figure 5.9). Consequently, it is hypothesised that the threshold conditions between the both sites were different.

The results of the WaTEM/SEDEM modelling (Table 5.4) illustrate that this proposed hypothesis on the differences between the two study sites is physically possible. Land cover scenario 7, with cropland area close to the rivers on low gradient slopes, results in Cortil in a higher sediment delivery compared with land cover scenario 8 in Sclage, with cropland area further away from the rivers (Figure 5.8 and Table 5.4). However, this interpretation is not confirmed by the first set of simulations. Scenario 1, 2, 3 and 4 (respectively 0, 10, 20 and 40% of cropland in the catchment) does not result in higher sediment delivery at Cortil compared to Sclage. Alternatively, this first set of simulations shows the possibility of a different hypothesis: the differences between the two study sites can be attributed to a earlier deforestation in Cortil compared to Sclage. Scenario 6 (80 % of cropland) results in Cortil in a significant higher sediment delivery compared with scenarios 2, 3 and 4 (respectively 10, 20 and 40% of cropland) in Sclage. This is partly confirmed by the higher scores on the first CCA-axis in Cortil compared to Sclage during the Roman and Medieval Period (Figure 5.7). But, the fact that our hypothesis on the differences in connectivity is not confirmed by the first set of simulations is probably due to the fact that the simple allocation model used in this study (equation 5.2) is not detailed enough. For instance, soil type and distance to rivers are not included in equation 5.2. As a consequence, deforestation only occurred further away from the rivers in scenarios 2, 3 and 4 (Figure 5.2). Distance to rivers and soil type should be included in the allocation model to provide more realistic land cover scenarios. Such realistic land-cover reconstructions at high spatial resolution are needed for accurate modelling of sediment fluxes in the past (e.g. De Brue and Verstraeten, 2014) and to correctly evaluate the proposed hypothesis.

Moreover, the modelling results of the WaTEM/SEDEM shows that study site Sclage appears to be more sensitive at high human impact, resulting in a higher sediment delivery, compared to Cortil. This can explain the higher sediment accumulation rate in Sclage (6 mm a^{-1}) compared to Cortil (4 mm a^{-1}), and the consequent high amount of sediment deposition in the floodplain in Sclage once a large fraction of the catchment is deforested.

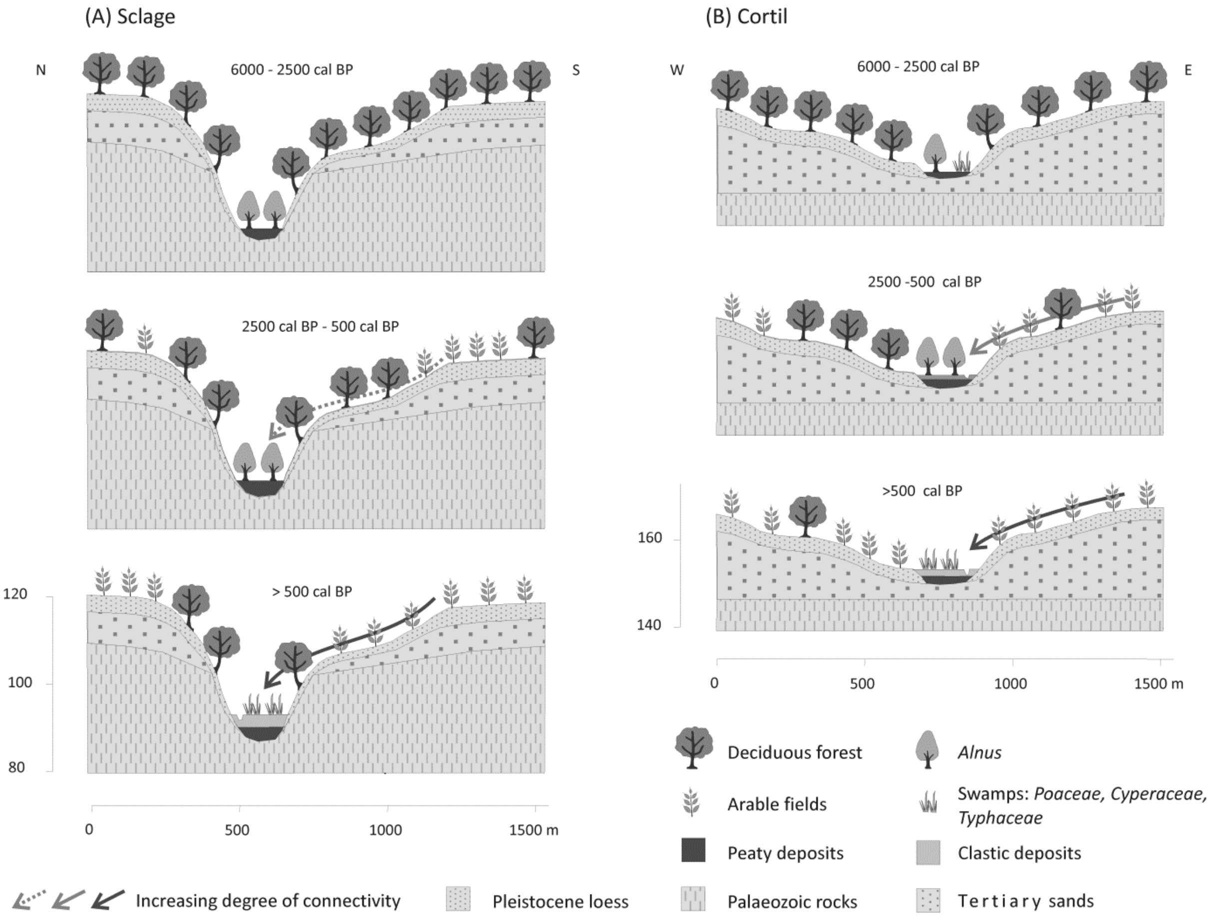

Figure 5.9. Schematic reconstruction of the floodplain and upland vegetation, for (A) Sclage and (B) Cortil.

5.6 Conclusions

This study demonstrates that floodplain geoecology (i.e. geomorphology and ecology) of two sites in the upstream part of the Dijle catchment changed during the Middle and Late Holocene under the influence of increased human impact in the catchment. Until ca. 2500 cal a BP, human impact was nearly absent or localized with no discernible influence on the floodplain geoecology. The river floodplain was relatively stable and consisted of a marshy environment where organic material accumulated. This marshy environment with Alder carr forests and shallow lakes and a multichannel drainage network is suggested to be the natural state of the Dijle catchment headwaters. From ca. 2500 cal a BP onwards, human impact gradually increased and forest cover previously dominated by *Tilia* and *Corylus* declined. Our results show that this first increase of human impact on the regional vegetation did not influence the floodplain geoecology dramatically, although the timing of the geoecological floodplain response of the two sites is slightly different depending on site-specific geomorphologic (valley slope) and archeological (occupation density) conditions. This can be confirmed by the WaTEM/SEDEM modelling, but more realistic land-cover reconstructions at high spatial resolution are needed for a more accurate modelling of sediment fluxes in the past. When anthropogenic land use further intensified after ca. 600 cal a BP and sediment delivery crossed a threshold, the floodplain geoecology changed with clearing of the Alder carr forest, the creation of a single channel river and the dominance of minerogenic overbank sedimentation.

The contemporary morphology of the floodplains in the Dijle catchment, with a meandering river bordered by levees and mineral floodplain deposits, has an anthropogenic origin. It contrasts widely with the Middle Holocene floodplains, which were dominated by peat formation in marshes and gyttja deposition in floodplain lakes, and which lack evidence of a well developed main channel. These floodplain geo-ecological changes are the indirect result of the intensification of cropland activities in the catchment, and comparable changes are also reported for other rivers in temperate West- and Central Europe (Notebaert and Verstraeten, 2010).

5.7 Annex

In this chapter 5, canonical correspondence analysis (CCA), was used to gain more insights into the changes in the pollen records through time and to compare the pollen record over the different study sites. In chapter 4, however, non-metric multidimensional scaling (NMDS) was used for this purpose, since NMDS has several advantages compared with other ordination techniques such as PCA (principal component analysis) and CCA: NMDS is the most robust unconstrained ordination method in ecology (Minchin, 1987), it does not make assumptions about the nature of the data and there are no hidden axes of variation unlike other ordination techniques (Legendre and Legendre, 1983; McCune and Grace, 2002).

In Figure 5.10, the scores on NMDS axis 1 (chapter 4; Figure 4.7) are compared with the scores on the first CCA axis (chapter 5; Figure 5.7), both plotted in function of time, for study site Sclage and Cortil. Figure 5.10 shows that the trends for both study sites are similar when using the two methods. Also the onset of the increase in scores is dated at the same time, namely at ca. 2700 cal a BP for Sclage and at ca. 2300 cal a BP for Cortil. Only at Cortil some differences are present. Between 6000 and 2500 cal a BP, the two different methods shows different variations. These variation are caused by variations in the pollen data between high values of *Pinus*, *Betula* and Poaceae and high values of *Quercus*, *Corylus* and *Tilia* (Figure 5.5b). The ordination used in CCA and NMDS is slightly different, resulting in different scores for these variations on the first axes. The results of the NMDS seems to better represent these variations in forest composition. Nevertheless, these different representations of the variations in forest composition does not affect the reconstruction of human impact after ca. 2500 cal a BP. The onset of the increase in human impact is dated at the same time and the subsequent trends are similar. Therefore, it is stated that the overall conclusions made based on the CCA remains valid and does not need a reinterpretation.

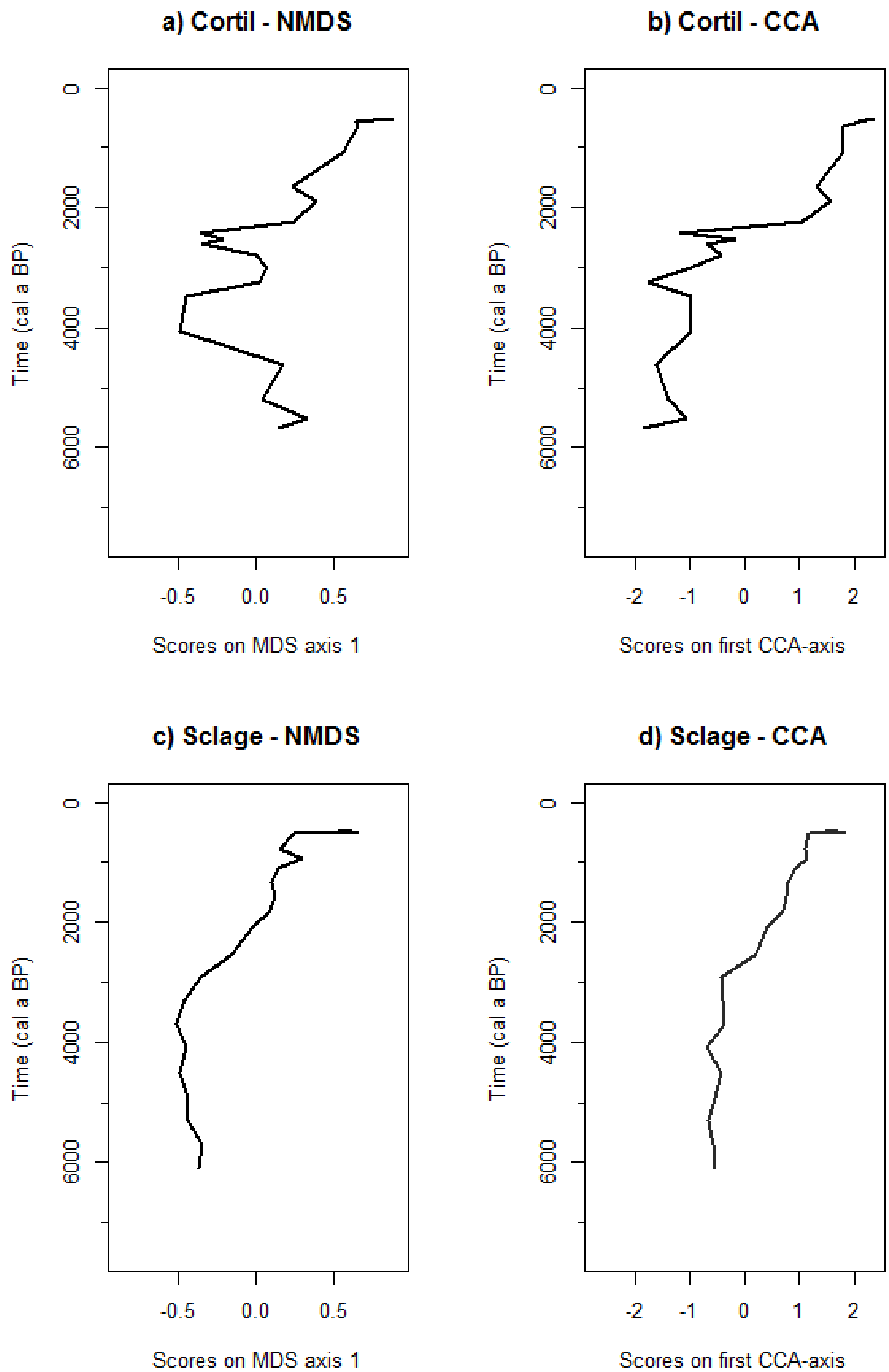

Figure 5.10. Scores on NMDS axis 1 (chapter 4) compared with scores on first CCA axis (chapter 5), plotted in function of time. For (a) and (b) Cortil, and (c) and (d) Sclage.

Chapter 6 Synthesis: Sensitivity of floodplain geoecology to human impact. A catchment-scale approach

This chapter is based on: Broothaerts N, Verstraeten G, Kasse C, Bohncke S, Vandenberghe J (under review) From natural to human-dominated floodplain geoecology – a Holocene perspective for the Dijle catchment. *Anthropocene.*

6.1 Introduction

From chapter 2 it is clear that floodplain geoecology of the River Dijle changed throughout the Holocene. During the Middle Holocene, the floodplain was a relatively stable environment and consisted of a strongly vegetated marshy environment (dominated by an alder carr forest), resulting in peat and gyttja accumulation. Floodplain geoecology changed with clearing of the alder carr forest, the creation of a single channel river and the dominance of minerogenic overbank sedimentation (Figure 2.14). Sediment input in the floodplain increased mainly in the last 1500 years (Figure 2.10). The detailed chronological analysis of these changes (chapter 3) reveals that the change in floodplain geoecology was diachronous at the scale of the catchment, and ranged between 6500 and 500 cal a BP. Moreover, the well-dated floodplain transect of Korbeek showed that floodplain changes are also asynchronous at cross-section scale. It was hypothesized that this gradual and spatially heterogeneous decrease in peat growth at catchment scale was the consequence of the heterogeneous and gradual nature of human impact in the catchment (section 3.5.4).

However, several questions remained unanswered. How exactly did the increasing human impact influence floodplain geoecology? How can the changes in floodplain geoecology be related to the increasing human impact? Why are changes in floodplain geoecology asynchronous? Can the differences in response between the various subcatchments be attributed to heterogeneity in the timing and nature of the external forcings, or to the difference in sensitivity towards human impact? Is the latter an indication of a non-linearity in the process-response relation? Finally, which threshold levels of human impact needed to be reached to trigger the observed changes in floodplain geoecology?

To provide an answer to these questions, and to attain a better understanding of the sensitivity of floodplain geoecology to human impact in the landscape, the observations on floodplain changes from chapter 2 and 3 will be evaluated against the available data on human impact. A detailed reconstruction of human impact in the Dijle catchment was extracted from palynological data based on the statistical analysis in chapter 4, and showed that human impact in the Dijle catchment is increasing from the Bronze Age onwards. In chapter 5, a similar integrating approach was used to investigate the relation between increasing human impact and the changes in floodplain geoecology for the headwaters of the Dijle catchment. In the present chapter, a catchment-wide approach will be followed as this will provide more insights in the differences among different subcatchments. The study area in the present chapter is the Dijle catchment upstream of Leuven (758 km²). Data of six study sites in the Dijle catchment are used (Figure 2.2). Detailed description of the Dijle catchment and the study sites is provided in chapter 2.

6.2 From natural to human-dominated floodplain geoecology

6.2.1 Natural situation

As argued in chapter 4, the statistical analyses of the pollen records (cluster analysis and non-metric multidimensional scaling (NMDS)) do not detect wide-scale forest clearance or catchment-wide human activities during the Mesolithic (11500 – 7200 cal a BP; Table 2.1) and Neolithic Period (7200 – 3900 cal a BP). The Dijle catchment was mainly covered by a deciduous forest dominated by *Corylus*, *Tilia* and *Quercus* (Figure 4.2), which is considered as the natural, interglacial, vegetation of the Dijle catchment. Human impact was low during these periods, as is shown by the NMDS (Figures 6.1, 6.2 and 6.3). The Neolithic human activities, however, could have been limited to local-scale clearings, which were hardly connected with the fluvial system. In this case, pollen of e.g. anthropogenic indicators are will not be easily represented in records from alluvial study sites (see chapter 4).

In the same period, the floodplain consisted of a strongly vegetated marshy environment, dominated by an *Alnion glutinosae* (alder carr forest) in most study sites (chapter 2 and Figures 6.1 and 6.2). It was an environment with limited sediment discharge and sediment deposition. Water transport occurred through a multi-channel or diffuse water-network, without a clear river channel (Appendix 2). Such a floodplain environment resulted in peat and gyttja accumulation. During the Mesolithic and Neolithic Period, almost the whole floodplain area in the Dijle catchment was under active peat growth (Figure 6.3). This is considered as it is the natural, interglacial, state of the floodplains in the Dijle catchment. There are no indications of direct human influence on the floodplain during this period, such as floodplain forest clearance. Similar natural floodplain situations can be found more downstream in the Dijle catchment, in the Dijle-Demer confluence area (De Smedt, 1973; Vandenberghe and De Smedt, 1979), and in other catchments in West and Central Europe e.g. in Germany (e.g. Lang and Nolte, 1999; Rittweger, 2000; Kalis et al., 2003; Houben, 2007) and in the Paris Basin (e.g. Pastre et al., 2002) for an overview, see Notebaert and Verstraeten (2010).

However, this overall picture of a dense vegetated catchment with alder carr forest dominating marshy valley bottoms, is not always valid. Some variations in the natural floodplain vegetation are observed at the study sites of Cortil and Sint-Agatha-Rode (Figure 6.1). Here, human impact, as expressed as scores on NMDS-axis 1, shows variations during the Mesolithic and Neolithic Period. These can be related to local variations in forest clearance and regrowth in the landscape at distances sufficiently close to the sampling site (see chapter 4 and 5). The variations in nearby forest clearance and regrowth can be coupled to the observed alternation in floodplain conditions. Wet floodplain stages dominated by Cyperaceae, Poaceae and Typhaceae corresponded with forest clearance and higher human impact in the landscape; dryer floodplain stages dominated by alder carr forest corresponded with forest regrowth in the landscape. This early and local deforestation could cause increased rates of infiltration on the slopes and interfluves and seepage in the river valley bottoms. Consequently, this will have resulted in wetter conditions in the floodplain and the alder carr forest could disappear (see e.g. Huybrechts, 1999). However, at both study sites, the floodplain morphology remained stable during these variations and the limited amount of sediment deposition did not abruptly end the gyttja and peat accumulation. Furthermore, these variations did not occur at the same moment for the two study sites. In Cortil, they occurred between ca. 6000 and 2500 cal a BP, in Sint-Agatha-Rode between ca. 7500 and 5500 cal a BP (Figure 6.1). These observations do suggest that the Neolithic forest clearances occurred only at a small scale and were semi-connected to the floodplain system. At other areas in the Dijle catchment, such Neolithic forest clearances cannot be excluded, but were probably located at a larger distance from the floodplain and were consequently not represented in the pollen records from these alluvial sites.

6.2.2 Towards human-dominated floodplain geoecology

The increase in human impact that can be observed throughout the Dijle catchment from the Bronze Age onwards (Figure 6.3) caused an increase in overland flow and soil erosion. Time-differentiated sediment budgets for the Dijle (Notebaert et al., 2009b) and Nethen catchment (Verstraeten et al., 2009b) indicated an increase in anthropogenic erosion and colluviation from this period onwards. Consequently, sediment input in the floodplain system could increase (Figures 6.3, and Notebaert et al. (2011b)). Coinciding with this increase in sediment input, floodplain geoecology changed from a marshy environment dominated by an alder carr forest towards a more open floodplain dominated by clastic overbank deposits. This can be observed in most study sites, i.e. in Archennes, Loonbeek, Korbeek, Cortil and Sclage (Figures 6.1 and 6.2). The timing of the increase in sediment input and the changes in floodplain geoecology differs, however, for the different study sites (Figures 6.1 and 6.2). Moreover, in the wide floodplains situated more downstream, such as Korbeek and Archennes, this change in floodplain geoecology does not occur simultaneously (Figures 3.7, 6.1 and 6.2). This gradual change can be coupled with the gradual increase in sediment supply in the floodplain first hampering peat growth near the channel(s) and only later on affecting peat growth in the distal floodplain parts (Figure 3.7). In narrow floodplains, such as Cortil and Sclage, the change in morphology is more abrupt (see chapter 5 and Figures 6.1 and 6.2). In Sint-Agatha-Rode, the floodplain morphology is changing before increasing human impact is detected by the pollen data for this study site (Figure 6.1). This is suggested to be related with the larger catchment area of this study site (ca. 190 km²). Study sites in a larger catchment reflect changes in a larger area and cumulate sediment supply from the entire catchment. Consequently, floodplain morphology can change before human impact is detected in the pollen data of a site. In Archennes and Korbeek (catchment area of 360 km² and 750 km² respectively) such a reverse temporal offset is not observed, since human impact is detected very early in the pollen records of these sites (Figure 6.1 and 6.2).

The diachronic change in floodplain geoecology in the individual sites resulted in a gradual decrease in proportion of floodplain area under active peat growth in the entire Dijle catchment, coinciding with the gradual increase in human impact from the Bronze Age onwards (Figure 6.3). Even from the beginning of the Neolithic period, peat growth slightly disappeared in some parts of the floodplain (Figure 6.3). The limited amount of sediment input associated with Neolithic human impact could cumulate downstream and could trigger a stop in peat growth in some floodplain areas in the downstream part of the catchment (e.g. in Sint-Joris-Weert; Notebaert et al. 2011a) (see also section 6.2.3).

During the Migration period (1750-1600 cal a BP; Table 2.1), human impact stagnated or even decreased in (Figures 6.1 and 6.2). This decrease can be coupled with floodplain changes, with a regrowth of the alder carr forest and an increase in the OM content (locally represented as a peaty layer), e.g. in Sint-Agatha-Rode, Loonbeek, Archennes (Figure 6.1) and Korbeek (Figure 6.2). It is suggested that the decrease in human impact caused a decrease in soil erosion and a decrease in hillslope-floodplain connectivity due to the regeneration of valley-side vegetation barriers (e.g. Houben et al., 2013). Consequently, sediment input in the floodplain decreased. This decrease in sediment input is not observed in the accumulated sediment mass curves (Figure 2.10) due to the averaging effects and the rather low time resolution of the sediment stratigraphy (e.g. Notebaert et al., 2011b). Furthermore, Figure 6.3 shows a stabilization phase in the decline of floodplain area under active peat growth during the Roman Period. Similar patterns of decrease in sediment supply into the floodplain system during the Roman and Migration Period are observed in SW Germany (Lang and Nolte, 1999; Houben et al., 2013), where they are coupled with the specific land use system during the Roman Period. In SW Germany, the floodplain was not part of the Roman land use system and floodplain forests could regenerate. Due to the regeneration of floodplain forests and valley-side vegetation barriers, the hillslope-floodplain connectivity decreased and sediments could not enter the floodplain (Houben et al., 2013). Quantitative and spatially distributed data of archeological findings for the entire Belgian loess belt, however, is still lacking to check if this is the case in the Dijle catchment. Nevertheless, archeological research in a limited part of the Dijle catchment suggests that Roman settlements are mainly found at some distance from the rivers (Van Hove et al., 2005). After the Migration Period, when human impact increased again, an important increase in sediment input in the floodplain system is observed (Figure 6.3). Consequently, the entire floodplain changed towards a floodplain with open vegetation, the creation of a single channel river and the dominance of minerogenic overbank sedimentation (Figures 6.1 and 6.2).

Overall, it is clear that the floodplain geoecology changed mainly as the indirect result of an intensification of agricultural activities in the catchment. Possibly, infrastructural works in the floodplain, such as mills, milldams and other hydraulic works could have an influence on the changing floodplain morphology. However, the known watermills in the Dijle catchment are located directly on the river channel or on a parallel canal, and no milldams damming the entire floodplain are observed – except for one milldam in the headwaters of the Dijle catchment. Also no milldams damming the entire floodplain are indicated on the *de Ferraris* map (ca. 1775). Moreover, the observed floodplain changes occurred before the introduction of mills in the catchment. Watermills in the Dijle catchment were mainly introduced from ca. 800 to 600 cal a BP onwards (Verstraeten et al., 2009b), although an extensive database of watermills in the catchment is still missing. Therefore, it is suggested that hydraulic works were not the dominant factor controlling the floodplain changes, as observed in e.g. Germany (Houben et al., 2013) and in Eastern USA (Walter and Merritts, 2008), although a better archaeological record on medieval mills can help to unravel their specific role on changing floodplain morphology. Also the clearing of the alder carr forest and reclamation of floodplains into wet meadows during the Medieval Period could have an influence on the changing floodplain geoecology, but identification of the relative importance of this direct impact was not possible by the available data. Model results showed that little evidence exists for the influence of climatic variations on floodplain changes in the Dijle catchment during the Middle and Late Holocene (Notebaert et al., 2011c). In contrast, the importance of climatic variability has been identified in some other areas in Europe (e.g. Macklin et al., 2006; Starkel et al., 2006). However the temporal resolution of our study does not allow an identification of the influence of short-term climatic variations or the influence of the interplay between land use changes and climatic events (e.g. Knox, 2001; Notebaert et al., 2011b). A more detailed temporal framework is needed for a detailed appraisal of the influence of climatic variations.

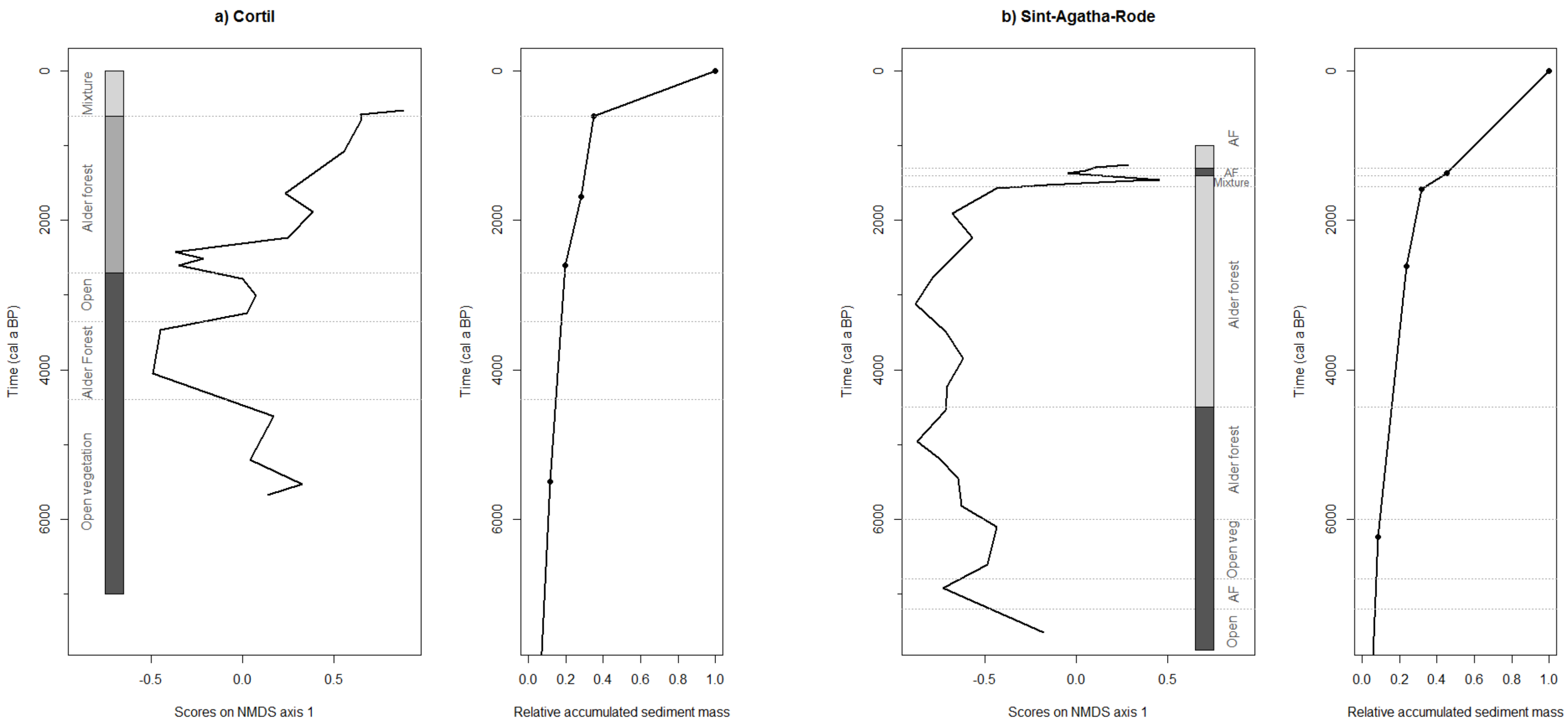

Figure 6.1. (left) Scores on axis 1 of non-metric multidimensional scaling (NMDS) of the pollen data, low scores represent low human impact, high scores represent high human impact (full explanation of NMDS is provided in chapter 4); and changes in floodplain geoecology (chapter 2); (right) relative accumulated sediment mass (chapter 2). For study site (a) Cortil, (b) Sint-Agatha-Rode, (c) Archennes and (d) Loonbeek. Black boxes represent peat accumulation, dark grey boxes represent organic overbank deposits, grey boxes represent clastic overbank deposits, horizontal lines represent changes in floodplain geoecology.

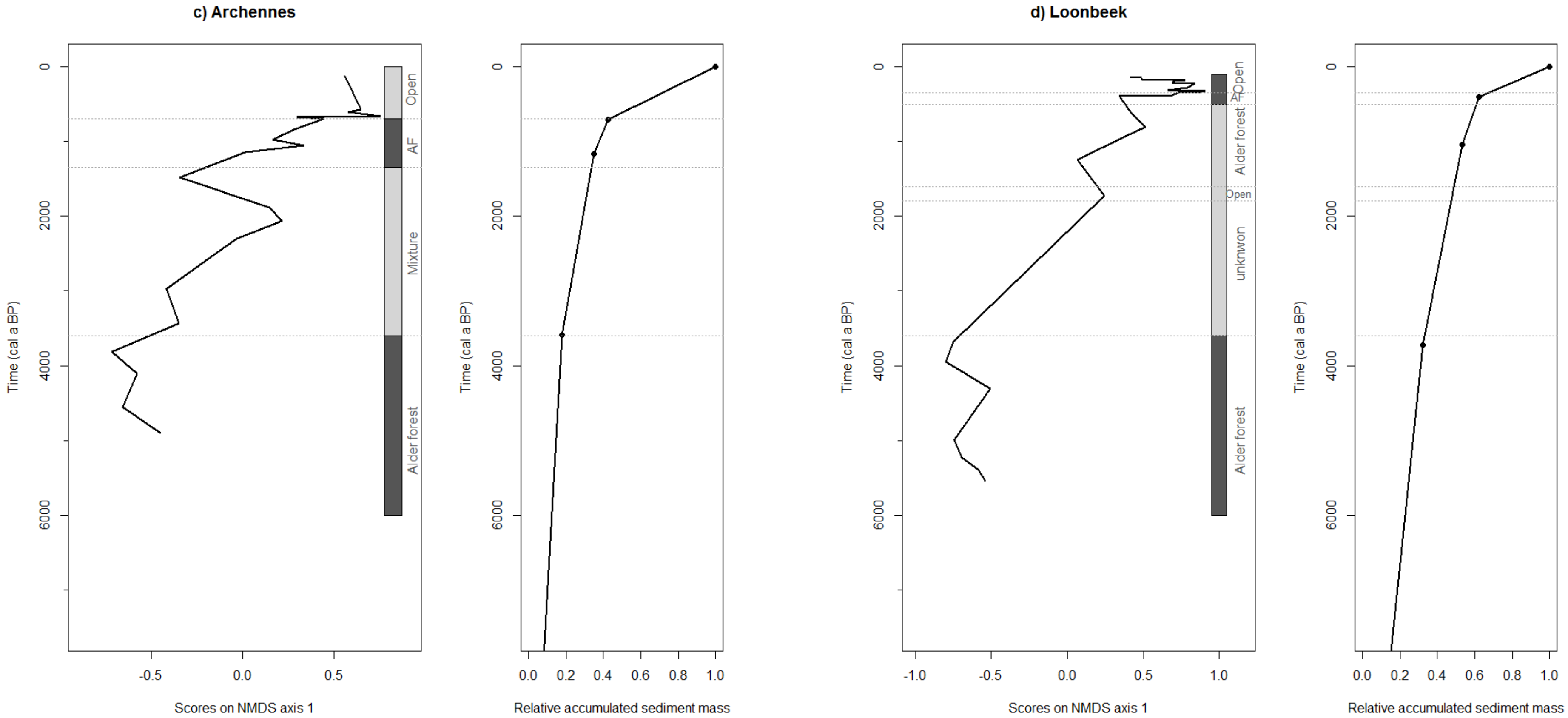

Figure 6.1 Cont.

6.2.3 Within-catchment variability

The timing of changes in floodplain geoecology differs for the different study sites (Table 6.1 and Figures 6.1 and 6.2), which is also shown by the cumulative probability functions (CPF) of the radiocarbon ages of the top of the peat layer in the Dijle catchment (Figure 3.3). This diachronic transition in floodplain morphology can be attributed partly to differences in topography and hillslope-floodplain connectivity, as argued in chapter 3 (section 3.5.4), but it is mainly interpreted as a consequence of the heterogeneous and gradual nature of human impact in the catchment. The intensity and onset of the increasing human impact differ between the different study sites, as shown in chapter 4 (Figure 4.7 and Table 6.1). Also the archeological record, although fragmentary, shows that there is spatial variation in human occupation at the catchment scale, e.g. for the Neolithic and Roman Period (Figure 4.1) (Crombé and Vanmontfort, 2007; Vanmontfort, 2007; Notebaert, 2009). Due to the different land cover history in the different subcatchments, the increased sediment input in the floodplain did not occur at the same moment for the different subcatchments (Figure 2.10), and consequently the changes in the floodplain geoecology were initiated at different moments (Table 6.1, Figure 3.3).

The diachronous pattern at the catchment scale can also be attributed to the location of the floodplain in the catchment. As stated above, floodplains in small catchments only reflect the changes in their small catchment. Floodplains in larger catchments on the other hand, can integrate the variable effects of the different sub-catchments (e.g. Steegen, 2001). Such downstream study sites reflect changes in a larger area and cumulate sediment supply from the entire catchment. Our data shows that floodplain changes in the downstream part of the Dijle catchment occurred earlier (from ca. 4000 cal a BP onwards), compared to the headwaters (ca. 600 cal a BP). More downstream, in the lower Scheldt catchment, floodplain changes are even dated from 4900 cal a BP onwards (Meylemans et al., 2013). This temporal difference is observed in other catchments as well, for instance in the Mark catchment, Belgium (Huybrechts, 1989). A possible explanation for this observed temporal difference is that also in the headwaters some study sites with early floodplain changes are present, but are not yet identified by previous studies (e.g. Notebaert, 2009) nor in our study. Sediment supply from these sites could accumulate downstream and initiate changes in the downstream part of the catchment. More geomorphic fieldwork is needed to check this hypothesis for the Dijle catchment. Another explanation could be hydrological changes within the catchment, related to land use changes. Land use changes can change suspended-sediment rating curves (Warrick and Rubin, 2007), and consequently, spatial differences in land use changes within a catchment can cause differences in rating curves along a river course. However, more research is needed to correctly understand the hydrological changes related to human induced land use changes. Other factors can be excluded to explain the time differences between the upstream and downstream part. For instance, no erosion of the top of peat layer occurred (see section 2.4 and 3.5), nor watermills and milldams can be indicated as a dominant factor controlling floodplain changes (see section 6.2.2). Overall, more research is needed to clearly understand the temporal difference between the headwaters and the downstream parts of the catchment.

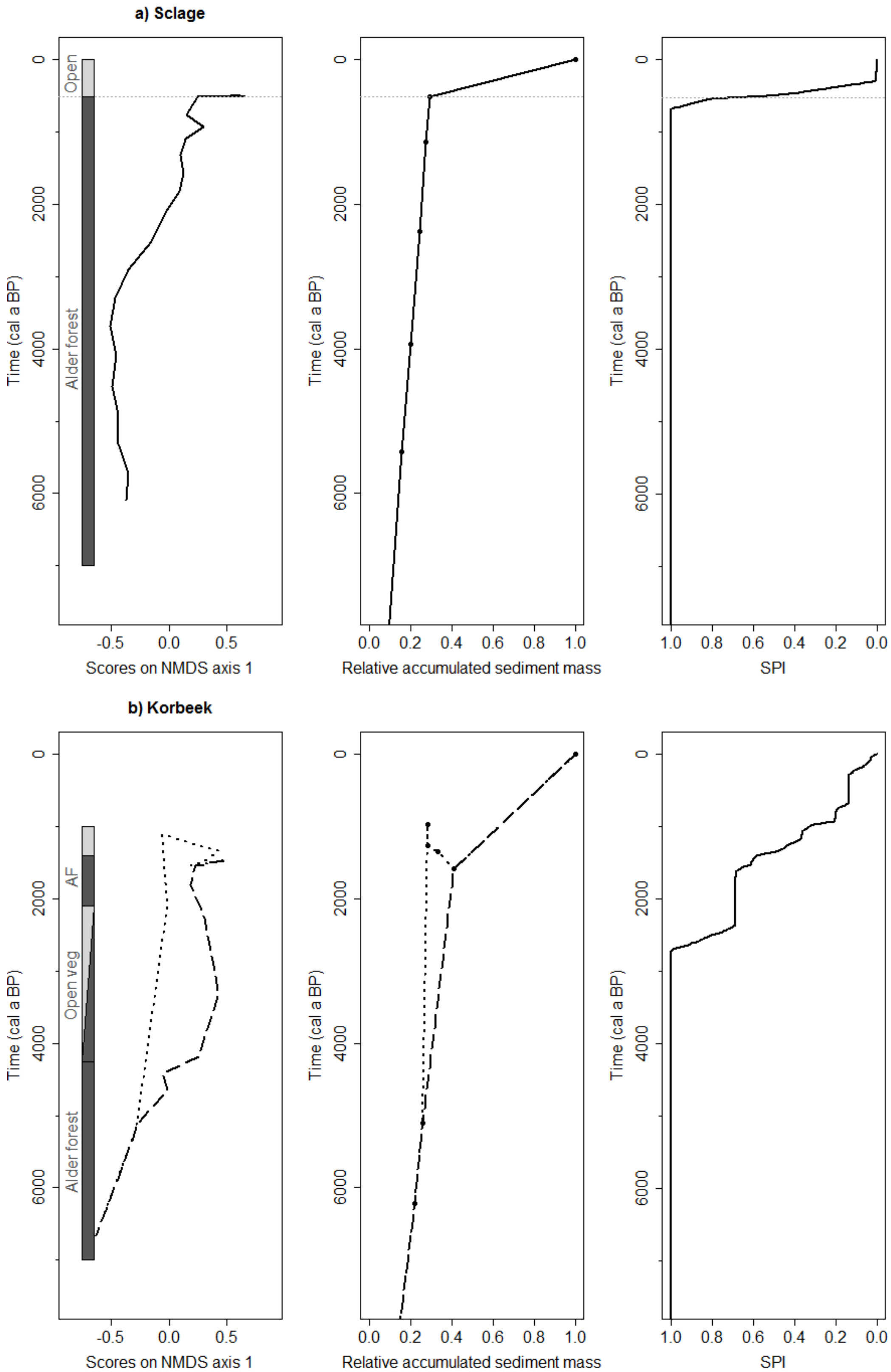

Figure 6.2. (left) Scores on axis 1 of non-metric multidimensional scaling (NMDS) of the pollen data, low scores represent low human impact, high scores represent high human impact (full explanation of NMDS is provided in chapter 4); and changes in floodplain geoecology (chapter 2); (middle) relative accumulated sediment mass (chapter 2); (right) SPI, proportion of floodplain area under active peat growth, based on radiocarbon ages of the top of the peat layer using Equation 3.3. For (a) Sclage and (b) Korbeek. For Korbeek, two age-depth scenarios are shown (see chapter 2 and 4). Black boxes represent peat accumulation, grey boxes represent clastic overbank deposits, horizontal lines represent changes in floodplain geoecology.

6.2.4 Thresholds in human impact

A temporal offset between the increasing human impact, as observed from the pollen data, and the changes in floodplain geoecology is observed in Sclage and Cortil (Figures 6.1 and 6.2, and Table 6.1). In these small subcatchments (< 20 km²), floodplain changes were only triggered when human impact in the subcatchment was large enough and thus reached a threshold. Limited human impact on the hillslopes resulted likewise in a limited connectivity between hillslopes and floodplains, and the eroded sediments were deposited and stored on foot slopes and in dry valley bottoms near their source area (see also Rommens, 2006; Verstraeten et al., 2009b; Notebaert et al., 2011b). Only when human impact was large enough and new land management techniques were used, hillslope-floodplain connectivity increased, for instance due to the removal of valley-side vegetation. Also the emergence of a network of dirt roads and sunken lanes (e.g. Houben et al., 2013) and the development of large gullies (e.g. Vanwalleghem et al., 2006) enhanced hillslope-floodplain connectivity. Hence sediment input in the floodplain could increase (Figure 2.10) and floodplain changes were triggered. The peat growth in these narrow floodplain sites decreased at the same moment as the increase in floodplain sedimentation (Figures 6.1 and 6.2), indicating that this increase in sediment input was high enough to trigger changes at the entire width of the narrow floodplain (see also Figure 3.7). The timing of this abrupt decrease in peat growth is different for each subcatchment, depending on the increase of sediment input in the floodplain (see chapter 5 and Figure 3.8). Such a temporal offset between the beginning of human impact and alluvial changes indicates a non-linearity in the impact-response relationship, and is observed in several catchments in West and Central Europe (e.g. Lang and Nolte, 1999; Trimble, 1999; De Moor and Verstraeten, 2008; Macklin et al., 2010; Houben et al., 2013). As argued in chapter 5, the differences in temporal offset between Cortil and Sclage (Table 6.1) and the different threshold conditions were caused by their specific topographic conditions (section 5.5.2).

Floodplains in larger catchments on the other hand, reflect the changes in the entire catchment and integrate the variable effects of the different sub-catchments. Moreover, in the wide floodplains in the downstream part of the catchment, floodplain changes occurred gradually, coinciding with the gradual increasing sediment supply in the floodplain (Figures 6.1 and 6.2). Consequently, a temporal offset between the increasing human impact, as observed from the pollen data, and the changes in floodplain geoecology is not observed in Sint-Agatha-Rode and Archennes (figure 6.1). In the two other study sites (Korbeek and Loonbeek), identifying a temporal offset is not possible due to a poor chronostratigraphical control of the human impact curve (Korbeek; Figures 2.8 and 6.2) or due to a gap in the pollen record (Loonbeek; Figure 6.1).

Table 6.1. Timing of regional vegetation transition (chapter 4) and local floodplain changes (chapter 2), and time lag between local and regional changes for the study sites in the Dijle catchment.

Study site	Timing of regional vegetation changes	Timing of local floodplain changes	Time lag
Cortil	ca. 2300 cal a BP	ca. 500 cal a BP	ca. 1800 a
Sclage	ca. 2700 cal a BP	ca. 600 cal a BP	ca. 2100 a
Sint-Agatha-Rode	ca. 1600 cal a BP	ca. 4500 cal a BP	- ca. 2900 a
Korbeek	ca. 4500 – 1500 cal a BP	ca. 4200 – 150 cal a BP	300 – 4000 a
Archennes	ca. 3600 cal a BP	ca. 3500 cal a BP	ca. 100 a
Loonbeek	ca. 3500 – 2000 cal a BP	ca. 3500 – 2000 cal a BP	0 – 1500 a

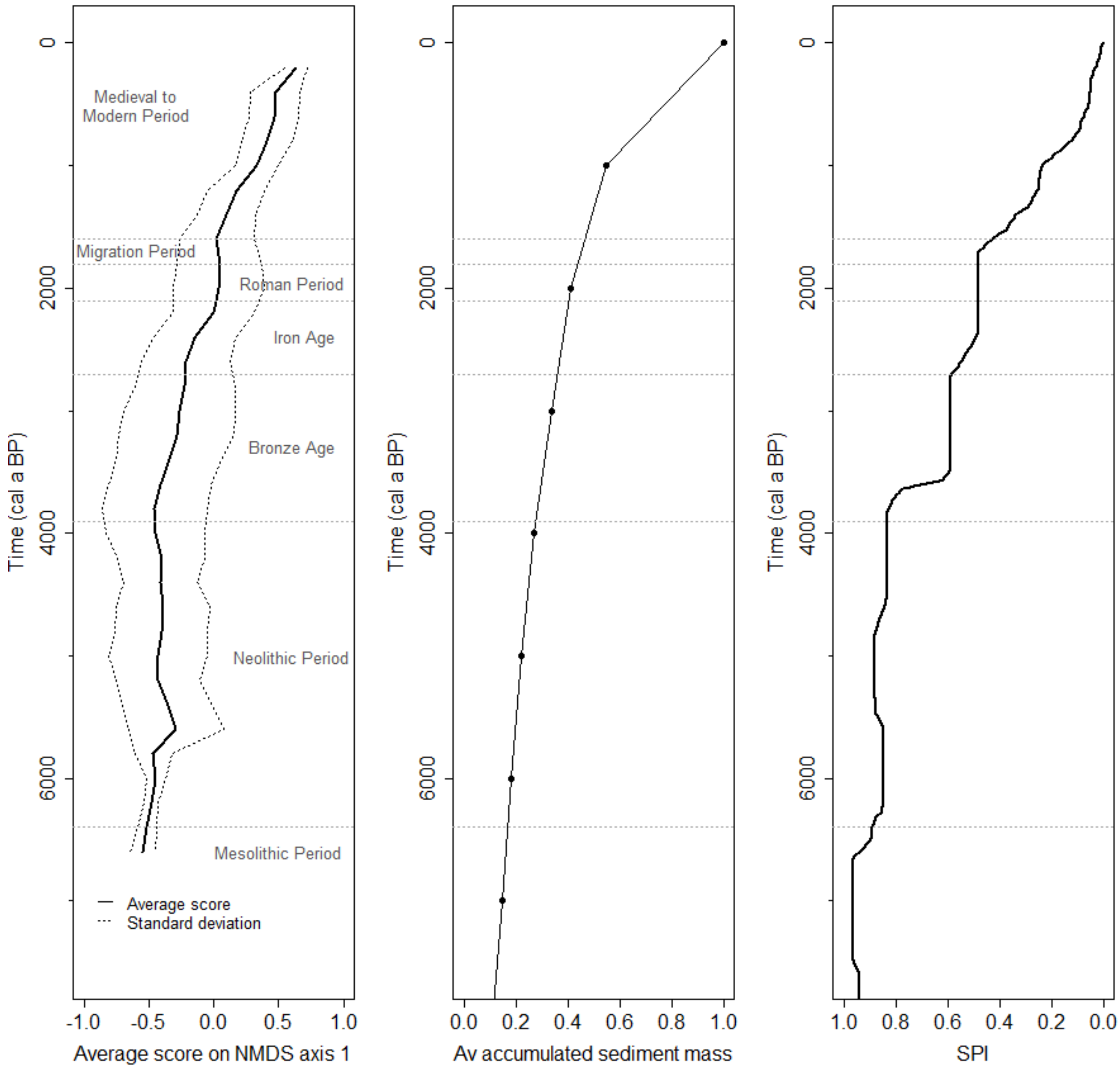

Figure 6.3. (Left) Average score on axis 1 of non-metric multidimensional scaling (NMDS) of the pollen data, for the five study sites (Korbeek is excluded). Low scores represent low human impact, high scores represent high human impact (full explanation of NMDS is provided in chapter 4); (Middle) average relative accumulated sediment mass for the different dated corings in alluvial deposits in the Dijle catchment (based on Notebaert et al. (2011b)); and (Right) SPI, the proportion of floodplain area under active peat growth in the Dijle catchment, using equation 3.3 (see chapter 3). With indication of the archaeological periods in the Belgian loess area.

6.3 Generalized model of floodplain development

The gradual decrease in floodplain area under active peat growth in the Dijle catchment shows a similar pattern as the gradual increase in human impact in the landscape (Figure 6.3), although some small differences are present, e.g. during the Neolithic Period (see above and Figure 6.3). This similarity suggests a linearity at the catchment scale between the external forcing (human impact) and geomorphic response (change in floodplain morphology) (Figure 6.4): when human impact gradually increased from the Bronze Age onwards, sediment input into the floodplain slightly increased, and the floodplain geoecology gradually changed. A small increase in the sediment input could be sufficient to trigger floodplain changes in a part of the wide floodplains (i.e. near the river channel(s)) in the downstream part of the catchment. In these wide floodplains, the geoecology started to change before the large increase in floodplain sedimentation. The observed linearity is not in contrast with the previously assumed non-linearity in sediment dynamics between the beginning of the agricultural hillslope colluviation and the massive alluvial aggradation, as observed in the Dijle catchment (Verstraeten et al., 2009b; Notebaert et al., 2011b), as well as in other West and Central European catchment (e.g. Lang and Nolte, 1999; Trimble, 1999; De Moor and Verstraeten, 2008; Macklin et al., 2010; Houben et al., 2013). Indeed, there is a time lag between the dramatic increase in sediment input towards the floodplain compared with the increase in human impact in the Dijle catchment (Figure 6.4).

Nevertheless, the observed linearity at catchment scale hides important variations between the various study sites (see also section 6.2.3). On the level of the individual study sites, the impact-response relationship is not necessarily linear. In the narrow floodplain sites (e.g. Sclage and Cortil) the gradual increase in human impact contrasts with the abrupt change in floodplain area under active peat growth (Figure 6.5a). Only when human impact reached a certain threshold and hillslopes were deforested and valley-side vegetation were removed, the hillslope-floodplain connectivity increased and sediments could reach the floodplain (see also section 6.2.4). The peat growth in these narrow floodplain sites decreased at the same moment as the increase in floodplain sedimentation (Figure 6.5a). The timing of this abrupt decrease in peat growth is different for each subcatchment, depending on the timing of first sediment input in the floodplain (Figure 6.5a and chapter 3 and 5). In the wide floodplain sites (e.g. Korbeek and Archennes) the impact-response relationship seems to be more linear (Figure 6.5b), although the limited chronostratigraphical control makes interpretation more difficult. The gradual change in floodplain geoecology more or less coincides with the gradual increase in human impact. The increase in human impact could cause a small increase in sediment input, since floodplains in larger catchments reflect the changes in their entire catchment and integrate the variable effects of the different sub-catchments. The small increase in sediment input could trigger floodplain changes close to the river channel(s), by the formation of levees. When the increasing human impact reached a certain threshold, the massive floodplain sedimentation was triggered and all floodplain parts became dominated by clastic overbank deposition (Figure 6.5b).

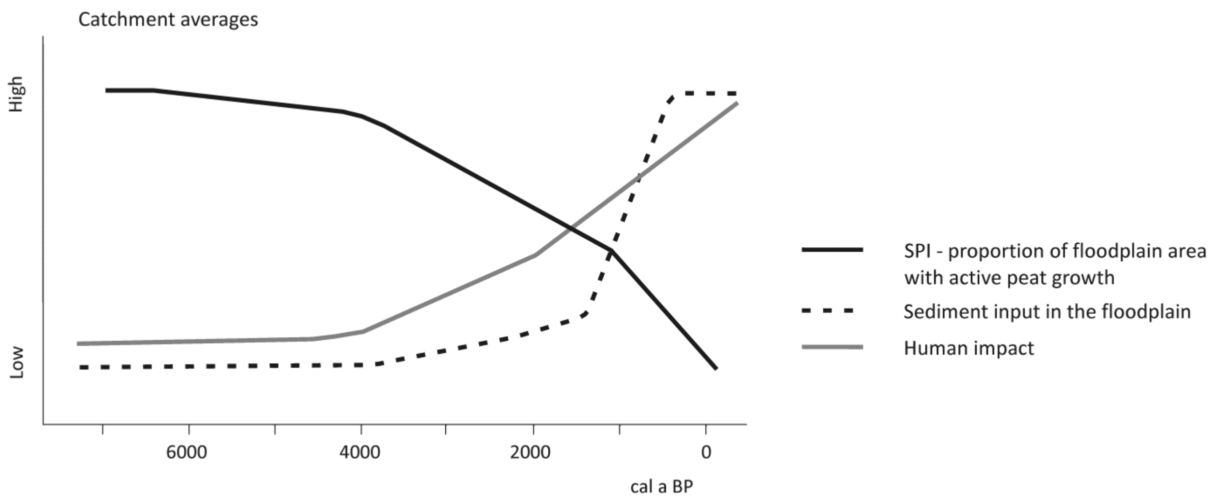

Figure 6.4 Conceptual model of floodplain response to increasing human impact for the entire Dijle catchment. Changes on centurial timescale are not displayed.

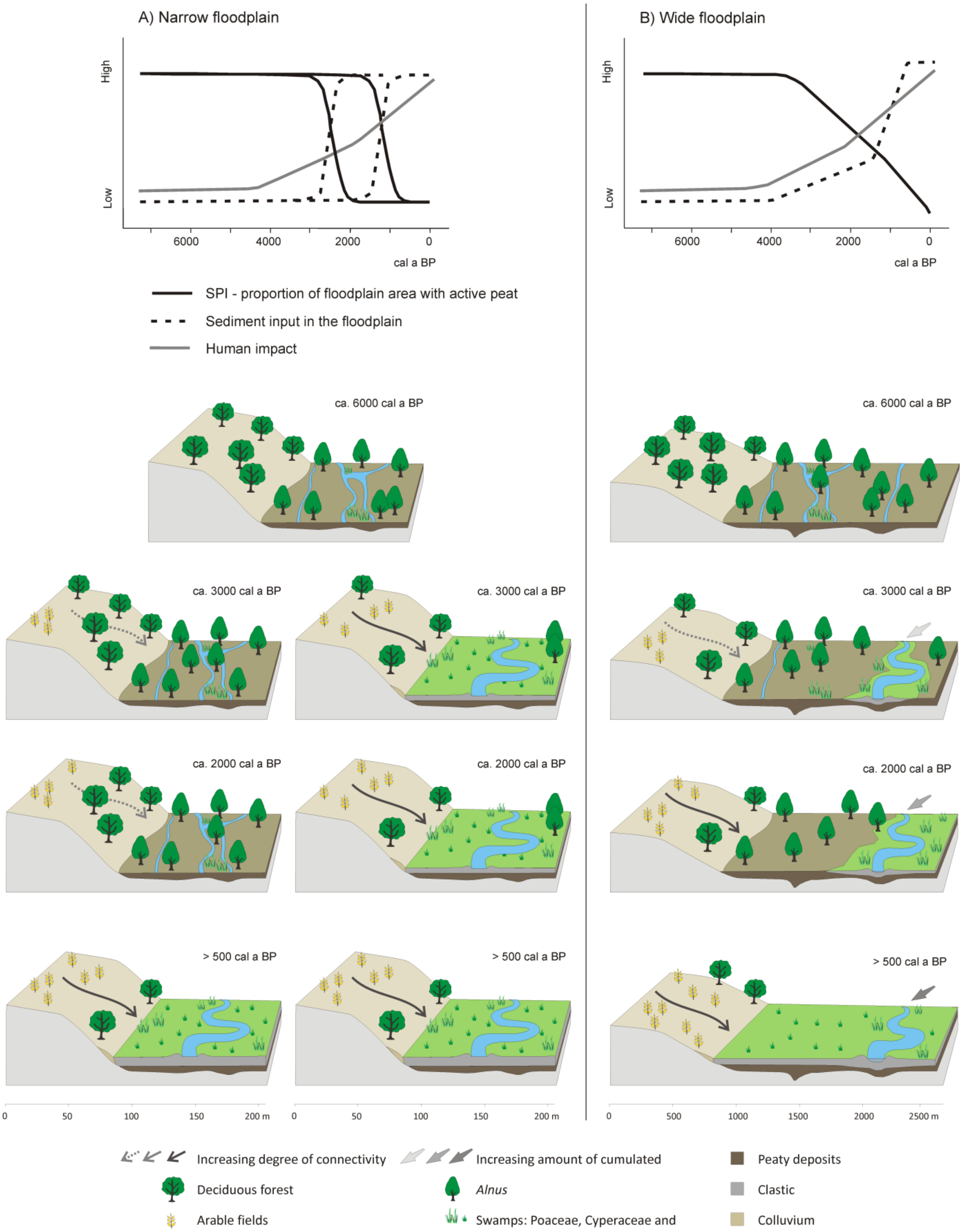

Figure 6.5. Conceptual model of floodplain response to increasing human impact. A) Narrow floodplains, headwaters; B) wide floodplains, main trunk valley. Changes on centurial timescale are not displayed.

6.4 Importance of high spatial and temporal resolution

The discussion from above and from the previous chapters indicates that floodplain changes are diachronous and non-uniform at the scale of the Dijle catchment (758 km²). Even for such a medium-sized catchment, the chronostratigraphy differs from the lithostratigraphy. For instance, the Holocene lithostratigraphical fluvial units previously defined in the Scheldt basin by Gullentops et al. (2001) are the Korbeek-Dijle Member (peat layer) and Rotspoel Member (silty overbank deposits). The chronostratigraphy coupled with these lithostratigraphical units are respectively the Early and Late Holocene (Gullentops et al., 2001). But, our results indicate that these changes in lithostratigraphy – the transition from peaty to clastic deposits – are diachronous at the scale of the Dijle catchment. Consequently, these changes in lithostratigraphy cannot be used to construct, for instance, time-differentiated sediment budgets.

Moreover, extrapolation of local dating results are not always justified (chapter 3), and conclusions with respect to the response of floodplain to variable intensities of human impact from one study site cannot be applied to an entire catchment. For instance, the floodplain response is different in small catchments compared to larger catchments, and the results of the headwaters (catchment area < 20 km²; chapter 5), cannot be extrapolated to the entire Dijle catchment (758 km²), let alone the Scheldt basin (ca. 20 000 km²). It also shows that results from one study site are insufficient to understand precisely all involved factors. When analyzing individual study sites, local effects are dominant and come forward, as the contrasting evolution of study sites Cortil and Sclage show (Chapter 5). Integrating data from different study sites on a catchment scale, however, can result in more insights in the overall pattern and dominant processes, and local variations will become less important. Therefore, a catchment-wide approach with results from different study sites and with multiple corings within one cross-section are necessary to fully understand floodplain changes and its interaction with environmental changes. Conclusions based on a few study sites should always be handled with caution.

This study also highlights the importance of a high temporal resolution. To understand the role humans have played in changing floodplain geoecology, data on human impact and on floodplain changes need to be collected with a high time-resolution (see also Verstraeten et al., 2009a). Understanding Holocene floodplain changes not only needs a sufficient amount of cross-sections and coring per cross-sections in one catchment (Notebaert et al., 2010), but also multiple dated corings within one cross-section and dating results for different study sites (see also chapter 3). Gathering more insights in the role of short-term climatic variations or the influence of the interplay between land use changes and climatic events requires even a more detailed temporal framework (see section 6.2.2). Moreover, a low temporal resolution results in averaging effects, which can hide small variations in the involved factors. For instance, small variations in sediment mass curves are missed due to averaging effects (see above and Notebaert et al. (2011b)). Also the gradual nature of the increasing human impact (Figure 6.3) can be the result of such averaging effects, which can hide short-scale, abrupt changes. Understanding the different involved factors will therefore largely be improved by advances in dating methodologies.

6.5 Uncertainties and scope for further research

The previous discussion provided more insights in sensitivity of floodplain geoecology to human impact. Nevertheless, several questions remained unanswered and point out prospects for further research.

First, the interaction between changing floodplain geomorphology and floodplain vegetation needs further investigation. Vegetation plays a significant role in trapping sediments in a floodplain, and vegetation itself is also influenced by the sediment input in the floodplain (e.g. Hughes, 1997). A better understanding of this interaction will provide more insights in the sensitivity of floodplain systems to environmental disturbances. Multi-proxy analysis, modern analogues or experiments can help to unravel this interaction. Also to role of beavers (*Castor fiber*) in the floodplain geoecology needs further investigation. In floodplain forests, they would have been dam-builders and could influence the peat growth in floodplains (e.g. Brown, 2002). An understanding of the ecological and geomorphological role beavers have played needs further investigation, to get a better understanding of floodplain changes during the Holocene Period, and to understand the future influence on the Dijle floodplain of the recently reintroduced beavers in the Dijle valley (e.g. Niewold, 2003; Nyssen et al., 2011).

Second, defining threshold values of human impact in terms of percentages of deforestation or area under cultivation remains problematic. Our reconstruction of human impact, based on the statistical analysis of pollen data, remains a semi-quantitative technique and cannot be considered as an absolute quantification of human impact (see chapter 4). The multiple scenario approach (MSA) of Bunting and Middleton (2009) can possibly be used to translate fossil pollen from alluvial sites into quantitative vegetation estimations (see Annex of chapter 4). But, in order to do so, more insight is needed in the pollen transport mechanisms and pollen source areas for pollen deposited in floodplains. If a significant part of the pollen influx in floodplains is dominated by waterborne pollen, the pollen source area of the aerial component and the pollen productivity estimates exclusively based on aerial pollen transport is a poor starting point for quantifying the changes in regional vegetation cover (e.g. Bonny, 1978; Xu et al., 2012), and model-based correction approaches, such as the Landscape Reconstruction Algorithm (Sugita, 2007b; Sugita, 2007a) and the Multiple Scenario Approach (Bunting and Middleton, 2009), need to be adjusted.

Beside the fact that our statistical analysis of the fossil pollen data remains a semi-quantitative technique, our study has proven the added value of statistical analysis of pollen data compared with the more traditional techniques, such as the indicator species approach (e.g. Behre, 1981) or the use of ratios of arboreal to non-arboreal pollen taxa (AP/NAP ratio) (e.g. Faegri and Iversen, 1989). Also future palynological research should focus on a (semi-)quantitative analysis of pollen data, using statistical methods (used in this study and in e.g. Lechterbeck et al., 2009; Lopez-Merino et al., 2012), the Landscape Reconstruction Algorithm (LRA; Sugita, 2007b; Sugita, 2007a), or Multiple Scenario Approach (MSA; Bunting and Middleton, 2005). Moreover, palynological studies should integrate results from different study sites. Focusing on one or a few pollen profiles will severely limit their potential in interpreting past land cover. Such (semi-)quantitative measures of human impact in the landscape during the Holocene at catchment scale are necessary to fully understand the role human impact has played to change sediment fluxes (e.g. Verstraeten et al., 2009a).

Moreover, it will be interesting to compare our human impact curves with other datasets, such as global databases of anthropogenic land use during the Holocene, which have recently been developed based on population and agricultural land per capita estimates (e.g. Kaplan et al., 2011; Klein Goldewijk et al., 2011). These models need further evaluation, which can be done based on detailed and well-dated palynological records. Also a comparison between our reconstruction of human impact with archaeological records will be interesting and can help to translate the scores on the NMDS-axes into quantitative estimates of area under cultivation. However a detailed archaeological database for the entire Belgian loess belt is still missing, as well as detailed data on land management and on the organization of the agricultural system.

References

Anderson NJ, Bugmann H, Dearing JA and Gaillard M-J (2006) Linking palaeoenvironmental data and models to understand the past and to predict the future. *Trends in ecology & evolution* 21: 696-704.

Assendelft R (2012) *Reconstruction of the human impact on the floodplain sedimentation and vegetational development in the Dijle catchment, Belgium, from the Neolithic period to the Middle Ages*. MSc thesis. Department of Earth Sciences, VU University Amsterdam.

Aufdenkampe AK, Mayorga E, Raymond PA, Melack JM, Doney SC, Alin SR, Aalto RE and Yoo K (2011) Riverine coupling of biogeochemical cycles between land, oceans, and atmosphere. *Frontiers in Ecology and the Environment* 9: 53-60.

Bakels C (2009) The Western European loess belt. *Agrarian History, 5300 BC–AD* 1000.

Bakker J, Kaniewski D, Verstraeten G, De Laet V and Waelkens M (2012) Numerically derived evidence for late-Holocene climate change and its impact on human presence in the southwest Taurus Mountains, Turkey. *The Holocene* 22: 425-438.

Behre K-E (1981) The interpretation of anthropogenic indicators in pollen diagrams. *Pollen spores* 23: 225-245.

Beug HJ (2004) *Leitfaden der Pollenbestimmung für Mitteleuropa und angrenzende Gebiete*. Munchen: Verlag Dr. Friedrich Pfeil.

Birks HJB (1985) Recent and Possible Future Mathematical Developments in Quantitative Paleoecology. *Palaeogeography Palaeoclimatology Palaeoecology* 50: 107-147.

Birks HJB, Line JM and Persson T (1988) Quantitative estimation of human impact on cultural landscape development. In: Birks HH, Birks HJB, Kaland PE and Moe D (ed.) *The Cultural Landscape - Past, Present and Future*. Cambridge: Cambridge University Press, 229-240.

Birks HJB, Lotter AF, Juggins S and Smol JP (2012) *Tracking environmental change using lake sediments. Data handling and numerical techniques.*: Springer.

Blaauw M (2010) Methods and code for 'classical' age-modelling of radiocarbon sequences. *Quaternary Geochronology* 5: 512-518.

Bohncke S and Vandenberghe J (1991) Palaeohydrological development in the Southern Netherlands during the last 15000 years. In: Starkel L, Gregory K and Thornes J (ed.) *Temperate palaeohydrology*. Chichester: Wiley & Sons, 253-281.

Bonny AP (1978) Effect of Pollen Recruitment Processes on Pollen Distribution over Sediment Surface of a Small Lake in Cumbria. *Journal of Ecology* 66: 385-416.

Borren W, Bleuten W and Lapshina ED (2004) Holocene peat and carbon accumulation rates in the southern taiga of western Siberia. *Quaternary Research* 61: 42-51.

Bradshaw RHW (2008) Detecting human impact in the pollen record using data-model comparison. *Vegetation History and Archaeobotany* 17: 597-603.

Bravard J-P and Peiry J-L (1999) The CM pattern as a tool for the classification of alluvial suites and floodplains along the river continuum. *Geological Society, London, Special Publications* 163: 259-268.

Broothaerts N (2008) *Geomorfologische opbouw van de Dijle vallei*. Bachelor thesis. Department of Earth and Environmental Sciences, KU Leuven.

Broothaerts N, Notebaert B, Verstraeten G, Kasse C, Bohncke S and Vandenberghe J (2014a) Non-uniform and diachronous Holocene floodplain evolution: a case study from the Dijle catchment, Belgium. *Journal of Quaternary Science* 29: 351-360.

Broothaerts N, Verstraeten G, Kasse C, Bohncke S, Notebaert B and Vandenberghe J (2014b) Reconstruction and semi-quantification of human impact in the Dijle catchment, central Belgium: a palynological and statistical approach. *Quaternary Science Reviews* 102: 96-110.

Broothaerts N, Verstraeten G, Kasse C, Bohncke S and Vandenberghe J (under review) From natural to human-dominated floodplain geoecology – a Holocene perspective for the Dijle catchment. *Anthropocene*.

Broothaerts N, Verstraeten G, Notebaert B, Assendelft R, Kasse C, Bohncke S and Vandenberghe J (2013) Sensitivity of floodplain geoecology to human impact: A Holocene perspective for the headwaters of the Dijle catchment, central Belgium. *The Holocene* 23: 1403-1414.

Brostrom A, Gaillard MJ, Ihse M and Odgaard B (1998) Pollen-landscape relationships in modern analogues of ancient cultural landscapes in southern Sweden - a first step towards quantification of vegetation openness in the past. *Vegetation History and Archaeobotany* 7: 189-201.

Broström A, Nielsen AB, Gaillard M-J, Hjelle K, Mazier F, Binney H, Bunting J, Fyfe R, Meltsov V, Poska A, Räsänen S, Soepboer W, Stedingk H, Suutari H and Sugita S (2008) Pollen productivity estimates of key European plant taxa for quantitative reconstruction of past vegetation: a review. *Vegetation History and Archaeobotany* 17: 461-478.

Brown A (1988) The palaeoecology of Alnus (alder) and the Postglacial history of floodplain vegetation. Pollen percentage and influx data from the West Midlands, United Kingdom. *New Phytologist* 110: 425-436.

Brown A, Harper D and Peterken G (1997) European floodplain forests: structure, functioning and management. *Global ecology and biogeography letters* 6.

Brown A, Toms P, Carey C and Rhodes E (2013) Geomorphology of the Anthropocene: time-trangressive discontinuities of human-induced alluviation. *Anthropocene* 1: 3-13.

Brown AG (2002) Learning from the past: palaeohydrology and palaeoecology. *Freshwater biology* 47: 817-829.

Brown AG (2008) Geoarchaeology, the four dimensional (4D) fluvial matrix and climatic causality. *Geomorphology* 101: 278-297.

Brown AG, Carpenter RG and Walling DE (2007) Monitoring fluvial pollen transport, its relationship to catchment vegetation and implications for palaeoenvironmental studies. *Review of Palaeobotany and Palynology* 147: 60-76.

Buijs M (2013) *Human impact on the floodplain sedimentation and vegetation of the area around the IJse valley during the Holocene*. MSc thesis. Department of Earth Sciences, VU University Amsterdam.

Buijse AD, Coops H, Staras M, Jans LH, Van Geest GJ, Grifts RE, Ibelings BW, Oosterberg W and Roozen FCJM (2002) Restoration strategies for river floodplains along large lowland rivers in Europe. *Freshwater biology* 47: 889.

Buntgen U, Tegel W, Nicolussi K, McCormick M, Frank D, Trouet V, Kaplan JO, Herzig F, Heussner KU, Wanner H, Luterbacher J and Esper J (2011) 2500 Years of European Climate Variability and Human Susceptibility. *Science* 331: 578-582.

Bunting MJ (2007) Pollen in wetlands: using simulations of pollen dispersal and deposition to better interpret the pollen signal. *Biodiversity and Conservation* 17: 2079-2096.

Bunting MJ and Middleton D (2005) Modelling pollen dispersal and deposition using HUMPOL software, including simulating windroses and irregular lakes. *Review of Palaeobotany and Palynology* 134: 185-196.

Bunting MJ and Middleton R (2009) Equifinality and uncertainty in the interpretation of pollen data: the Multiple Scenario Approach to reconstruction of past vegetation mosaics. *Holocene* 19: 799-803.

CAI (2014) Centrale Archeologische Inventaris. http://cai.erfgoed.net.

Campbell ID and Campbell C (1994) Pollen preservation: Experimental wet-dry cycles in saline and desalinated sediments. *Palynology* 18: 5-10.

Chaopricha NT and Marin-Spiotta E (2014) Soil burial contributes to deep soil organic carbon storage. *Soil Biology & Biochemistry* 69: 251-264.

Chiverrell RC, Foster GC, Thomas GSP, Marshall P and Hamilton D (2009) Robust chronologies for landform development. *Earth Surface Processes and Landforms* 34: 319-328.

Chiverrell RC, Thorndycraft VR and Hoffmann TO (2011) Cumulative probability functions and their role in evaluating the chronology of geomorphological events during the Holocene. *Journal of Quaternary Science* 26: 76-85.

Coenen B (2013) *Bepaling van sedimentatiemilieus in de Dijle vallei aan de hand van textuuranalyse*. Bachelor thesis. Division of Geography, Department of Earth and Environmental Sciences, KU Leuven.

Crombé P and Vanmontfort B (2007) The neolithisation of the Scheldt basin in western Belgium. In: Whittle A and Cummings V (ed.) *Going over: the Mesolithic-Neolithic transition in north-west Europe*. Oxford: Proceedings of the British Academy, Oxford University Press, 263-285.

De Brue H and Verstraeten G (2014) Impact of the spatial and thematic resolution of Holocene anthropogenic land-cover scenarios on modeled soil erosion and sediment delivery rates. *The Holocene* 24: 67-77.

De Moor JJW, Kasse C, van Balen R, Vandenberghe J and Wallinga J (2008) Human and climate impact on catchment development during the Holocene — Geul River, the Netherlands. *Geomorphology* 98: 316-339.

De Moor JJW and Verstraeten G (2008) Alluvial and colluvial sediment storage in the Geul River catchment (The Netherlands) — Combining field and modelling data to construct a Late Holocene sediment budget. *Geomorphology* 95: 487-503.

De Smedt P (1973) Paleogeografie en kwartair-geologie van het confluentiegebied Dijle-Demer. *Acta Geographica Lovaniensia* 11: 141.

Deforce K, Storme A, Bastiaens J, Debruyne S, Denys L, Ervynck A, Meylemans E, Stieperaere H, Van Neer W and Crombé P (2014) Middle-Holocene alluvial forests and associated fluvial environments: A multi-proxy reconstruction from the lower Scheldt, N Belgium. *The Holocene*: 0959683614544059.

Dimbleby GW (1957) Pollen analysis of terrestrial soils. *New Phytologist* 56: 12-28.

Dotterweich M (2008) The history of soil erosion and fluvial deposits in small catchments of central Europe: Deciphering the long-term interaction between humans and the environment — A review. *Geomorphology* 101: 192-208.

Enters D, Dorfler W and Zolitschka B (2008) Historical soil erosion and land-use change during the last two millennia recorded in lake sediments of Frickenhauser See, northern Bavaria, central Germany. *Holocene* 18: 243-254.

Erkens G (2009) Sediment dynamics in the Rhine catchment: Quantification of fluvial response to climate change and human impact. *Netherlands Geographical Studies* 388: 278.

Erkens G, Hoffmann T, Gerlach R and Klostermann J (2011) Complex fluvial response to Lateglacial and Holocene allogenic forcing in the Lower Rhine Valley (Germany). *Quaternary Science Reviews* 30: 611-627.

Etienne D, Ruffaldi P, Dupouey JL, Georges-Leroy M, Ritz F and Dambrine E (2013) Searching for ancient forests: A 2000 year history of land use in northeastern French forests deduced from the pollen compositions of closed depressions. *Holocene* 23: 678-691.

Faegri K and Iversen J (1989) *Textbook of pollen analysis*. New Jersey: Blackburn Press.

Favre E, Escarguel G, Suc J-P, Vidal G and Thévenod L (2008) A contribution to deciphering the meaning of AP/NAP with respect to vegetation cover. *Review of Palaeobotany and Palynology* 148: 13-35.

FODEconomie (2013) Kerncijfers landbouw - De landbouw in België in cijfers.

Foulds SA and Macklin MG (2006) Holocene land-use change and its impact on river basin dynamics in Great Britain and Ireland. *Progress in Physical Geography* 30: 589-604.

Fyfe R, Roberts N and Woodbridge J (2010) A pollen-based pseudobiomisation approach to anthropogenic land-cover change. *Holocene* 20: 1165-1171.

Gaillard M-J, Sugita S, Bunting MJ, Middleton R, Broström A, Caseldine C, Giesecke T, Hellman SEV, Hicks S, Hjelle K, Langdon C, Nielsen A-B, Poska A, Stedingk H and Veski S (2008) The use of modelling and simulation approach in reconstructing past landscapes from fossil pollen data: a review and results from the POLLANDCAL network. *Vegetation History and Archaeobotany* 17: 419-443.

Gaillard MJ (2007) *Pollen methods and studies: Archaeological applications*. Amsterdam: Elsevier.

Geurts AM (1976) Genèse et stratigraphie des travertins de fond de vallée en Belgique. *Acta Geographica Lovaniensia* 16.

Ghilardi B and O'Connell M (2013) Early Holocene vegetation and climate dynamics with particular reference to the 8.2 ka event: pollen and macrofossil evidence from a small lake in western Ireland. *Vegetation History and Archaeobotany* 22: 99-114.

Gibbard P and Lewin J (2002) Climate and related controls on interglacial fluvial sedimentation in lowland Britain. *Sedimentary Geology* 151: 187-210.

Gullentops F, Bogemans F, De Moor G, Paulissen E and Pissart A (2001) Quaternary lithostratigraphic units (Belgium). *Geologica Belgica* 4: 153-164.

Hammer O and Harper D (2006) *Paleontological data analysis*. Oxford: Blackwell Publishing.

Hellman S, Gaillard M-J, Broström A and Sugita S (2008) The REVEALS model, a new tool to estimate past regional plant abundance from pollen data in large lakes: validation in southern Sweden. *Journal of Quaternary Science* 23: 21-42.

Hoek WZ, Bohncke SJ, Ganssen GM and Meijer T (1999) Lateglacial environmental changes recorded in calcareous gyttja deposits at Gulickshof, southern Netherlands. *Boreas* 28: 416-432.

Hoffmann T, Erkens G, Cohen K, Houben P, Seidel J and Dikau R (2007) Holocene floodplain sediment storage and hillslope erosion within the Rhine catchment. *The Holocene* 17: 105-118.

Hoffmann T, Erkens G, Gerlach R, Klostermann J and Lang A (2009) Trends and controls of Holocene floodplain sedimentation in the Rhine catchment. *Catena* 77: 96-106.

Hoffmann T, Lang A and Dikau R (2008) Holocene river activity: analysing 14C-dated fluvial and colluvial sediments from Germany. *Quaternary Science Reviews* 27: 2031-2040.

Houben P (2007) Geomorphological facies reconstruction of Late Quaternary alluvia by the application of fluvial architecture concepts. *Geomorphology* 86: 94-114.

Houben P, Nolte S, Rittweger H and Wunderlich J (2001) Lateglacial and Holocene environmental change indicated by floodplain deposits of the Hessian Depression (Central Germany). In: Maddy D, Macklin MG and Woodward JC (ed.) *River Basin Sediment Systems: Archives of Environmental Change*. Roterdam: Balkema, 249-264.

Houben P, Schmidt M, Mauz B, Stobbe A and Lang A (2012) Asynchronous Holocene colluvial and alluvial aggradation: A matter of hydrosedimentary connectivity. *The Holocene* doi: 10.1177/0959683612463105.

Houben P, Schmidt M, Mauz B, Stobbe A and Lang A (2013) Asynchronous Holocene colluvial and alluvial aggradation: A matter of hydrosedimentary connectivity. *The Holocene* 23: 544-555.

Houbrechts G, Hallot E, Levecq Y, Denis A-C, Van Campenhout J, Peeters A and Petit F (2013) Images CM de Passega des rivières ardennaises. *Bulletin de la Société Géographique de Liège* 61: 37-68.

Huggett R (2007) *Fundamentals of geomorphology*. Routledge.

Hughes FM (1997) Floodplain biogeomorphology. *Progress in Physical Geography* 21: 501-529.

Huybrechts W (1989) Palaeohydrologic conditions in the Mark River basin during the last 15000 years. *Geologie En Mijnbouw* 68: 175-187.

Huybrechts W (1999) Post-pleniglacial floodplain sediments in Central Belgium. *Geologica Belgica* 2: 29-37.

Jones AF, Brewer PA, Johnstone E and Macklin MG (2007) High-resolution interpretative geomorphological mapping of river valley environments using airborne LiDAR data. *Earth Surface Processes and Landforms* 32: 1574-1592.

Juggins S (2007) *C2 Version 1.5 User Guide. Software for ecological and palaeoecological data analysis and visualisation*. Newcastle: Newcaste University.

Kalicki T, Sauchyk, S, Calderoni, G, Simakova, G (2008) Climatic versus human impact on the Holocene sedimentation in river valleys of different order: Examples from the upper Dnieper basin, Belarus. *Quaternary International* 189: 91-105.

Kalis AJ, Merkt J and Wunderlich J (2003) Environmental changes during the Holocene climatic optimum in central Europe - human impact and natural causes. *Quaternary Science Reviews* 22: 33-79.

Kaniewski D, Paulissen E, Van Campo E, Al-Maqdissi M, Bretschneider J and Van Lerberghe K (2008) Middle East coastal ecosystem response to middle-to-late Holocene abrupt climate changes. *Proceedings of the National Academy of Sciences* 105: 13941-13946.

Kaplan JO, Krumhardt KM, Ellis EC, Ruddiman WF, Lemmen C and Goldewijk KK (2011) Holocene carbon emissions as a result of anthropogenic land cover change. *The Holocene* 21: 775-791.

Kerig T and Lechterbeck J (2004) Laminated sediments, human impact, and a multivariate approach: a case study in linking palynology and archaeology (Steisslingen, Southwest Germany). *Quaternary International* 113: 19-39.

Klein Goldewijk K, Beusen A, Van Drecht G and De Vos M (2011) The HYDE 3.1 spatially explicit database of human-induced global land-use change over the past 12,000 years. *Global Ecology and Biogeography* 20: 73-86.

Klimo E and Hager H (2001) *The floodplain forests in Europe: current situation and perspectives*. Leiden: European Forest Institute.

Knox JC (2001) Agricultural influence on landscape sensitivity in the Upper Mississippi River Valley. *Catena* 42: 193-224.

Kruskal JB (1964) Nonmetric multidimensional scaling: a numerical method. *Psychometrika* 29: 115-129.

Lang A (2008) Recent advances in dating and source tracing of fluvial deposits. In: Schmidt J CT, Phillips C, et al. (ed.) *Sediment Dynamics in Changing Environments*. Wallingford, Oxon, UK: IAHS Press, 3-12.

Lang A, Bork HR, Mackel R, Preston N, Wunderlich E and Dikau R (2003) Changes in sediment flux and storage within a fluvial system: some examples from the Rhine catchment. *Hydrological Processes* 17: 3321-3334.

Lang A and Nolte S (1999) The chronology of Holocene alluvial sediments from the Wetterau, Germany, provided by optical and C-14 dating. *Holocene* 9: 207-214.

Langohr R (2001) L'anthropisation du paysage pédologique agricole de la Belgique depuis le Néolithique ancien - Apports de l'archéopédologie. *Étude et Gestion des Sols* 8: 103-118.

Lechterbeck J, Kalis AJ and Meurers-Balke J (2009) Evaluation of prehistoric land use intensity in the Rhenish Loessboerde by canonical correspondence analysis—A contribution to LUCIFS. *Geomorphology* 108: 138-144.

Legendre L and Legendre P (1983) *Numerical ecology*. Amsterdam: Elsevier.

Lespez L, Clet-Pellerin M, Limondin-Lozouet N, Pastre J, Fontugne M and Marcigny C (2008) Fluvial system evolution and environmental changes during the Holocene in the Mue valley (Western France). *Geomorphology* 98: 55-70.

Lewin J, Macklin MG and Johnstone E (2005) Interpreting alluvial archives: sedimentological factors in the British Holocene fluvial record. *Quaternary Science Reviews* 24: 1873-1889.

Lopez-Merino L, Sanchez NS, Kaal J, Lopez-Saez JA and Cortizas AM (2012) Post-disturbance vegetation dynamics during the Late Pleistocene and the Holocene: An example from NW Iberia. *Global and Planetary Change* 92-93: 58-70.

Macklin MG, Benito G, Gregory KJ, Johnstone E, Lewin J, Michczyńska DJ, Soja R, Starkel L and Thorndycraft VR (2006) Past hydrological events reflected in the Holocene fluvial record of Europe. *Catena* 66: 145-154.

Macklin MG, Jones AF and Lewin J (2010) River response to rapid Holocene environmental change: evidence and explanation in British catchments. *Quaternary Science Reviews* 29: 1555-1576.

Macklin MG, Jones AF and Lewin J (2011) Comment: Cumulative probability functions and their role in evaluating the chronology of geomorphological events during the Holocene. *Journal of Quaternary Science* 26: 238-240.

Macklin MG and Lewin J (2003) River sediments, great floods and centennial-scale Holocene climate change. *Journal of Quaternary Science* 18: 101-105.

Marin-Spiotta E, Chaopricha NT, Plante AF, Diefendorf AF, Mueller CW, Grandy AS and Mason JA (2014) Long-term stabilization of deep soil carbon by fire and burial during early Holocene climate change. *Nature Geosci* 7: 428-432.

Mazier F, Gaillard MJ, Kunes P, Sugita S, Trondman AK and Brostrom A (2012) Testing the effect of site selection and parameter setting on REVEALS-model estimates of plant abundance using the Czech Quaternary Palynological Database. *Review of Palaeobotany and Palynology* 187: 38-49.

McCune B and Grace JB (2002) *Analysis of ecological communities*. Gleneden Beach, Oregon: MjM Software Design.

Meylemans E, Bogemans F, Storme A, Perdaen Y, Verdurmen I and Deforce K (2013) Lateglacial and Holocene fluvial dynamics in the Lower Scheldt basin (N-Belgium) and their impact on the presence, detection and preservation potential of the archaeological record. *Quaternary International* 308-309: 148-161.

Minchin PR (1987) An Evaluation of the Relative Robustness of Techniques for Ecological Ordination. *Vegetatio* 69: 89-107.

Montgomery DR (2008) Dreams of Natural Streams. *Science* 319: 291-292.

Moore PD, Webb JA and Collinson ME (1991) *Pollen analysis*. Oxford: Blackwell Scentific Publications.

Mullenders W and Gullentops F (1957) Palynologisch en geologisch onderzoek in de alluviale vlakte van de Dijle te Heverlee-Leuven. *Agricultura* Band V: 57-64.

Mullenders W, Gullentops F, Lorent J, Coremans M and Gilot E (1966) Le remblement de la vallée de la Nethen. *Acta Geographica Lovaniensia* IV: 169-181.

Munaut A (1967) Recherches paleo-ecologiques en Basse et Moyenne Belgique. *Acta Geographica Lovaniensia* 6: 1-191.

Newson MD and Large ARG (2006) 'Natural' rivers, 'hydromorphological quality' and river restoration: a challenging new agenda for applied fluvial geomorphology. *Earth Surface Processes and Landforms* 31: 1606-1624.

Nielsen AB (2003) *Pollen-based quantitative estimation of land cover-relationships between pollen sedimentation in lakes and land cover as seen on historical maps in Denmark AD 1800*. Doctoral thesis, University of Copenhagen.

Niewold FJJ (2003) *Haalbaarheidsonderzoek naar de herkolonisatie van de bever in het bekken van de Schelde en de Dijle*. Wageningen: Alterra.

Notebaert B (2009) *Sensitivity of river systems to human actions and climatic events across different environments: a Holocene perspective*. Leuven: PhD thesis. Department of Earth and Environmental Sciences, KU Leuven.

Notebaert B, Houbrechts G, Verstraeten G, Broothaerts N, Haeckx J, Reynders M, Govers G, Petit F and Poesen J (2011a) Fluvial architecture of Belgian river systems in contrasting environments: implications for reconstructing the sedimentation history. *Netherlands Journal of Geosciences-Geologie En Mijnbouw* 90: 31-50.

Notebaert B and Verstraeten G (2010) Sensitivity of West and Central European river systems to environmental changes during the Holocene: A review. *Earth-Science Reviews* 103: 163-182.

Notebaert B, Verstraeten G, Govers G and Poesen J (2009a) Qualitative and quantitative applications of LiDAR imagery in fluvial geomorphology. *Earth Surface Processes and Landforms* 34: 217-231.

Notebaert B, Verstraeten G, Govers G and Poesen J (2010) Quantification of alluvial sediment storage in contrasting environments: Methodology and error estimation. *Catena* 82: 169-182.

Notebaert B, Verstraeten G, Rommens T, Vanmontfort B, Govers G and Poesen J (2009b) Establishing a Holocene sediment budget for the river Dijle. *Catena* 77: 150-163.

Notebaert B, Verstraeten G, Vandenberghe D, Marinova E, Poesen J and Govers G (2011b) Changing hillslope and fluvial Holocene sediment dynamics in a Belgian loess catchment. *Journal of Quaternary Science* 26: 44-58.

Notebaert B, Verstraeten G, Ward P, Renssen H and Van Rompaey A (2011c) Modeling the sensitivity of sediment and water runoff dynamics to Holocene climate and land use changes at the catchment scale. *Geomorphology* 126: 18-31.

Nyssen J, Pontzeele J and Billi P (2011) Effect of beaver dams on the hydrology of small mountain streams: example from the Chevral in the Ourthe Orientale basin, Ardennes, Belgium. *Journal of Hydrology* 402: 92-102.

Oksanen J, Blanchet FG, Kindt R, Legendre L, Minchin PR, O'Hara RB, Simpson GL, Solymos P, Stevens MHH and Wagner H (2012) vegan: Community Ecology Package. R package version2.0-5. http://CRAN.R-project.org/package=vegan.

Oswald WW, Faison EK, Foster DR, Doughty ED, Hall BR and Hansen B (2007) Post-glacial changes in spatial patterns of vegetation across southern New England. *Journal of Biogeography* 34: 900-913.

Ovenden L (1990) Peat accumulation in northern wetlands. *Quaternary Research* 33: 377-386.

Passega R (1957) Texture as characteristic of clastic deposition. *AAPG Bulletin* 41: 1952-1984.

Pastre JF, Leroyer C, Limondin-Lozouet N, Orth P, Chaussé P, Fotugne M, Gauthier A, Kunesch S, Le Jeune Y and Saad MC (2002) Variations paléoenvironmentales et paléohydrologiques durant les 15 derniers millénaires: les réponses morphosédimentaires des vallées du Bassin Parisien (France). In: Bravard JP and Magny M (ed.) *Les fleuves ont une histoire. Paléo-environnement des rivières et des lacs français depuis 15 000 ans*. Paris: Errance, 29-44.

Paus A (2013) Human impact, soil erosion, and vegetation response lags to climate change: challenges for the mid-Scandinavian pollen-based transfer-function temperature reconstructions. *Vegetation History and Archaeobotany* 22: 269-284.

Peeters I (2007) Spatial modelling of sediment redistribution patterns on a millennial time scale. *status: published*.

Petit RJ, Hu FS and Dick CW (2008) Forests of the past: A window to future changes. *Science* 320: 1450-1452.

Prentice IC (1985) Pollen Representation, Source Area, and Basin Size - toward a Unified Theory of Pollen Analysis. *Quaternary Research* 23: 76-86.

Qian J (2013) *Reconstruction of palaeoenvironmental change in a paleomeander in Dijle River from Late Glacial to ealry Holocene*. MSc thesis. Division of Geography, Department of Earth and Environmental Sciences, KU Leuven.

Ramsey CB (2009) Bayesian Analysis of Radiocarbon Dates. *Radiocarbon* 51: 337-360.

Reimer PJ, Bard E, Bayliss A, Beck JW, Blackwell PG, Ramsey CB, Grootes PM, Guilderson TP, Haflidason H and Hajdas I (2013) IntCal13 and Marine13 radiocarbon age calibration curves 0–50,000 years cal BP. *Radiocarbon* 55: 1869-1887.

Rittweger H (2000) The "Black Floodplain Soil" in the Amoneburger Becken, Germany: a lower Holocene marker horizon and indicator of an upper Atlantic to Subboreal dry period in Central Europe? *Catena* 41: 143-164.

Rommens T (2006) *Holocene sediment dynamics in a small river catchment in central Belgium*. Leuven: PhD thesis. Department of Earth and Environmental Sciences, KU Leuven.

Rommens T, Verstraeten G, Bogman P, Peeters I, Poesen J, Govers G, Van Rompaey A and Lang A (2006) Holocene alluvial sediment storage in a small river catchment in the loess area of central Belgium. *Geomorphology* 77: 187-201.

Rommens T, Verstraeten G, Peeters I, Poesen J, Govers G, Van Rompaey A, Mauz B, Packman S and Lang A (2007) Reconstruction of late-Holocene slope and dry valley sediment dynamics in a Belgian loess environment. *Holocene* 17: 777-788.

Rommens T, Verstraeten G, Poesen J, Govers G, Van Rompaey A, Peeters I and Lang A (2005) Soil erosion and sediment deposition in the Belgian loess belt during the Holocene: establishing a sediment budget for a small agricultural catchment. *Holocene* 15: 1032-1043.

Schumm S (1973) Geomorphic thresholds and complex response of drainage systems. *Fluvial geomorphology* 6: 69-85.

Seddon AW, Mackay AW, Baker AG, Birks HJB, Breman E, Buck CE, Ellis EC, Froyd CA, Gill JL and Gillson L (2014) Looking forward through the past: identification of 50 priority research questions in palaeoecology. *Journal of Ecology* 102: 256-267.

Sheldon ND and Retallack GJ (2001) Equation for compaction of paleosols due to burial. *Geology* 29: 247-250.

Shennan S (1997) *Quantifying Archaeology*. Edinburgh: Edinburgh University Press.

Shennan S, Downey SS, Timpson A, Edinborough K, Colledge S, Kerig T, Manning K and Thomas MG (2013) Regional population collapse followed initial agriculture booms in mid-Holocene Europe. *Nature Communications* 4.

Shepard RN (1962a) The analysis of proximities: Multidimensional scaling with an unknown distance function. I. *Psychometrika* 27: 125-140.

Shepard RN (1962b) The analysis of proximities: Multidimensional scaling with an unknown distance function. II. *Psychometrika* 27: 219-246.

Soepboer W, Sugita S and Lotter AF (2010) Regional vegetation-cover changes on the Swiss Plateau during the past two millennia: A pollen-based reconstruction using the REVEALS model. *Quaternary Science Reviews* 29: 472-483.

Starkel L, Soja R and Michczyńska DJ (2006) Past hydrological events reflected in Holocene history of Polish rivers. *Catena* 66: 24-33.

Steegen A (2001) *Sediment deposition in and export from small agricultural catchments*. Leuven: PhD thesis. Department of Earth and Environmental Sciences, KU Leuven.

Sugita S (1994) Pollen Representation of Vegetation in Quaternary Sediments - Theory and Method in Patchy Vegetation. *Journal of Ecology* 82: 881-897.

Sugita S (2007a) Theory of quantitative reconstruction of vegetation I: pollen from large sites REVEALS regional vegetation composition. *Holocene* 17: 229-241.

Sugita S (2007b) Theory of quantitative reconstruction of vegetation II: all you need is LOVE. *The Holocene* 17: 243-257.

Sugita S, Gaillard MJ and Brostrom A (1999) Landscape openness and pollen records: a simulation approach. *Holocene* 9: 409-421.

Tabacchi E, Correll DL, Hauer R, Pinay G, Planty-Tabacchi AM and Wissmar RC (1998) Development, maintenance and role of riparian vegetation in the river landscape. *Freshwater biology* 40: 497-516.

Tauber H (1967) Investigations of the mode of pollen transfer in forested areas. *Review of Palaeobotany and Palynology* 3: 277-286.

Ter Braak CJ (1986) Canonical correspondence analysis: a new eigenvector technique for multivariate direct gradient analysis. *Ecology* 67: 1167-1179.

Thomas DS and Allison RJ (1993) *Landscape sensitivity*. John Wiley & Sons Ltd.

Thorndycraft VR and Benito G (2006a) The Holocene fluvial chronology of Spain: evidence from a newly compiled radiocarbon database. *Quaternary Science Reviews* 25: 223-234.

Thorndycraft VR and Benito G (2006b) Late Holocene fluvial chronology of Spain: The role of climatic variability and human impact. *Catena* 66: 34-41.

Tinner W and Lotter AF (2006) Holocene expansions of Fagus silvatica and Abies alba in Central Europe: where are we after eight decades of debate? *Quaternary Science Reviews* 25: 526-549.

Tockner K and Stanford JA (2002) Riverine flood plains: present state and future trends. *Environmental Conservation* 29.

Törnqvist T, de Jong A, Oosterbaan WA and der Borg K (1992) Accurate dating of organic deposits by AMS 14C measurement of macrofossils. *Radiocarbon* 34: 566-577.

Trimble SW (1999) Decreased Rates of Alluvial Sediment Storage in the Coon Creek Basin, Wisconsin, 1975-93. *Science* 285: 1244-1246.

Trofimov V (2009) Paradoxes of modern geoecology. *Moscow University Geology Bulletin* 64: 203-213.

Turner J (1962) The *Tilia* decline: an anthropogenic interpretation. *New Phytologist* 61: 328-341.

Van Asselen S (2011) The contribution of peat compaction to total basin subsidence: implications for the provision of accommodation space in organic-rich deltas. *Basin Research* 23: 239-255.

van Asselen S, Stouthamer E and Smith ND (2010) Factors Controlling Peat Compaction in Alluvial Floodplains: A Case Study in the Cold-Temperate Cumberland Marshes, Canada. *Journal of Sedimentary Research* 80: 155-166.

Van De Wiel MJ and Coulthard TJ (2010) Self-organized criticality in river basins: Challenging sedimentary records of environmental change. *Geology* 38: 87-90.

Van der Woude JD (1983) Holocene paleoenvironmental evolution of a perimarine fluviatile area. Geology and paleobotany of the area surrounding the archeological excavation at the Hazendonk river dune (Western Netherlands). *Analecta Praehistorica Leidensia* 16.

Van Geel B (1978) A palaeoecological study of holocene peat bog sections in Germany and The Netherlands; based on the analysis of pollen, spores and macro- and microscopic remains of fungi, algae, cormophytes and animals. *Review of Palaeobotany and Palynology* 25: 1-120.

Van Geel B, Hallewas DP and Pals JP (1983) A late Holocene deposit under the Westfriese Zeedijk near Enkhuizen (Prov. of Noord-Holland, The Netherlands): palaeoecological and archaeological aspects. *Review of Palaeobotany and Palynology* 38: 269-335.

Van Hove D, Vanmontfort B, Verstraeten G, Van Rompaey A, De Man J and Van Peer P (2005) Mens & landschap in het Dijlebekken Eindraport Fase 2. Studie uitgevoerd in opdracht van het Vlaamse Gewest Afdeling Monumenten en Landschappen.

Van Oost K, Govers G and Desmet P (2000) Evaluating the effects of changes in landscape structure on soil erosion by water and tillage. *Landscape Ecology* 15: 577-589.

Van Oost K, Verstraeten G, Doetterl S, Notebaert B, Wiaux F, Broothaerts N and Six J (2012) Legacy of human-induced C erosion and burial on soil-atmosphere C exchange. *Proceedings of the National Academy of Sciences* 109: 19492-19497.

Van Rompaey AJJ, Verstraeten G, Van Oost K, Govers G and Poesen J (2001) Modelling mean annual sediment yield using a distributed approach. *Earth Surface Processes and Landforms* 26: 1221-1236.

van Schilt J (2013) *Fluvial and vegetational development of the Dijle catchment(Belgium) from the late Pleistocene until present, focusing on human impact*. MSc Thesis. Department of Earth Sciences, VU University Amsterdam.

Vandenberghe J (1995) Timescales, climate and river development. *Quaternary Science Reviews* 14: 631-638.

Vandenberghe J and De Smedt P (1979) Palaeomorphology in the Eastern Scheldt Basin (Central Belgium) - The Dijle-Demer-Grote Nete confluence area. *Catena* 6: 73-105.

Vanmontfort B (2007) Bridging the gap. The Mesolithic-Neolithic transition in a frontier zone. *Documenta Praehistorica* 34: 105-118.

Vanwalleghem T, Bork HR, Poesen J, Dotterweich M, Schmidtchen G, Deckers J, Scheers S and Martens M (2006) Prehistoric and Roman gullying in the European loess belt: a case study from central Belgium. *The Holocene* 16: 393-401.

Vanwalleghem T, Poesen J, Van Den Eeckhaut M, Nachtergaele J and Deckers J (2005) Reconstructing rainfall and land-use conditions leading to the development of old gullies. *Holocene* 15: 378-386.

Vanwalleghem T, Van Den Eeckhaut M, Poesen J, Deckers J, Nachtergaele J, Van Oost K and Slenters C (2003) Characteristics and controlling factors of old gullies under forest in a temperate humid climate: a case study from the Meerdaal Forest (Central Belgium). *Geomorphology* 56: 15-29.

Verstraeten G (2012) Combining quantitative field and modelling approaches towards understanding landscape dynmics: an evolution of ideas spanning Jef Vandenberghe's research career. *Netherlands Journal of Geosciences-Geologie En Mijnbouw* 91: 133-244.

Verstraeten G, Lang A and Houben P (2009a) Human impact on sediment dynamics - quantification and timing Introduction. *Catena* 77: 77-80.

Verstraeten G and Poesen J (2001) Factors controlling sediment yield from small intensively cultivated catchments in a temperate humid climate. *Geomorphology* 40: 123-144.

Verstraeten G, Rommens T, Peeters I, Poesen J, Govers G and Lang A (2009b) A temporarily changing Holocene sediment budget for a loess-covered catchment (central Belgium). *Geomorphology* 108: 24-34.

Verstraeten G, Van Oost K, Van Rompaey A, Poesen J and Govers G (2002) Evaluating an integrated approach to catchment management to reduce soil loss and sediment pollution through modelling. *Soil Use and Management* 18: 386-394.

Walter RC and Merritts DJ (2008) Natural Streams and the Legacy of Water-Powered Mills. *Science* 319: 299-304.

Ward PJ, van Balen RT, Verstraeten G, Renssen H and Vandenberghe J (2009) The impact of land use and climate change on late Holocene and future suspended sediment yield of the Meuse catchment. *Geomorphology* 103: 389-400.

Warrick JA and Rubin DM (2007) Suspended-sediment rating curve response to urbanization and wildfire, Santa Ana River, California. *Journal of Geophysical Research: Earth Surface* 112: F02018.

Wilkinson BH and McElroy BJ (2007) The impact of humans on continental erosion and sedimentation. *Geological Society of America Bulletin* 119: 140-156.

Wilmshurst JM and McGlone MS (2005) Origin of pollen and spores in surface lake sediments: Comparison of modem palynomorph assemblages in moss cushions, surface soils and surface lake sediments. *Review of Palaeobotany and Palynology* 136: 1-15.

Wohl E, Angermeier PL, Bledsoe B, Kondolf GM, MacDonnell L, Merritt DM, Palmer MA, Poff NL and Tarboton D (2005) River restoration. *Water Resources Research* 41.

Woodbridge J, Fyfe RM, Roberts N, Downey S, Edinborough K and Shennan S (2012) The impact of the Neolithic agricultural transition in Britain: a comparison of pollen-based land-cover and archaeological C date-inferred population change. *Journal of Archaeological Science*.

Xu Q, Tian F, Bunting MJ, Li Y, Ding W, Cao X and He Z (2012) Pollen source areas of lakes with inflowing rivers: modern pollen influx data from Lake Baiyangdian, China. *Quaternary Science Reviews* 37: 81-91.

Zimmermann A, Hilpert J and Wendt KP (2009) Estimations of Population Density for Selected Periods Between the Neolithic and AD 1800. *Human Biology* 81: 357-380.

Zolitschka B, Behre, K., Schneider, J. (2003) Human and climatic impact on the environment as derived from colluvial, fluvial and lacustrine archives - examples from the Bronze Age to the Migration period,Germany. *Quaternary Science Reviews* 22: 81-100.

List of publications

Articles in international journals

Broothaerts N, Kissi E, Poesen J, Van Rompaey A, Getahun A, Van Ranst E, Diels J (2012) Spatial patterns, causes and consequences of landslides in the Gilgel Gibe catchment, SW Ethiopia. *Catena*, 97: 127-136.

Broothaerts N, Verstraeten G, Notebaert B, Assendelft R, Kasse C, Bohncke S and Vandenberghe J (2013) Sensitivity of floodplain geoecology to human impact: A Holocene perspective for the headwaters of the Dijle catchment, central Belgium. *The Holocene* 23: 1403-1414.

Broothaerts N, Notebaert B, Verstraeten G, Kasse C, Bohncke S and Vandenberghe J (2014a) Non-uniform and diachronous Holocene floodplain evolution: a case study from the Dijle catchment, Belgium. *Journal of Quaternary Science* 29: 351-360.

Broothaerts N, Verstraeten G, Kasse C, Bohncke S, Notebaert B and Vandenberghe J (2014b) Reconstruction and semi-quantification of human impact in the Dijle catchment, central Belgium: a palynological and statistical approach. *Quaternary Science Reviews* 102: 96-110.

Broothaerts N, Verstraeten G, Kasse C, Bohncke S and Vandenberghe J (under review) From natural to human-dominated floodplain geoecology – a Holocene perspective for the Dijle catchment. *Anthropocene*.

Notebaert B, Houbrechts G, Verstraeten G, Broothaerts N, Haeckx J, Reynders M, Govers G, Petit F and Poesen J (2011) Fluvial architecture of Belgian river systems in contrasting environments: implications for reconstructing the sedimentation history. *Netherlands Journal of Geosciences-Geologie En Mijnbouw* 90: 31-50.

Van Oost K, Verstraeten G, Doetterl S, Notebaert B, Wiaux F, Broothaerts N and Six J (2012) Legacy of human-induced C erosion and burial on soil-atmosphere C exchange. *Proceedings of the National Academy of Sciences* 109: 19492-19497.

Presentations at international conferences

Broothaerts N, Notebaert B, Verstraeten G (2013) Asynchronicity in floodplain processes. An example from the Dijle catchment, Central Belgium. IAG International Conference on Geomorphology. Paris, 27-31 August 2013.

Broothaerts N, Verstraeten G, Kasse C, Bohncke S, Notebaert B and Vandenberghe J (2013) Human impact on floodplain geoecology. A Holocene perspective for the Dijle catchment, Central Belgium. IAG International Conference on Geomorphology. Paris, 27-31 August 2013.

Broothaerts N, Verstraeten G, Kasse C, Bohncke S, Notebaert B and Vandenberghe J (2013) The meandering Dijle River in the western European loess region: an anthropogenic landscape. EGU General Assembly 2012. Vienna, 07-12 April 2013.

Broothaerts N, Verstraeten G, Notebaert B, Assendelft R, Kasse C, Bohncke S and Vandenberghe J (2012) Humans reshaped the floodplain geoecology in NW Europe through intense agricultural impact. EGU General Assembly 2012. Vienna, 22-27 April 2012.

Broothaerts N, Notebaert B, Verstraeten G (2011) The changing geo-ecology of the Dijle floodplain (Belgium) during the Holocene in relation to human impact. XVII INQUA Bern 2011. Bern, Switzerland, 21-27 July 2011.

Kissi E, Poesen J, Diels J, Van Rompaey A, Broothaerts N, Vanopstal M (2011) Spatial and temporal variability of sediment yield of Gilgel Gibe catchment, Southwestern Ethiopia. Water 2011, integrated water resources management in tropical and subtropical drylands. Mekelle University, Mekelle, Ethiopia, 19-26 September 2011.

Notebaert B, Broothaerts N, Berger JF, Verstraeten G (2013) Non-linearities in Holocene floodplain sediment storage. EGU General Assembly 2012. Vienna, 07-12 April 2013.

Notebaert B, Broothaerts N, Verstraeten G, Kasse K, Bohncke S (2012). Development of an Anthropogenic Landscape in the Belgian Loess Belt after 5000 Years of Agriculture. International Symposium on Archaeometry: “50 years of ISA”. Leuven, 28 May – 1 June 2012.

Van Oost K, Verstraeten G, Doetterl S, Notebaert B, Wiaux F, Broothaerts N and Six J (2012) Carbon emissions as a result of land use change and accelerated soil erosion: perspectives in time & space. EGU General Assembly 2012. Vienna, 22-27 April 2012

Verstraeten G, Van Oost K, Broothaerts N, Notebaert B, Doetterl S, Wiaux F (2013) Humans have impacted atmospheric C-exchange since the introduction of agriculture by changing the geomorphic cascade. IAG International Conference on Geomorphology. Paris, 27-31 August 2013.

Verstraeten G, Notebaert B, D’Haen K, Broothaerts N, De Brue H (2013) Variability in geomorphic response to anthropogenic disturbance. EGU General Assembly 2012. Vienna, 07-12 April 2013.

Presentations at national conferences

Broothaerts N, Verstraeten G, Kasse C, Bohncke S, Notebaert B and Vandenberghe J (2014) Reconstructing human impact based on pollen analysis and MDS. A Holocene perspective for the Dijle catchment (Belgium). Meeting of the Belgian archaeobotanists. Brussels, 31 January 2014.

Broothaerts N, Verstraeten G, Notebaert B, Assendelft R, Kasse C, Bohncke S and Vandenberghe J (2012) Humans reshaped the floodplain geoecology of the Dijle catchment through intense agricultural impact. Belqua 2012 Annual Scientific Workshop, Brussels, Belgium, 1 March 2012

External reports

Lambrechts B, Broothaerts N, Vanmontfort B (2011) Mechelen De Nekker – Archeologisch en paleolandschappelijk onderzoek. EPA rapport 23.

Presentations at universities

Broothaerts et al., 2011. Doctoral plan: A geoecological reconstruction of the Dijle floodplain during the last 7 ka in relation with human impact. KU Leuven, June 2011.

Broothaerts et al., 2011. A geoecological reconstruction of the Dijle floodplain during the last 7 ka in relation with human impact. VU Amsterdam, October 2011.

Broothaerts et al., 2011. A geoecological reconstruction of the Dijle floodplain during the last 7 ka in relation with human impact. KU Leuven, 1 December 2011.

Broothaerts et al., 2012. Changing geoecology of the Dijle floodplain through intense agricultural impact. KU Leuven, 5 November 2012.

Broothaerts et al., 2013. Workshop R: Correspondence analysis of pollen data in R. KU Leuven, 11 January 2013.

Broothaerts et al., 2014. Reconstruction and semi-quantification of human impact in the Dijle catchment. KU Leuven, 2 April 2014.

Supervision of M.Sc. and B.Sc. theses

Assendelft R (2012) *Reconstruction of the human impact on the floodplain sedimentation and vegetational development in the Dijle catchment, Belgium, from the Neolithic period to the Middle Ages*. MSc thesis. Department of Earth Sciences, VU University Amsterdam.

Buijs M (2013) *Human impact on the floodplain sedimentation and vegetation of the area around the IJse valley during the Holocene*. MSc thesis. Department of Earth Sciences, VU University Amsterdam.

Coenen B (2013) *Bepaling van sedimentatiemilieus in de Dijle vallei aan de hand van textuuranalyse*. Bachelor thesis. Division of Geography, Department of Earth and Environmental Sciences, KU Leuven.

Qian J (2013) *Reconstruction of palaeoenvironmental change in a paleomeander in Dijle River from Late Glacial to ealry Holocene*. MSc thesis. Division of Geography, Department of Earth and Environmental Sciences, KU Leuven.

van Schilt J (2013) *Fluvial and vegetational development of the Dijle catchment(Belgium) from the late Pleistocene until present, focusing on human impact*. MSc Thesis. Department of Earth Sciences, VU University Amsterdam.

Appendices

Appendix 1 - Radiocarbon ages for the Dijle catchment

nr	Sample ID	Lab-code	Conventional age (BP)	calibrated Radiocarbon age (Cal BP) ± 1-σ error	location	depth (cm)	dated material	Stratigraphic position	Ch. 3		Source
1	COR-103-D4	Beta-308864	620 ± 30	604 ± 33	Cortil	245	terrestrial plant remains	top peat layer	top	*	This study
2	COR-D12	Beta-323481	1770 ± 30	1683 ± 52	Cortil	269	plant remains	floodplain fines	-	*	This study
3	COR-103-D1	Beta-308862	2520 ± 30	2606 ± 77	Cortil	320	wood remains	top gyttja layer	-	*	This study
4	COR-103-D3	Beta-308863	4760 ± 40	5495 ± 72	Cortil	370	terrestrial plant remains	gyttja layer	-	*	This study
5	SCL 4-2	Beta-257424	430 ± 40	470 ± 55	Sclage	230	wood remains	top peat layer	top		Notebaert et al., 2011b
6	NB-SCL-50-9	Beta-297818	300 ± 40	376 ± 61	Sclage	270	wood remains	top peat layer	top		This study
7	NB-SCL-50-17	Beta-297819	9080 ± 50	10247 ± 53	Sclage	515	wood remains	base gyttja layer	base		This study
8	NB-SCL102-D1	Beta-302449	480 ± 30	520 ± 14	Sclage	304	wood remains	top peat layer	top	*	This study
9	SCL-102-4-D5	Beta308870	1210 ± 30	1137 ± 50	Sclage	319	terrestrial plant remains	peat layer	-	*	This study
10	NB-SCL102-D9	Beta-302450	2350 ± 30	2377 ± 49	Sclage	339	terrestrial plant remains	peat layer	-	*	This study
11	SCL-102-4-15	Beta-308869	3620 ± 30	3933 ± 48	Sclage	371	terrestrial plant remains	peat layer	-	*	This study
12	NB-SCL102-D12	Beta-302451	4700 ± 30	5424 ± 77	Sclage	399	terrestrial plant remains	peat layer	-	*	This study
13	SCL 3-2	Beta250211	450 ± 40	494 ± 43	Sclage	330	wood remains	top peat layer	top		Notebaert et al., 2011b
14	NB-SCL-53-9	Beta-297820	510 ± 40	543 ± 36	Sclage	340	wood remains	top peat layer	top		This study
15	NB-SCL-53-17	Beta-297821	2230 ± 40	2237 ± 56	Sclage	490	terrestrial plant remains	bottom gyttja layer	-		This study
16	SCL 2-1	Beta2577361	670 ± 40	620 ± 40	Sclage	320	terrestrial plant remains	top peat layer	top		Notebaert et al., 2011b
17	SCL 2-7	Beta-257243	9870 ± 60	11304 ± 88	Sclage	500	wood remains	base peat layer	base		Notebaert et al., 2011b
18	SAR-100-D5-2	Beta-309758	1490 ± 30	1373 ± 36	St-Agatha-Rode	240	woody plant remains	org floodplain fines	-	*	This study
19	SAR-D13	Beta-321659	1670 ± 30	1580 ± 46	St-Agatha-Rode	300	woody plant remains	floodplain fines	-	*	This study
20	SAR-D16	Beta-323484	2530 ± 30	2618 ± 78	St-Agatha-Rode	335	wood remains	org floodplain fines	-	*	This study
21	SAR-100-D1	Beta-308865	1630 ± 30	1512 ± 52	St-Agatha-Rode	380	plant remains	top peat layer	top	*	This study
22	SAR-D18	Beta-323485	1730 ± 30	1639 ± 43	St-Agatha-Rode	383	plant remains	top peat layer	top		This study
23	SAR-100-D2	Beta-308866	5430 ± 40	6234 ± 46	St-Agatha-Rode	414	plant remains	peat layer	-	*	This study
24	NB-ARC-D20-3	Beta-352395	780 ± 30	705 ± 20	Archennes	322	wood remains	top upper peat layer	-	*	This study
25	NB-ARC-D21	Beta-352396	1230 ± 30	1164 ± 55	Archennes	379	wood remains	base upper peat l.	-	*	This study
26	NB-ARC-D9	Beta-352394	3350 ± 30	3586 ± 49	Archennes	486	wood remains	top peat layer	top	*	This study

27	Arch 73-5	Beta - 257380	9450 ± 50	10709 ± 116	Archennes	717	wood remains	base peat layer	base		Notebaert et al., 2011b
28	NB-LNB-D5	Beta-352397	360 ± 30	408 ± 56	Loonbeek	190	seeds:Fabaceae	org floodplain fines	-	*	This study
29	NB-LNB-D6	Beta-352398	1140 ± 30	1044 ± 50	Loonbeek	235	seeds: Bidens	floodplain fines	-	*	This study
30	NB-LNB-D7	Beta-352399	3450 ± 30	3725 ± 58	Loonbeek	341	plant remains	top peat layer	top	*	This study
31	ijlbk 02-4	Beta - 250207	3450 ± 40	3722 ± 63	Loonbeek	290	wood	top peat layer	top		Notebaert et al., 2011b
32	NB-ROT100-D2	Beta-343910	2610 ± 30	2742 ± 27	Rotselaar	152	top peat layer	wood remains	-	*	This study
33	NB-ROTZ-D41	Beta-352401	8860 ± 40	9988 ± 113	Rotselaar	200	peat layer	wood remains	-	*	This study
34	NB-ROTZ-D42	Beta-352402	9310 ± 50	10504 ± 82	Rotselaar	232	bottom peat layer	carex seeds	-	*	This study
35	ROTZ200-D44	Beta-352403	10060 ± 40	11588 ± 123	Rotselaar	330	top of unit 1	pollen	-	*	This study
36	KOR_04C	UtC 14830	1280 ± 36	1219 ± 44	Korbeek	330	charcoal	top peat layer	top		Notebaert et al., 2011b
37	KOR_0163	UtC 14827	2473 ± 35	2560 ± 96	Korbeek	290	organic C residue	top peat layer	top		Notebaert et al., 2011b
38	NB-KOR60-2	Beta-302444	160 ± 30	154 ± 86	Korbeek	650	terrestrial plant remains	top peat layer	top		This study
39	NB-KOR50-10	Beta-297802	1040 ± 40	960 ± 47	Korbeek	240	terrestrial plant remains	top peat layer	top		This study
40	NB-KOR-D40	Beta-352400	1060 ± 30	975 ± 36	Korbeek	233-234	seeds	top peat layer	top	*	This study
41	NB-KOR58-3-1	Beta-297808	1440 ± 40	1340 ± 31	Korbeek	105	wood remains	top peat layer	top		This study
42	NB-KOR52-11	Beta-302442	1490 ± 30	1373 ± 36	Korbeek	300	terrestrial plant remains	top peat layer	top		This study
43	NB-KOR68-11	Beta-302445	1650 ± 30	1550 ± 50	Korbeek	381	terrestrial plant remains	top peat layer	top		This study
44	NB-KOR56-9-1	Beta-297804	2440 ± 40	2241 ± 57	Korbeek	270	wood and plant remains	top peat layer	top		This study
45	NB-KOR54-4	Beta-302443	800 ± 30	715 ± 24	Korbeek	195	terrestrial plant remains	top peat layer	top		This study
46	KOR_0164	UtC 14828	6646 ± 48	7524 ± 40	Korbeek	460	plant remains	base peat layer	base		Notebaert et al., 2011b
47	102-5B-5	Beta - 240527	9000 ± 50	10145 ± 93	Korbeek	497-500	wood	base peat layer	base		Notebaert et al., 2011b
48	NB-KR71-16-1	Beta-297816	4780 ± 40	5510 ± 60	Korbeek	500	plant remains	base peat layer	base		This study
49	NB-KR74-11-1	Beta-297817	8380 ± 50	9395 ± 64	Korbeek	450	plant remains	base peat layer	base		This study
50	NB-KOR50-15	Beta-297803	8740 ± 50	9732 ± 108	Korbeek	390	plant remains	base peat layer	base		This study
51	NB-KOR56-12	Beta297806	8860 ± 50	9975 ± 132	Korbeek	400	wood and plant remains	base peat layer	base		This study
52	NB-KOR68-17	Beta-302446	9220 ±40	10380 ± 70	Korbeek	470	plant remains	base peat layer	base		This study
53	NB-KOR80-13	Beta-297812	9500 ± 50	10835 ± 141	Korbeek	510	plant remains	base peat layer	base		This study
54	NB-KOR62-21	Beta-297811	9530 ± 50	10888 ± 128	Korbeek	820	wood	base peat layer	base		This study
55	NB-KOR58-8-1	Beta-297809	9670 ± 50	11036 ±127	Korbeek	330	plant remains	base peat layer	base		This study
56	KOR110-D2	Beta-321656	1670 ± 30	1580 ± 46	Korbeek	184	wood remains	floodplain fines	-	*	This study
57	KOR110-D4	Beta-323482	1470 ± 30	1355 ± 39	Korbeek	208	seeds	floodplain fines	-	*	This study
58	KOR110-D6	Beta-321657	1340 ± 40	1260 ± 40	Korbeek	232	terrestrial plant remains	peat layer	-	*	This study
59	KOR110-D7	Beta-321658	4450 ± 30	5108 ± 107	Korbeek	245	seeds	peat layer	-	*	This study

60	KOR110-D8	Beta-323483	5400 ± 30	6221 ± 49	Korbeek	265	terrestrial plant remains	peat layer	-	*	This study
61	BN1	Beta-192001	7380 ± 40	8214 ± 70	Beauvechain	365-375	Organic C residue	top peat layer	top		Rommens et al., 2006
62	cer8-2	Beta - 250192	900 ± 40	827 ± 54	Cerise	72	wood remains	top peat layer	top		Notebaert et al., 2011b
63	HMW	Beta-192000	1300 ± 40	1229 ± 43	Hamme-Mille	235	Organic C residue	top peat layer	top		Rommens et al., 2006
64	VZ	Beta-191999	920 ± 40	841 ± 49	Nethen	165	Organic C residue	top peat layer	top		Rommens et al., 2006
65	SJW22-445	Beta - 226190	5500 ± 40	6305 ± 47	St-Joris-Weert	445	wood remains	top peat layer	top		Notebaert et al., 2011b
66	SJW20-340	Beta - 226189	5770 ± 40	6570 ± 53	St-Joris-Weert	340	wood remains	top peat layer	top		Notebaert et al., 2011b
67	suz 6-1	Beta - 250212	4140 ± 40	4685 ± 82	Suzeril	420	wood remains	top peat layer	top		Notebaert et al., 2011b
68	Bon 01-6	Beta - 257409	9530 ± 60	10885 ± 134	Bonlez I	520-540	wood remains	base peat layer	base		Notebaert et al., 2011b
69	Bon 5-14	Beta - 257412	8660 ± 60	9640 ± 81	Bonlez II	815	wood remains	base peat layer	base		Notebaert et al., 2011b
70	TLA 4-8	Beta - 257427	9970 ± 40	11432 ± 107	Terlanen	540-545	terrestrial plant remains	base peat layer	base		Notebaert et al., 2011b

Asterisk (*) indicate radiocarbon ages used for the age-depth modelling (Figure 2.9)

Appendix 2 - Floodplain transects

Appendix 2. Floodplain transects in the Dijle catchment, with indication of the different lithostratigraphical units (see Table 2.3). White dots indicate the location of radiocarbon samples (Appendix 1). Dotted rectangulars indicate location of pollen profiles, vertical lines indicate location and bottom of the individual corings.

Legend

	Unit	**Texture**	**Interpreted deposition environment**
	Unit 1A	Compact silty to loamy sediments	Loamy Pre-Holocene river deposits
	Unit 1B	Loamy sands to coarse sands	Sandy Pre-Holocene river deposits
	Unit 2	Gyttja	Gyttja
	Unit 3	Peat	Peat
	Unit 4	Calciumcarbonate rich deposits	Calciumcarbonate rich deposits
	Unit 5	Silty clay loam to loam	Overbank deposits
	Unit 5A	Organic silty clay loam to loam	Organic overbank deposits
	Unit 6A	Alterations of organic silty clay loam and fine sand	Low energetic channel deposits
	Unit 6B	Sandy loam and sands	Channel and point bar deposits
	Unit 7	Alternating silty clay loam to sand	Alternation of colluvial and overbank deposits

Anthropogenic heightened

Location and bottom of the individual corings

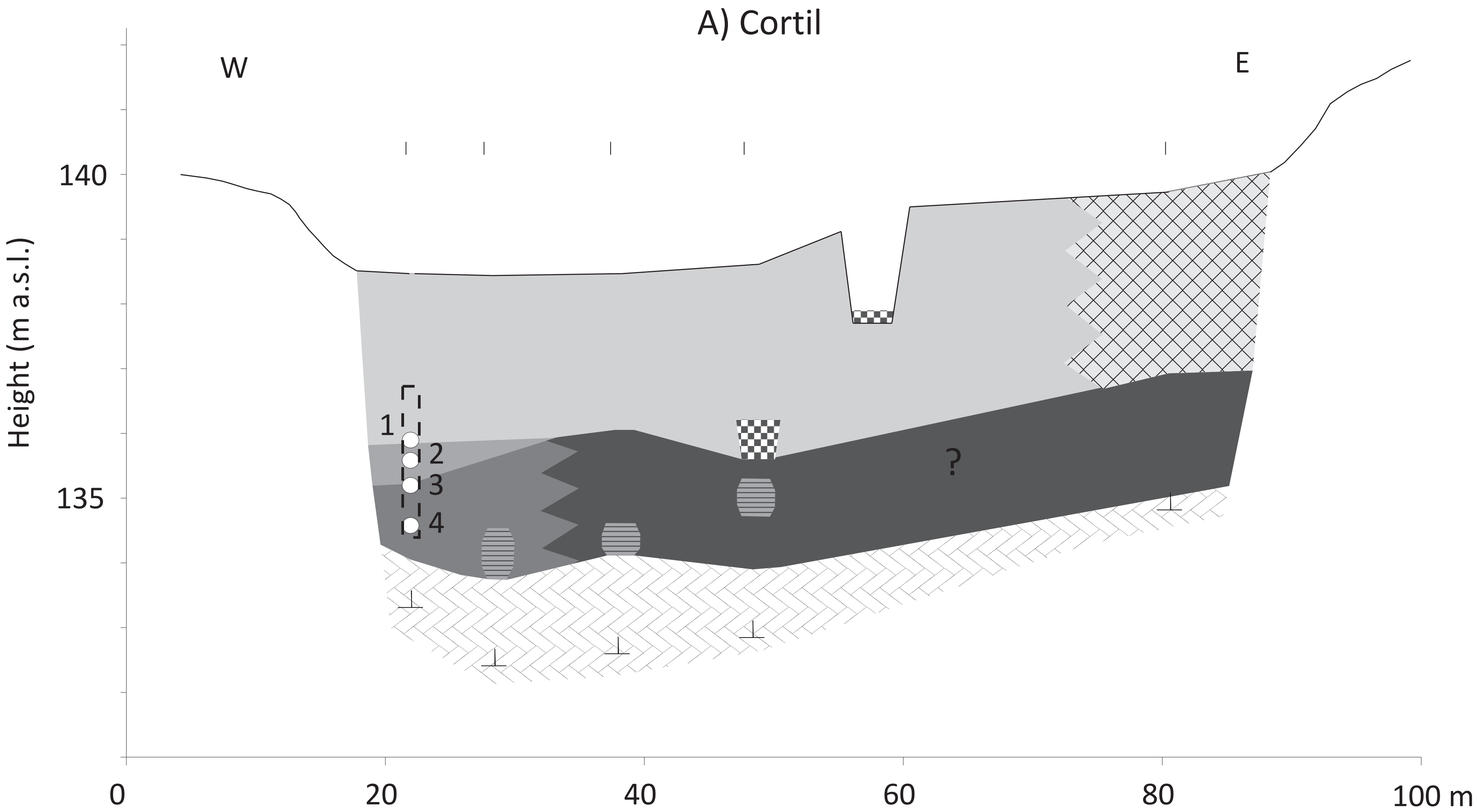
A) Cortil
W
E
Height (m a.s.l.)
140
135
1
2
3
4
?
0
20
40
60
80
100 m

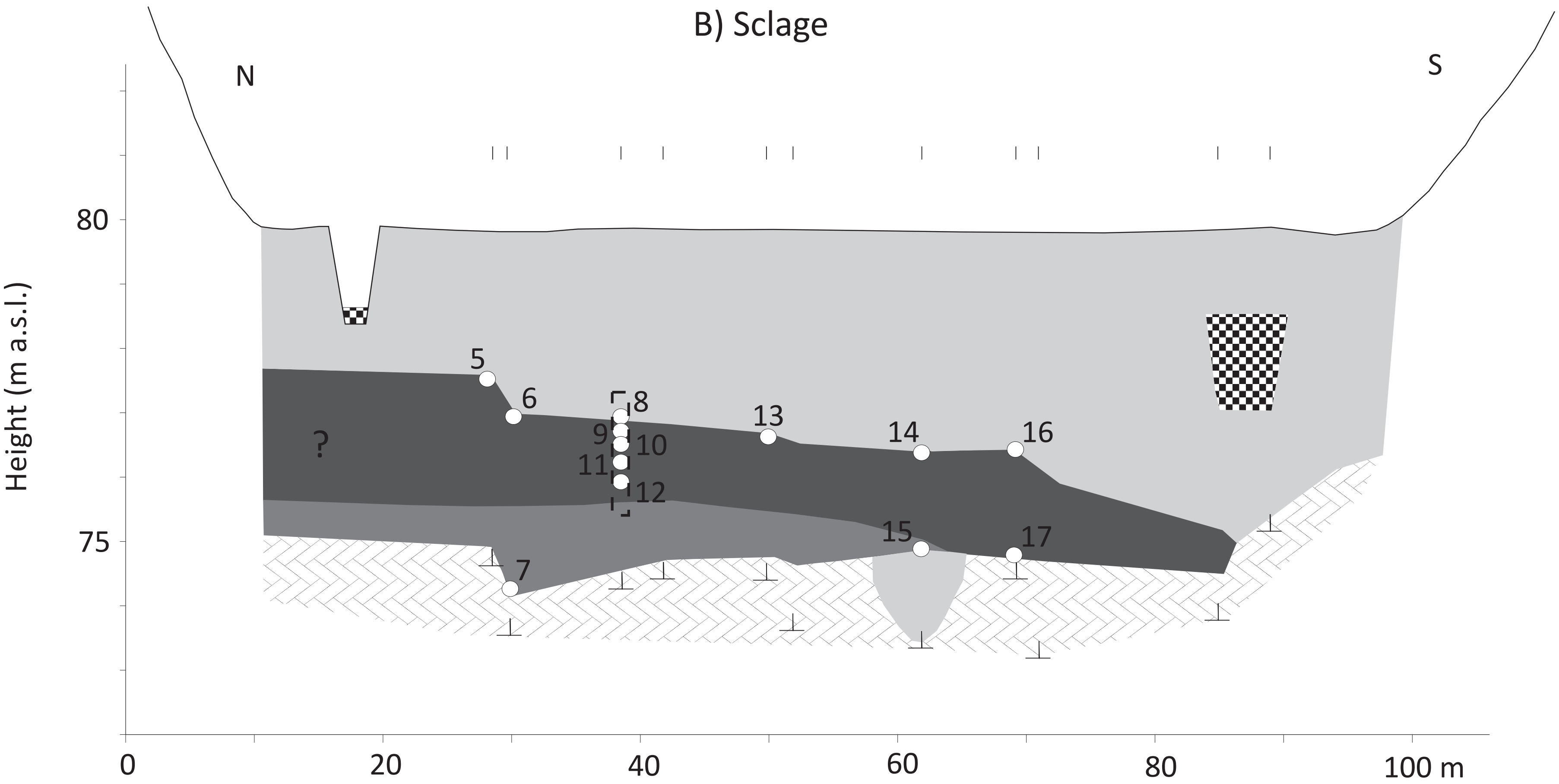
B) Sclage
N
S
80
75
Height (m a.s.l.)
5
6
7
8
9
10
11
12
13
14
15
16
17
?
0
20
40
60
80
100 m

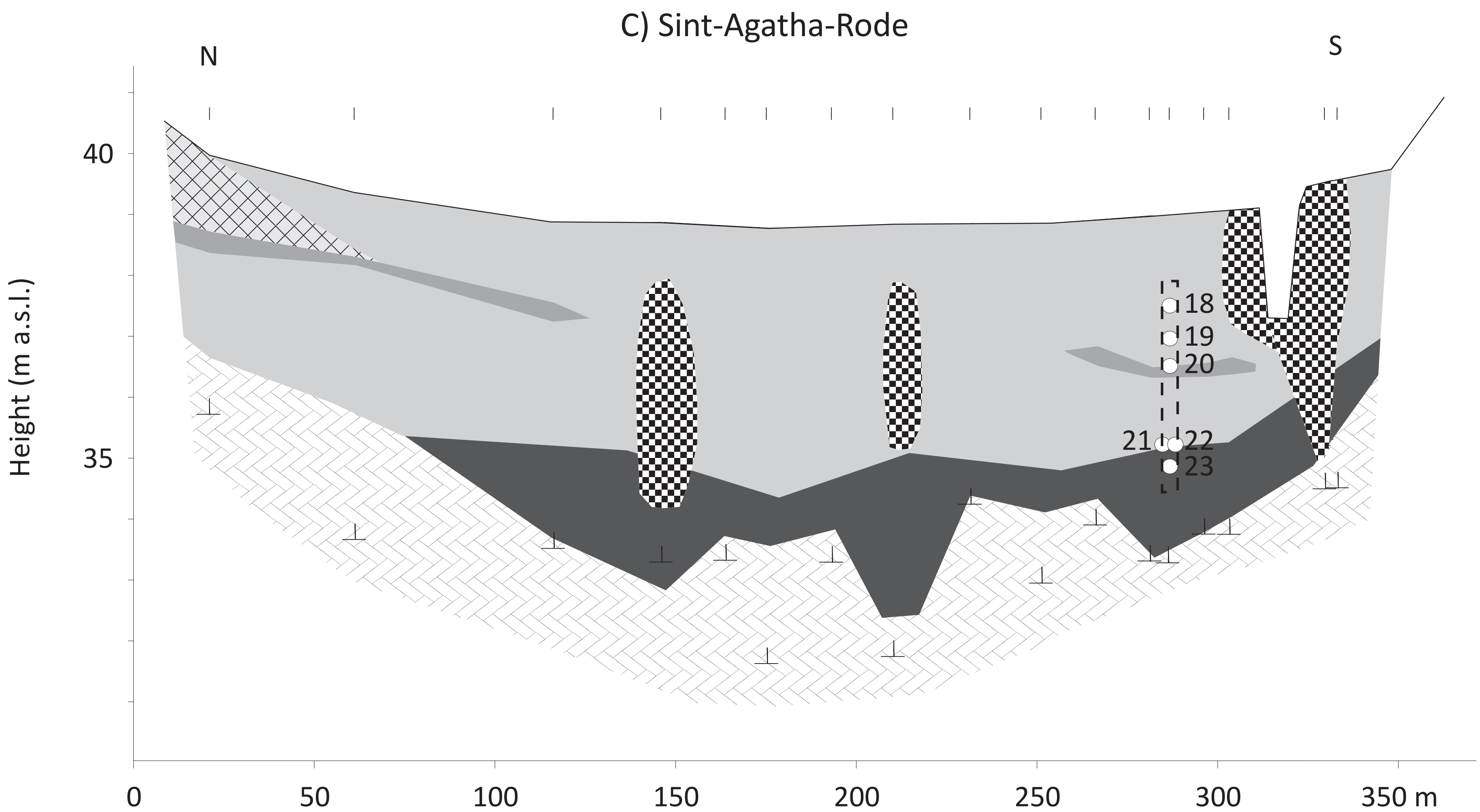

C) Sint-Agatha-Rode
N
S
Height (m a.s.l.)
40
35
18
19
20
21
22
23
0
50
100
150
200
250
300
350 m

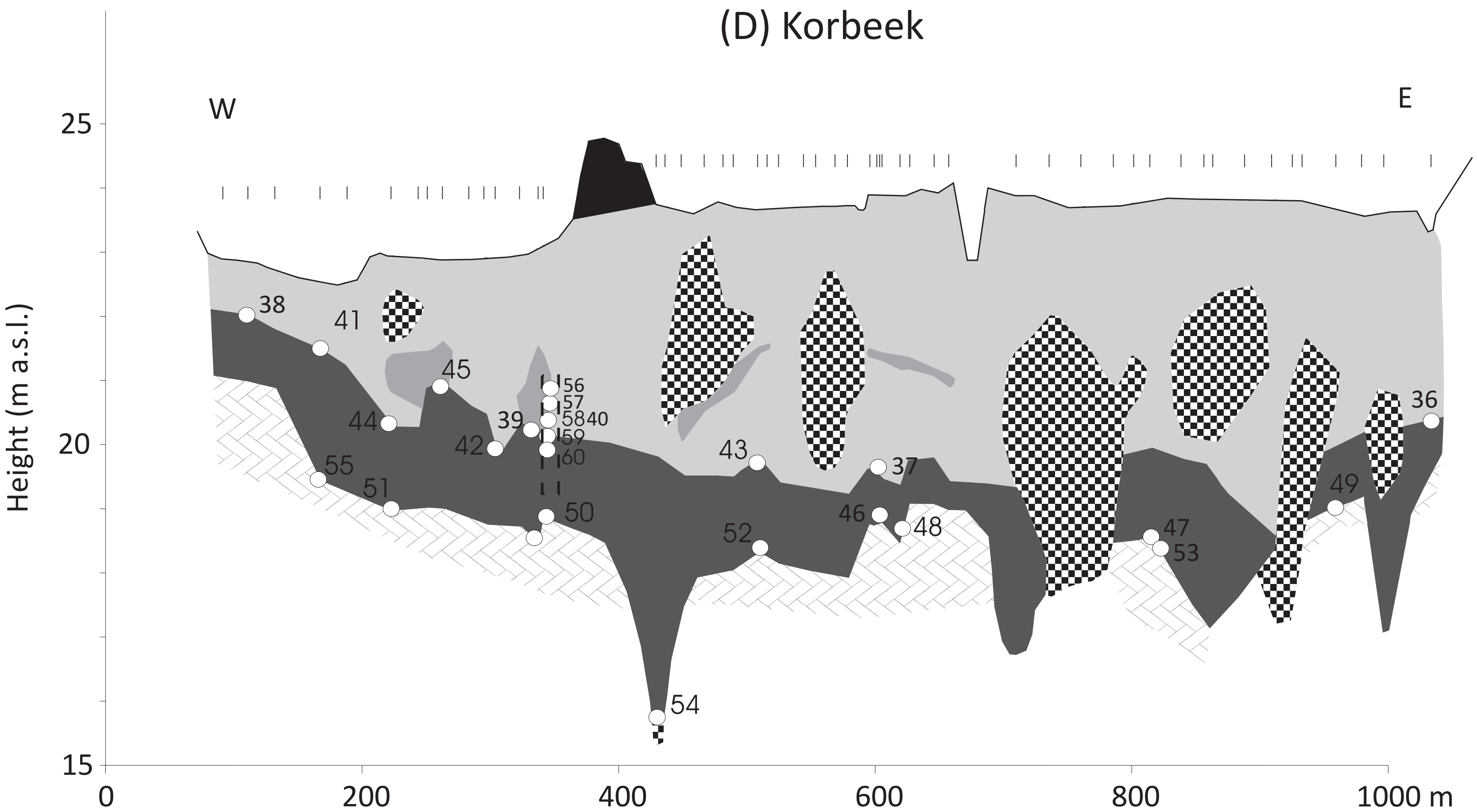

(D) Korbeek
W
E
Height (m a.s.l.)
25
20
15
0
200
400
600
800
1000 m
38
41
45
44
39
42
56
57
58
40
59
60
55
51
50
54
43
52
46
37
48
47
53
49
36

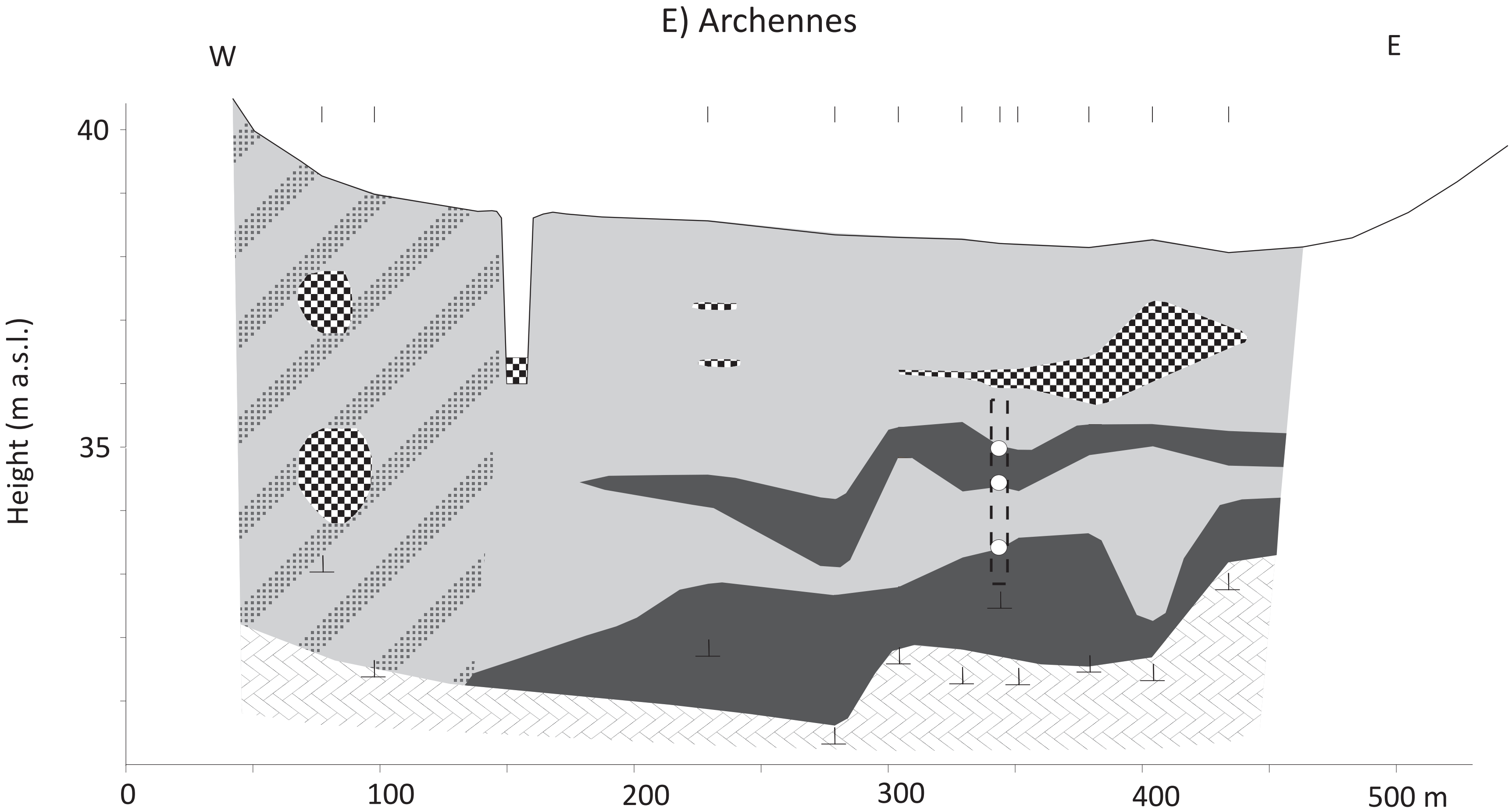
E) Archennes
W
E
40
35
Height (m a.s.l.)
0
100
200
300
400
500 m

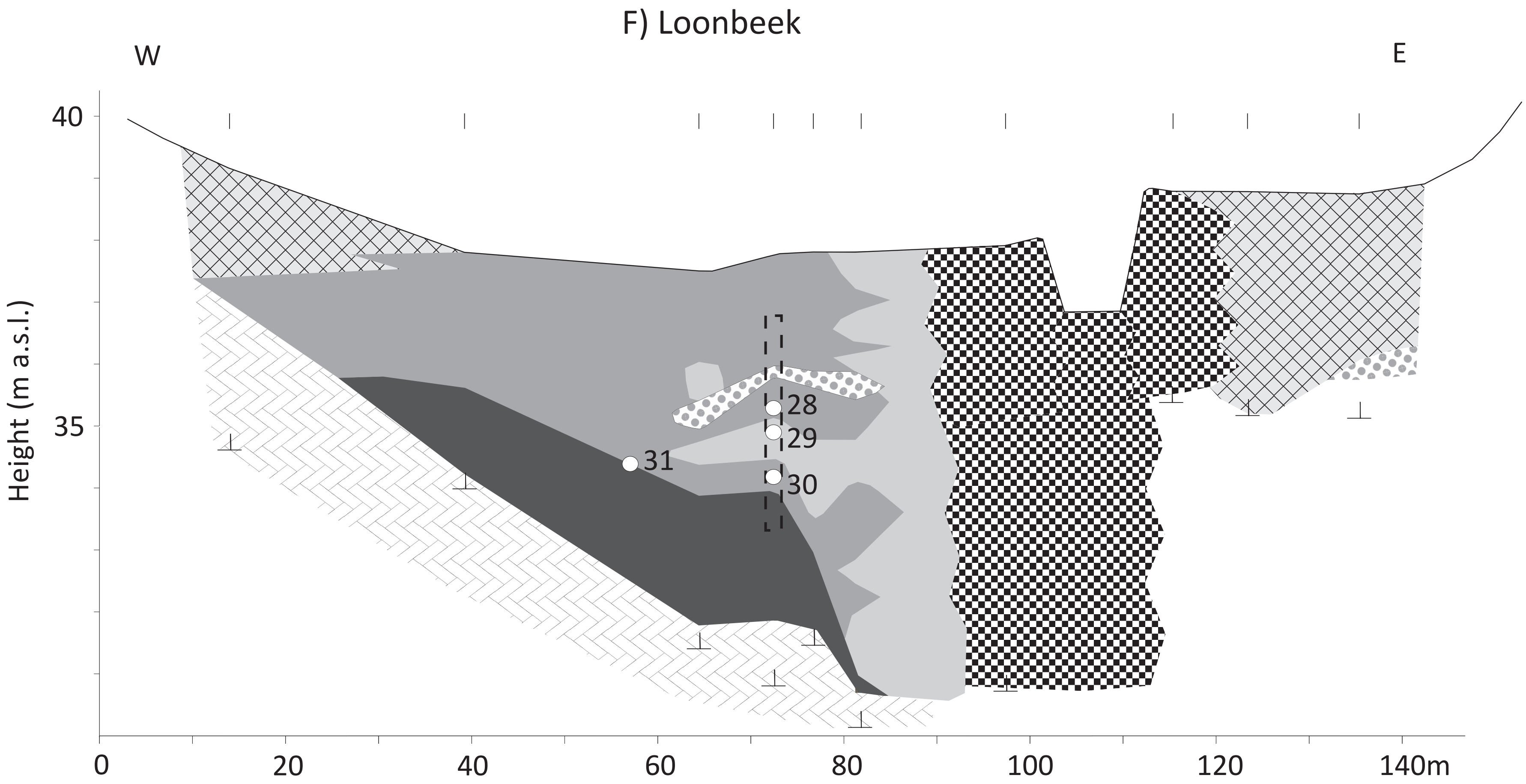

F) Loonbeek
W
E
40
35
Height (m a.s.l.)
28
29
30
31
0
20
40
60
80
100
120
140m

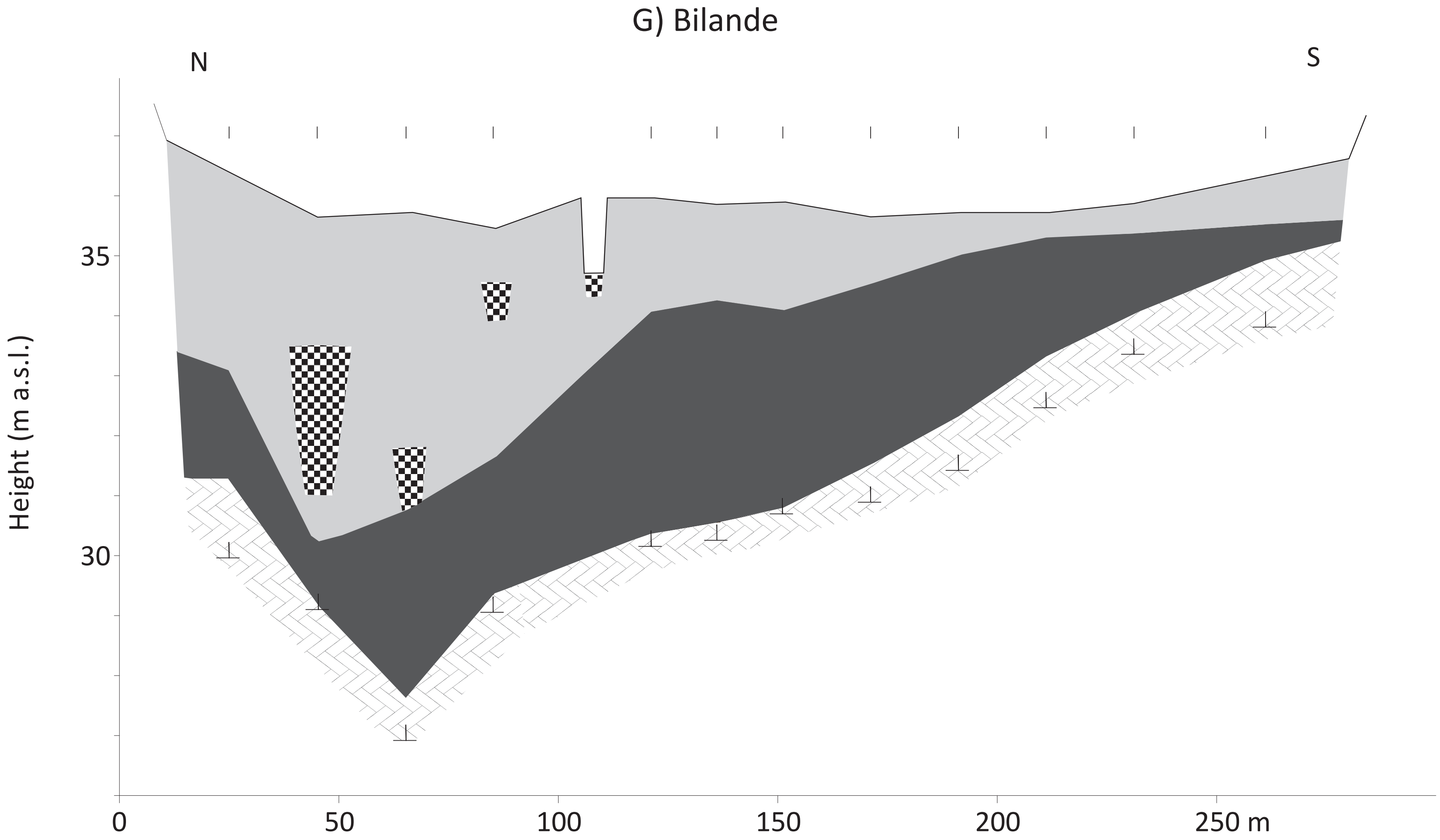
G) Bilande
N
S
Height (m a.s.l.)
35
30
0
50
100
150
200
250 m

H) Thy

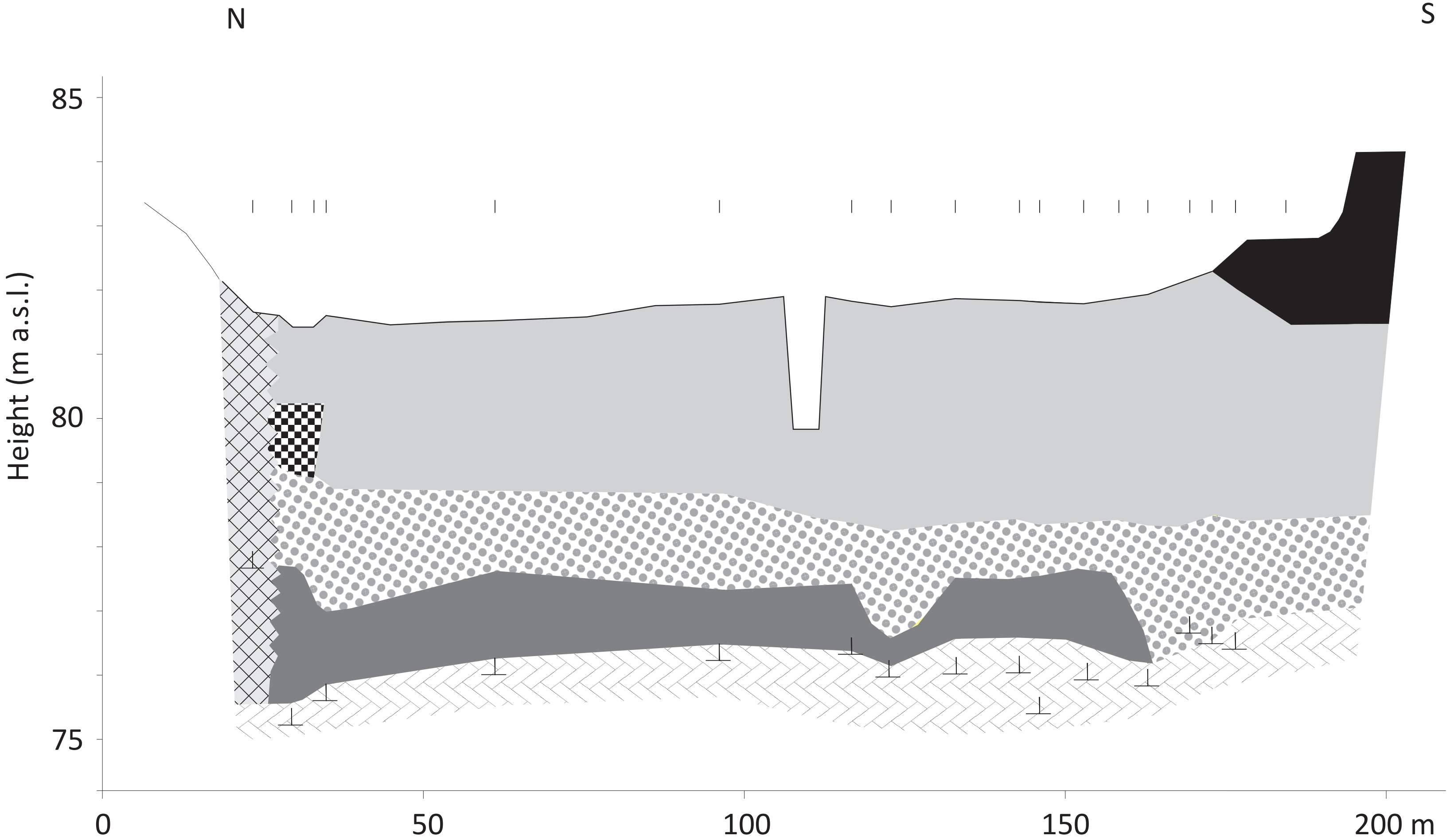

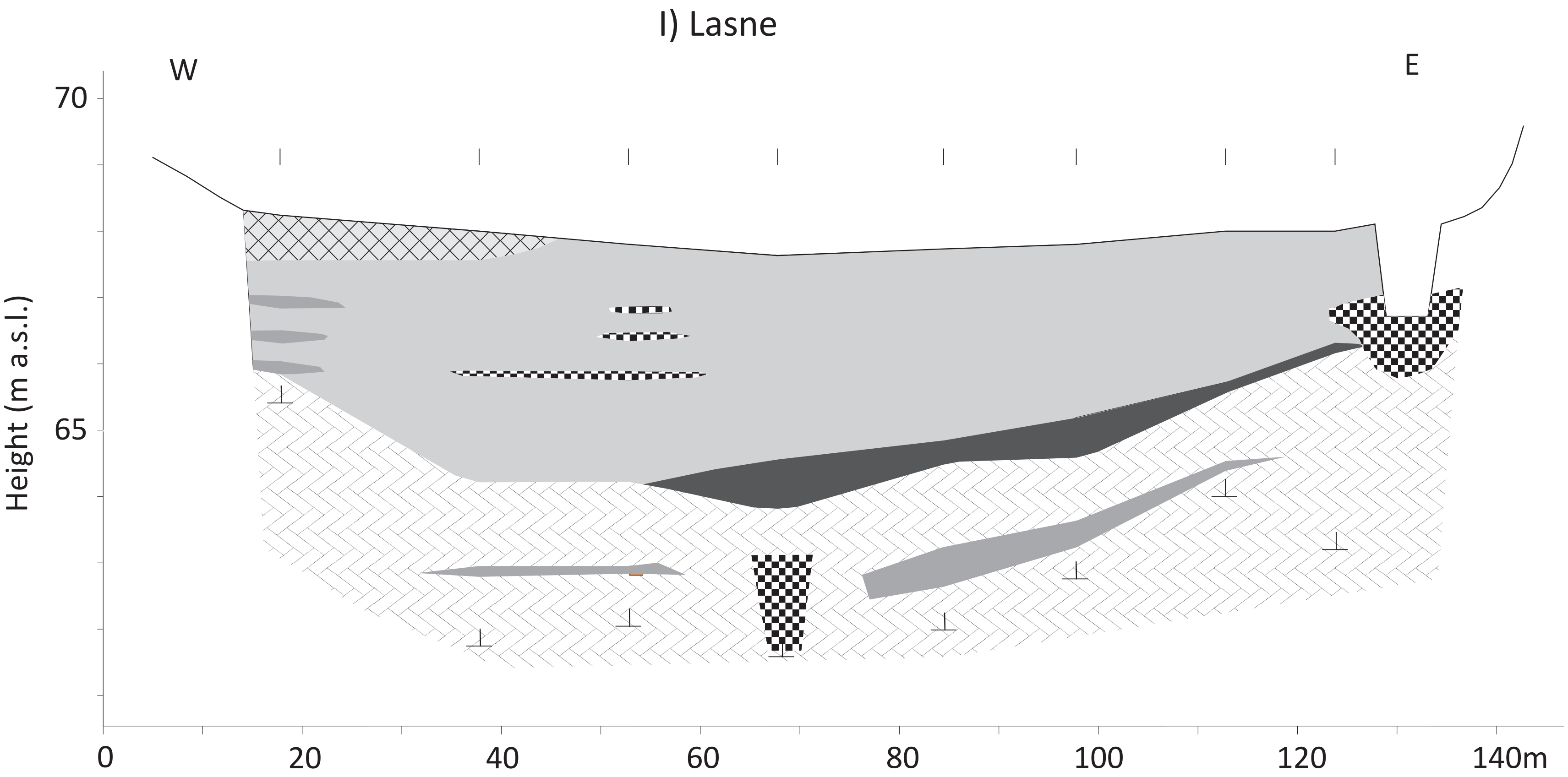

I) Lasne
W
E
Height (m a.s.l.)
70
65
0
20
40
60
80
100
120
140m

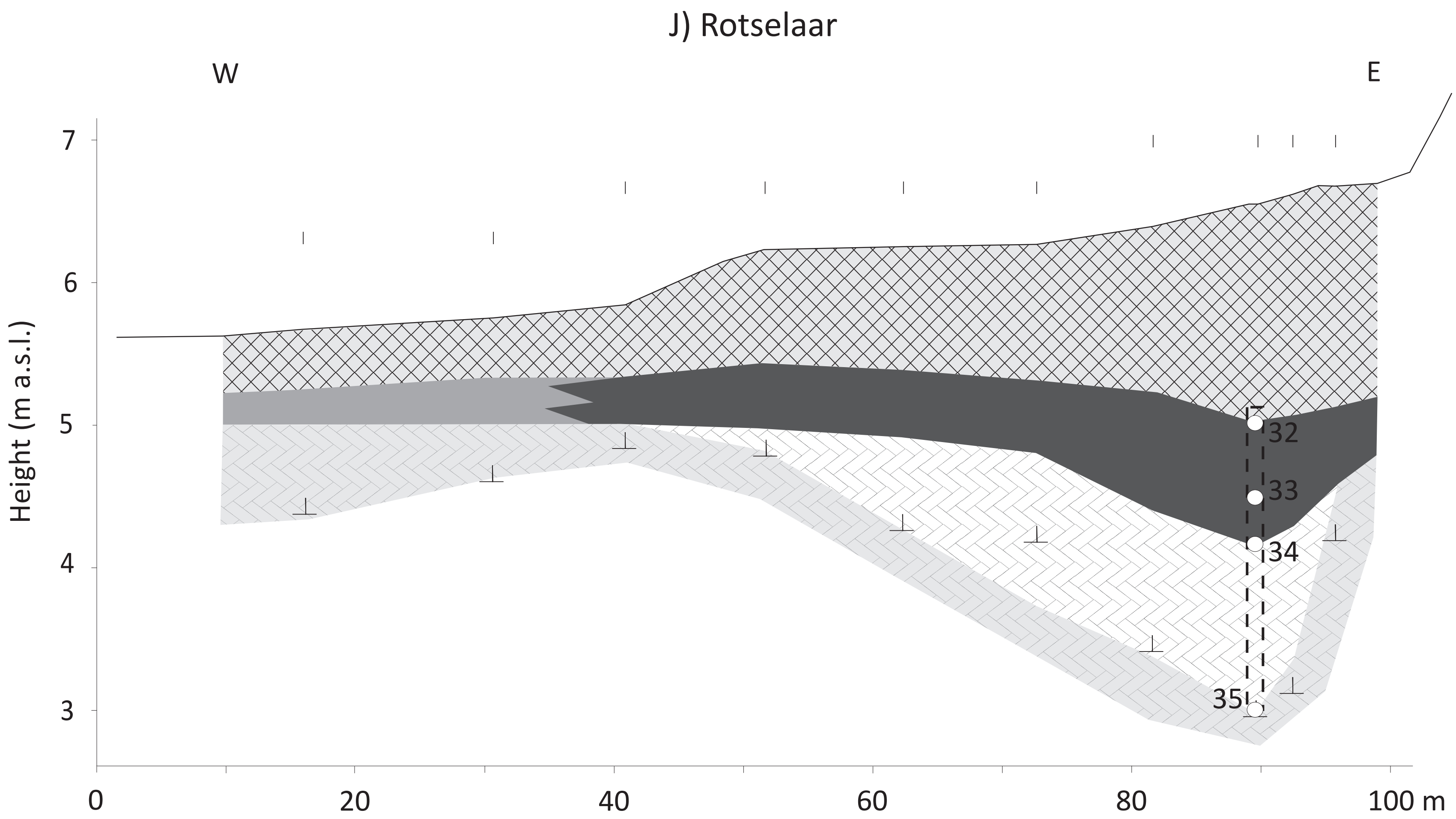

J) Rotselaar
W
E
Height (m a.s.l.)
7
6
5
4
3
0
20
40
60
80
100 m
32
33
34
35

Appendix 3 – Pollen tables

The pollen tables used in this study are available via the digital repository of KU Leuven (Lirias; https://lirias.kuleuven.be/).

Appendix 4 - Cluster trees

Clustering tree for the local pollen signal from each study sites. Sample names are indicated by the sample depth. The height of each branch represents the distance between the two objects being connected.

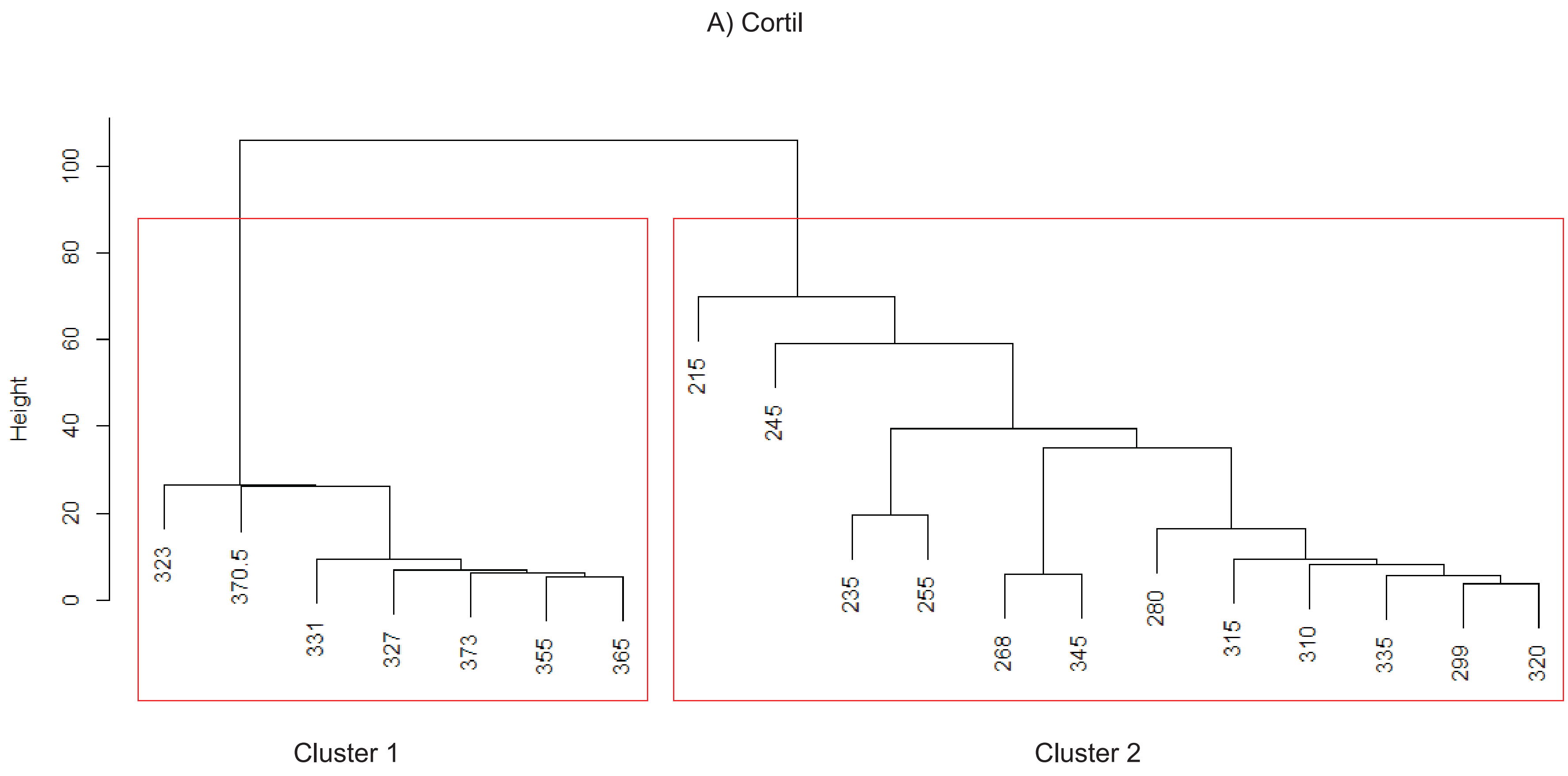

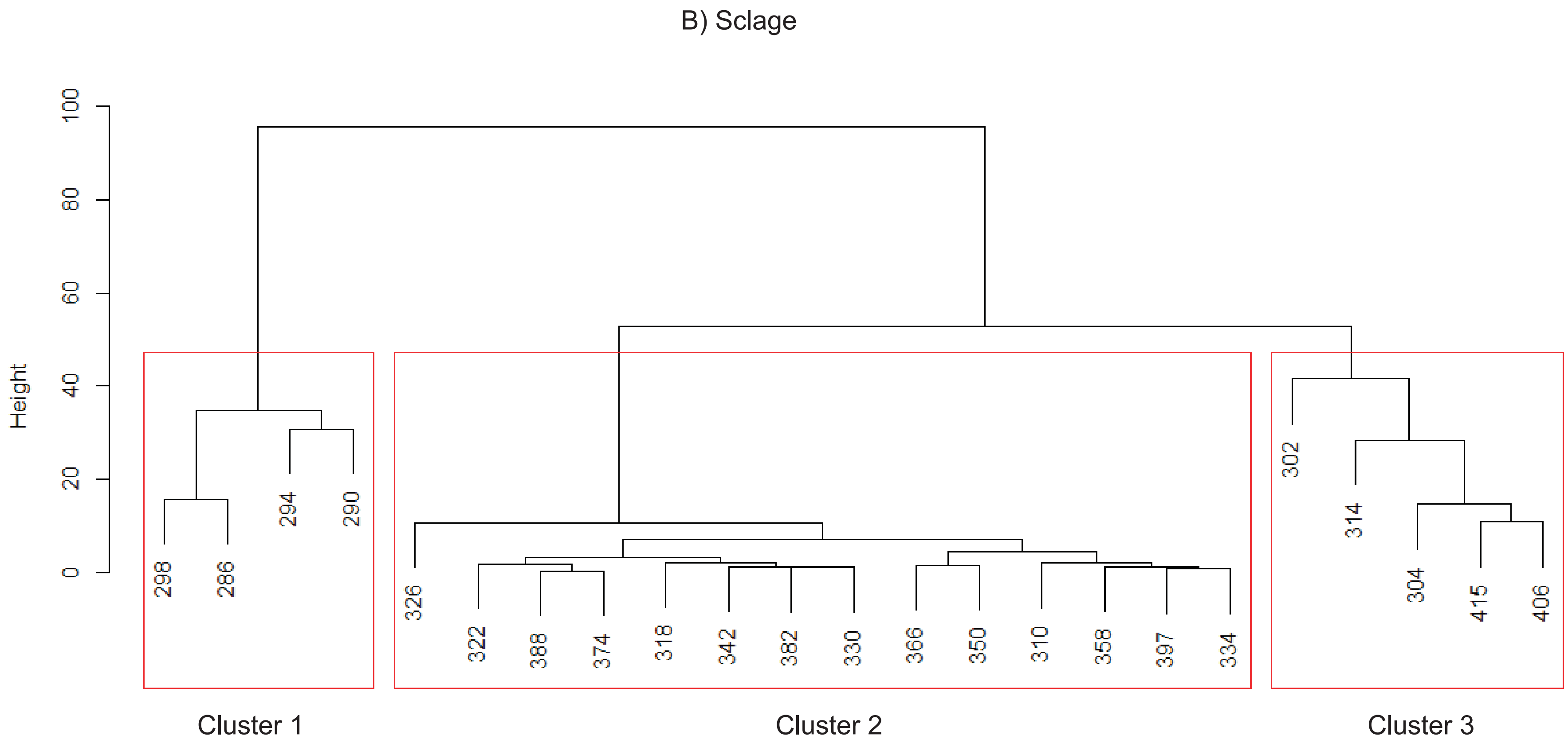
B) Sclage
Height
100
80
60
40
20
0
298
286
294
290
326
322
388
374
318
342
382
330
366
350
310
358
397
334
302
314
304
415
406
Cluster 1
Cluster 2
Cluster 3

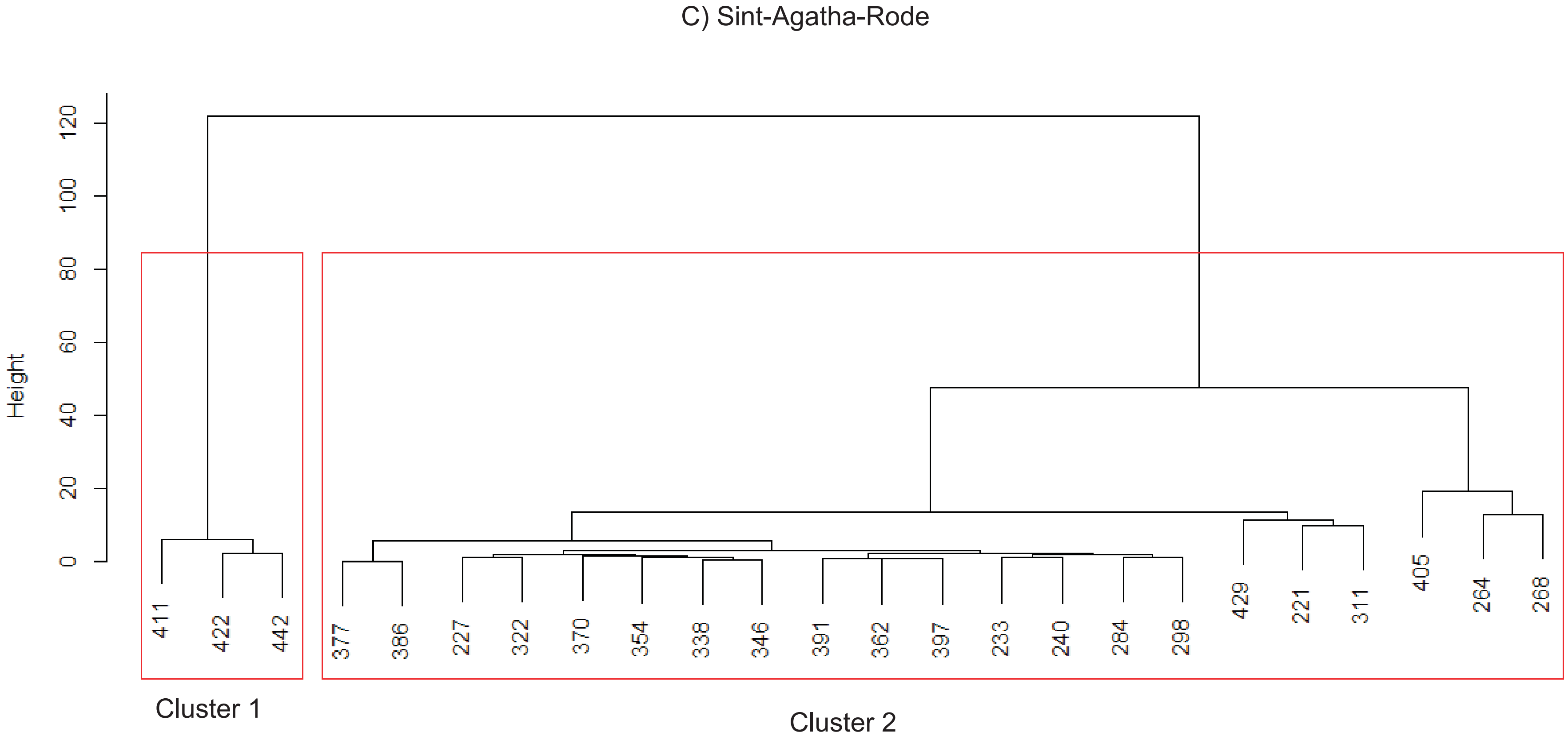
C) Sint-Agatha-Rode
Height
0
20
40
60
80
100
120
411
422
442
377
386
227
322
370
354
338
346
391
362
397
233
240
284
298
429
221
311
405
264
268
Cluster 1
Cluster 2

D) Korbeek

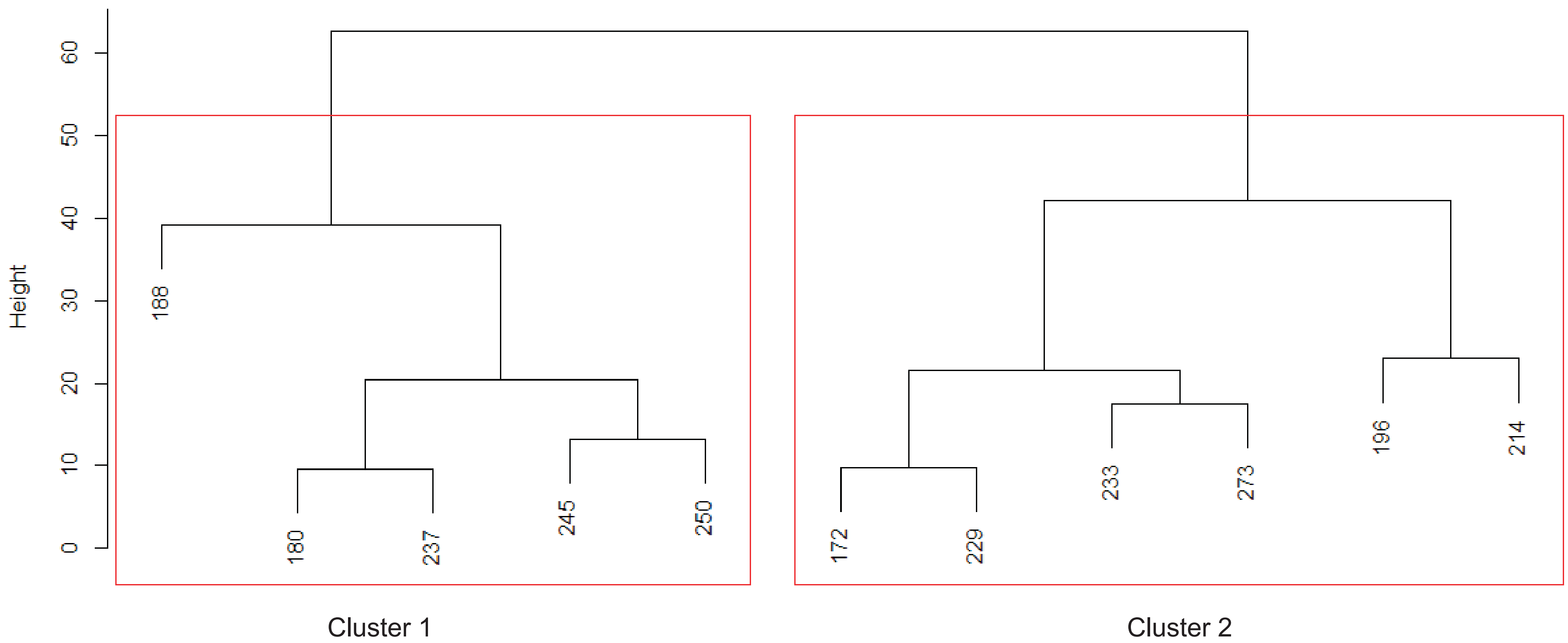

Height
0
10
20
30
40
50
60
188
180
237
245
250
172
229
233
273
196
214
Cluster 1
Cluster 2

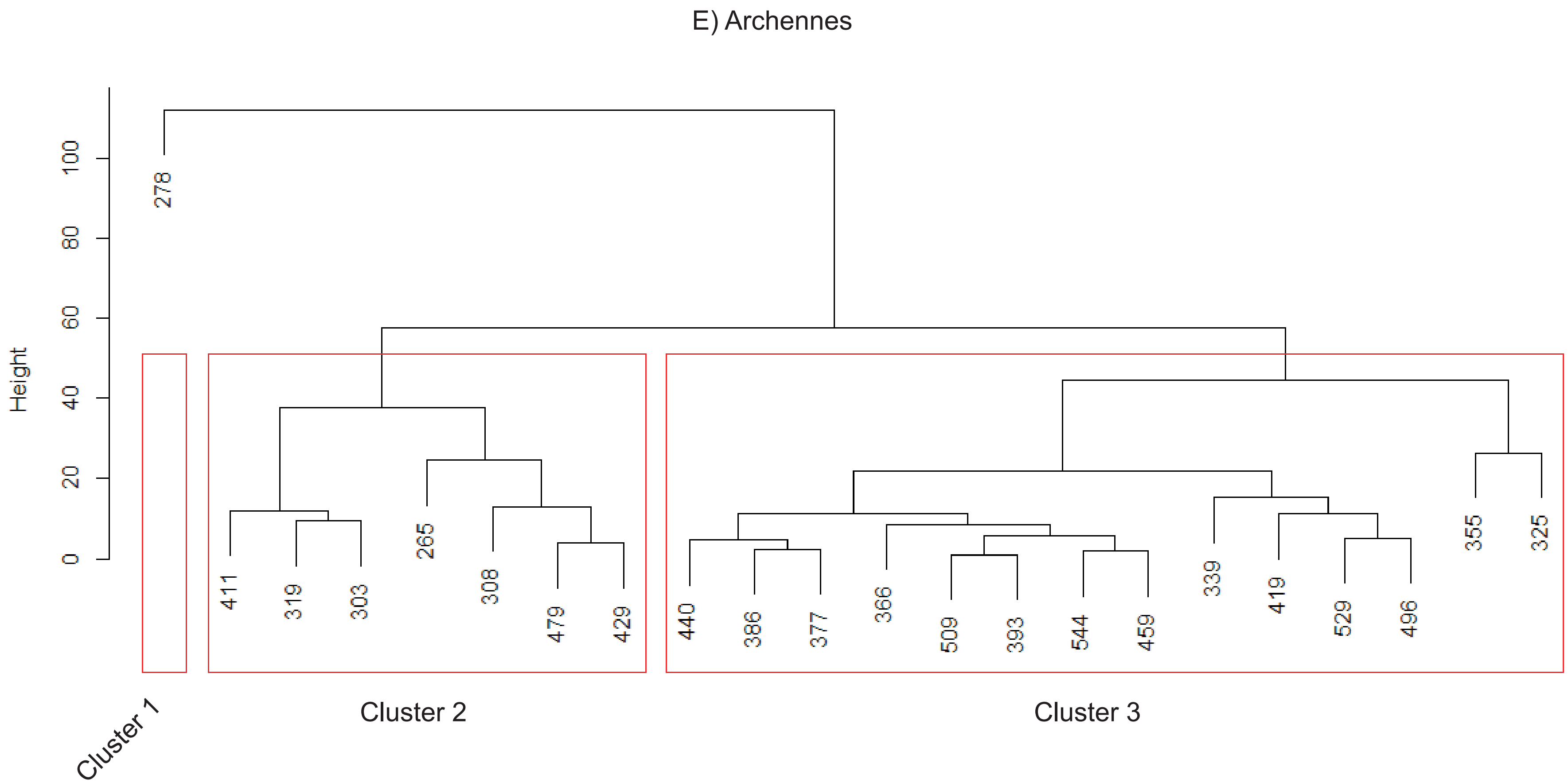
E) Archennes
Height
0
20
40
60
80
100
278
411
319
303
265
308
479
429
440
386
377
366
509
393
544
459
339
419
529
496
355
325
Cluster 1
Cluster 2
Cluster 3

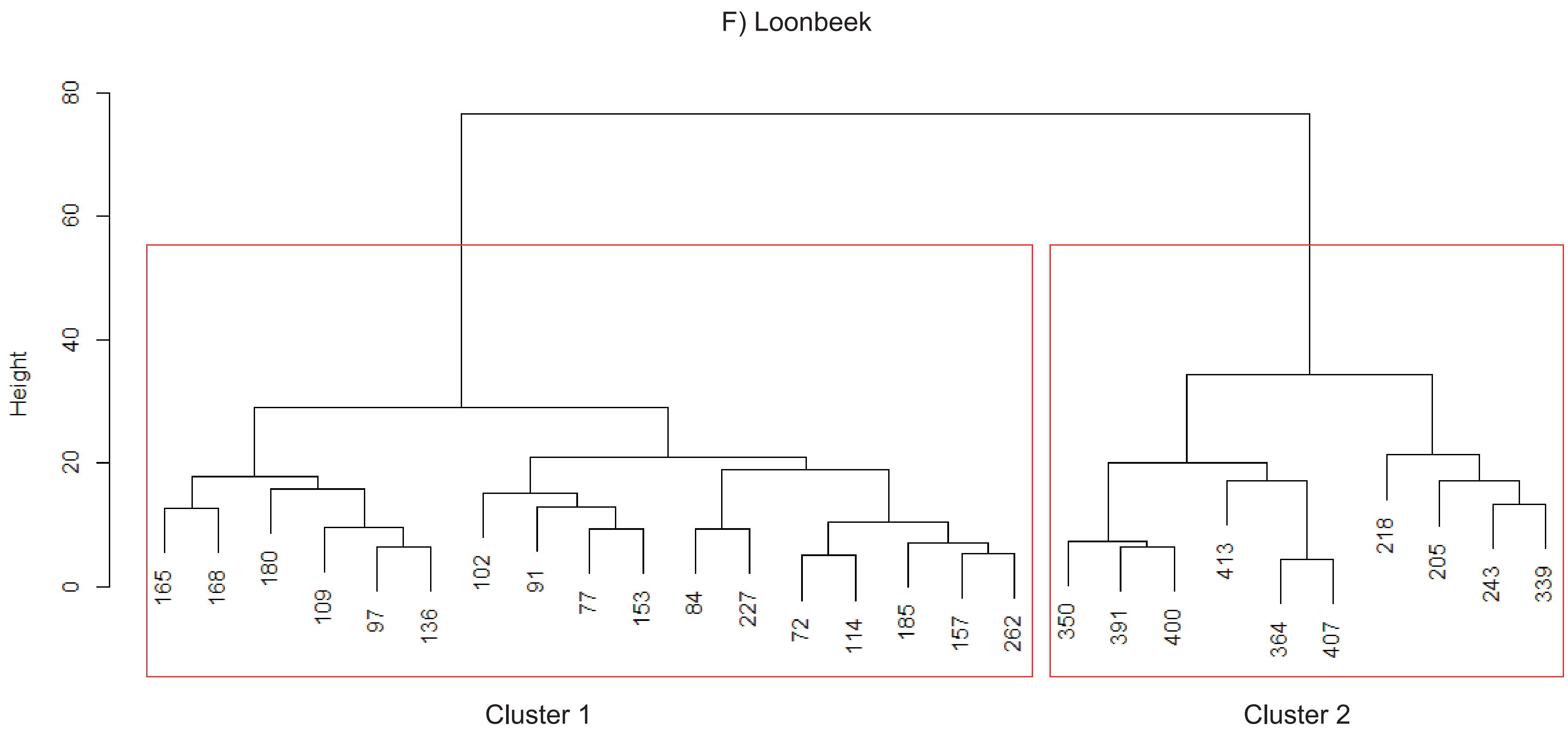
F) Loonbeek
Height
0
20
40
60
80
165
168
180
109
97
136
102
91
77
153
84
227
72
114
185
157
262
350
391
400
413
364
407
218
205
243
339
Cluster 1
Cluster 2

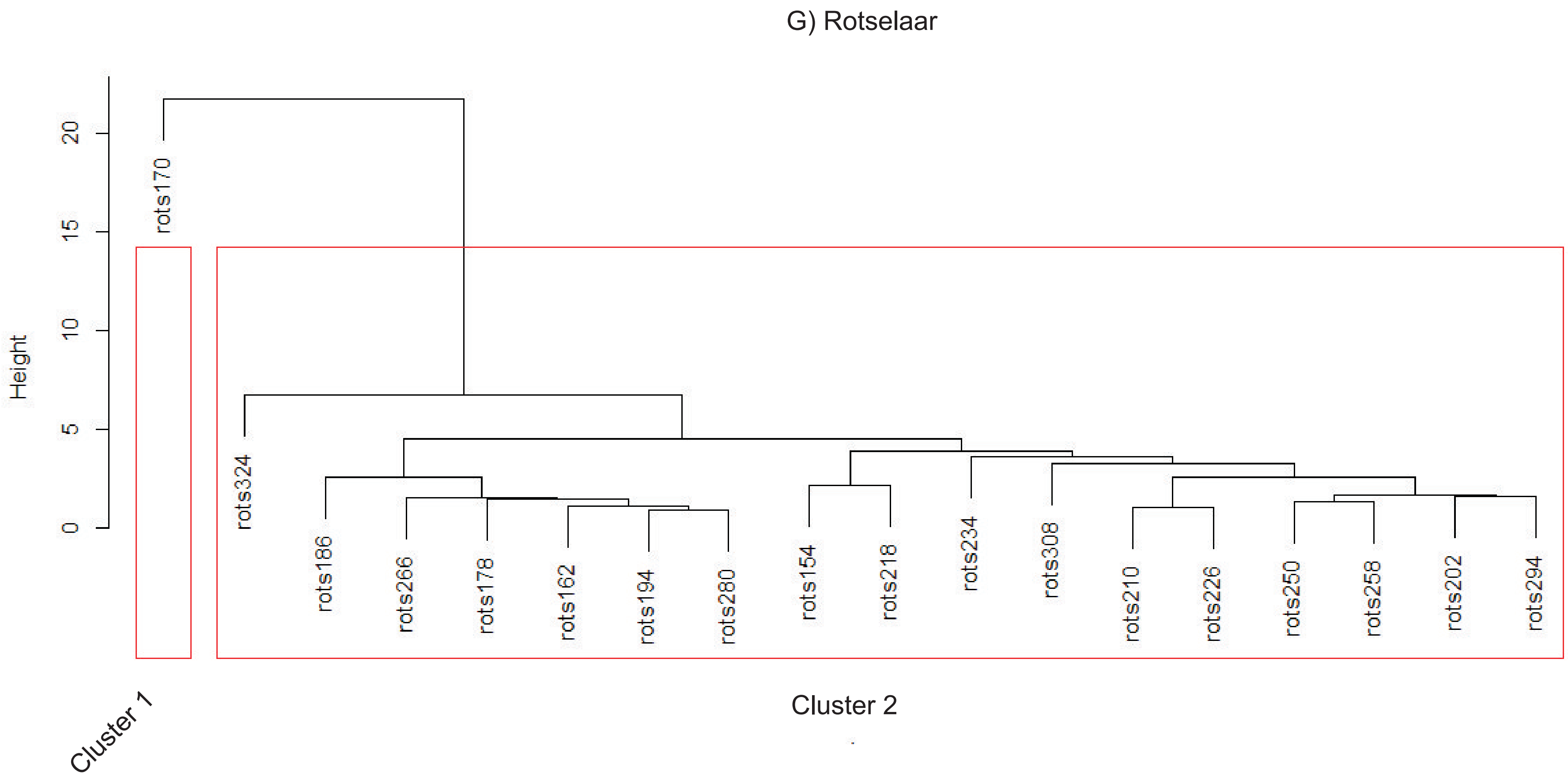

G) Rotselaar
Height
0
5
10
15
20
rots170
rots324
rots186
rots266
rots178
rots162
rots194
rots280
rots154
rots218
rots234
rots308
rots210
rots226
rots250
rots258
rots202
rots294
Cluster 1
Cluster 2

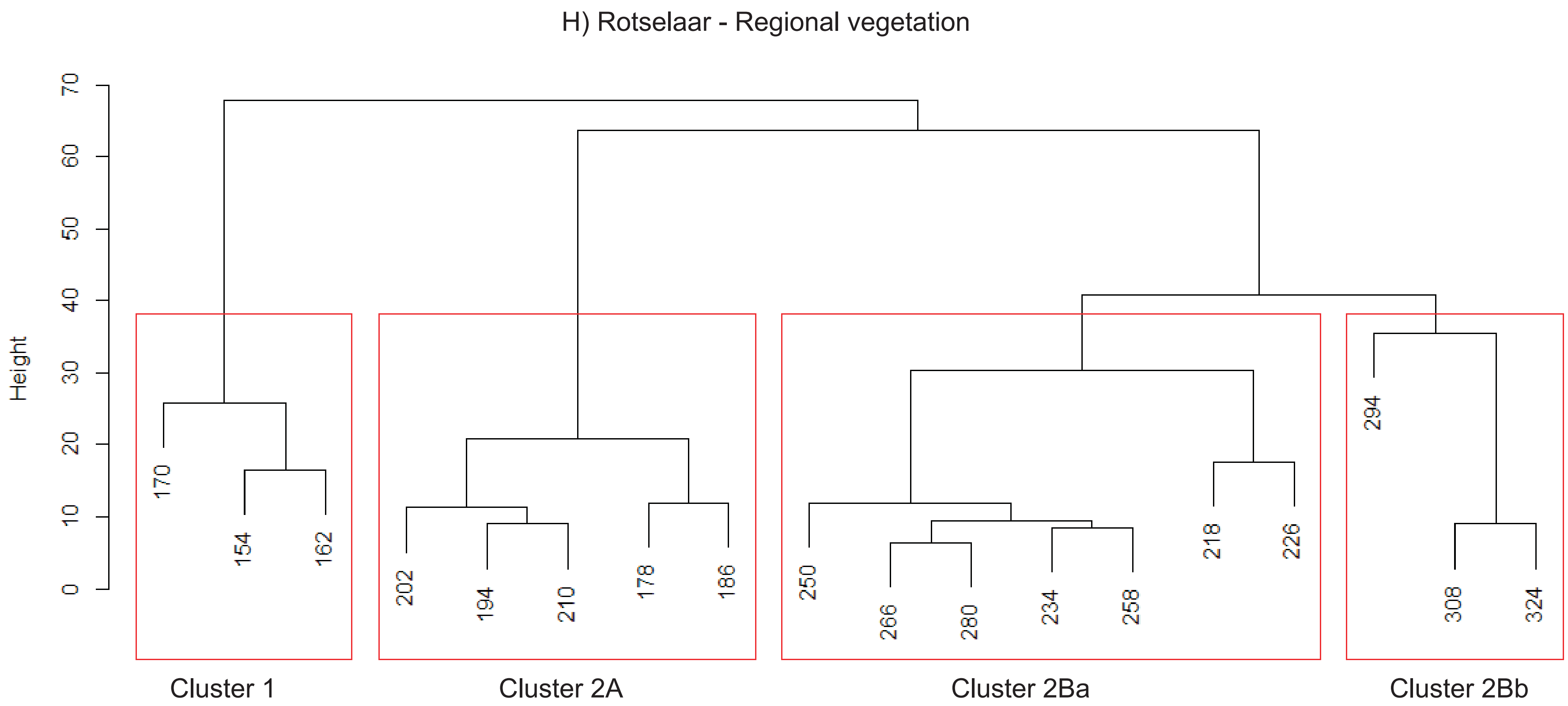
H) Rotselaar - Regional vegetation
Height
0
10
20
30
40
50
60
70
170
154
162
202
194
210
178
186
250
266
280
234
258
218
226
294
308
324
Cluster 1
Cluster 2A
Cluster 2Ba
Cluster 2Bb